



UNIFORMED SERVICES UNIVERSITY OF THE HEALTH SCIENCES
F. EDWARD HÉBERT SCHOOL OF MEDICINE
4301 JONES BRIDGE ROAD
BETHESDA, MARYLAND 20814-4799



March 12, 2007

BIOMEDICAL
GRADUATE PROGRAMS

Ph.D. Degrees

Interdisciplinary
Emerging Infectious Diseases
Molecular & Cell Biology
Neuroscience

Departmental
Clinical Psychology
Environmental Health Sciences
Medical Psychology
Medical Zoology
Pathology

Doctor of Public Health (Dr.P.H.)

Physician-Scientist (MD/Ph.D.)

Master of Science Degrees

Molecular & Cell Biology
Public Health

Masters Degrees

Comparative Medicine
Military Medical History
Public Health
Tropical Medicine & Hygiene

Graduate Education Office

Dr. Eleanor S. Metcalf, Associate Dean
Janet Anastasi, Program Coordinator
Tanice Acevedo, Education Technician

Web Site

www.usuhs.mil/geo/gradpgm_index.html

E-mail Address

graduateprogram@usuhs.mil

Phone Numbers

Commercial: 301-295-9474
Toll Free: 800-772-1747
DSN: 295-9474
FAX: 301-295-6772

APPROVAL SHEET

Title of Dissertation: "Molecular Factors and Biological Pathways Associated with Malaria Fever and the Pathogenesis of Cerebral Malaria"

Name of Candidate: Miranda Oakley
Doctor of Philosophy Degree
9 April 2007

Dissertation and Abstract Approved:

Richard Andre, Ph.D.
Department of Preventive Medicine & Biometrics
Committee Chairperson

12 April 2007
Date

Thomas McCutchan, Ph.D.
Department of Preventive Medicine & Biometrics
Committee Member

11 April 2007
Date

D. Scott Merrell, Ph.D.
Department of Microbiology & Immunology
Committee Member

4/12/2007
Date

John Cross, Ph.D.
Department of Preventive Medicine & Biometrics
Committee Member

11 April 2007
Date

Dechang Chen, Ph.D.
Department of Preventive Medicine & Biometrics
Committee Member

12 April 2007
Date



UNIFORMED SERVICES UNIVERSITY OF THE HEALTH SCIENCES
F. EDWARD HÉBERT SCHOOL OF MEDICINE
4301 JONES BRIDGE ROAD
BETHESDA, MARYLAND 20814-4799



March 14, 2007

**BIOMEDICAL
GRADUATE PROGRAMS**

Ph.D. Degrees

Interdisciplinary
-Emerging Infectious Diseases
-Molecular & Cell Biology
-Neuroscience

Departmental
-Clinical Psychology
-Environmental Health Sciences
-Medical Psychology
-Medical Zoology
-Pathology

Doctor of Public Health (Dr.P.H.)

Physician Scientist (MD/Ph.D.)

Master of Science Degrees

-Molecular & Cell Biology
-Public Health

Masters Degrees

-Comparative Medicine
-Military Medical History
-Public Health
-Tropical Medicine & Hygiene

Graduate Education Office

Dr. Eleanor S. Metcalf, Associate Dean
Janet Anastasi, Program Coordinator
Tanice Acevedo, Education Technician

Web Site

www.usuhs.mil/geo/gradpgm_index.html

E-mail Address

graduateprogram@usuhs.mil

Phone Numbers

Commercial: 301-295-9474
Toll Free: 800-772-1747
DSN: 295-9474
FAX: 301-295-6772

**FINAL EXAMINATION FOR THE DEGREE
OF DOCTOR OF PHILOSOPHY**

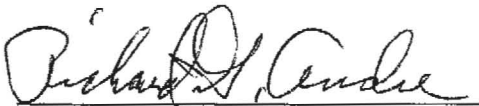

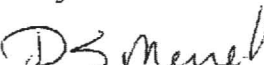
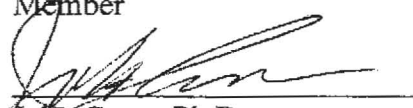
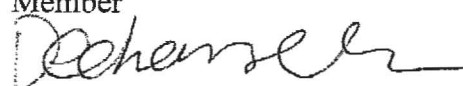
Name of Student: Miranda Oakley

Date of Examination: 9 April 2007

Time: 1:00

Place: Lecture Room C

DECISION OF EXAMINATION COMMITTEE MEMBERS:

	PASS	FAIL
 Richard Andre, Ph.D. Department of Preventive Medicine & Biometrics Chairperson	X	—
 Thomas McCutchan, Ph.D. Department of Preventive Medicine & Biometrics Major Advisor	X	—
 D. Scott Merrell, Ph.D. Department of Microbiology & Immunology Member	✓	—
 John Cross, Ph.D. Department of Preventive Medicine & Biometrics Member	✓	—
 Dechang Chen, Ph.D. Department of Preventive Medicine & Biometrics Member	pass	—

The author hereby certifies that the use of any copyrighted material in the thesis manuscript entitled:

"Molecular Factors and Biological Pathways Associated with Malaria Fever
and the Pathogenesis of Cerebral Malaria"

is appropriately acknowledged and, beyond brief excerpts, is with the permission of the copyright owner.

A handwritten signature in black ink, appearing to read 'MOakley', with a stylized flourish at the end.

Miranda Oakley
Emerging Infectious Diseases Program
Uniformed Services University

Molecular Factors and Biological Pathways Associated with Malaria
Fever and the Pathogenesis of Cerebral Malaria

By

Miranda S.M. Oakley

Emerging Infectious Diseases Program

Uniform Services University of the Health Sciences

Abstract

Title of Thesis: Molecular Factors and Biological Pathways Associated with Malaria Fever and the Pathogenesis of Cerebral Malaria

Name: Miranda S.M. Oakley

Thesis Directed by: Thomas F. McCutchan
Principle Investigator, Regulation of Growth and Development Section
Laboratory of Malaria and Vector Research
National Institute of Allergy and Infectious Diseases, NIH

Fever is the most benign and common, and cerebral malaria is the most severe but rare consequence of malaria pathogenesis. However, the molecular mechanisms underlining these clinical syndromes are poorly defined. As a result, therapy against malaria is solely based on drugs that eliminate parasites in an infected host; no anti-disease interventions are available to alleviate the pathological symptoms of malaria. In this dissertation, I have investigated the molecular factors and biological pathways that are associated with febrile illness and cerebral malaria. Febrile illness studies were done with intra-erythrocytic stage *Plasmodium falciparum* parasites, while cerebral malaria studies were done in the experimental *Plasmodium berghei* ANKA murine model of cerebral malaria (ECM).

Using a combination of microarray-based global gene expression profiling, in depth computational analysis, bioinformatics, and biological assays, we have identified parasitic factors associated with malaria febrile illness and host factors associated with cerebral malaria. Fever-induced changes in the parasite include upregulation of parasite virulence factors, down-regulation of the ubiquitin pathway, and a major extrusion of parasite proteins into the erythrocyte cytoplasm and membrane. In ECM, we observed transcriptional changes of a wide

array of host proteins including molecules involved in immunopathogenesis and neuroprotection.

Among the molecules with significantly altered expression, protein expression of p21 and galectin-3 in brain samples from ECM was confirmed by western blot, making these molecules strong candidates for reliable biomarkers of cerebral malaria. The identification of associated molecules and biological pathways opens up new avenues for understanding the parasite cell biology, immunopathogenesis of disease, and for identifying 1) future biomarkers for early prediction of disease and 2) novel targets for drugs and vaccines.

Acknowledgements

This work was completed with the support and assistance of many people and organizations. I would like to express my gratitude to the following individuals.

I thank Dr. Thomas McCutchan for directing my dissertation project and for giving me the opportunity to work as an NIH-pre IRTA fellow in his laboratory at the Regulatory and Growth Development Section, Laboratory of Malaria and Vector Research, National Institute of Allergy and Infectious Diseases, NIH.

I'm grateful to Professor Richard Andre, Professor John Cross, Assistant Professor D. Scott Merrell and Associate Professor Dechang Chen from the Uniformed Services University of the Health Sciences for serving as members of my dissertation committee and for their continuous guidance and support. Dr. Andre served as the committee chair. I also thank Professor Eleanor Metcalf for her help as a committee member during the early part of my research and also for her guidance as Director of the USUHS EID program. I am thankful to Ms. Janet Anastasi at USUHS for providing administrative assistance throughout my graduate studies.

I express my gratitude to my collaborators Drs. Sanjai Kumar and Babita Mahajan, and Mr. Hong Zheng and Ms. Victoria Majam from the Division of Emerging and Transfusion Transmitted Diseases at the FDA.

I am also thankful to Drs. Guojian Jiang and Tim Myers at the NIAID Microarray Research Facility for assistance with microarray studies and Dr. Jerry Ward, Mr. Larry Faucette, and Ms. Cindy Erekson from the Infectious Disease Pathogenesis Section at NIAID for their assistance and for teaching me details of histopathology.

Drs. Aravind Iyer and Vivek Anantharaman at the National Center for Biotechnology Information at NIH are thanked for their help and guidance with the bioinformatics and annotation and analysis of febrile temperature induced Plasmodium genes.

I would also like to extend my sincere thanks to my numerous coworkers and friends at the Laboratory of Malaria and Vector Research at NIAID and my colleagues at USUHS. I'd especially like to thank Rosanne Hearn, Kasima Brown, and Margery Sullivan for their contribution to my research.

In the end, I express my gratitude to my parents, Mr. and Mrs. William and Victoria Oakley for their life-long inspiration and support.

Sincerely,

Miranda Oakley

List of Figures

Figure 1. Life Cycle of human malaria.....	4
Figure 2. Pathogenesis of malaria.....	5
Figure 3. Effect of febrile temperature on parasite growth and survival.....	33
Figure 4. TUNEL assay of parasites treated at 37°C and 41°C.....	35
Figure 5. Effect of febrile temperature on expression of HSP-70 and chitinase parasite proteins.....	39
Figure 6. Flow cytometric analysis of heat-induced erythrocyte surface expression of PfEMP1.....	46
Figure 7. Tree of DnaJ family showing lineage-specific expansion.....	51
Figure 8. Effect of febrile temperature on ubiquitination of parasite proteins.....	54
Figure 9. Tree of R45 protein kinase family showing lineage-specific expansion.....	57
Figure 10. Cell cartoon depicting sub-cellular localization of proteins showing altered mRNA levels under febrile temperatures.....	62
Figure 11. Histological features of ECM.....	87
Figure 12. Symptoms exhibited in a moribund and in a non-moribund mouse.....	97
Figure 13. Analysis of genes altered in expression in brain and spleen tissue.....	105
Figure 14. Parasitemia curves of susceptible and resistant mice.....	108
Figure 15. Boxplots for spleen size data.....	110
Figure 16. OX40 immunohistological staining of brain sections.....	118
Figure 17. CD8 ⁺ T cell-mediated expression of galectin-3.....	123
Figure 18. A summary of the chemokine network altered during CD8 ⁺ T cell-mediated pathogenesis of ECM.....	126

Figure 19. Diagram of Microarray Analysis.....	165
Figure 20. p21 protein expression during ECM.....	176

List of Tables

Table 1. Febrile temperature induced alterations in the <i>P. falciparum</i> genome and assigned biologic functions.....	37
Table 2. Biologic functions of a subset of genes induced by febrile temperature.....	41
Table 3. Groups of Mice used in Microarray Hybridizations.....	104
Table 4. Relationship between susceptibility to ECM and spleen Size.....	111
Table 5. Effect of the <i>CD8a</i> and <i>pfpr</i> genes on tissue-specific gene expression.....	113
Table 6. Effect of <i>CD8</i> and <i>perforin</i> genes on brain and spleen gene expression in uninfected mice.....	115
Table 7. Mediators of apoptosis in the brain during ECM.....	119
Table 8. Genes altered by presence of perforin during a Pb-A infection.....	127
Table 9. Criteria used for classification of mice into moribund, non-moribund, and resistant groups.....	161
Table 10. Groups of Mice used in Microarray Hybridizations.....	162
Table 11. Biological functions of a subset of ECM related genes.....	166
Table S1. Annotation and functional predictions of parasites genes altered by febrile temperature.....	69
Table S2. Differential gene expression in relation to WT C57BL6 mice with ECM and CD8 ⁺ KO C57BL6 with no ECM in the Brain.....	134
Table S3. Differential gene expression in relation to WT C57BL6 mice with ECM and CD8 ⁺ KO C57BL6 with no ECM in the spleen.....	141

Table S4. Differential gene expression in relation to WT C57BL6 mice with ECM and PFP-KO C57BL6 with no ECM in the Brain.....	149
Table S5. Differential gene expression in relation to WT C57BL6 mice with ECM and PFP-KO C57BL6 with no ECM in the Spleen.....	150
Table S6. A complete list of ECM related genes in our study.....	184

Table of Contents

Title Page.....	i
Abstract.....	ii
Acknowledgements.....	iv
List of Figures.....	vi
List of Tables.....	viii
Introduction I: Malaria the disease.....	1
Introduction II: Malaria and Fever.....	8
Intra-erythrocytic parasite growth cycle, clinical febrile illness and regulation of parasite density.....	9
Malaria toxins and febrile illness.....	11
Febrile illness and the regulation of parasite development and growth.....	13
Febrile temperatures and parasite virulence factors.....	14
Febrile illness and the pathogenesis of cerebral malaria.....	15
Molecular Factors and Biochemical Pathways Induced by Febrile Temperature in <i>Plasmodium falciparum</i> Parasites.....	20
Abstract.....	21
Introduction.....	23
Material and Methods.....	26
Results and Discussion.....	32
Effect of febrile temperature on the survival of <i>P. falciparum</i> parasites.....	32
Measuring febrile temperature-induced alterations in the expression profile of <i>P. falciparum</i>	35

Annotation of febrile temperature-regulated hypothetical malarial genes.....	39
Biologic characteristics of the febrile temperature-regulated genes.....	40
Trafficking.....	43
Febrile illness and cerebral malaria: the role of EMP-1.....	44
Secreted and cell surface molecules.....	47
Heat-shock response and protein stability.....	49
Cytoplasmic systems and signal transduction.....	55
RNA metabolism.....	58
Nuclear functions.....	58
General metabolism.....	59
Introduction III: The Pathogenesis of Cerebral Malaria.....	83
Background.....	84
The Pathogenesis of CM.....	85
Sequestration.....	85
Experimental CM.....	86
T cells.....	87
CD4 ⁺ T cells.....	88
CD8 ⁺ T cells.....	88
Perforin.....	89
Blood brain barrier.....	90
Soluble mediators and effector molecules.....	90
Hemostasis.....	91

CD8 ⁺ T cell-Mediated Pathogenesis of Cerebral Malaria.....	95
Abstract.....	96
Introduction.....	97
Material and Methods.....	101
Results and Discussion.....	107
CD8 ⁺ -KO and PFP-KO mice are resistant to ECM.....	107
Relationship between susceptibility to ECM and spleen size.....	108
Measuring the alterations in the gene expression during ECM.....	111
Measuring alterations in gene expression in uninfected knockout mice.....	113
CD8 ⁺ T cells and the pathogenesis of ECM.....	116
Activation of CD8 ⁺ T cells.....	116
Apoptosis.....	118
CTL mediated cytotoxicity.....	119
Suppressors of apoptosis.....	121
Galectin-3.....	122
Chemokines.....	124
Perforin and pathogenesis of ECM.....	126
Effect of perforin on the expression of CCL21b.....	127
Host Molecular Markers of Cerebral Malaria.....	155
Abstract.....	156
Introduction.....	157
Material and Methods.....	160

Results and Discussion.....	164
Measuring the alterations in the gene expression during ECM.....	164
Immune modulators of pathogenesis.....	169
Changes in hemoglobin content.....	171
Stress response.....	171
Transcription factors.....	173
Signal transduction.....	174
Cell cycle.....	175
Receptors.....	176
Cytoskeleton.....	177
Discussion of Results.....	192

Malaria the disease

Malaria is one of the top ranking infectious diseases in the world, and in terms of human suffering and economic loss, it inflicts a great burden on mankind. In spite of the modern advances in medical sciences, the problem of malaria is on the rise; today there are more clinical cases of malaria than 30 years ago. Each year, there are approximately 300 - 500 million clinical cases and more than 1 million deaths, mostly in young children, that are directly attributed to malaria infections (1). Several factors including the exponential rise in human population, environmental degradation, policies against the use of residual insecticides in house, human migration and probably most importantly the rapid emergence and spread of parasite strains that have developed resistance against the major anti-malaria drugs are responsible for the deteriorating situation (2, 8).

Malaria is caused by infections with protozoan parasites belonging to the genus *Plasmodium*. There are more than 100 species of *Plasmodium* that infect reptiles, birds and mammals of which only four species, *Plasmodium falciparum*, *Plasmodium vivax*, *Plasmodium ovale*, and *Plasmodium malariae* are known to cause infections in human.

The life cycle of *Plasmodium* parasites consists of asexual stages completed in a vertebrate host and sexual stages in the mosquito vector of over 40 species of female *Anopheles* (Greek for hurtful). Malaria infection is commenced following the inoculation of sporozoites during a blood meal. Within a span of 30 minutes or less, inoculated sporozoites find and invade liver cells to begin the intra-hepatic stage of development. In human malarias, the hepatic stages normally last between 6 to 15 days, although some strains of *P. vivax* are known to remain dormant inside the liver for more than 21 months (3). During the liver stage, a single uninucleated sporozoite, replicates into 10,000 - 40,000 liver form merozoites. Following the rupture of the infected liver cell, merozoites are released into circulation and invade erythrocytes, thus

beginning the intra-erythrocytic stage of the cycle. Within erythrocytes, development progresses from ring, trophozoite and finally into multi-nucleated schizonts resulting in 8 – 32 merozoites. Rupturing schizonts release merozoites into the circulation that invade new erythrocytes. This repeated cycle of invasion, replication, and rupture continues until the infected host reaches a threshold parasitemia. In human *Plasmodium*, the intra-erythrocytic cycle lasts 48–72 hrs depending on the species. A subset of the blood form merozoites undergo gametocytogenesis and develop into male and female gametocytes that can survive in circulation for an extended period before they are picked up by a mosquito during a blood meal. Once inside the mosquito vector, the gametocytes undergo a process of further maturation that is followed by fertilization resulting in the formation of a zygote. The zygotes undergo differentiation into motile ookinetes which penetrate the epithelial brush border of the midgut cells and become oocysts. After an extensive amount of nuclear division, each oocyst gives rise to up to 3000 sporozoites that are released into the mosquito haemocoel, from where they are carried by the hemolymph and may invade the salivary gland. Infectious mosquitoes release the sporozoites into a host during a blood meal. The complete life cycle of malaria parasites and implicated immune mechanisms are depicted in figure 1 (4).

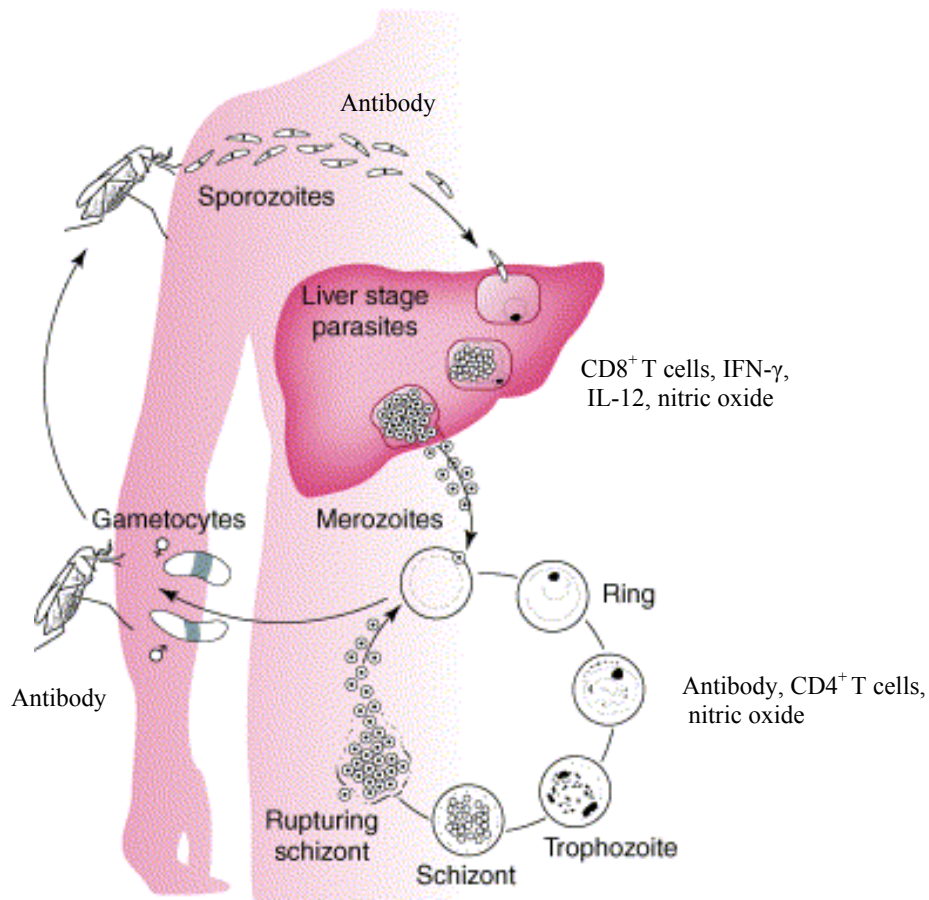


Figure 1. The life cycle of human malaria and immune mechanisms associated with each stage (figure modified from reference 4).

Only intra-erythrocytic stages of malaria parasites are known to cause clinical disease in humans; pre-erythrocytic stages (sporozoite and liver forms) cause no symptoms. Malarial infections present a wide range of clinical symptoms: malaria paroxysm is the most common and mildest form, and severe anemia and cerebral malaria are the most severe forms of malaria pathogenesis (FIG. 2).

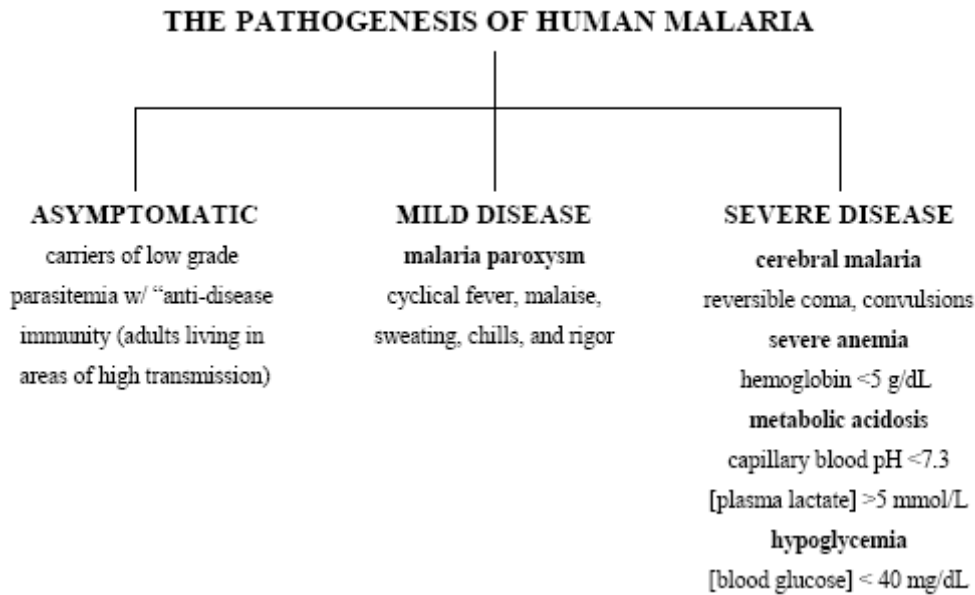


Figure 2. The pathogenesis of human malaria. Infection with *Plasmodium* can result in clinical symptoms that range in both severity and frequency.

Rupturing infected erythrocytes and releasing merozoites are known to cause malaria fever and chills, the clinical symptoms most closely associated with malaria. Another common feature of malaria is the presence of severe anemia mostly experienced during primary infections. The degree of anemia experienced during malaria is not always directly proportional to the parasite density and has been shown to be caused by destruction of both infected and uninfected erythrocytes and dyserythropoiesis (7). Sequestration, a process defined as binding of infected erythrocytes to the deep capillary venules especially in the brain tissues leads to obstruction in blood flow and is considered the primary cause of the pathogenesis of cerebral malaria. Sequestration is a parasite defense mechanism that prevents filtration of mature infected erythrocytes through the spleen, thus enabling parasites to evade immune destruction (5). A unique feature of the biology of *P. falciparum* parasites is that only early ring form parasites are detected in blood films; trophozoite and schizont forms sequester in different organs, including

the brain (6). Among the four *Plasmodium* species, *P. falciparum* alone is responsible for more than 90% of malaria related deaths; approximately 90% of these deaths occur in children under the age of five living in sub-Saharan Africa. Why *P. falciparum* has evolved to causes the most virulent form of malaria is not clear; however, the majority of *falciparum*-associated deaths in young children are caused by the pathological syndromes of cerebral malaria and severe anemia. It is also important to note that the clinical syndromes of cerebral malaria are caused by only *P. falciparum* infections, although some murine malarias also display the patho-physiological symptoms that closely resemble the human cerebral malaria disease.

Current anti-malarial drugs are known to function by being effective against the parasite. None of these drugs are designed to directly block the pathological symptoms of severe disease. Similarly, current vaccine development efforts are directed either to prevent infection or reduce parasitemia in a vaccinated host. To reduce malaria morbidity and mortality, it is imperative that a new generation of ‘anti-disease’ drugs and vaccines are designed that ameliorate the pathological symptoms of malaria, as well as reduce the parasite burden. However, design of ‘anti-disease’ intervention strategies requires a close understanding of both the parasite and host molecules and their related biological pathways that render protection from and also contribute towards the pathogenesis of malaria.

In this Ph.D. dissertation, results will be presented from studies that were designed to 1) determine the effect of febrile temperature on the survival of *P. falciparum* parasites and its potential effect on host pathogenesis due to changes encountered by the parasites in response to febrile temperature conditions and 2) identification of the molecular factors and biological pathways that are responsible for resistance to or susceptibility to the pathological consequences of cerebral malaria in a murine malaria model.

REFERENCES

1. **Breman, J. G., A. Egan, and G. T. Keusch.** 2001. The intolerable burden of malaria: a new look at the numbers. *Am J Trop Med Hyg* **64**:iv-vii.
2. **Hay, S. I., C. A. Guerra, A. J. Tatem, A. M. Noor, and R. W. Snow.** 2004. The global distribution and population at risk of malaria: past, present, and future. *Lancet Infect Dis* **4**:327-336.
3. **Krotoski, W. A.** 1989. The hypnozoite and malarial relapse. *Prog Clin Parasitol* **1**:1-19.
4. **Miller, L.H. and Hoffman S. L.** 1996. Perspectives on Malaria Vaccine Development. ASM, Washington D.C (1-9).
5. **Langreth, S. G., and E. Peterson.** 1985. Pathogenicity, stability, and immunogenicity of a knobless clone of *Plasmodium falciparum* in Colombian owl monkeys. *Infect Immun* **47**:760-766.
6. **Newbold, C., A. Craig, S. Kyes, A. Rowe, D. Fernandez-Reyes, and T. Fagan.** 1999. Cytoadherence, pathogenesis and the infected red cell surface in *Plasmodium falciparum*. *Int J Parasitol* **29**:927-937.
7. **Newton, C. R., P. A. Warn, P. A. Winstanley, N. Peshu, R. W. Snow, G. Pasvol, and K. Marsh.** 1997. Severe anaemia in children living in a malaria endemic area of Kenya. *Trop Med Int Health* **2**:165-178.
8. **Sachs, J. D.** 2002. A new global effort to control malaria. *Science* **298**:122-124.

Chapter 1
Malaria and Fever

Several centuries before the discovery by Charles Louis Alphonse Laveran in 1880 that malaria is caused by infection of erythrocytes with *Plasmodium* parasites, in ancient civilizations, the disease of malaria was characterized by a high cyclical fever, lasting for a few hours at a time followed by rigors and chills. Subsequent studies established an association between the time required by a *Plasmodium* species to develop inside the erythrocyte and recurrence of malaria fever, leading to the conclusion that toxic products released by rupturing schizonts are responsible for the febrile illness that is a hallmark of malaria infection. Observations arising from neurosyphilis studies performed in the 1930s and 1940s (5) and from a few recent studies have led many researchers to believe that malaria febrile illness is an evolutionary adaptation that benefits both the parasite and its host (25, 47). According to this hypothesis, elevated host temperature induces a cascade of molecular events that maintain the total parasite burden at a threshold level by limiting its replication rate, allowing host defense mechanisms to activate and mature. Although inhibition of exponential parasite growth caused by febrile temperature may appear to aid only the host, it may also provide the parasite sufficient time to further transmit infection, making it a potential parasite survival strategy. Given the important role of febrile temperature on the survival and virulence of malaria parasites, surprisingly, information remains very limited regarding the molecular factors and the associated biological pathways induced in malaria parasites in response to febrile illness.

Intra-erythrocytic parasite growth cycle, clinical febrile illness and regulation of parasite density. The periodicity of clinical febrile illness in an infected patient is known to coincide with the release of merozoites from the rupturing schizonts. The intraerythrocytic cycle is completed in 48 h for *P. falciparum*, *P. vivax* and *P. ovale* parasites, and 72 h for *P. malariae* (19). In line with their schizogony cycle, infections with *P. falciparum*, *P. vivax* and *P. ovale* species cause incidents of febrile episodes that occur every 48 h, hence the name TERTIAN

intervals. Febrile reactions caused by *P. vivax* infections are known to most closely correspond to the 48 h division cycle and following each cycle of schizont rupture, the patient's temperature rises and then in the course of several hours returns to normal (19). However, it is frequently observed that once the infections are well established in a naïve host, two broods of infections might simultaneously exist giving rise to daily pyrogenic episodes at 24 h intervals known as QUOTIDIAN paroxysms. The developmental cycle of *P. malariae* requires 72 h, which is called a QUARTAN infection. In this group, one, two or three pyrogenic broods of infections could be present that could result in single, double or triple QUARTAN clinical activity. These clinical observations were the basis for the establishment of a cause and effect relationship between the *Plasmodium* developmental cycle and malaria infection-induced clinical paroxysms. In a malaria naïve host, during each paroxysm cycle, temperatures as high as 39.44°C to 40.55°C are commonly observed, although temperatures of 41.67°C or higher lasting for several hours were also observed.

In the 1930s and 40s, malaria infections were used as therapeutic agents in the treatment of neuro-syphilis (5, 33). These studies have provided the most comprehensive knowledge of clinical malariology in previously malaria naïve individuals without interference of preexisting immunity. Close monitoring of parasite burden at the onset of and at the terminal stages of the febrile episodes triggered by malaria infections has directly allowed the determination of the effect of febrile temperatures on the regulation of parasite density. The neurosyphilis studies have provided the most accurate information on the dynamics of infection in a controlled setting that closely mimics the conditions of infection acquired in endemic areas.

The minimal parasite density required to trigger a febrile response (a temperature of 100°F or higher) is termed the PYROGENIC DENSITY or THRESHOLD. This threshold is known to vary greatly based on the *Plasmodium* species and the host's immune status. Ross and

Thompson had established in 1910 that in malaria, a certain parasite density is necessary before a febrile response is triggered (42). Subsequently, it was demonstrated that there was an inverse correlation between the existing malaria immunity and threshold pyrogenic parasite density. In a prospective study of children (aged 3 – 7 years) and adults infected with *P. falciparum*, the geometric mean (GM) parasite densities in febrile children were much higher (GM: 17, 277 per μl) than in adults (GM: 881 per μl) (29). In a four-month period longitudinal study in cohorts ranging from one month to 83 year, there was an age-dependent threshold effect during *P. falciparum* infection and the risk of acquiring fever (41). This threshold was the maximum at one year of age (2.45 trophozoites per leukocyte) and a minimum at 60 years of age (0.5 trophozoite per leukocyte) (41). This paradigm of lower pyrogenic-threshold with advancing age is true only in areas of high transmission. In areas of lower endemicity, there is a diminished difference in pyrogenic threshold between children and adults (7, 37). These field studies strongly suggest that repeated parasite exposure leads to the evolution of ‘anti-febrile’ immunity that progressively increases with age.

Malaria toxins and febrile illness. The fact that malaria febrile illness is induced by the parasite products released by rupturing schizonts was recognized as early as 1886 (15). In later years, it was postulated that the toxic products that are responsible for the clinical symptoms of febrile illness are of host-origin. This theory was further strengthened by the subsequent studies showing that key clinical features and cytokine profiles observed during bacterial endotoxemia and acute malarial infection share several common features (11). Certain cytokines such as tumor necrosis factor (TNF), interleukin (IL) 1 β and IL-6 are also shown to be elevated during clinical malaria (12). Furthermore, administration of monoclonal anti-TNF antibodies led to a reduction in febrile illness in children (22). These studies demonstrate that TNF is the primary mediator of malaria fever.

Several parasite factors have been identified as candidate “malaria toxins” that induce malaria fever and are responsible for other aspects of malaria pathogenesis such as upregulation of the host endothelial receptors (45), severe anemia (27), and several physiological disturbances such as acute acidosis and hypoglycemia (10). The most studied malaria toxin for *P. falciparum* is glycosylphosphatidylinositol (GPI), a glycolipid that is a constituent of several surface membrane proteins (44). GPI molecules act on monocytes to produce excess amounts of the cytokines TNF – α and IL – 1 that initiate a systematic inflammatory cascade of events including renal failure, multi-organ inflammation, hypoglycemia, lactic acidosis and death (43). Purified malaria GPIs are also shown to increase the expression of the host adhesion molecules (ICAM, VCAM, and E-selectin) and nitric oxide production in endothelial cells through a cytokine-independent pathway (46). These events could lead to increased binding of infected erythrocytes in the brain vasculature, a process that is considered to be responsible for the pathogenesis of cerebral malaria. In a recent study, *P. falciparum* GPIs, like bacterial lipopolysaccharide (LPS), have been shown to induce apoptosis in vitro and in vital organs in mice (49).

Another major candidate toxin molecule is malaria pigment – hemozoin (Hz) that was first implicated in 1912 as the parasite factor responsible for the malaria paroxysm (9). Although immunologically inert, recent studies suggest that *P. falciparum* Hz can serve as a novel non-DNA ligand for Toll-like receptor (TLR) 9 and activate the innate immune response to produce cytokines, chemokines, and up-regulation of co-stimulatory molecules (13). Another recent study suggests that Hz itself is immunologically inert but facilitates the activation of innate immunity by presenting malaria DNA to TLR-9 (36). It has also been demonstrated that Hz acquired by monocytes leads to a suppression in the production of peripheral blood macrophage migration inhibitory factor that is associated with enhanced severe anemia in African children (2).

Febrile illness and the regulation of parasite development and growth. Several in vitro and in vivo studies suggest that febrile temperatures play an important role in the regulation of parasite density (19, 21, 23). In vitro studies have conclusively demonstrated that cultivation of *P. falciparum* parasites at febrile temperatures adversely affects their development inside erythrocytes with a maximum effect against the mature forms, while ring form parasites are relatively resistant to elevated temperatures (21). In vitro periodic elevations in temperature lead to synchronized parasite growth that raises the possibility that febrile temperatures cause synchronized growth in vivo (17, 21). Synchronized parasite growth might offer a selective advantage by minimizing the cycles of merozoite bursts and thus reducing the massive release of pro-inflammatory cytokines such as TNF- α in a non-immune host.

Neurosyphilis studies suggest that cyclical episodes of febrile illness play a direct role in the regulation of parasite density in vivo. In one such study, a relationship between febrile illness and parasite density was determined during an acute *P. vivax* infection. During a 12 h (8 AM to 8 PM) phase of malaria paroxysm, parasite density rose from 8,300 per cu. mm at 9 AM to a peak of over 21,000 during the rigor (chill phase) and then gradually dropped to 10,870 at 8 PM (19). Based on this observation, it is reasonable to infer that the febrile episode during the malaria paroxysm was responsible for reduction in total parasite burden observed at the end of the 12 h observation period. Together these in vitro and in vivo studies clearly demonstrate that febrile temperatures are deleterious for the development of malaria parasites. It is highly possible that febrile illness-mediated death of malaria parasites is an evolutionary advantage whereby regulation of parasite density permits host survival and thereby allows sufficient time for further parasite transmission. Exposure of *P. falciparum* parasites to febrile temperatures also triggers the process of gametocytogenesis (1), a step essential for parasite survival.

Febrile temperatures and parasite virulence factors. Elevated body temperature is a natural response to invading pathogens including viral, bacterial and parasitic infections. A well-studied adaptive response to elevation in the host temperature is the heat shock response that involves increased expression of several proteins including chaperones, proteases, sigma factors and other regulatory and structural proteins (16). Induction of the heat shock proteins has a wide ranging effect on both the pathogen and its host. In bacteria, the heat shock response improves the ability to endure environmental changes including thermotolerance, salt tolerance, and tolerance to heavy metals (18, 20, 24, 48). Proteins induced by the heat shock response are required for the virulence of several bacteria. For example, heat shock proteins facilitate the binding of *Salmonella typhimurium* to mucosal cells (14) and chaperone 10 is responsible for the osteolytic activity of *Mycobacterium tuberculosis* in Pott's diseases (26). A temperature shift of 2°C in the host has been shown to restrict the growth of *Haemophilus influenzae* (34) thus demonstrating temperature regulated in vivo growth of a pathogenic bacterium.

In *P. falciparum*, elevated temperature conditions are known to induce the expression of a variety of heat shock proteins and virulence factors. Among these, the most characterized proteins (HSP60, HSP70 and HSP90) are expressed during the intra-erythrocytic stages of parasite development (3). In higher eukaryotes, HSP90 is a multi-complex chaperone, that in conjunction with HSP60 and HSP70, facilitates folding of newly synthesized proteins and is involved in the regulation of cell cycle and development (30, 31, 38). In line with its important role in other eukaryotes, HSP90 function is found to be essential for the growth of intra-erythrocytic *P. falciparum* parasites (3). HSP90, in conjunction with HSP70 and other accessory proteins, was found to facilitate not only protein folding but also control the activities of transcription factors and protein kinases (3). Due to their highly conserved nature and immunogenicity during natural infection and in experimental models, *Plasmodium* HSPs are also considered good

vaccine targets (32). These observations suggest that, similar to other pathogens, heat shock response proteins play a critical role in the development and survival of malaria parasites and are therefore attractive drug and vaccine targets.

Febrile illness and the pathogenesis of cerebral malaria. The effect of *Plasmodium* infection induced febrile illness on its pathogenesis in the human host is not clear. Nonetheless, it is well known that the characteristic clinical features of malaria fever are experienced only in young children and non-immune adults suggesting that multiple exposures lead to immunity against pyrogenic toxins released by malaria parasites. In *P. falciparum* infections, only early parasite forms (rings) are detected in circulation while the mature forms (trophozoites and schizonts) are known to sequester in deep venules of different vital organs by binding to endothelial cells (including brain) leading to organ dysfunction. Sequestration, mediated by a classical host receptor-parasite ligand process, is considered a sophisticated defense mechanism to avoid parasite clearance by the host spleen and its immune system.

During the erythrocytic stage of development, several parasite proteins are expressed on the surface of host erythrocytes that could serve as ligands in binding to host endothelial cells (28). In *P. falciparum*, one such identified ligand is PfEMP-1 (erythrocyte membrane protein-1), the most characterized malarial virulence protein, which has sequence domains that bind to CD36 (4, 6, 35), ICAM-1 (6) and CSA (39, 40) on endothelial cells. In one study, pretreatment of ring and trophozoite stage *P. falciparum*-infected erythrocytes at 40°C (a febrile temperature) allowed their binding to vascular adherence receptors CD36 and ICAM (47). Parasites treated at 37°C did not bind to these adherence receptors. The authors claimed that this heat-induced cytoadherence was mediated by EMP-1 since heat shock parasites had a higher surface expression of this molecule. Based on these results, they speculated that in an infected naïve host, malaria fever might increase the cytoadherence of infected red cells and thus contribute

towards the pathogenesis of cerebral malaria. This hypothesis could be supported by the observation that use of anti-pyretic drugs slows parasite clearance (8) and thus could exacerbate the effects of malaria pathogenesis. These results raise the possibility that malaria fever is not the benign clinical symptom resulting from *Plasmodium* infection but in fact contributes towards the pathogenesis of cerebral malaria, the most severe syndrome of *P. falciparum* malaria.

REFERENCES

1. **Adedeji, A. A., F. A. Fehintola, B. A. Fateye, T. C. Happi, A. O. Amoo, G. O. Gbotosho, and A. Sowunmi.** 2005. *Plasmodium falciparum* malaria in Nigerian children during high and low transmission seasons: gametocyte carriage and response to oral chloroquine. *J Trop Pediatr* **51**:288-294.
2. **Awandare, G. A., Y. Ouma, C. Ouma, T. Were, R. Otieno, C. C. Keller, G. C. Davenport, J. B. Hittner, J. Vulule, R. Ferrell, J. M. Ong'echa, and D. J. Perkins.** 2007. Role of monocyte-acquired hemozoin in suppression of macrophage migration inhibitory factor in children with severe malarial anemia. *Infect Immun* **75**:201-210.
3. **Banumathy, G., V. Singh, S. R. Pavithra, and U. Tatu.** 2003. Heat shock protein 90 function is essential for *Plasmodium falciparum* growth in human erythrocytes. *J Biol Chem* **278**:18336-18345.
4. **Barnwell, J. W., A. S. Asch, R. L. Nachman, M. Yamaya, M. Aikawa, and P. Ingravallo.** 1989. A human 88-kD membrane glycoprotein (CD36) functions in vitro as a receptor for a cytoadherence ligand on *Plasmodium falciparum*-infected erythrocytes. *J Clin Invest* **84**:765-772.
5. **Becker, F. T.** 1949. *Induced Malaria as a therapeutic agent*, vol. II. W.B. Saunders Company, Philadelphia and London.
6. **Berendt, A. R., D. L. Simmons, J. Tansey, C. I. Newbold, and K. Marsh.** 1989. Intercellular adhesion molecule-1 is an endothelial cell adhesion receptor for *Plasmodium falciparum*. *Nature* **341**:57-59.
7. **Boisier, P., R. Jambou, L. Raharimalala, and J. Roux.** 2002. Relationship between parasite density and fever risk in a community exposed to a low level of malaria transmission in Madagascar highlands. *Am J Trop Med Hyg* **67**:137-140.
8. **Brandts, C. H., M. Ndjave, W. Graninger, and P. G. Kremsner.** 1997. Effect of paracetamol on parasite clearance time in *Plasmodium falciparum* malaria. *Lancet* **350**:704-709.
9. **Brown, W. D.** 1912. Malarial Pigment (Hematin) as a Factor in the Production of the Malarial Paroxysm. *J Exp Med* **15**:579-597.
10. **Clark, I. A., F. M. al Yaman, and L. S. Jacobson.** 1997. The biological basis of malarial disease. *Int J Parasitol* **27**:1237-1249.
11. **Clark, I. A., L. M. Alleva, A. C. Mills, and W. B. Cowden.** 2004. Pathogenesis of malaria and clinically similar conditions. *Clin Microbiol Rev* **17**:509-539, table of contents.
12. **Clark, I. A., and W. B. Cowden.** 2003. The pathophysiology of *falciparum* malaria. *Pharmacol Ther* **99**:221-260.

13. **Coban, C., K. J. Ishii, T. Kawai, H. Hemmi, S. Sato, S. Uematsu, M. Yamamoto, O. Takeuchi, S. Itagaki, N. Kumar, T. Horii, and S. Akira.** 2005. Toll-like receptor 9 mediates innate immune activation by the malaria pigment hemozoin. *J Exp Med* **201**:19-25.
14. **Ensgraber, M., and M. Loos.** 1992. A 66-kilodalton heat shock protein of *Salmonella typhimurium* is responsible for binding of the bacterium to intestinal mucus. *Infect Immun* **60**:3072-3078.
15. **Golgi, C.** 1886. *Ach Sci Med* **10**:109-135.
16. **Gophna, U., and E. Z. Ron.** 2003. Virulence and the heat shock response. *Int J Med Microbiol* **292**:453-461.
17. **Haynes, J. D., J. K. Moch, and D. S. Smoot.** 2002. Erythrocytic malaria growth or invasion inhibition assays with emphasis on suspension culture GIA. *Methods Mol Med* **72**:535-554.
18. **Inbar, O., and E. Z. Ron.** 1993. Induction of cadmium tolerance in *Escherichia coli* K-12. *FEMS Microbiol Lett* **113**:197-200.
19. **Kitchen, S. F.** 1949. *Symptomatology: General Considerations*, vol. 72. Humana Press, Totowa, N.J.
20. **Kusukawa, N., and T. Yura.** 1988. Heat shock protein GroE of *Escherichia coli*: key protective roles against thermal stress. *Genes Dev* **2**:874-882.
21. **Kwiatkowski, D.** 1989. Febrile temperatures can synchronize the growth of *Plasmodium falciparum* *in vitro*. *J Exp Med* **169**:357-361.
22. **Kwiatkowski, D., M. E. Molyneux, S. Stephens, N. Curtis, N. Klein, P. Pointaire, M. Smit, R. Allan, D. R. Brewster, G. E. Grau, and et al.** 1993. Anti-TNF therapy inhibits fever in cerebral malaria. *Q J Med* **86**:91-98.
23. **Kwiatkowski, D., and M. Nowak.** 1991. Periodic and chaotic host-parasite interactions in human malaria. *Proc Natl Acad Sci U S A* **88**:5111-5113.
24. **LaRossa, R. A., and T. K. Van Dyk.** 1991. Physiological roles of the DnaK and GroE stress proteins: catalysts of protein folding or macromolecular sponges? *Mol Microbiol* **5**:529-534.
25. **Long, H. Y., B. Lell, K. Dietz, and P. G. Kremsner.** 2001. *Plasmodium falciparum*: in vitro growth inhibition by febrile temperatures. *Parasitol Res* **87**:553-555.
26. **Meghji, S., P. A. White, S. P. Nair, K. Reddi, K. Heron, B. Henderson, A. Zaliani, G. Fossati, P. Mascagni, J. F. Hunt, M. M. Roberts, and A. R. Coates.** 1997. *Mycobacterium tuberculosis* chaperonin 10 stimulates bone resorption: a potential contributory factor in Pott's disease. *J Exp Med* **186**:1241-1246.
27. **Menendez, C., A. F. Fleming, and P. L. Alonso.** 2000. Malaria-related anaemia. *Parasitol Today* **16**:469-476.
28. **Miller, L. H., D. I. Baruch, K. Marsh, and O. K. Doumbo.** 2002. The pathogenic basis of malaria. *Nature* **415**:673-679.
29. **Miller, M. J.** 1958. Observations on the natural history of malaria in the semi-resistant West African. *Trans R Soc Trop Med Hyg* **52**:152-168.
30. **Nathan, D. F., M. H. Vos, and S. Lindquist.** 1997. In vivo functions of the *Saccharomyces cerevisiae* Hsp90 chaperone. *Proc Natl Acad Sci U S A* **94**:12949-12956.
31. **Neckers, L. M., E., and Schulte, T.W. .** 1998. Stress Proteins: Handbook to Experimental Pharmacology, vol. 136. Springer-Verlag, Heidelberg.
32. **Newport, G. R.** 1991. Heat shock proteins as vaccine candidates. *Semin Immunol* **3**:17-24.

33. **Nicol, W. D., Hutton, E.L.** 1937. Neurosyphilis: its treatment and prophylaxis. *Br J Venereal Dis* **13**:141-166.
34. **O'Reilly, T., and O. Zak.** 1992. Elevated body temperature restricts growth of *Haemophilus influenzae* type b during experimental meningitis. *Infect Immun* **60**:3448-3451.
35. **Oquendo, P., E. Hundt, J. Lawler, and B. Seed.** 1989. CD36 directly mediates cytoadherence of *Plasmodium falciparum* parasitized erythrocytes. *Cell* **58**:95-101.
36. **Parroche, P., F. N. Lauw, N. Goutagny, E. Latz, B. G. Monks, A. Visintin, K. A. Halmen, M. Lamphier, M. Olivier, D. C. Bartholomeu, R. T. Gazzinelli, and D. T. Golenbock.** 2007. Malaria hemozoin is immunologically inert but radically enhances innate responses by presenting malaria DNA to Toll-like receptor 9. *Proc Natl Acad Sci U S A* **104**:1919-1924.
37. **Prybylski, D., A. Khaliq, E. Fox, A. R. Sarwari, and G. T. Strickland.** 1999. Parasite density and malaria morbidity in the Pakistani Punjab. *Am J Trop Med Hyg* **61**:791-801.
38. **Queitsch, C., T. A. Sangster, and S. Lindquist.** 2002. Hsp90 as a capacitor of phenotypic variation. *Nature* **417**:618-624.
39. **Reeder, J. C., A. F. Cowman, K. M. Davern, J. G. Beeson, J. K. Thompson, S. J. Rogerson, and G. V. Brown.** 1999. The adhesion of *Plasmodium falciparum*-infected erythrocytes to chondroitin sulfate A is mediated by *P. falciparum* erythrocyte membrane protein 1. *Proc Natl Acad Sci U S A* **96**:5198-5202.
40. **Rogerson, S. J., S. C. Chaiyaroj, K. Ng, J. C. Reeder, and G. V. Brown.** 1995. Chondroitin sulfate A is a cell surface receptor for *Plasmodium falciparum*-infected erythrocytes. *J Exp Med* **182**:15-20.
41. **Rogier, C., D. Commenges, and J. F. Trape.** 1996. Evidence for an age-dependent pyrogenic threshold of *Plasmodium falciparum* parasitemia in highly endemic populations. *Am J Trop Med Hyg* **54**:613-619.
42. **Ross, R.** 1910. *The Prevention of Malaria*. E.P. Dutton and Co., New York.
43. **Schofield, L., and F. Hackett.** 1993. Signal transduction in host cells by a glycosylphosphatidylinositol toxin of malaria parasites. *J Exp Med* **177**:145-153.
44. **Schofield, L., M. C. Hewitt, K. Evans, M. A. Siomos, and P. H. Seeberger.** 2002. Synthetic GPI as a candidate anti-toxic vaccine in a model of malaria. *Nature* **418**:785-789.
45. **Schofield, L., S. Novakovic, P. Gerold, R. T. Schwarz, M. J. McConville, and S. D. Tachado.** 1996. Glycosylphosphatidylinositol toxin of *Plasmodium* up-regulates intercellular adhesion molecule-1, vascular cell adhesion molecule-1, and E-selectin expression in vascular endothelial cells and increases leukocyte and parasite cytoadherence via tyrosine kinase-dependent signal transduction. *J Immunol* **156**:1886-1896.
46. **Schwarzer, E., H. Kuhn, E. Valente, and P. Arese.** 2003. Malaria-parasitized erythrocytes and hemozoin nonenzymatically generate large amounts of hydroxy fatty acids that inhibit monocyte functions. *Blood* **101**:722-728.
47. **Udomsangpetch, R., B. Pipitaporn, K. Silamut, R. Pinches, S. Kyes, S. Looareesuwan, C. Newbold, and N. J. White.** 2002. Febrile temperatures induce cytoadherence of ring-stage *Plasmodium falciparum*-infected erythrocytes. *Proc Natl Acad Sci U S A* **99**:11825-11829.
48. **Volker, U., H. Mach, R. Schmid, and M. Hecker.** 1992. Stress proteins and cross-protection by heat shock and salt stress in *Bacillus subtilis*. *J Gen Microbiol* **138**:2125-2135.

49. **Wichmann, D., R. T. Schwarz, V. Ruppert, S. Ehrhardt, J. P. Cramer, G. D. Burchard, B. Maisch, and F. Debierre-Grockiego.** 2007. *Plasmodium falciparum* glycosylphosphatidylinositol induces limited apoptosis in liver and spleen mouse tissue. Apoptosis.

Chapter 2

Molecular Factors and Biochemical Pathways Induced by Febrile Temperature in *Plasmodium falciparum* Parasites

Published as: Miranda S. M. Oakley, Sanjai Kumar, Vivek Anantharaman, Hong Zheng, Babita Mahajan, J. David Haynes, J. Kathleen Moch, Rick Fairhurst, Thomas F. McCutchan, and L. Aravind. 2007. Molecular Factors and Biochemical Pathways Induced by Febrile Temperature in Intraerythrocytic *Plasmodium falciparum* Parasites. Infect. Immunity. 75(4): 2012-2025.

Abstract

Intermittent episodes of febrile illness are the most benign and recognized symptom of infection with malaria parasites, although the effect on parasite survival and virulence remains unclear. In this study, we identified the molecular factors altered in response to febrile temperature by measuring differential expression levels of individual genes using high-density oligonucleotide microarray technology and by performing biological assays in asexual-stage *Plasmodium falciparum* parasite cultures incubated at 37°C and 41°C (an elevated temperature that is equivalent to malaria induced febrile illness in the host). Elevated temperature had a profound influence on expression of individual genes; 336 of approximately 5300 genes (6.3% of the genome) had altered expression profiles. Of these, 163 genes (49%) were upregulated by 2 fold or greater, and 173 genes (51%) were downregulated by 2 fold or greater. In-depth sensitive sequence-profile analysis revealed that febrile temperature-induced responses caused significant alterations in the major parasite biologic networks and pathways, and that these changes are well coordinated and intricately linked. One of the most notable transcriptional changes occur in genes encoding proteins containing the predicted Pexel motifs that are exported into the host cytoplasm or inserted into the host cell membrane and are likely to be associated with erythrocyte remodeling and parasite sequestration functions. Using our sensitive computational analysis, we were also able to assign biochemical or biologic functional predictions for at least 100 distinct genes previously annotated as “hypothetical”. We find that cultivation of *P. falciparum* parasites at 41°C leads to parasite death in a time-dependent manner. Presence of the “crisis forms” and the TUNEL-positive parasites following heat treatment strongly supports the notion that an apoptosis-like-cell-death mechanism might be induced in response to febrile temperatures. These studies enhance the possibility for designing vaccines and drugs based on

disruption in molecules and pathways of parasite survival and virulence activated in response to febrile temperatures.

Introduction

Febrile illness is the most common and benign feature of malaria pathogenesis. Historically, malaria has been associated with a unique pattern of cyclical fever, later recognized to coincide with schizont rupture, which varies (depending on the length of the erythrocytic-stage cycle) between *Plasmodium* species (27). The duration of the erythrocytic stage cycle and, hence, pattern of cyclical fever for *Plasmodium falciparum*, *P. vivax*, and *P. ovale* is 48 h, and for *P. malariae*, 72 h.

Febrile illness, defined by an elevated host body temperature, is a common clinical symptom seen in response to distress caused by several pathogens, autoimmune diseases, and many other diseases including cancers (15). In malaria, febrile illness is induced via a poorly defined immunologic mechanism activated by malaria toxins and hemoglobin metabolites released from the ruptured, infected red blood cells (IRBCs) (30). It has been argued that malarial febrile illness is an evolutionary adaptation that benefits both the parasite and its host. Cultivation at febrile temperatures has been shown to inhibit in vitro growth of *P. falciparum* cultures (31). It is possible that during acute malaria infection, elevated host temperature induces a cascade of molecular events that maintain the total parasite burden at a threshold level by limiting its replication rate, allowing host defense mechanisms to activate and mature. Although inhibition of exponential parasite growth caused by febrile temperature may appear to aid only the host, it may also provide the parasite sufficient time to further transmit infection, making it a potential parasite survival strategy.

Notwithstanding the possible beneficial effects of malaria-induced febrile illness, a recent study suggests that fever may, in fact, augment the pathogenesis of malaria by enhancing cytoadherence of parasite IRBCs to CD36 and ICAM-1 molecules that serve as host receptors on endothelial cells (48). The authors found an increased level of the variant antigen erythrocyte

membrane protein-1 (EMP-1) (a parasite ligand that mediates binding to host receptors on endothelial cells) on the surface of ring and trophozoite IRBCs when heated to 40°C, leading them to speculate that the enhanced cytoadherence observed could be due to increased trafficking of EMP-1 to the surface of IRBCs.

In mammalian cells, an increase in temperature can lead to a number of changes within the cell including protein denaturation, transient cell-cycle arrest, and changes in membrane fluidity (4, 12). Heat-shock proteins (HSPs), the primary mediators of the heat-shock response, act as molecular chaperones by preventing aggregation and promoting folding of cellular proteins (41). In humans, HSPs appear to be possible regulators of key apoptotic pathways, and targeting HSPs that interact with the cellular apoptotic machinery is emerging as a novel approach for pharmacologic intervention in cancer (45). To understand the molecular changes that occur and biochemical pathways altered in *P. falciparum* parasites in response to febrile temperatures, we compared the genome-wide gene expression profiles of parasites cultivated at 37°C and 41°C. We used a combination of gene expression data and computational sequence analyses to reconstruct a detailed picture of the response of the parasite to elevated temperature. The use of sensitive sequence profile analysis methods allowed the detection of conserved domains and sequence motifs that are known to greatly assist in elucidating the biologic role of uncharacterized proteins. Furthermore, various forms of contextual information gleaned from comparative genomics, such as presence of lineage-specific gene expansions and gene losses, phyletic profiles and shared gene ontology, also complement the results obtained from direct sequence analysis of the proteins themselves. Accordingly, we carried out in-depth sequence and comparative genomic analyses of all the proteins encoded by the genes showing noticeable changes in response to temperature elevation. We confirmed a subset of the findings, based on transcriptional activation of genes with biologically relevant assays, by measuring the expression

of EMP-1 on the surface of *P. falciparum* IRBCs and by detecting the ubiquitination of total parasite proteins using an anti-ubiquitin antibody. We also investigated whether the febrile temperature induced in vitro killing of *P. falciparum* parasites ((31), and this study) is mediated by apoptosis-like cell death.

The results of our analyses suggest that a number of parasite pathways are strongly altered at the level of gene expression—particularly those involved with protein stability and folding, RNA metabolism, and a significant component of the secretome that is transported from the parasite into the host cell. We also find a positive TUNEL activity in the heat-treated parasites suggesting the existence of apoptosis-like- cell-death mechanism in blood-form malaria parasites. We believe that the identification of heat-inducible parasite factors and biochemical pathways that contribute to the regulation of parasite density, and potentially influence their virulence in a non-immune host, could lead to new antimalarial drug and vaccine targets.

Material and Methods

Parasites. The 3D7 strain of *Plasmodium falciparum* was cultured according to the procedures used in our laboratory (47). Briefly, parasites were cultured in modified RPMI-1640 with 25 mM HEPES equilibrated with 5% CO₂ 5% O₂ 90% N₂ and containing 10% pooled heat-inactivated human-type O+ serum (obtained commercially) and human type O+ RBCs from blood. The blood was collected in CPDA bags, filtered to remove leukocytes, and handled as a biological hazardous substance. Cultures were maintained in suspension at 2.5% to 5% hematocrit with 0.02% to 5% of the RBCs infected by parasites. For growth inhibition studies, parasites were synchronized using a temperature cycling incubator as described by Haynes et al (19).

Parasite survival studies. The effect of febrile temperature on parasite survival was evaluated in both synchronous and asynchronous cultures of *P. falciparum*. Parasite cultures with an initial parasitemia of 3% and hematocrit of 2.5% were grown at either 37°C or 41°C for 48 h in a final volume of 10 ml. Over the course of the experiment, parasitemias were enumerated from Giemsa-stained thin blood films prepared at 2, 8, 16, 24, 32, 40 and 48 h time points. Experiments were replicated three times for synchronous cultures and two times for asynchronous cultures. Temperature-dependent survival rate at each time point was defined as follows: parasitemia at 41°C/ parasitemia at 37°C.

TUNEL assay. For monitoring apoptosis, terminal-deoxy-nucleotidyl-transferase-mediated dUTP-biotin nick end labeling (TUNEL) assay (In Situ Cell Death Detection Kit, Roche Diagnostic Incorporation, Indianapolis, IL) was used. *P. falciparum* schizont stage parasites were cultured at 37°C and 41°C for two h. The air dried blood films were fixed for one hour in freshly prepared fixative (4% paraformaldehyde in PBS, pH 7.4). The slides were rinsed with PBS and incubated with permeabilisation solution (0.1 % Triton X-100 in 0.1% sodium

citrate dihydrate) for 2 min on ice. The positive controls slides were treated with DNase I (300 U/ml in 50 mM Tris-HCl, pH 7.5, 2 mg/ml BSA) for 10 min. The slides were washed twice with PBS and 50 µl of TUNEL reaction mixture was added on to the slides. The slides were incubated for 60 min at 37°C in a humidified atmosphere in the dark. The slides were rinsed thrice with PBS for 5 min each and were mounted using VectaShield mounting media for fluorescence (Vector Laboratories Inc., Burlingame, CA). The images were viewed in a Zeiss Axioplan II Imaging microscope. Images were transferred to PC version of Adobe Photoshop 5.5 for labeling and printing.

Heat-shock treatment of parasites and RNA preparation. A seed culture of asynchronous *P. falciparum* parasites at approximately 3% parasitemia was divided into two flasks, and parasites were grown at either 37°C or 41°C in a final volume of 50 ml. After two hours of incubation, total RNA was isolated from parasite cultures by saponin lysis of RBCs, followed by RNA extraction with Trizol. RNA quantity was determined by optical densitometry, and its quality was evaluated by agarose gel electrophoresis. Microarray expression profiles were determined from RNA samples isolated in five independent experiments.

Microarray expression analysis. The effect of febrile temperature on parasite global gene expression was examined in *P. falciparum* cultures by cDNA microarray expression analysis. Labeled target was synthesized from 30 µg of RNA extracted from parasites incubated at 37°C and 41°C for two hours. Briefly, cDNA was labeled with 50 nmol of dUTP-cy3 or dUTP-cy5 during a reverse transcription reaction at 42°C for 90 min in a sample mixture containing 300 mM DTT, 15 mM each of dATP, dCTP, dGTP, and dTTP, mixture of polyT and random hexamer primers and 300 U Superscript II. After incorporation of label, RNA was degraded by the addition of NaOH, and labeled cDNA was purified and concentrated by ultrafiltration through a vivaspin 500 column (VivaScience, now Sartorius, Goettingen,

Germany). Labeled cDNA was then hybridized to a *P. falciparum* oligonucleotide chip containing 6168 70 base probes printed in duplicate (Qiagen, Valencia, CA), and the slide was scanned by a GenePix microarray scanner. Microarray data was analyzed with GenePix Pro 4.0 software (Axon Instruments, Inc. Union City, CA), filtered using the NIAID microarray database tools (<http://madb-niaid.cit.nih.gov>), and extracted spots were normalized to the precalculated 50th percentile (median). The criterion for an altered gene expression in an individual gene induced by febrile temperature was defined as a 2-fold or greater increase (upregulation) or decrease (downregulation) and a cut-off p value of <0.05 by two-tailed Student t-test in at least 4 of 5 biological replicates.

Real-time PCR. To confirm microarray data, a small subset of genes varying in abundance (upregulation or downregulation) by array was quantified using real-time PCR. Primers (20-23 bp) with a T_m of 55-60°C were designed to yield a 90-150 bp product containing an exon/intron boundary. Total RNA (2 µg) was treated with 1 U of RNase free DNase I (Invitrogen, San Diego, Calif), and synthesis of cDNA was performed for 50 min at 42°C using 50 U of reverse transcriptase (superscript II, Invitrogen), 100 mM of MgCl₂, 40 U of RNaseOUT (Invitrogen), 200 mM of DTT, 10 mM of dNTP mix and random hexamer primers. The reaction was then subjected to RNase-H treatment with 2 U of enzyme for 20 min at 37°C. Real-time quantitative PCR was performed in a 20 µl reaction volume containing 10 µl of a dilution of cDNA preparation, 2 µl of FastStart DNA Master SYBR Green I (Roche, Nutley, NJ) and 10 µM of gene-specific primers. Amplification and detection of specific product were performed with the MX4000 LightCycler with the following cycle profile: one cycle at 95°C for 2 min, 40 cycles with 30 s denaturation at 95°C and 1 min annealing-elongation at 60°C. A standard curve derived from 10-fold serial dilutions of purified PCR products of the target gene was used to determine absolute concentration of target RNA/DNA.

Gene annotation, ontology and identification of biological pathways. The non-redundant (NR) database of protein sequences (National Center for Biotechnology Information, NIH, Bethesda, MD) was searched using the BLASTP program. All large scale BLAST searches were run using a parallelized version of the BLASTP program running on 1250 compute nodes of the NIH Biowulf cluster. Profile searches were conducted using the PSI-BLAST program (1) with either a single sequence or an alignment used as the query, with a default profile inclusion expectation (E) value threshold of 0.01 (unless specified otherwise), and was iterated until convergence. For all searches involving membrane-spanning domains or low complexity sequences, we used a statistical correction for compositional bias to reduce false positives due to the general hydrophobicity of these proteins. Hidden Markov Models (HMMs) were built from alignments using the *hmmbuild* program and searches were carried out using the *hmmsearch* program from the HMMer package (10). Multiple alignments were constructed using the T_Coffee program (36) followed by manual correction based on the PSI-BLAST results. A library of a large set of alignments of conserved protein domains including those from the PFAM database (<http://www.sanger.ac.uk/Software/Pfam/index.shtml>) as well as an additional set of unpublished conserved domains was used for domain searches with the HMMER package (HMMs) or with PSI-BLAST (PSSM - position-specific score matrices). Signal peptides were predicted using the SignalP program (www.cbs.dtu.dk/services/SignalP-2.0/). Multiple alignments of the N-terminal regions of proteins were used additionally to verify the presence of a conserved signal peptide, and only those signal peptides that were conserved across orthologous groups of proteins were considered as true positives. Transmembrane regions were predicted in individual proteins using the TMPRED, TMHMM2.0 and TOPRED1.0 programs with default parameters (21, 28). For TOPRED1.0, the organism parameter was set to “eukaryote” (<http://bioweb.pasteur.fr/seqanal/interfaces/toppred.html>). All large-scale sequence

analysis procedures were carried out using the TASS package (S. Balaji, V. Anantharaman, L.A., unpublished). The recently reported *Plasmodium*-specific motif for protein export into the host cells, the Pexel motif, was detected using a HMM, constructed using the alignment of the *bona fide* Pexel containing proteins. The proteins encoded by the genes affected by elevated temperature were searched with this HMM and constrained by position towards the N-terminal of the polypeptide and confirmed by further searching for an upstream hydrophobic signal. Secondary structure predictions based on multiple alignments were carried out using the Jpred2 program (6).

Similarity-based clustering of proteins was carried out using the BLASTCLUST program (<ftp://ftp.ncbi.nih.gov/blast/documents/blastclust.txt>). Phylogenetic analysis was carried out using the maximum-likelihood, neighbor-joining and least-squares methods. Briefly, this process involved the construction of a least-squares tree using the FITCH program or a neighbor-joining tree using the NEIGHBOR program (both from the Phylip package), followed by local rearrangement using the Protml program of the Molphy package to arrive at the maximum likelihood (ML) tree (13, 18). The statistical significance of various nodes of this ML tree was assessed using the relative estimate of logarithmic likelihood bootstrap (Protml REL-LL-BP), with 10,000 replicates. All large-scale sequence and structure analysis procedures were carried out using the TASS package, which operates similarly to the SEALS package (S. Balaji, V. Anantharaman, LMI, LA unpublished). Text versions of all alignments reported in this study can be downloaded from: (ftp://ftp.ncbi.nih.gov/pub/aravind/plasmodium_aln.txt).

Flow cytometry. Mouse polyclonal antiserum (kindly provided by Dr. Morris O. Makobongo) was raised against an externalized segment (CIDR1) of EMP-1 expressed by the 3D7.41 parasite line. Approximately 1×10^6 erythrocytes at 1% parasitemia were stained with antiserum at various dilutions (1:200, 1:400, 1:800, and 1:1600) in PBS containing 2% fetal calf

serum for 45 minutes at 25°C and then washed. Bound antibody was detected using Alexa 488-conjugated anti-mouse IgG (Molecular Probes, Carlsbad, Calif.). Parasitized erythrocytes were stained with ethidium bromide (2 µg/mL) for 30 min. A FACSort instrument (Becton-Dickinson, San Jose, Calif.) and FlowJo software were used to acquire 500,000 events from each sample and to determine the median fluorescence intensity of populations of antibody-reactive, parasitized erythrocytes.

Ubiquitin bioassay. Total ubiquitination of parasite proteins was assayed by western blot after growth of *P. falciparum* 3D7 parasites (5% initial parasitemia and 5% hematocrit) at 37°C 2 h or 41°C 2 h. After incubation, erythrocytes were lysed with saponin and parasite protein was then extracted and washed with M-PER Protein Extraction Reagent (Pierce 78503). Total parasite protein (5 µg) was loaded per well, and ubiquitination of proteins was detected and quantitated using a rabbit anti-ubiquitin antibody (Pierce 89899) and a commercially obtained chemiluminescence-linked western blot kit (Western Light Tropic, Bedford, Mass.).

Results and Discussion

Effect of febrile temperature on the survival of *P. falciparum* parasites. During the course of an acute *P. falciparum* infection, elevated temperatures as high as 41°C that last between 2-6 h are experienced in children and non-immune adults. The malaria paroxysm is generally known to occur between the cycles of schizont rupture and persists for several hours. The rupture of malaria schizonts is known to release toxins such as hemozoin pigments and glycerophosphoinositol anchor moieties. These toxins activate the host monocytes to release TNF- α , a major fever-inducing cytokine during malaria infection (29, 49).

We studied the effect of febrile temperature on the survival of synchronous and asynchronous asexual erythrocytic stage cultures of *P. falciparum* parasites by comparing the survival rate of parasites grown at 37°C and 41°C over the period of 48 h. Our results show that elevated temperature had a deleterious effect on parasite survival in both synchronous and asynchronous cultures. In synchronous ring stage cultures, in relation to survival at 37°C, following 2, 8, 16, and 24 h of cultivation at 41°C, parasite survival was reduced by 25%, 60%, 95%, and 88% respectively (FIG. 3). Thirty-two hours of cultivation at 41°C caused elimination of 100% of cultured *P. falciparum* parasites. In asynchronous cultures, following 2 and 8 hours of cultivation at 41°C, parasite survival was reduced by 23% and 66%, respectively, and 16 h of cultivation at febrile temperature resulted in the death of 100% of cultured parasites (FIG. 3). The prolonged survival of synchronous cultures can be attributed to the fact that the starting cultures were solely comprised of ring stage parasites that have been shown to be less susceptible to cultivation at elevated temperature than the mature forms (29).

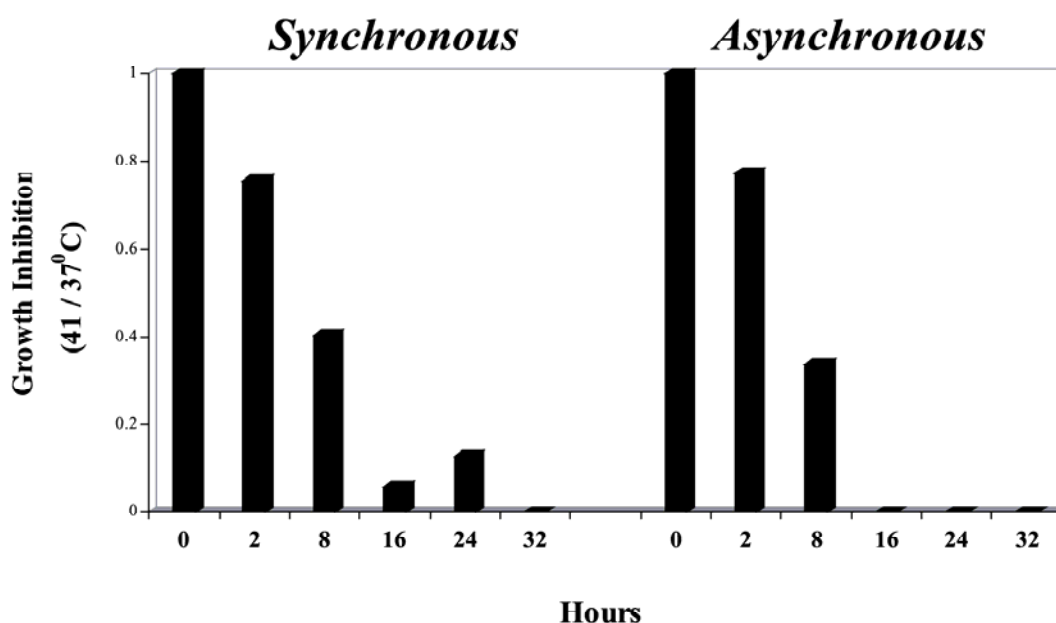


Figure 3. The effect of febrile temperature on the survival of asexual erythrocytic stage synchronous and asynchronous cultures of *Plasmodium falciparum*. Parasite survival rate, defined as parasitemia at 41°C divided by parasitemia at 37°C, was determined over a period of 48 hours.

To further explore the effect of febrile temperatures on stage-specific killing of blood form parasites, we examined the Giemsa-stained *P. falciparum* blood films for the presence of pyknotic “crisis forms” that give the appearance of parasites undergoing death. Morphological analysis of different developmental stages treated at 41°C by light microscopy revealed the distinct presence of “crisis form” trophozoites and schizonts while rings appear to be immune to heat-induced destruction. However, numbers and morphological appearance of “crisis forms” was significantly more evident following 4 h treatment at 41°C (data not shown). Previously, “crisis forms” of trophozoites and schizonts have been described in *P. falciparum* cultures undergoing death induced by treatment with anti-malaria drugs and other experimentally induced forms of stress (7, 38). It is important to note that the presence of “crisis forms” has been

ascribed as a marker of apoptotic cell death in malaria parasites (7). These results are in agreement with an earlier report showing an inhibitory effect of temperatures characteristic of the malaria paroxysm on in vitro parasite growth (29, 31) and suggest that the malaria paroxysm plays a significant role in limiting the exponential growth of parasites in a non-immune host.

To understand the mechanism of febrile temperature induced death in *P. falciparum* parasites, we performed the *in situ* terminal-deoxy-nucleotidyl-transferase-mediated dUTP-biotin nick end labeling (TUNEL) assay in segmented *P. falciparum* schizonts cultivated at 37°C and following a 2 hr heat shock at 41°C. The TUNEL assay is widely used as a marker for apoptotic cell death in eukaryotic cells. Our results show a strong TUNEL-activity in 41°C cultured parasites (FIG. 4A). By counting the number of fluorescent-positive cells, we find that approximately 60% of all infected red cells were TUNEL-positive. In comparison, barely detectable reactivity was observed in parasites cultured at 37°C (FIG. 4B). In fact, the intensity of fluorescence signal in 41°C cultured parasites almost reached the level seen in DNase treated cells that serve as positive control. The existence of TUNEL-positive reaction in liver forms and mid-gut stages is well documented (16, 23). While our results clearly demonstrate a TUNEL-positive assay, existence of TUNEL-reactivity in blood forms of malaria parasites has been a subject of controversy. In a recent review article, Deponte and Becker reported TUNEL-activity in *P. falciparum* blood stage schizonts treated with anti-malaria drugs and H₂O₂ (7). Other studies have failed to detect a TUNEL-positive assay in *P. falciparum* parasites treated *in vitro* with known anti-malarial drugs (38, 39). Taken together, presence of “crisis forms” and TUNEL-positive parasites suggests that febrile temperature induced parasites killing is mediated by the mechanism of apoptotic cell death. However, further studies demonstrating the presence of additional markers of apoptotic cell death in heat shocked parasites will be needed to firmly establish this conclusion.

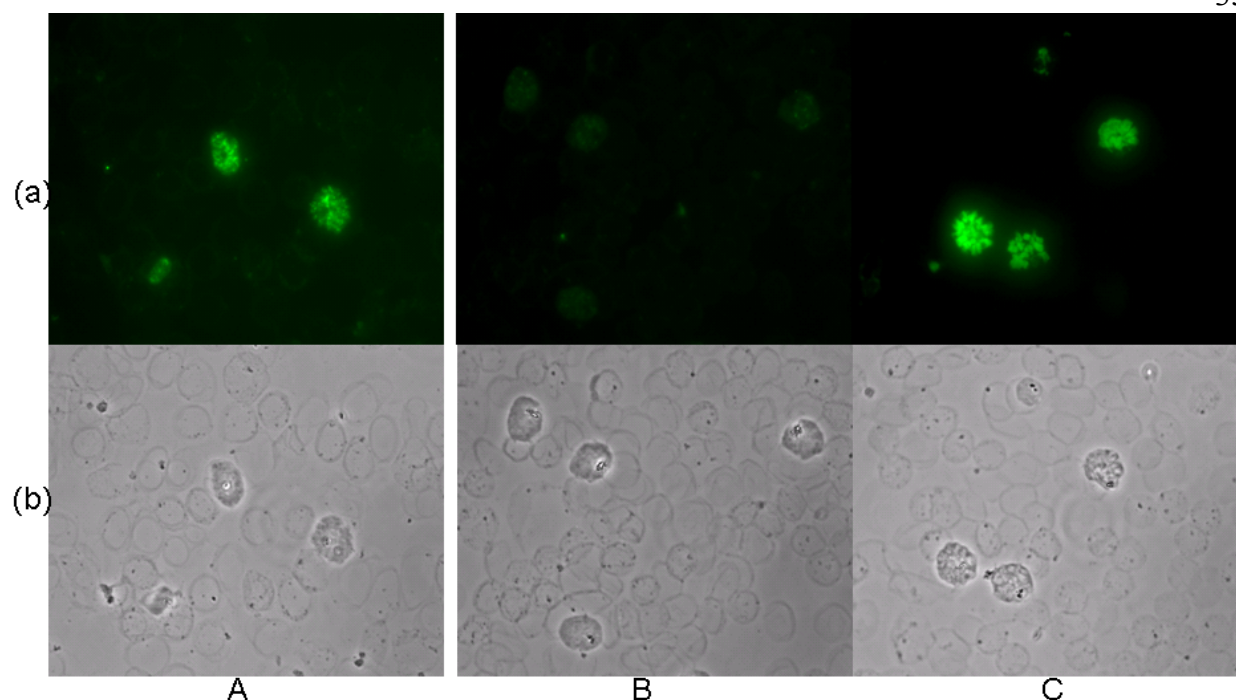


Figure 4. Evidence of *in situ* DNA fragmentation as monitored by TUNEL assay in *P.*

falciparum blood form schizonts following the exposure to febrile temperature. (A) *P.*

falciparum parasites cultured at 41 °C for two h, (B) *P. falciparum* parasites cultured at 37°C for two h, and (C) *P. falciparum* parasites treated with DNase I used as a positive control.

Panel (a) are the parasites stained with TUNEL reaction mixture, and Panel (b) are the phase contrast images of the same fields.

Measuring febrile temperature-induced alterations in the expression profile of

***P. falciparum*.** The molecular factors and biologic pathways triggered in response to febrile illness during a malaria infection are not known. We compared the global gene expression profiles in *P. falciparum* parasites cultivated at 37°C and after heat induction at 41°C for 2 h. A 2 h heat-induction period was selected based on the following reasons. First, during a primary malaria infection, the duration of febrile illness in patients typically lasts between 2–6 h. Second, in our studies, we found that a 2 h heat exposure had a minimal effect on the parasite growth and

morphology and allowed for the preparation of high quality RNA. Asynchronous *P. falciparum* parasites at approximately 3% parasitemia were incubated at 37°C and 41°C for 2 h, and parasite RNA samples were prepared. To measure temperature-induced differential global gene transcription, cy3- and cy5-labeled cDNA probes were prepared by reverse transcription of the isolated total RNA samples. The labeled probes were hybridized to a *P. falciparum* oligonucleotide microarray representing 6168 open reading frames. To ascertain that the transcription levels determined were the true measure of gene expression and not artifacts introduced by experimental variations, we performed microarray hybridizations with RNA samples isolated in five independent experiments. An altered expression response was defined as more than a 2-fold increase (upregulation) or a 2-fold decrease (downregulation) in the individual gene expression measured in response to heat induction and a cut-off p value of <0.05 by two-tailed Student t-test. Our input data were 5 arrays, and gene expression was considered altered only if this criterion was met in at least 4 of 5 microarray experiments. By this criterion, in the 6168 oligonucleotide array, 772 genes were excluded for being present in less than four of five arrays, and 4976 genes were excluded for having an (unaltered) fold change ratio between .5 and 2 in at least two arrays. A total of 46 arrayed sequences were excluded because they did not correspond to any assigned gene in the currently submitted release of the *Plasmodium* genes in the GenBank database.

We find that, of approximately 5300 *P. falciparum* genes analyzed, 337 protein-coding genes consistently show noticeably altered expression patterns in response to elevated temperature, with approximately equal numbers of genes being transcriptionally upregulated (49%) and downregulated (51%) (Table 1). Of these 337 genes, 208 genes were annotated as “hypothetical proteins” in the *P. falciparum* genome database.

TABLE 1. Febrile temperature induced alterations in the *P. falciparum* genome and assigned biologic function

Category	Genes _{total}	Genes _{up}	Genes _{down}
Stress Response/ Protein Stability	22	15	7
DNA Repair/Replication	6	2	4
Chromatin/Basal Transcription	10	8	2
RNA Processing	19	17	2
Translation	18	4	14
Ubiquitin-Proteasome Pathway	10	0	10
Secretion/Protein Trafficking System	10	0	10
Glycosylation/GPI-anchors	6	1	5
Signal Transduction	10	8	2
Cytoskeleton	5	4	1
Lipid/ Fatty Acid/Isoprenid metabolism	14	6	8
Known Transporters	7	0	7
Cell Surface and Adhesion	28	24	4
Basic Metabolism	14	4	10
Miscellaneous	30	9	21
Apicomplexa Specific	8	3	5
<i>Plasmodium</i> Specific	72	26	46
<i>P. falciparum</i> Specific	7	6	1
Low Complexity	21	19	2
No hits	19	7	12
Total	336	163	173

Six genes with altered expression profiles were randomly selected for additional analysis by real-time PCR to verify that the changes in mRNA abundance observed by microarray were true measures of febrile temperature-induced alterations of expression and not experimental artifacts of microarray chip analysis. Measurements of changes in mRNA abundance by real-time PCR for heat-shock 70 kDa protein (7.42), protein with DNAJ domain (6.05), rifin (2.13), acyl carrier protein (-2.80), ribosomal protein L20 (-1.69), and UDP-galactose transporter (-2.69) are in general accordance with our microarray results: heat-shock 70 kDa protein (5.29), protein with DNAJ domain (9.51), rifin (4.38), acyl carrier protein (-2.96), ribosomal protein L20 (-2.9), and UDP-galactose transporter (-4.34).

To determine if there was a relationship between the individual mRNA levels and protein expression, we compared the levels of PfHSP-70 in asynchronous *P. falciparum* parasites cultivated at 37⁰C and 41⁰C. Protein levels were measured as intensity of specific-antibody reactive bands in ECL-based semi-quantitative assays. By the immuno-precipitation assay, for PfHSP-70 at 37⁰C and 41⁰C, integrated optical densities (IOD) values of 507 and 1894 (a 3.7-fold change) were obtained (FIG. 5A); corresponding change in RNA transcription by microarray was 7.4-fold. By western blot, for chitinase (FIG. 5B), the IOD values at 37⁰C and 41⁰C were 371 and 660 (a 1.8-fold change) while a 3.1-fold change in RNA level was observed by microarray. These results demonstrate a close concordance between the febrile temperature-induced alterations in mRNA levels and the resultant protein expression.

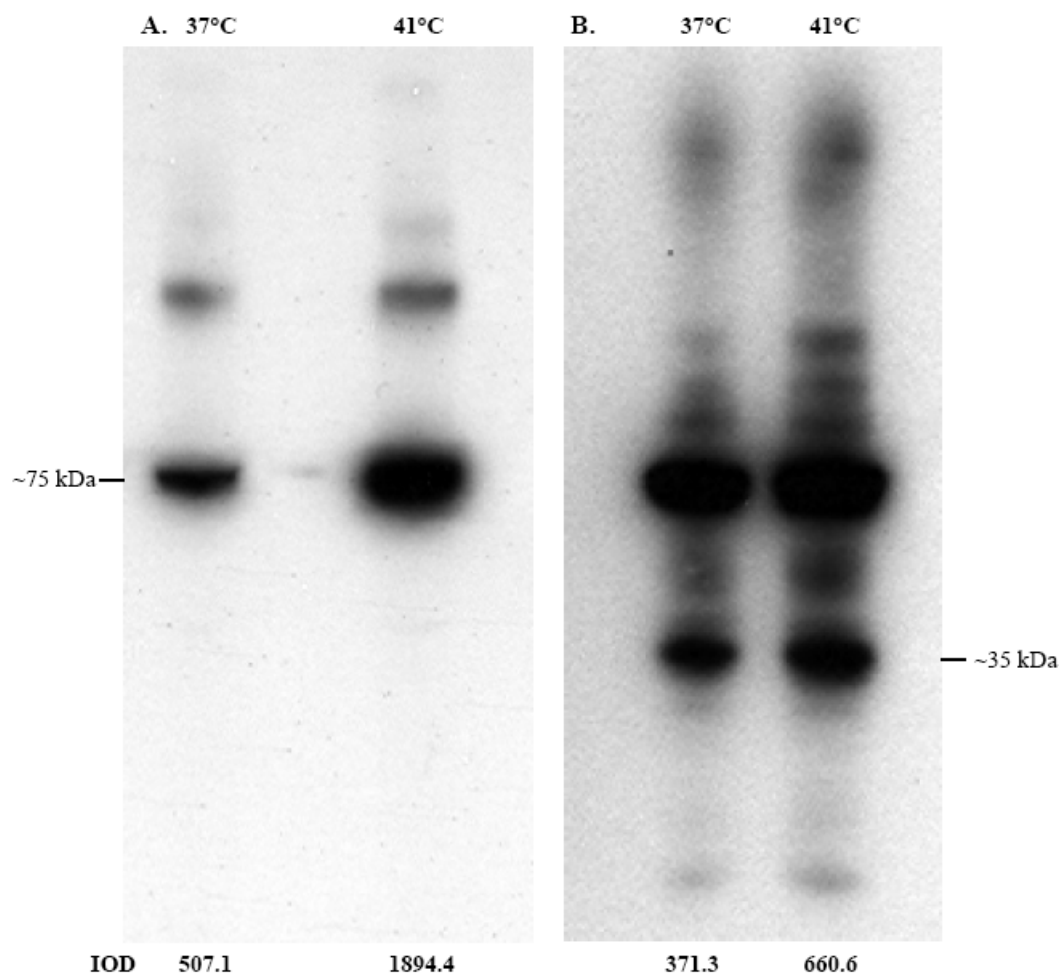


Figure 5. Effect of febrile temperature on expression of HSP-70 (A) and chitinase (B) parasite proteins. HSP-70 protein expression was measured by immunoprecipitation, and chitinase protein expression was measured by western blot analysis following incubation for 2 h. Integrated optical densities (IOD) for each lane were measured using Meta Morph 6.1 software.

Annotation of febrile temperature-regulated hypothetical malarial genes. To better understand the functional role of these genes during febrile illness, and to improve the quality of annotations in the malaria genome database, we analyzed these genes by using sequence analysis techniques (see Methods for details). As a result, we were able to detect conserved protein domains in 101 of these “hypothetical proteins”, annotate them, and consequently make new

functional predictions at differing levels of detail (Table S1). Of the remaining set, 76 showed conserved regions that were restricted to other *Plasmodium* species or other apicomplexans like *Theileria*. Another 28 proteins of the remaining set seemed to be entirely composed of low-complexity regions and seemed not to have any significant hits to other proteins in the non-redundant protein database. A list of the newly annotated genes and their assigned functional/structural predictions is available in the supplemental data (Table S1).

Biologic characteristics of the febrile temperature-regulated genes. To obtain a specific representation of the cellular systems that might be altered in response to temperature stress, we systematically analyzed all the proteins encoded by the responding genes and classified them into specific biologic functional classes based on the presence of conserved motifs and the pathways to which their orthologs belong (Tables 1 and 2). Several striking changes were seen across different functional classes, and we discuss the transcriptional changes in terms of these specific biologic classes below.

TABLE 2. Biologic functions in a subset of genes in our dataset regulated by febrile temperature

Function ¹	Gene Name	Accession No.	Average Fold Δ^2
Stress Response/ Protein Stability	protein with DNAJ domain (resa-like)	PFL0055c	9.5
	heat shock 70 kDa protein	PF08_0054	5.3
	ring-infected erythrocyte surface antigen 2	PF11_0512	3.6
	protein with DNAJ domain, dnj1/sis1 family	PFA0660w	3.4
	<i>P. falciparum</i> RESA-like protein with DnaJ domain	PFA0675w	3.3
	serine protease	MAL8P1.126	2.5
	heat shock protein 86	PF07_0029	2.4
	gamma-glutamylcysteine synthetase	PFI0925w	2.3
	Leu/Phe-tRNA protein transferase	PFB0585w	-2.6
	ATP-dependent CLP protease	PFC0310c	-2.6
	peptidyl-prolyl cis-trans isomerase precursor	PF08_0121	-2.8
	methionine aminopeptidase	MAL8P1.140	-3.6
DNA Repair/ Replication	helicase	PF10_0369	2.8
	DNA mismatch repair protein Msh2p	PF14_0254	-2.3
	replication factor C subunit 5	PF11_0117	-2.6
Chromosome/ Basal Transcription	histone H2B	PF11_0062	2.5
	transcriptional regulatory protein sir2 hom.	PF13_0152	2.4
	histone H4	PF11_0061	1.9
	CCAAT-box DNA binding protein subunit B	PF11_0477	-2.8
RNA Processing	small nuclear ribonucleoprotein polypeptide g, 65009- 64161	MAL8P1.48	5.5
	zinc finger protein	PFE1245w	4.5
	mago nashi protein homolog	MAL7P1.139	-2.1
Ubiquitin Proteasome Pathway	ubiquitin carboxyl-terminal hydrolase	PFE1355c	-2.4
	ubiquitin carboxyl-terminal hydrolase	PF14_0576	-2.3
	proteasome precursor	PFI1545c	-2.5
	ubiquitin-protein ligase	PFC0845c	-2.7
	skp1 family protein	MAL13P1.337	-2.7
	proteasome subunit alpha type 5	PF07_0112	-2.9
	proteasome subunit	MAL13P1.270	-3
Secretion/ Protein Trafficking System	translocation protein sec62	PF14_0361	-2.1
	vacuolar protein sorting 29	PF14_0064	-2.2
	ras family GTP-ase	PFI0155c	-2.4
	G-protein coupled receptor	PFE1265w	-2.4
	Rab5B protein	PF13_0057	-2.4

	protein disulfide isomerase related protein	PF11_0352	-2.7
	signal peptidase	MAL13P1.167	-2.8
	transmembrane protein Tmp21 homologue	MAL13P1.171	-2.9
	signal peptidase	PFI0215c	-3.2
	ADP-ribosylation factor-like protein	PF10_0337	-4.4
Glycosylation/ GPI-Anchors	chitinase	PFL2510w	3
	GPI8p transamidase	PF11_0298	-3.2
Signal Transduction	<i>Plasmodium falciparum</i> trophozoite antigen r45-like protein	PFD1175w	3.7
	calcium dependent protein kinase	PFC0420w	3.4
	Ser/Thr protein kinase	PF14_0423	3.3
	serine/threonine protein kinase	PFA0380w	3.0
	serine/threonine protein kinase	PFC0060c	2.1
	calmodulin	PF14_0323	-1.9
	protein kinase	MAL13P1.196	-2.0
Cytoskeleton	tubulin	PF14_0725	3.4
	dynein Heavy Chain	MAL7P1.162	2.6
	actin-depolymerizing factor	PF13_0326	-2.3
Known Transporters	transporter	PFC0725c	-2.2
	nucleoside transporter	MAL8P1.32	-2.5
	vacuolar ATP synthase subunit g	PF13_0130	-2.6
	vacuolar ATP synthase subunit F	PF11_0412	-2.8
	triose or hexose phosphate / phosphate translocator	PFE0410w	-3.2
	UDP-galactose transporter	PF11_0141	-4.3
Cell Surface and Adhesion	EMP1 (5)		2.6 to 3
	rifins (12)		2.3 to 8.2
	glycophorin Binding Related Antigen	PF14_0010	5.6
	MAEBL	PF11_0486	2.5
	MSP7-like Protein	PF13_0193	2.4
	rhopty associated protein	PFE0075c	-2
	CLAG	PFI1730w	-2.5
	RAP2	PFE0080c	-2.5
	MSP7-like protein	MAL13P1.174	-3.9

¹ Biologic function assigned by PlasmoDB

² Average Fold Δ was calculated from 5 independent microarray experiments. For a complete list of genes in our dataset and their annotation by our group, see Table S1 in the supplemental data

Trafficking. About 47% of the genes that show altered transcription are predicted to be either transmembrane or secreted proteins, suggesting that a major component of the transcriptional response to temperature is directed at altering the cell-surface and/or interactions with the host. About 22% (75 proteins) of the transcriptionally altered genes are predicted to contain the recently described Pexel motif or host target signal (consensus R/KxLxE/Q) (20, 33). The Pexel motif has been demonstrated to serve as a key signal for protein export into the erythrocytes, and such exported proteins are known to reside either in the host cytoplasm or the host membrane. In *P. falciparum*, 400 proteins (8% of the genome) are predicted to contain the putative Pexel motif. Of these, 225 proteins are identified as virulence proteins, and 160 are thought to be involved in the remodeling of the host erythrocyte (33). Pexel motifs are fairly reliably detected, especially if constrained with the condition requiring them to be closely associated with a signal peptide, and show a more extended general amino acid compositional similarity around the motif. Furthermore, for several of the proteins with confidently identified Pexel motifs, e.g., the Rifins, Pfemp1, Psurf 4.2, some R45-like kinases and RESA-like DnaJ domain proteins, there is prior evidence for host targeting, supporting the predictive value of this motif (20, 33, 52). Nonetheless, further experimental evidence presented by additional molecules containing the Pexel motifs should fully authenticate the validity of the “Pexel motif rule.”

In our studies, 72% of the proteins (54 of 75) with reliably predicted Pexel motifs encoded by the temperature-affected genes are upregulated, suggesting that there is a major extrusion of proteins into the host cytoplasm or membrane upon temperature elevation. The most prominent group of genes encoding Pexel motif-containing proteins in our dataset are the rifins. Several of the uncharacterized Pexel motif containing proteins that show altered expression levels are *Plasmodium*-specific predicted-membrane proteins with large, low complexity

segments and might be involved in remodeling the erythrocyte and mediating interactions with the host, such as cytoadherence-mediated immune evasion. These results suggest that febrile illness conditions result in the *en masse* upregulation of proteins that might contribute toward parasite-host interactions and cause necessary modifications in the host-cell membrane to facilitate parasite sequestration.

Febrile illness and cerebral malaria: the role of EMP-1. The effect of febrile illness on malaria pathogenesis is not well understood. A generalized upregulation in the expression of genes that are identified as virulence factors and potential erythrocyte remodeling proteins strongly suggest that febrile illness directly affects malaria pathogenesis. In this regard, we paid especial attention to EMP-1, the most studied virulence protein of *P. falciparum*. We find that in 4 of 5 microarray experiments, there was a consistent upregulation in the expression of 5 *var* genes (average fold change 2.8, range 2.6–3.0). Among these, 4 *var* transcripts encode full-length *var* proteins, and one of the transcripts is a truncated transcript (specifying only 88 aa of the *var* protein) and could have a regulatory role. How elevated temperature upregulated the expression of multiple *var* genes is not known. While simultaneous transcription of multiple *var* genes in a parasite isolate culture has been described earlier (5), of the 60 *var* genes present in the *P. falciparum* genome, in a single parasite at a given time, only one *var* gene is expressed. The regulation of the expression of *var* family genes is thought to be controlled by several factors. One recently identified factor is a transcriptional regulatory protein, PfSir2, a molecule that has been shown to maintain the sub-telomeric *var* genes in a silent state by deacetylating the histones that are bound to their promoter (14, 40). Interestingly, we find that following heat shock, there is an average 2.4-fold increase in the level of PfSir2 expression.

Some malaria researchers believe that a permutation of events, such as frequent recombinations, deletions and gene conversions, give rise to a limitless *var* repertoire for

antigenic variation, and thus make it impossible to attain sterilizing immunity against blood-form parasites (9). It is reasonable to assume that in an endemic area, clinically immune adults possess immunity against a multitude of *var* alleles. How febrile illness influences *var*-mediated malaria pathogenesis is not known. In sub-Saharan Africa, the regulation of *var* gene expression in young children, who are the most susceptible to cerebral malaria, has not been studied.

Nonetheless, based on our results, it is tempting to hypothesize that malaria-induced fever causes enhanced expression of multiple *var* proteins leading to enhanced cytoadherence in vivo, thereby modulating the pathogenesis of disease in a susceptible host. Similarly, fever-induced expression of multiple *var* proteins may accelerate the development of the anti-disease immunity that prevents cytoadherence-mediated pathogenesis in adults living in malaria endemic areas.

We next wanted to determine whether febrile temperatures increase the amount of EMP-1 present at the IRBC surface. We used flow cytometry to examine the reactivity of unfixed (live) parasitized erythrocytes to a mouse polyclonal antibody specific for the EMP-1 variant expressed by the mature trophozoite stage of *P. falciparum* line 3D7.41. We found that the median fluorescent intensities (MFI) of parasitized erythrocyte populations incubated for 2 h at 41°C were slightly lower than those incubated for 2 h at 37°C (MFI ratio 41°C/37°C, mean + s.d., 0.93 + 0.03, $P = 0.0002$, one sample t test of the mean). Similar results (0.95 + 0.03, $P = 0.04$) were obtained after incubation for an additional 2 h at 37°C to enable sufficient time for translation and subsequent transport of EMP-1 to the erythrocyte surface (FIG. 6).

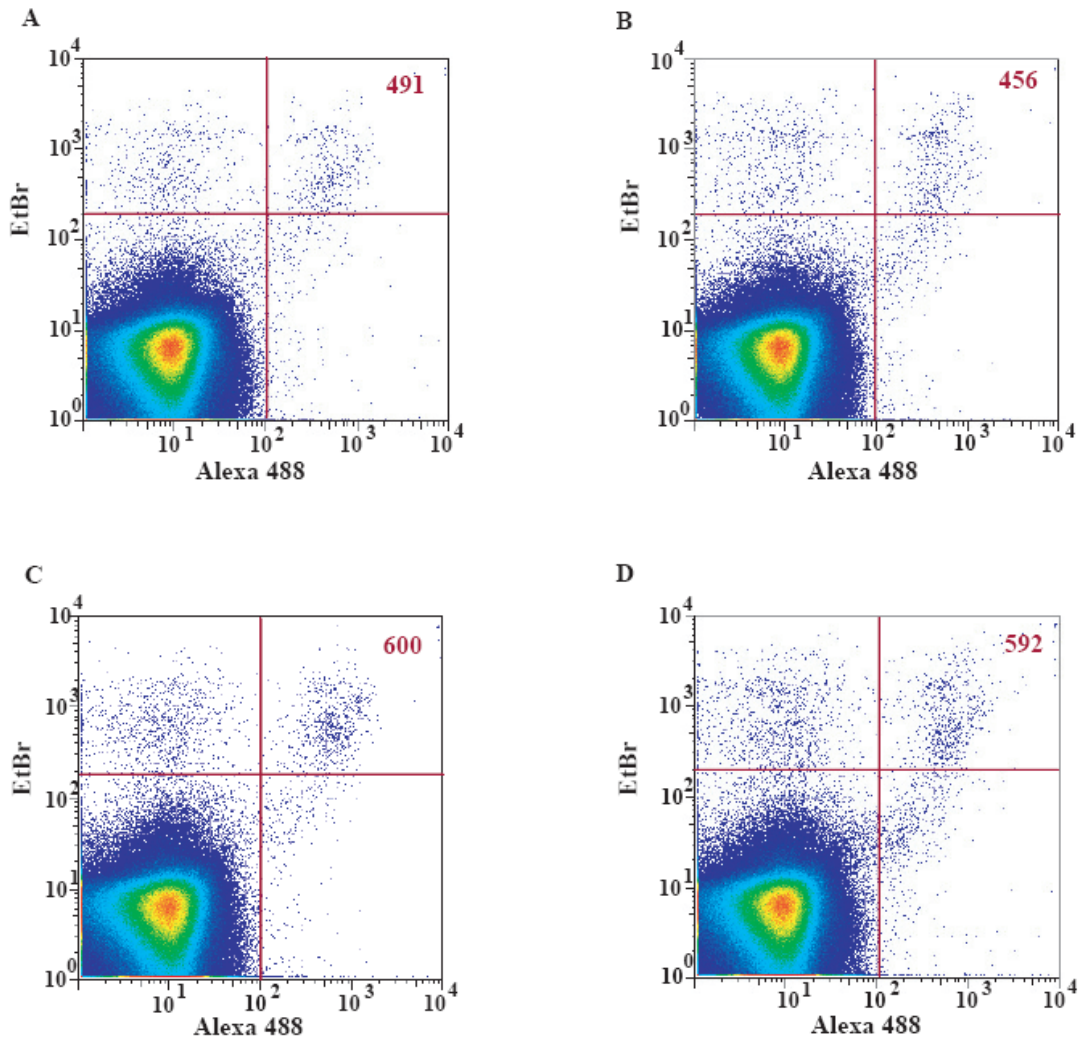


Figure 6. Flow cytometric analysis of heat induced PfEMP-1 expression on erythrocytes parasitized with the mature trophozoite stage of *P. falciparum* parasites. Parasitized erythrocytes cultured at 37°C 2 h (A), 41°C 2 h (B), 37°C 4 h (C), and 41°C 2 h + 37°C 2 h recovery period (D) were stained with ethidium bromide and probed with mouse polyclonal antibody specific for the extracellular CIDR1 domain of the PfEMP-1 molecule. Parasitized erythrocytes reactive to antibody appeared as clustered populations in the upper right quadrants (red numbers indicate the median fluorescent intensities or MFI). MFI ratio at T_{2h} (A/B) = .93 + 0.03, $P=0.0002$ and at T_{4h} (C/D) = .95 + 0.03, $P=0.04$.

These data suggest that heat shock does not increase the amount of EMP-1 expressed at the cell surface. These results somewhat differ from those reported earlier by Udomsangpeth et al., who detected EMP-1 expression on the surface of ring and mature trophozoite IRBCs incubated at 40°C but not at 37°C (48). Among the possible reasons for disagreement observed in the level of EMP-1 expressed on the surface of red cells following treatment at febrile temperatures may include the different *P. falciparum* parasites used in the study and differences in assay sensitivity. It is important to note that we were able to detect EMP-1 expression on the surface of IRBC incubated at 37°C. Nonetheless, further studies will be needed to determine how febrile illness influences EMP-1-mediated cytoadherence. It is feasible that elevated temperature could influence the conformational folding of adhesion moieties on EMP-1 (e.g., CSA, CD36 and ICAM) or alter the distribution of EMP1 on IRBCs making it more accessible for binding to endothelial cells. Precedence exists for such a possibility. In West African children, the presence of the homozygous haemoglobin CC genotype is associated with an increased protection against *P. falciparum* malaria (35). *P. falciparum* infected CC erythrocytes display an abnormal cell-surface distribution of EMP-1, and consequently have a reduced binding affinity to endothelial cells expressing CD36 and ICAM-1 (11).

These in vitro studies suggest that in an infected host, febrile illness could have both protective and deleterious effects. While febrile temperature could directly kill in vivo parasites by causing physiologic stress, it can also simultaneously prevent parasite immunologic clearance by allowing enhanced sequestration within the deep venules of the host tissues that could contribute toward the pathogenesis of cerebral malaria.

Secreted and cell surface molecules. This class is basically defined as those parasite-encoded polypeptides that are secreted outside the parasite cell or anchor themselves in the

parasite membrane or host cell or membrane. The most striking molecules that showed a strong tendency for over-expression are the *rif* and *var* proteins that are predicted to localize to the erythrocyte membrane. Proteins of the *rif* and *var* families are known to be involved in the binding of malaria parasites to receptors on the host cells causing rosetting and sequestration, two phenomena that are associated with malaria pathogenesis. Two other surface molecules encoded by sub-telomerically located genes are also upregulated, namely PFA0135w, a homolog of the *P. falciparum*, merozoite-associated tryptophan-rich antigen, and *P. yoelii*, pAg-3 (37) and a homolog of Psurf 4.2, a *P. falciparum* protein related to *P. vivax* vir proteins (52). Along with these proteins, other surface molecules that are overexpressed include an ortholog of the ookinete expressed protein SOAP of *P. berghei* (murine malaria), the so-called glycophorin-binding related antigen, a surface molecule with the anthrax-protective antigen domain (46), a protein with the MAC-perforin domain that has been implicated in invasion (3, 24-26), the merozoite surface protein 7, and the erythrocyte-binding protein 3, a paralog of MAEBL. The elevated expression of the *P. falciparum* SOAP at febrile temperatures is of interest because this molecule is expressed in the micronemes of the ookinete in *P. berghei* malaria and plays a role in adhesion to the mosquito basement layer (8). If this temperature-induced increase in expression of *P. falciparum* SOAP also occurs at the level of translation, it could mean that *P. falciparum* SOAP may have acquired a different function, or that this gene may have an additional function in the blood stages of the vertebrate host that was previously unknown. In a similar vein, the *P. falciparum* chitinase, a parasite enzyme shown to play an important role in the degradation of the insect peritrophic membrane (50), was also over-expressed in our study. These data again suggest a second function for this enzyme in modifying the deglycosylation of host molecules. However, direct biochemical studies will be needed to confirm the precise effect of the altered expression of individual surface molecules in mediating different interactions with host cells.

In contrast, other membrane proteins, such as at least six distinct small molecule transporters predicted to be localized to the parasite membrane and two subunits of the vacuolar ATPase, are downregulated. The genome of *P. falciparum* possesses an intact pathway for the synthesis of GPI anchors for membrane proteins, and this is consistent with the presence of several GPI-anchored proteins on the parasite membranes (46). In this study, five key enzymes in the GPI anchor biosynthesis pathway, including GPI transamidase and glycosyltransferase are consistently downregulated. This suggests that in response to elevated temperature, GPI-anchored proteins are likely to be depleted from the parasite membrane. This observation, taken together with the over-expression of proteins released into the host, suggests that some type-I membrane proteins on the parasite membrane might possibly be modulated to allow the aforesaid export. Interestingly, we also observed that a predicted secreted/cell-surface glycosyl transferase (PF11_0487) is downregulated under febrile conditions. Sequence analysis showed that it contains a glycosyltransferase domain of the O-linked N-acetylglucosamine transferase family related to the plant Spindly-type proteins (17). We predicted that this protein might mediate as yet unnoticed glycosylation of serine and threonine residues in host or parasite proteins, which might be shut-down or modulated in the febrile response.

Heat-shock response and protein stability. The next functional category in which genes showed dramatic changes in expression were those involved in the heat-shock response and protein stability. Not surprisingly, two chaperones, the HSP70 and HSP90 orthologs, which have been implicated in the heat-shock response across the phylogenetic spectrum of life, show an increased expression. *P. falciparum*, in contrast to other *Plasmodium* species and other Apicomplexa, shows a dramatic lineage-specific expansion of a particular family of DnaJ-domain proteins (3). Outside of Apicomplexa, orthologs of these proteins are currently encountered only in plants, further suggesting an ultimate origin from the plastid progenitor

(FIG. 7). Nine members of this DnaJ expansion show an elevated expression in our study. In *P. falciparum*, these proteins are characterized by an additional C-terminal domain that is predicted to form a multi-helical bundle enriched in charged amino acids that may serve as a surface for mediating interactions with specific protein targets. These DnaJ-domain proteins also contain an N-terminal hydrophobic signal and a Pexel motif, suggesting that they are secreted into the host cell, wherein, they might stabilize certain complexes by acting in conjunction with their usual functional partner, HSP70. In addition to the nine members of this expansion that are expressed in the elevated temperature conditions (FIG. 7), we observed that there are several other members of the expansion, which are not. This observation suggests that after the recent lineage-specific expansion in *P. falciparum*, some were adapted for specific roles in the febrile response, whereas other members of the expansion may be deployed under as-yet-unknown conditions. This suggests that the expansion of this family might have a role in terms of multiple specific adaptations of *P. falciparum*.

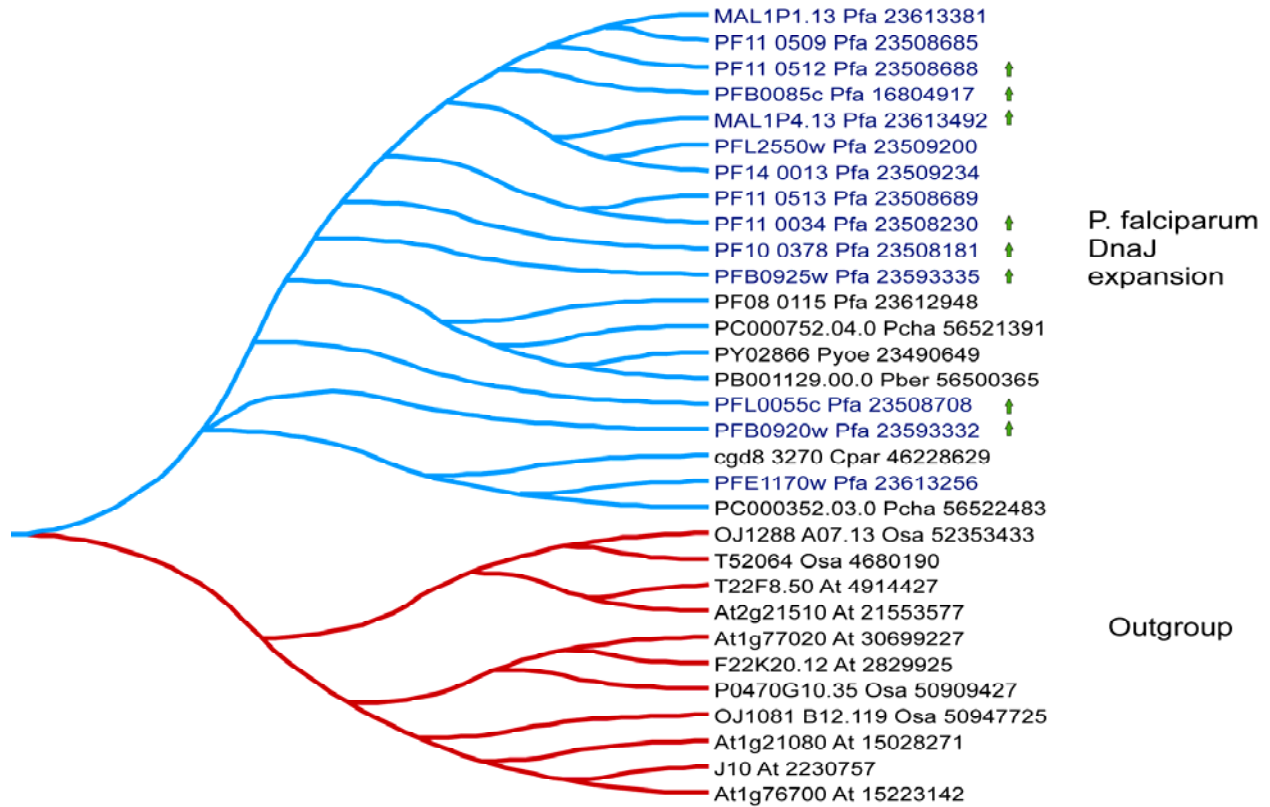


Figure 7. Tree of DnaJ family showing lineage-specific expansion. A phylogenetic tree of the DnaJ lineage-specific expansion in *Plasmodium falciparum*, with other eukaryotes as outgroup is shown. The *P. falciparum* proteins found to be upregulated in this study are marked with green arrows. The proteins are denoted by their gene name followed by the species abbreviation and GenBank Identifier. The species abbreviations are: At : *Arabidopsis thaliana*; Chom: *Cryptosporidium hominis*; Cpar: *Cryptosporidium parvum*; Osa: *Oryza sativa*; Pber: *Plasmodium berghei*; Pcha: *Plasmodium chabaudi*; Pfa: *Plasmodium falciparum*; Pyoe: *Plasmodium yoelii*

Most of these *P. falciparum*-specific RESA-type DnaJ-domain proteins were found to contain an additional conserved N-terminal domain. We accordingly named this conserved domain the PRESAN domain, for Plasmodium RESA N-terminal domain. Overall, we detected at least 67 proteins in *P. falciparum* (supplementary material) with complete copies of the

PRESAN domain, and several additional fragmentary versions (~5–10) of the domain which might represent mis-predicted genes or pseudogenes. In the publicly available draft of protein sequences of *P. yoelii*, *P. berghei* and *P. vivax* in the GenBank database, we detected at least one protein each with a copy of the PRESAN domain. No versions of this domain were detected in other apicomplexan genera, suggesting that the domain was “invented” after the divergence of the lineage leading to genus *Plasmodium*, but underwent a dramatic proliferation only in *P. falciparum*. A secondary structure prediction based on the amino acid frequency, a hidden Markov model, and a position-specific-score matrix derived from the multiple alignment of the PRESAN family revealed that it is composed of an all- α helical fold (JPred2 program, see Methods for details). The core domain is predicted to contain six conserved helical segments, which are likely to form a compact bundle. Most of the highly conserved positions seen throughout the family are hydrophobic residues that are likely to form the buried core of the helical bundle. Less conserved regions are enriched in both positively and negatively charged polar residues and likely comprise the exposed surface, which suggests a role for the PRESAN domain in protein-protein interactions. Further iterative searches with the PRESAN domain led to the identification of the conserved extra-cellular domains within the Vir superfamily of proteins, including the *P. falciparum* protein PfSURFIN4.2. Both of these domains are α -helical and share a similar pattern of secondary structural elements; however, the Vir superfamily contains conserved cysteines that are absent in the PRESAN domains. This suggests that the two domains are likely to have emerged from a common ancestor, with the Vir superfamily specializing in extracellular interactions, whereas the PRESAN superfamily specialized in cytoplasmic interactions.

Paradoxically, ten different genes for proteins of the ubiquitin metabolism system were observed to be consistently downregulated in this study. These include proteasomal enzymes,

different E1 and E3 enzymes, as well as some ubiquitin C-terminal hydrolases. As a validation of our microarray results, we noted that polyubiquitin (PFL0585w), the only ubiquitin pathway gene found to be upregulated in our dataset (1.53 fold change), was also upregulated in response to elevated temperature in an earlier published report (22). An overall depression of the ubiquitin pathway suggests that modulation of protein degradation could be a parasite survival mechanism to increase the half-life of certain proteins under stressful conditions.

To establish a relationship between our microarray data and its biologic relevance, we measured total ubiquitination of proteins isolated from parasites incubated at 37°C and 41°C, using a rabbit polyclonal bovine anti-ubiquitin antibody. Comparison of expression levels obtained by ECL-based semi-quantitative western blot analysis of *P. falciparum* parasite extracts collected after incubation at 37°C or 41°C 2 h demonstrated that temperature elevation causes a generalized downregulation in the ubiquitination process. Based on its immuno-reactivity with anti-ubiquitin antibody, there is a significant depression in ubiquitination of both high-molecular mass and low-molecular-mass protein adducts following treatment at 41°C (FIG. 8). A quantitative analysis based on intensities of bands measured between the areas marked by asterisks that includes the high and low molecular weight proteins from parasites incubated at 37°C and 41°C gave IOD units of 19,047 and 1291, respectively, demonstrating a 14.8-fold downregulation in the ubiquitination process.

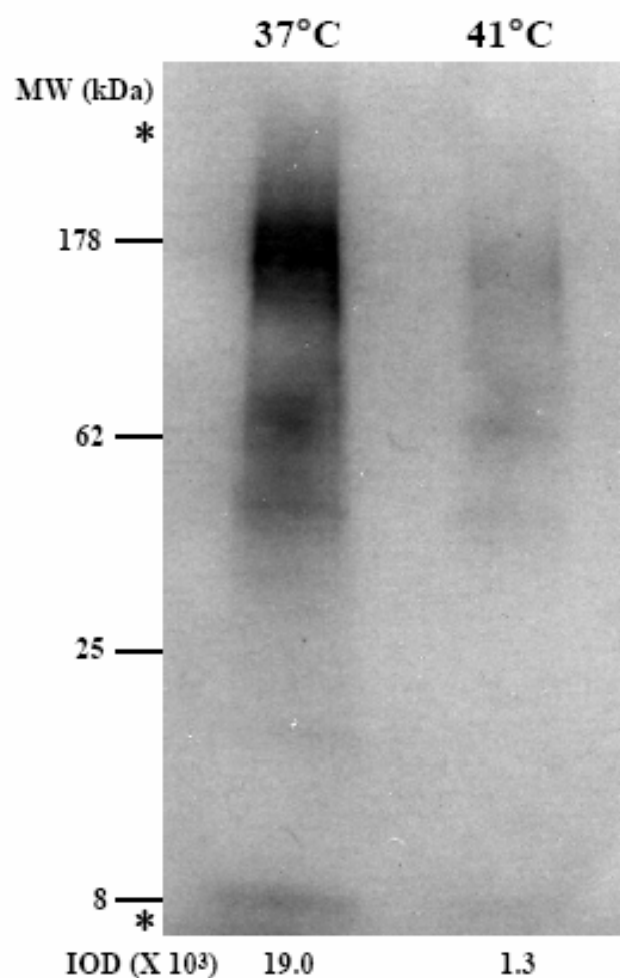


Figure 8. Effect of febrile temperature on ubiquitination of parasite proteins. Total ubiquitination of 5 μ g protein from *P. falciparum* parasites was measured by western blot analysis using an anti-ubiquitin antibody following incubation at *lane 1*: 37°C 2 h, *lane 2*: 41°C 2 h. Protein bands were visualized following incubation with the ECL western blotting detection reagents and the integrated optical densities (IOD) for each lane were measured using Meta Morph 6.1 software. Asterisks denote the area in each lane of the blot where IOD was determined.

The significance of this biologic assay is twofold. First, it confirms that changes in expression are occurring at the protein as well as the mRNA level. Second, while our microarray

data capture changes in expression of individual enzymes in the ubiquitin pathway, this assay quantifies total ubiquitination of all parasite proteins. It may seem rather counter-intuitive that the ubiquitin pathway is downregulated in response to elevated temperature, which undoubtedly results in the accumulation of misfolded proteins that may become toxic to the cell if not removed. However, depression of the ubiquitin pathway may be a mechanism to increase the half-life of certain proteins under stressful conditions. A recent study suggested that protein degradation by ubiquitination and heat-shock protein-assisted refolding do, in fact, act in concert with one another and may even at times compete for the same substrates (misfolded proteins) (32). Another plausible explanation for a generalized depression in the ubiquitin pathway could be a parasite strategy to conserve energy at times of duress. It is estimated that approximately 30% of nascent proteins are degraded by the proteasome in unstressed cells (43); therefore, even a slight decrease in the ubiquitin pathway will result in a considerable increase in energy available for other cellular processes.

Cytoplasmic systems and signal transduction. We found that four of the five genes encoding conserved cytoskeletal proteins that were recovered in our study were upregulated, including tubulin and a homolog of the *Drosophila* actin-binding protein kelch. The only downregulated gene in this category was ADF3, an actin-depolymerizing factor related to gelsolin. A probable explanation for the observed expression pattern may be that the cytoskeleton is strengthened to compensate for the destabilizing effects of elevated temperature. All ten genes related to cytoplasmic protein trafficking, vacuolar sorting and secretion that were recovered in this study were found to be consistently downregulated. These included various small GTPases of the vesicular biogenesis and fusion pathway, a potential vesicular cargo-binding protein with the conserved GOLD domain (2), the microsomal signal peptidase, and one of the luminal disulfide bond isomerases. Similarly, 12 ribosomal protein genes and two genes

for proteins with ribosome-associated functions were downregulated. This apparent downregulation of several components of the protein synthesis and protein-trafficking apparatus as well as the ubiquitin-dependent protein degradation system (noted above) might indicate a multi-level process to slow down the synthesis and turnover of proteins.

In terms of signal transduction, members of three distinct families of protein kinases are upregulated. Most interesting of these are the protein kinases of the Apicomplexa-specific R45 family. These predicted serine/threonine kinases are thus far found only in Apicomplexa and are characterized by several structural features that distinguish them from all other S/T kinases that have been characterized to date. These unique structural features include the peculiar structure of the ATP-binding site in the N-terminal sub-domain of the kinase and a conserved extension with a characteristic tryptophan, N-terminal to the kinase domain. These features suggest that these kinases target a unique set of substrates. Furthermore, they possess a conserved Pexel motif, which has been shown to be required for their translocation to the host cytoplasm and are likely to phosphorylate targets in the host cytoplasm. The R45 family shows a lineage-specific expansion unique to the *falciparum* species of *Plasmodium* (FIG. 9), of which three members were found to be consistently upregulated. The fact that none of the other members of this large lineage-specific expansion in *Plasmodium* are upregulated suggests that there is again a functional diversification of this recently diversified family, just as in the earlier-mentioned DNAJ proteins, with some members being recruited in the context of the febrile response.

In addition to the R45 family, two paralogous kinases of the GCN2-family of kinases, which are involved in regulating translation by phosphorylating components of the translation machinery (51), are also upregulated. These kinases may also be exported to the host cytoplasm and may thereby interfere with the basic metabolism of the host cell. Two members of the calcium-dependent kinase family with EF-hand domains fused to the kinase domains are also

strongly over-expressed. This family shows a lineage-specific expansion in various alveolates and might be widely used by organisms of this lineage in various signaling contexts (32). In contrast, two genes for predicted calcium-binding proteins with EF-hand domains, and a MAP kinase are downregulated. Beyond this, no conserved signaling genes appear to be under any kind of regulation. This suggests that the transcriptional response to elevated temperature specifically affects only a small set of phosphorylation-dependent signaling pathways.

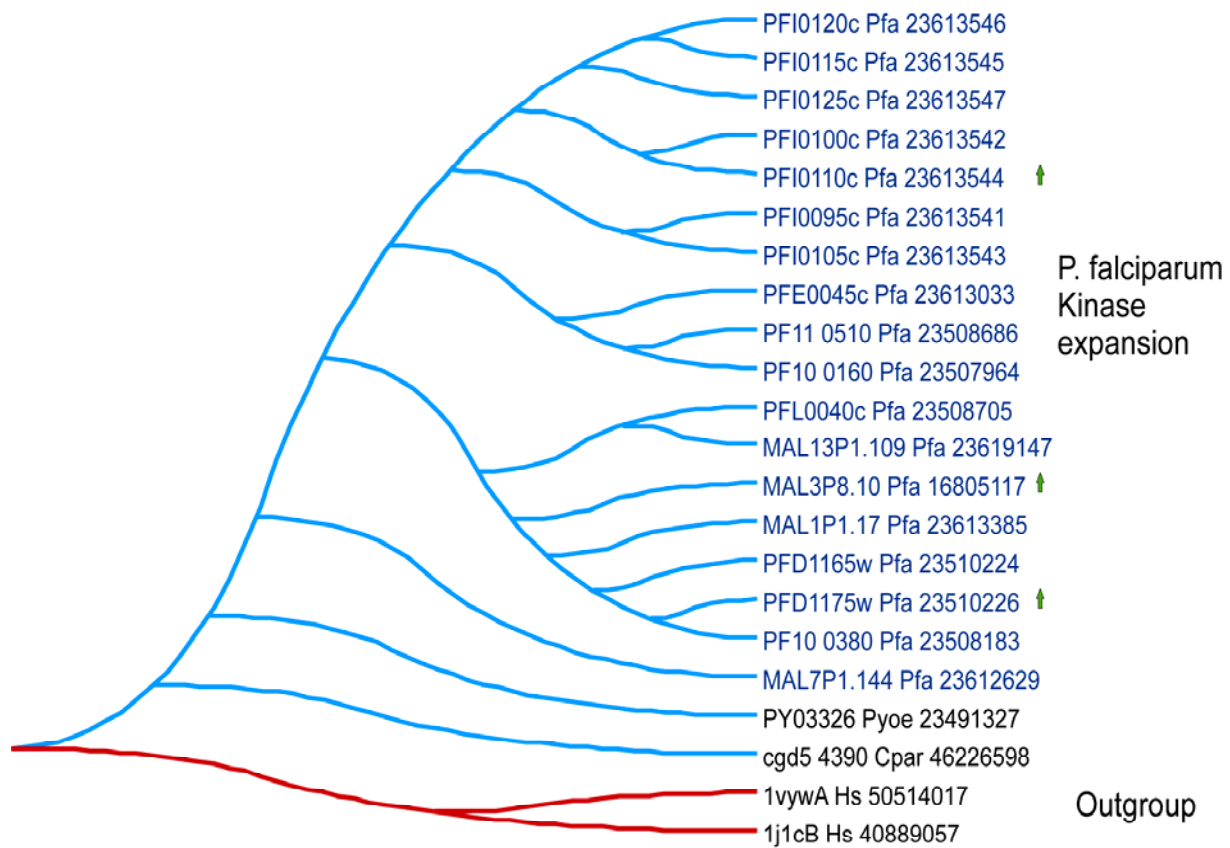


Figure 9. Tree of R45 protein kinase family showing lineage-specific expansion. A phylogenetic tree of the R45 protein kinase lineage-specific expansion in *Plasmodium falciparum*, with human kinases with structures as outgroup, is shown. The *P. falciparum* proteins, which are found to be upregulated in this study, are marked with green arrows. The proteins are denoted by their gene name followed by the species abbreviation and GenBank Identifier. The species abbreviations are as in Figure 7 and Hs: *Homo sapiens*.

RNA metabolism. We found that 17 genes for proteins involved in different aspects of RNA metabolism, particularly splicing, mRNA maturation, and post-transcriptional gene regulation, are over-expressed, as against only three genes for RNA-metabolism proteins that are downregulated. A striking, opposite regulation of two genes for Sm proteins was observed in our study. The classical Sm protein, Sm-G, which is a core component of the U1, U2, U4 and U5 spliceosomal particles, is strongly upregulated, whereas LSM6, which is a component of the U6 spliceosomal particle and decapping-dependent RNA degradation pathway, is downregulated. This pattern might indicate a change in stoichiometry of the spliceosomal components, which might affect the splicing or stability of specific mRNAs. We had earlier reported a family of predicted RNA-binding proteins with multiple Zn-chelating CCCH domains (typified by PFE1245w), which show a lineage-specific expansion in *Plasmodium* (46). Two members of this expansion show a strong over-expression in response to temperature stress and might participate in an Apicomplexa-specific post-transcriptional regulatory mechanism. These observations point to a major potential regulatory input occurring at the level of mRNA stability and perhaps splicing.

Nuclear functions. Eight genes for chromatin components are upregulated; in comparison, only two genes are downregulated. The upregulated genes include the histones (H2B and H4) and the NAD-dependent histone deacetylase of the Sir2p family (PfSir2). Several genes of the DNA replication and repair systems, including the RP-A and RF-C are downregulated, whereas a Rad25-like helicase/ATPase and a DNA repair nuclease, Dem1p of the RecB family are upregulated. The exact implication of these changes in the expression pattern of the nuclear proteins is unclear, but it might indicate a tendency for condensation of chromatin and a possible slow-down in replication. A few DNA-binding proteins, other than the

histones, associated with chromatin structure maintenance also show an upregulation, namely the BRIGHT domain protein (MAL6P1.39), which is likely to be a component of the SWI2/SNF2-dependent chromatin remodeling complexes, and the histone-type nuclear factor Y homolog (PF14_0374). We observed that the mRNA levels of three predicted specific transcription factors show noticeable changes in response to elevated temperature. Two of these, PFL0455c with two C-terminal C2H2 zinc finger domains, and PFD0200c with the recently identified ApiAP2 DNA-binding domain, are upregulated. In contrast, the third transcription factor, PFE1025c, has a DNA-binding domain related to the plant p24/PBF-2 transcription factors and the ciliate TIF1 transcription factor and is downregulated. In ciliates, the orthologous transcription factor TIF1 is known to be required for the transcription of rDNA in ribosomal biogenesis (42). It is likely that the *Plasmodium* protein plays a similar role and its downregulation is consistent with the downregulation of several other ribosomal components (See above).

Another striking observation we made was that about 26% (90 genes) of the genes showing a change in transcription in response to febrile conditions map to the sub-telomeric gene arrays that, in addition to members of the *rif*, *var* and DNAJ families, also encode several other proteins. This observation indicates a strong bias in the preferential regulation of genes associated with chromosome ends (<0.001 chance probability of obtaining the observed numbers by the Chi square test) and points to probable special chromatin-related changes in the sub-telomeric regions. In particular, we noticed that at least 70% of sub-telomeric genes found in our data set were over-expressed, suggesting there might be an increased accessibility of particular regions of sub-telomeric chromatin to allow increased transcription of certain genes.

General metabolism. We did not observe expression patterns suggesting systematic down- or up-regulation of entire metabolic pathways; however, expression of genes for specific components of a few metabolic pathways did seem to show alterations. The most striking

alterations were seen in the case of lipid metabolism. *Plasmodium* possesses multiple paralogs of a fatty acyl-CoA synthetase, some of which have been shown to function on long-chain fatty acids. Recently, these proteins have been demonstrated to be exported in specific vesicular structures to the host cell (34). We observed that three members of this family are strongly or moderately over-expressed under temperature stress. Furthermore, a serine C-palmitoyltransferase (ortholog of yeast Lcb2p), which functions in sphingolipid biosynthesis, is also upregulated, and this protein is predicted on the basis of the Pexel motif to be exported into the host cell. Likewise, two paralogous genes encoding phospholipases that are predicted to convert fatty acid monoglycerides to free fatty acids are also over-expressed. Interestingly, the gene for an enzyme catalyzing the opposite step in the pathway, a membrane-associated lysophosphatidic acyltransferase, is strongly downregulated, implying a two-level modification of the pathway in the same general direction. These patterns suggest potential mechanisms for modification of the lipids of the host and the parasite that might be conducive for the localization of the parasite proteins and also allow the formation and maintenance of the parasitophorous membrane.

PFB0590w encodes a predicted monooxygenase related to the bacteria antibiotic biosynthesis monooxygenases (44) and is downregulated under febrile conditions. It would be of interest to further investigate whether it might be involved in the modification of as-yet-unknown metabolites in the parasite. The gene for the allantoinase, which is involved in purine degradation, is also quite strongly upregulated. This suggests that under heat shock there might be a shift to utilization of purine break-down products as a secondary nitrogen source. A Cof-like phosphatase of the HAD superfamily of hydrolases, which belongs to a family of highly conserved hydrolases, is strongly over-expressed in our study. However, the functional implications of this protein remain largely unclear.

We believe that a combination of gene expression data, sequence analysis, and biologic experiments has helped us piece together the potential activities involved in the febrile temperature response in *P. falciparum* and is depicted in Fig. 10. We note, particularly, that a large number of polypeptides that are predicted or known to be exported into the host cell or expressed on the host cell surface are over-expressed to varying degrees under temperature stress. In particular, the PRESAN domain proteins, such as the DNAJ family, might form specific complexes in the host cytoplasm and modify its properties in response to the temperature elevation. In terms of a general intracellular response, the upregulation of several genes related to mRNA metabolism and splicing appears to suggest a major post-transcriptional regulatory response. In terms of protein stability, trafficking, and protein synthesis itself, a general tendency to slow down synthesis of new proteins and degradation of existing proteins is suggested by our data. On a more pragmatic note, we observe that several *Plasmodium*- or Apicomplexan-specific gene families and other enzymes with no close homologs in humans are over-expressed. If this observation were to reflect in comparable elevation protein levels, then they might serve as potential targets for therapeutic intervention or as vaccine candidates. In summary, our data present for the first time a comprehensive view of the alterations in gene expression and predicted biochemical pathways in *P. falciparum* parasites exposed in vitro to temperatures characteristic of febrile illness, independent of confounding factors such as host genetics and immune status.

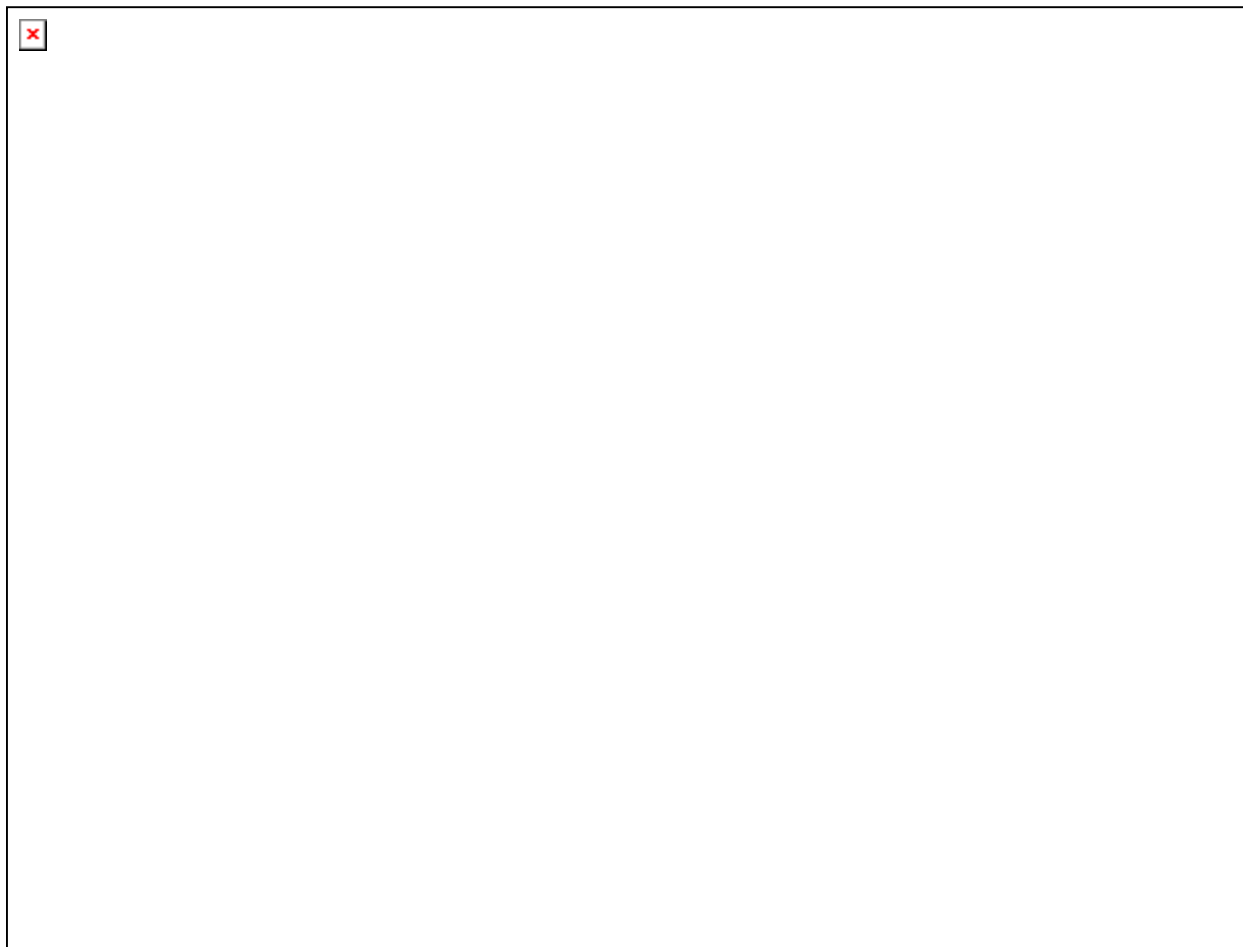


Figure 10. Cell cartoon with sub-cellular localization of various proteins showing altered mRNA levels under febrile temperatures. The cells and organelles are schematically shown and not drawn to scale. The membranous system depicted on the right section of the parasite cell is the Golgi and vesicular transport system. The alveolar membrane or ER system is shown to the extreme right. The domain architectures of proteins that show altered temperature response and their localizations are indicated. The representative protein name is given, and the number of proteins, if any, is given in round brackets. The function legend is given on the top of the figure, and each protein is marked with a function symbol when its function is known. Green arrows indicate upregulation, while Red arrows indicate downregulation. Abbreviations: RF – Ring Finger; GBPH2 - Glycophorin-binding protein homolog 2. ZnF- is a zinc finger domain. All the GPI anchor biosynthesis related proteins are shown inside the parasite cell and are likely to co-

localize with the Golgi and vesicular transport system involved in secretion and maturation of proteins.

ACKNOWLEDGMENTS

We thank Guojian Jiang and Tim Myers at the NIAID microarray research facility for assistance with the microarray studies, and Nancy Shulman for editorial assistance. We than Richard Andre, John Cross, Dechang Chen, and D. Scott Merrell at the Uniformed Services University of the Health Sciences for assistance in research design and analysis of these studies. We also thank Nirbhay Kumar for anti-PfHSP-70, Morris Makobongo for anti-EMP-1 and Sanjay Singh for anti-Pfchitinase antibodies. The views and opinions expressed here are those of the authors and should not be construed as the official opinion of the Food and Drug Administration.

The abbreviations used are: IRBC, infected red blood cell; HSP, heat-shock protein; EMP-1, erythrocyte membrane protein-1; GPI, Glycosyl phosphatidyl inositol.

REFERENCES

1. **Altschul, S. F., T. L. Madden, A. A. Schaffer, J. Zhang, Z. Zhang, W. Miller, and D. J. Lipman.** 1997. Gapped BLAST and PSI-BLAST: a new generation of protein database search programs. *Nucleic Acids Res* **25**:3389-3402.
2. **Anantharaman, V., and L. Aravind.** 2002. The GOLD domain, a novel protein module involved in Golgi function and secretion. *Genome Biol* **3**:research0023.
3. **Aravind, L., L. M. Iyer, T. E. Wellems, and L. H. Miller.** 2003. *Plasmodium* biology: genomic gleanings. *Cell* **115**:771-785.
4. **Beere, H. M., and D. R. Green.** 2001. Stress management - heat shock protein-70 and the regulation of apoptosis. *Trends Cell Biol* **11**:6-10.
5. **Chen, Q., V. Fernandez, A. Sundstrom, M. Schlichtherle, S. Datta, P. Hagblom, and M. Wahlgren.** 1998. Developmental selection of var gene expression in *Plasmodium falciparum*. *Nature* **394**:392-395.
6. **Cuff, J. A., and G. J. Barton.** 2000. Application of multiple sequence alignment profiles to improve protein secondary structure prediction. *Proteins* **40**:502-511.
7. **Deponte, M., and K. Becker.** 2004. *Plasmodium falciparum*-do killers commit suicide? *Trends Parasitol* **20**:165-169.
8. **Dessens, J. T., I. Siden-Kiamos, J. Mendoza, V. Mahairaki, E. Khater, D. Vlachou, X. J. Xu, F. C. Kafatos, C. Louis, G. Dimopoulos, and R. E. Sinden.** 2003. SOAP, a novel malaria ookinete protein involved in mosquito midgut invasion and oocyst development. *Mol Microbiol* **49**:319-329.
9. **Dzikowski, R., M. Frank, and K. Deitsch.** 2006. Mutually exclusive expression of virulence genes by malaria parasites is regulated independently of antigen production. *PLoS Pathog* **2**:e22.
10. **Eddy, S. R.** 1998. Profile hidden Markov models. *Bioinformatics* **14**:755-763.
11. **Fairhurst, R. M., D. I. Baruch, N. J. Brittain, G. R. Ostera, J. S. Wallach, H. L. Hoang, K. Hayton, A. Guindo, M. O. Makobongo, O. M. Schwartz, A. Tounkara, O. K. Doumbo, D. A. Diallo, H. Fujioka, M. Ho, and T. E. Wellems.** 2005. Abnormal display of PfEMP-1 on erythrocytes carrying haemoglobin C may protect against malaria. *Nature* **435**:1117-1121.
12. **Feder, M. E., and G. E. Hofmann.** 1999. Heat-shock proteins, molecular chaperones, and the stress response: evolutionary and ecological physiology. *Annu Rev Physiol* **61**:243-282.
13. **Felsenstein, J.** 1989. PHYLIP -- Phylogeny Inference Package (Version 3.2). **5**:164-166.
14. **Freitas-Junior, L. H., R. Hernandez-Rivas, S. A. Ralph, D. Montiel-Condado, O. K. Ruvalcaba-Salazar, A. P. Rojas-Meza, L. Mancio-Silva, R. J. Leal-Silvestre, A. M. Gontijo, S. Shorte, and A. Scherf.** 2005. Telomeric heterochromatin propagation and histone acetylation control mutually exclusive expression of antigenic variation genes in malaria parasites. *Cell* **121**:25-36.
15. **Gove, S.** 2000. Integrated management of childhood illness, p. 125-140. *In* A. J. Magill and G. T. Strickland (ed), *Hunter's Tropical Medicine and Emerging Infectious Diseases*, W. B. Saunders Co., Philadelphia, Pa.

16. **Guha, M., S. Kumar, V. Choubey, P. Maity, and U. Bandyopadhyay.** 2006. Apoptosis in liver during malaria: role of oxidative stress and implication of mitochondrial pathway. *Faseb J* **20**:1224-1226.
17. **Hartweck, L. M., C. L. Scott, and N. E. Olszewski.** 2002. Two O-linked N-acetylglucosamine transferase genes of *Arabidopsis thaliana* L. Heynh. have overlapping functions necessary for gamete and seed development. *Genetics* **161**:1279-1291.
18. **Hasegawa, M., H. Kishino, and N. Saitou.** 1991. On the maximum likelihood method in molecular phylogenetics. *J Mol Evol* **32**:443-445.
19. **Haynes, J. D., and J. K. Moch.** 2002. Automated synchronization of *Plasmodium falciparum* parasites by culture in a temperature-cycling incubator. *Methods Mol Med* **72**:489-497.
20. **Hiller, N. L., S. Bhattacharjee, C. van Ooij, K. Liolios, T. Harrison, C. Lopez-Estrano, and K. Haldar.** 2004. A host-targeting signal in virulence proteins reveals a secretome in malarial infection. *Science* **306**:1934-1937.
21. **Hofmann K. and Stoffel, W.** 1993. TMbase—a database of membrane spanning proteins segments. *Biol. Chem. Hoppe-Seyler* **374**:166.
22. **Horrocks, P., and C. I. Newbold.** 2000. Intraerythrocytic polyubiquitin expression in *Plasmodium falciparum* is subjected to developmental and heat-shock control. *Mol Biochem Parasitol* **105**:115-125.
23. **Hurd, H., K. M. Grant, and S. C. Arambage.** 2006. Apoptosis-like death as a feature of malaria infection in mosquitoes. *Parasitology* **132 Suppl**:S33-47.
24. **Ishino, T., Y. Chinzei, and M. Yuda.** 2005. A *Plasmodium* sporozoite protein with a membrane attack complex domain is required for breaching the liver sinusoidal cell layer prior to hepatocyte infection. *Cell Microbiol* **7**:199-208.
25. **Kadota, K., T. Ishino, T. Matsuyama, Y. Chinzei, and M. Yuda.** 2004. Essential role of membrane-attack protein in malarial transmission to mosquito host. *Proc Natl Acad Sci U S A* **101**:16310-16315.
26. **Kaiser, K., N. Camargo, I. Coppens, J. M. Morrissey, A. B. Vaidya, and S. H. Kappe.** 2004. A member of a conserved *Plasmodium* protein family with membrane-attack complex/perforin (MACPF)-like domains localizes to the micronemes of sporozoites. *Mol Biochem Parasitol* **133**:15-26.
27. **Kitchen, S. F.** 1949. Symptomatology: General considerations, p. 966-1045, vol. Vol. 72. Humana Press, Totowa, N. J.
28. **Krogh, A., B. Larsson, G. von Heijne, and E. L. Sonnhammer.** 2001. Predicting transmembrane protein topology with a hidden Markov model: application to complete genomes. *J Mol Biol* **305**:567-580.
29. **Kwiatkowski, D.** 1989. Febrile temperatures can synchronize the growth of *Plasmodium falciparum* in vitro. *J Exp Med* **169**:357-361.
30. **Kwiatkowski, D.** 1995. Malarial toxins and the regulation of parasite density. *Parasitol Today* **11**:206-212.
31. **Long, H. Y., B. Lell, K. Dietz, and P. G. Kremsner.** 2001. *Plasmodium falciparum*: in vitro growth inhibition by febrile temperatures. *Parasitol Res* **87**:553-555.

32. **Marques, C., W. Guo, P. Pereira, A. Taylor, C. Patterson, P. C. Evans, and F. Shang.** 2006. The triage of damaged proteins: degradation by the ubiquitin-proteasome pathway or repair by molecular chaperones. *Faseb J* **20**:741-743.
33. **Marti, M., R. T. Good, M. Rug, E. Knuepfer, and A. F. Cowman.** 2004. Targeting malaria virulence and remodeling proteins to the host erythrocyte. *Science* **306**:1930-1933.
34. **Matesanz, F., M. M. Tellez, and A. Alcina.** 2003. The *Plasmodium falciparum* fatty acyl-CoA synthetase family (PfACS) and differential stage-specific expression in infected erythrocytes. *Mol Biochem Parasitol* **126**:109-112.
35. **Modiano, D., G. Luoni, B. S. Sirima, J. Simpore, F. Verra, A. Konate, E. Rastrelli, A. Olivieri, C. Calissano, G. M. Paganotti, L. D'Urbano, I. Sanou, A. Sawadogo, G. Modiano, and M. Coluzzi.** 2001. Haemoglobin C protects against clinical *Plasmodium falciparum* malaria. *Nature* **414**:305-308.
36. **Notredame, C., D. G. Higgins, and J. Heringa.** 2000. T-Coffee: A novel method for fast and accurate multiple sequence alignment. *J Mol Biol* **302**:205-217.
37. **Ntumngia, F. B., M. K. Bouyou-Akotet, A. C. Uhlemann, B. Mordmuller, P. G. Kremsner, and J. F. Kun.** 2004. Characterisation of a tryptophan-rich *Plasmodium falciparum* antigen associated with merozoites. *Mol Biochem Parasitol* **137**:349-353.
38. **Nyakeriga, A. M., H. Perlmann, M. Hagstedt, K. Berzins, M. Troye-Blomberg, B. Zhivotovsky, P. Perlmann, and A. Grandien.** 2006. Drug-induced death of the asexual blood stages of *Plasmodium falciparum* occurs without typical signs of apoptosis. *Microbes Infect* **8**:1560-1568.
39. **Pankova-Kholmyansky, I., A. Dagan, D. Gold, Z. Zaslavsky, E. Skutelsky, S. Gatt, and E. Flescher.** 2003. Ceramide mediates growth inhibition of the *Plasmodium falciparum* parasite. *Cell Mol Life Sci* **60**:577-587.
40. **Ralph, S. A., and A. Scherf.** 2005. The epigenetic control of antigenic variation in *Plasmodium falciparum*. *Curr Opin Microbiol* **8**:434-440.
41. **Riezman, H.** 2004. Why do cells require heat shock proteins to survive heat stress? *Cell Cycle* **3**:61-63.
42. **Saha, S., A. Nicholson, and G. M. Kapler.** 2001. Cloning and biochemical analysis of the tetrahymena origin binding protein TIF1: competitive DNA binding in vitro and in vivo to critical rDNA replication determinants. *J Biol Chem* **276**:45417-45426.
43. **Schubert, U., L. C. Anton, J. Gibbs, C. C. Norbury, J. W. Yewdell, and J. R. Bennink.** 2000. Rapid degradation of a large fraction of newly synthesized proteins by proteasomes. *Nature* **404**:770-774.
44. **Sciara, G., S. G. Kendrew, A. E. Miele, N. G. Marsh, L. Federici, F. Malatesta, G. Schimperna, C. Savino, and B. Vallone.** 2003. The structure of ActVA-Orf6, a novel type of monooxygenase involved in actinorhodin biosynthesis. *Embo J* **22**:205-215.
45. **Sreedhar, A. S., and P. Csermely.** 2004. Heat shock proteins in the regulation of apoptosis: new strategies in tumor therapy: a comprehensive review. *Pharmacol Ther* **101**:227-257.

46. **Templeton, T. J., L. M. Iyer, V. Anantharaman, S. Enomoto, J. E. Abrahante, G. M. Subramanian, S. L. Hoffman, M. S. Abrahamsen, and L. Aravind.** 2004. Comparative analysis of Apicomplexa and genomic diversity in eukaryotes. *Genome Res* **14**:1686-1695.
47. **Trager, W., and J. B. Jensen.** 1976. Human malaria parasites in continuous culture. *Science* **193**:673-675.
48. **Udomsangpetch, R., B. Pipitaporn, K. Silamut, R. Pinches, S. Kyes, S. Looareesuwan, C. Newbold, and N. J. White.** 2002. Febrile temperatures induce cytoadherence of ring-stage *Plasmodium falciparum*-infected erythrocytes. *Proc Natl Acad Sci U S A* **99**:11825-11829.
49. **van Hensbroek, M. B., A. Palmer, E. Onyiorah, G. Schneider, S. Jaffar, G. Dolan, H. Memming, J. Frenkel, G. Enwere, S. Bennett, D. Kwiatkowski, and B. Greenwood.** 1996. The effect of a monoclonal antibody to tumor necrosis factor on survival from childhood cerebral malaria. *J Infect Dis* **174**:1091-1097.
50. **Vinetz, J. M., J. G. Valenzuela, C. A. Specht, L. Aravind, R. C. Langer, J. M. Ribeiro, and D. C. Kaslow.** 2000. Chitinases of the avian malaria parasite *Plasmodium gallinaceum*, a class of enzymes necessary for parasite invasion of the mosquito midgut. *J Biol Chem* **275**:10331-10341.
51. **Wilson, W. A., and P. J. Roach.** 2002. Nutrient-regulated protein kinases in budding yeast. *Cell* **111**:155-158.
52. **Winter, G., S. Kawai, M. Haeggstrom, O. Kaneko, A. von Euler, S. Kawazu, D. Palm, V. Fernandez, and M. Wahlgren.** 2005. SURFIN is a polymorphic antigen expressed on *Plasmodium falciparum* merozoites and infected erythrocytes. *J Exp Med* **201**:1853-1863.

SUPPLEMENTARY DATA

Table S1. Annotation and functional predictions of parasites genes altered by febrile temperature.

Function	Protein Name	gi	PlasmoDB Description	Annotation	Fold Δ
RNA processing	PF13_0035	23619008	Hypothetical protein	Ydr449cp / Utp6p; small (ribosomal) subunit (SSU) processosome (contains U3 snoRNA). HAT. Splicing	4.1623
	MAL8P1.48	23612793	Small nuclear ribonucleoprotein polypeptide g, 65009- 64161, putative	Sm. SMALL NUCLEAR RIBONUCLEOPROTEIN G (SNRNP-G) RUXG. Splicing	5.5298
	PFE1245w	23613271	Zinc finger protein, putative	PFE1245w_Pfal-like CCCH expansion	4.5157
	PF14_0236	23509458	Hypothetical protein	PFE1245w_Pfal-like CCCH expansion	3.7052
	PF11_0191	23508382	Hypothetical protein	nucleolar protein NOP56/Sik1p. Pre-mRNA splicing factor prp31; Sik1p. Splicing	2.2293
	PF14_0151	23509372	Hypothetical protein	NOVA-like. KH domain. PTGR. .	2.2087
	PF14_0113	23509334	Hypothetical protein	NIC+MI domains containing protein. nucampholin/yeast Cwc22p like protein involved in mRNA splicing	2.8640
	PFL0830w	23508862	Hypothetical protein	Mrd1p-like. 5RRMs Splicing Related	2.5258
	MAL6P1.300	23612206	Hypothetical protein, conserved	MJ1157-like thiouridine synthase (ZnRibbon+PPloopAtpase+Zn ribbon). involved in RNA metabolism.	4.7584
	MAL3P3.13, PFC0390w	16805183	Hypothetical protein, conserved	CG11596/YNL092w-like predicted mRNA methylase Cysteine rich repeat (C_tripleX) in the middle.	2.8625
	PF13_0236	23619363	Hypothetical protein, conserved	MJ0710-like(Thump+Methylase)	2.6947
	PF11510w	23613824	Hypothetical protein	N terminal Nucleolar protein,Nop52. (Nop52/Rrp1p/NNP-1 family)	2.3569
	PFD0320c	23510054	Hypothetical protein	NYN domain nuclease (novel RNase)	2.5650
	MAL8P1.70	23612835	Hypothetical protein	F11M21.28-like 3 CCCH RNA binding domain involved in RNA Metabolism . Splicing	1.9573
	PF11_0347	23508538	Hypothetical protein	FHA+RRM	3.9075
	PF14_0193	23509414	Hypothetical protein	3x Zn Knuckles domains. splicing factor YT521 -like. no arches cleavage and polyadenylation specific factor 4. CCCH. PTGR	2.0815
	PFL0355c	23508768	Hypothetical protein	Esf1p, involved in biogenesis	2.3212

				of 18S rRNA	
	MAL7P1.139	23612624	Mago nashi protein homolog, putative	Mago Nashi-like protein. Component of exon-junction complex	0.4786
	PF13_0142	23619200		Sm. LSM6. Splicing	
	MAL3P6.15, PFC0780w	16805261	Hypothetical protein	CPSF A subunit region.	0.3613
	PF14_0061	23509282	Hypothetical protein	pentatricopeptide PPR repeats	0.3039
Signal transduction	MAL3P8.10, PFC0060c	16805117	Serine/threonine protein kinase, putative	Serine/Threonine protein kinase PFI0110c-like	2.1223
	PFI0110c	23613544	Hypothetical protein	Serine/Threonine protein kinase PFI0110c-like	4.0695
	PFD1175w	23510226	Plasmodium falciparum trophozoite antigen r45-like protein	Serine/Threonine protein kinase PFI0110c-like	3.6933
	PF14_0423	23509645	Ser/Thr protein kinase, putative	Gcn2-like Ser/thr protein kinase.	3.3058
	MAL1P2.04, PFA0380w	23613435	Serine/threonine protein kinase, putative	Gcn2-like Ser/thr protein kinase.	2.9825
	PF11_0239	23508430	Hypothetical protein	CDP1. calcium/calmodulin dependent protein kinase with a 2EF hand + S/T kinase domain and 4 calmodulin like EF hands	3.0830
	MAL3P3.17, PFC0420w	23957748	Calcium-dependent protein kinase, putative	calcium/calmodulin dependent protein kinase with a S/T kinase domain and 4 calmodulin like EF hands 23508430	3.4104
	MAL13P1.196	23619326	Protein kinase, putative	protein kinase, CMGC/MAPK group	0.4981
	PF14_0323	23509545	Calmodulin	calmodulin. EF hands	0.5189
	PF14_0607	23509829	Hypothetical protein	Signal and Tm + EFhand?. Plasmodium specific.	0.4382
Chromatin/ basal-transcription	PFL0455c	23508788	Hypothetical protein	C term 2*C2H2	3.1357
	PFD0200c	23510029	Hypothetical protein	ApiAP2 transcription factor	3.0273
	MAL6P1.39	23612118	Hypothetical protein	ARID/BRIGHT DNA binding domain +tms. **check	3.0394
	PF14_0374	23509596	Hypothetical protein	N terminal Histone-like transcription factor (CBF/NF-Y) and archaeal histone	2.1555
	PF13_0152	23619221	Transcriptional regulatory protein sir2 homologue, putative	Sir2 family of transcriptional regulators NAD-dependent deacetylase 1 (DHS-like NAD/FAD-binding domain fold)	2.4447
	PF11_0061	23508257	Histone H4, putative	Histone H4.	1.8993
	PF11_0062	23508258	Histone H2B	histone H2B	2.4556
	PF07_0030	23612468	<i>P. falciparum</i> strain 3D7 heat shock protein 86	Nuclear NF-kappaB activating protein homolog (possible DNA binding protein)	3.4084
	PF11_0297	23508488	Hypothetical protein	CCR4-NOT transcription	2.7734

				complex, subunit 2; NOT2. C terminal Regena domain.	
	PF13_0060	23619049	Hypothetical protein	Coiled coil. Meiosis-specific nuclear structural protein 1 *	3.0638
	MAL13P1.75	23619093	Hypothetical protein	1 .. 250 pinin/SDK/memA/ protein conserved region. Also found in C term of M3KA map kinase.	2.5965
	PF11_0477	23508664	CCAAT-box DNA binding protein subunit B	CCAAT-box DNA binding protein . has C terminal Histone-like transcription factor (CBF/NF-Y) and archaeal histone	0.3613
	MAL13P1.275	23619478	Hypothetical protein	RNA pol II carboxy terminal domain phosphatase of the HAD superfamily with a BRCT domain at the C-terminus	0.4287
Stress response/ protein stability	PF11_0034	23508230	Hypothetical protein	Tms + DnaJ (expansion in falciparum). Caj1p/ SPBC3E7.11c	3.4855
	PFB0920w	23593332	Hypothetical protein	Tms + DnaJ (expansion in falciparum). Caj1p/ SPBC3E7.11c	2.7892
	PFB0925w	23593335	Hypothetical protein	Tms + DnaJ (expansion in falciparum). Caj1p/ SPBC3E7.11c	3.1013
	PFL0055c	23508708	Protein with DNAJ domain (resa-like), putative	Tms + DnaJ (expansion in falciparum). Caj1p/ SPBC3E7.11c	9.5113
	PF11_0512	23508688	Ring-infected erythrocyte surface antigen 2, RESA-2 - malaria parasite (Plasmodium falciparum)-re	Tms + DnaJ (expansion in falciparum). Caj1p/ SPBC3E7.11c	3.6282
	PFB0085c	16804917	Hypothetical protein	tm + DnaJ (expansion in falciparum). Caj1p/ SPBC3E7.11c	2.9966
	PFB0090c	23593261	Hypothetical protein, conserved	tm + DnaJ (expansion in falciparum). Caj1p/ SPBC3E7.11c	3.1575
	PF10_0378	23508181	Hypothetical protein	Tm + DnaJ (expansion in falciparum). Caj1p/ SPBC3E7.11c	4.1891
	PFA0660w	23613489	Protein with DNAJ domain, dnj1/sis1 family	DnaJ (expansion in falciparum). Caj1p/ SPBC3E7.11c	3.4420
	MAL1P4.13, PFA0675w	23613492	<i>P. falciparum</i> RESA-like protein with DnaJ domain	DnaJ (expansion in falciparum). Caj1p/ SPBC3E7.11c. N term plasmodium specific	3.2830
	PFD0080c	23510008	Hypothetical protein	N terminal locomplexity + c term domain common with N term of Caj1p/ SPBC3E7.11c. No DnaJ	2.8611
	PF08_0054	23612827	Heat shock 70 kDa protein	dnaK-type molecular chaperone hsp70. RnaseH fold	5.2863
	PF07_0029	23612467	Heat shock protein	Hsp90a ATPase	2.3642

			86		
	PFI0925w	23613707	Gamma-glutamylcysteine synthetase	GSH1-like gamma-glutamylcysteine synthetase (Glutamate-cysteine ligase)	2.3342
	MAL8P1.126	23612937	Serine protease, putative	DegP Serine protease.	2.4816
	PF08_0121	23612960	Peptidyl-prolyl cis-trans isomerase precursor	cyclophilin type peptidyl-prolyl cis-trans isomerase	0.3560
	PF11_0124	23508316	Hypothetical protein	TPR repeats (thats found in c term on other PPIs, but N term does not have ppi)	0.3650
	MAL3P2.31, PFC0310c	16805167	ATP-dependent CLP protease, putative	?. signal? + ATP-dependent Clp protease. Bacterial transfer	0.3868
	PFB0585w	16805016	Leu/Phe-tRNA protein transferase, putative	C terminal Leu/Phe-tRNA protein transferase	0.3891
	PF11_0443	23508632	Hypothetical protein, conserved	Signal and Tm. Signal+DnaJ+Tm+Tm	0.4718
	PF11_0216	23508407	Hypothetical protein	Heat shock factor binding protein 1 Hsbp1 protein	0.2629
	MAL8P1.140	23612964	Methionine aminopeptidase, putative	Secreted??. methionine aminopeptidase (with MYND finger at N-terminus - degraded??)	0.2785
Ubiquitin-proteasome pathway	PFE1355c	23613293	Ubiquitin carboxyl-terminal hydrolase, putative	Ubp6p-like Ubiquitin carboxyl-terminal hydrolase 6	0.4220
	PF11_0271	23508462	Hypothetical protein, conserved	ubiquitin-activating enzyme E1 Atg7p-like. ThiF domain +ZnF	0.4564
	PF14_0576	23509798	Ubiquitin carboxyl-terminal hydrolase, putative	Ubiquitin carboxyl-terminal esterase L3	0.4259
	MAL3P6.28, PFC0845c	16805275	Ubiquitin--protein ligase, putative	RING finger domain Ubiquitin-E3 Ligase	0.3755
	PF14_0315	23509537	Hypothetical protein	3 RingFingers (possible E3?)	0.4065
	PF07_0112	23612640	Proteasome subunit alpha type 5, putative	Pup2p/PSA5-like Proteasome subunit. Ntn hydrolase-like fold	0.3473
	MAL13P1.270	23619461	Proteasome subunit, putative	proteasome subunit alpha2, protease of the acylase family and NTN hydrolase fold	0.3367
	PF11545c	23613831	Proteasome precursor, putative	Pre3p/proteasome regulatory subunit beta type 6, NTN hydrolase fold	0.4070
	PF13_0264	23619427	Hypothetical protein	N term ThiF. Smt3 activating enzyme 1	0.3541
	MAL13P1.337	23619591	Skp1 family protein, putative	Skp1-like POZ+Skp1 dimerisation domain-like	0.3696
Cytoskeleton	PF14_0725	23509947	Tubulin, putative	tubulin Tub2p-like	3.4060
	PF13_0238	23619368	Conserved protein, putative	POZ+kelch domain protein with kelch repeats at the C-terminus	3.2512
	MAL7P1.162	23612663	Dynein heavy chain, putative	Dynein heavy chain	2.5838
	PFI1450c	23613812	Hypothetical protein, conserved	KPL2 (Highly conserved cytoskeletal protein, probably associated with the	2.1624

				microtubules)	
	PF13_0326	23619535	Actin-depolymerizing factor, putative	ADF3 actin-depolymerizing factor 3 (Gelsolin-like fold)	0.4425
Cell Surface and adhesion	PF10_0006	23507812	Rifin	Signal and Tm. RIFIN	8.2227
	PF11_0529	23508221	Rifin	RIFIN.	4.1527
	MAL3P8.2,PFC0010c	16805109	Rifin	RIFIN <i>Plasmodium falciparum</i> expansion	3.6979
	MAL6P1.11	23612085		RIFIN	
	PFL0025c	23508702		RIFIN	
	PFE0020c,PF E0025c	23613031	Rifin	RIFIN	2.3079
	MAL3P7.54, PFC1115w	16805327	Rifin (3D7-rifT3-7)	RIFIN	4.1643
	PFA0710c,PF A0760w	23613505	Rifin	RIFIN	4.3384
	MAL1P1.9a, PFA0010c	23613364	Rifin	RIFIN	3.4359
	PF10010c	23613525	Rifin	RIFIN	2.2716
	PF14_0006	23509229	Rifin	RIFIN	4.3802
	PFD0015c	23509996	Rifin	RIFIN	4.5094
	PFD0030c	23509999	Rifin	RIFIN	3.8534
	PF14_0040	23509261	Hypothetical protein	Secreted. 2*CxxxC..Cx CxCxC cluster. Ortholog of ookinite SOAP	4.6892
	PF13_0193	23619287	MSP7-like protein	Signal and Tm. merozoite surface protein 7 precursor. <i>falciparum</i> expansion 23619289	2.3551
	PF14_0010	23509233	Glycophorin binding protein-related antigen	TM + Glycophorin-binding repeats. Glycophorin-binding protein	5.6427
	PF08_0050	23612822	Hypothetical protein	Tm+MAC/Perforin domain. The membrane-attack complex (MAC) of the complement system forms transmembrane channels. These channels disrupt the phospholipid bilayer of target cells,	4.5025
	MAL8P1.135	23612951	Hypothetical protein	<i>C.elegans</i> DPY-19-like protein KIAA0877-like transmembrane protein. Involved in host interactions (Animal transfer)	0.2786
	MAL1P3.12, PFA0650w	23613486	Hypothetical protein	Plasmodium specific. N term conserved domain in vir proteins with Cs	2.9194
	MAL7P1.1,MAL7P1.55	23612504	erythrocyte membrane protein 1 (PfEMP1)	erythrocyte membrane protein 1. Plasmodium <i>falciparum</i> erythrocyte membrane protein (PFEMP)	2.7521
	PF11830c	23613888	Erythrocyte membrane protein 1 (PfEMP1)	erythrocyte membrane protein 1. Plasmodium <i>falciparum</i> erythrocyte membrane protein (PFEMP)	2.8396
	PFL1950w	23509084	Erythrocyte membrane protein 1 (PfEMP1)	erythrocyte membrane protein 1. Plasmodium <i>falciparum</i> erythrocyte membrane protein (PFEMP)	3.0453

	MAL6P1.1	23612086		erythrocyte membrane protein 1. Plasmodium falciparum erythrocyte membrane protein (PFEMP)	
	PFB0975c	23593349	Erythrocyte membrane protein 1 (PFEMP1), truncated	erythrocyte membrane protein 1. PFEMP1 . Fragment	2.9507
	PF14_0491	23509713	Hypothetical protein	Apicomplexa group. carbohydrate binding beta fold Anthrax protective antigen IACC.	2.4579
	PF11_0486	23508673	MAEBL, putative	Signal and Tm. maeb1-like erythrocyte binding protein	2.4793
	MAL13P1.174	23619289	MSP7-like protein	Secreted. merozoite surface protein 7 precursor. falciparum expansion 23619287	0.2597
	PFE0075c	23613039	Rhoptry-associated protein, putative	Secreted. rhoptry-associated protein 3 23613040 ?	0.4930
	PFE0080c	23613040	Rhoptry-associated protein 2	Secreted. rhoptry-associated protein 3 23613039 ?	0.3951
	PF11730w	23613868	Cytoadherence linked asexual protein (CLAG)	cytoadherence linked asexual protein	0.4067
Secretion/ protein trafficking system	PF11_0352	23508543	Protein disulfide isomerase related protein	ER-lumen PDA6-like protein disulfide isomerase. Thioredoxin domain	0.3672
	PF10_0337	23508140	ADP-ribosylation factor-like protein	ADP-ribosylation factor ARF-like small GTPases	0.2285
	PF10215c	23613565	signal peptidase, putative	microsomal signal peptidase SP22-like	0.3111
	PF14_0361	23509583	Translocation protein sec62, putative	SEC62-like transmembrane protein	0.4756
	MAL13P1.51, PF13_0057	23619044	Rab5B protein	RAS small GTPases RIC1/ypt1	0.4101
	PF10155c	23613553	Ras family GTP-ase, putative	Secreted. Rab7 GTPase	0.4085
	PF14_0064	23509285	Vacuolar protein sorting 29, putative	vacuolar protein sorting 29 (derived version of the Calcineurin-like phosphoesterase fold)	0.4536
	MAL13P1.171	23619274	Transmembrane protein Tmp21 homologue, putative	Signal and Tm, G252-like Glycoprotein 25L2. emp24/gp25L/p24 family GOLD domain	0.3396
	MAL13P1.167	23619255	Signal peptidase, putative	Tm + Sec11p-like signal peptidase 18 (Peptidase S24-like) +2 Tms	0.3554
	PFE1265w	23613275	G-protein coupled receptor, putative	Belongs to the family of LanC like lantothionine synthesizing enzyme (Cysteine+didehydroserine/threonine= lantothionine)	0.4185
Known transporters	PF11_0412	23508602	Vacuolar ATP synthase subunit F, putative	Vacuolar ATP synthase subunit F,	0.3537
	PF13_0130	23619182	Vacuolar ATP synthase subunit g, putative	Vacuolar ATP synthase subunit G 1 . No ATPase	0.3921
	PF11_0141	23508332	UDP-galactose	UDP-Gal transporter	0.2303

			transporter, putative		
	PFE0410w	23613106	Triose or hexose phosphate / phosphate translocator, putative	triose phosphate/3-phosphoglycerate/phosphate Transporter	0.3093
	MAL8P1.32	23612771	Nucleoside transporter, putative	nucleoside transporter,	0.4034
	PFB0535w	23593300	Hypothetical protein	GDP-fucose transporter 1	0.4416
	MAL3P6.6,PFC0725c	16805250	Transporter, putative	formate/nitrite transporter	0.4564
	MAL1P1.40, PFA0245w	23613408	Hypothetical protein	Novel Major facilitator superfamily transporter	0.3877
Glycosylation/ GPI-anchor	PFL2510w	23509192	Chitinase	Secreted. chitinase. Glycosyl hydrolases family 18. Tim-Barrel only	2.9820
	MAL13P1.165	23619250	Hypothetical protein	Tms + GPI transamidase component PIG-U (Phosphatidylinositol-glycan biosynthesis, class U protein)	0.3533
	PF11_0298	23508489	GPI8p transamidase	Signal and Tm. gpi8 transamidase. Signal + Peptidase C13 family+TM	0.3398
	MAL13P1.210	23619347	Hypothetical protein	PigB. phosphatidylinositol glycan, class B (Alg9-like mannosyltransferase family). dolichyl-phosphate-mannose-glycolipid alpha-mannosyltransferase involved in GPI anchor biosynthesis	0.4608
	PFL0685w	23508834	Hypothetical protein	Gpi13p/PIGO-like. Tm + Type I phosphodiesterase / nucleotide pyrophosphatase + Tms	0.2917
	PFB0515w	16805002	Hypothetical protein	Signal and Tm . CG6308-like Signal + Glycosyltransferase family 28 N-terminal domain (UDP-Glycosyltransferase/glycogen phosphorylase fold 1NLM) + tms	0.3880
	PF11_0487	23508674	Hypothetical protein	* has Tm. TM . Found in Apicomplexans, plant and Dictyostelium O-linked N-acetylglucosamine transferase, SPINDLY family [Posttranslationalmodification, protein turnover, chaperones	0.3870
DNA repair/ Replication/ cell division	PF10_0369	23508172	Helicase, putative	RAD25 DNA Helicase	2.7682
	PF14_0560	23509782	Hypothetical protein	Dem1p-like. RecB family nuclease	2.6910
	MAL13P1.229	23619383	Hypothetical protein	kinetochore protein Spc25 spindle pole body component 25	0.4871
	PF11_0249	23508440	Hypothetical protein	Smc like ABC ATPase involved in DNA repair	0.4008

	PF11_0332	23508523	Hypothetical protein	RP-A-like OB-fold nucleic acid binding domain	0.3539
	PF11_0117	23508310	Replication factor C subunit 5, putative	replication factor C. P-loop atpase	0.3798
	PF14_0254	23509476	DNA mismatch repair protein Msh2p, putative	Msh2/MutS like ABC ATPase involved in DNA repair	0.4426
	PFD0530c	23510096	Hypothetical protein	ylqF-like GTPase	2.2745
	PF14_0339	23509561	Hypothetical protein	Era-like GTPase	2.5875
	PFL0835w	23508863	GTP-binding protein, putative	ENGA-like GTPase. GTP-binding protein (bacterial)	3.1707
	MAL7P1.93	23612555	Mitochondrial ribosomal protein S8, putative	30S ribosomal protein S8	2.0939
	PF14_0027	23509248	Ribosomal S27a, putative	ubiquitin / ribosomal protein S27a Ubiquitin+Znr Ubi3p. Translation	0.2346
	PF14_0240	23509462	Ribosomal protein L21e, putative	ribosomal protein L21	0.2732
	PF13_0171	23619260	60S ribosomal protein L23, putative	ribosomal protein L23, putative	0.3581
	PF14_0709	23509931	Ribosomal protein L20, putative	ribosomal protein L20	0.3455
	MAL3P2.27, PFC0290w	16805163	40S ribosomal protein S23, putative	ribosomal protein S23. S1 domain RBD. Translation	0.3663
	PF13_0045	23619020	40S ribosomal protein S27, putative	ribosomal protein S27	0.2989
	MAL3P2.28, PFC0295c	16805164	40S ribosomal protein S12, putative	ribosomal protein S12. Pelota. Translation	0.3289
	PF11_0382	23508572	Ribosomal protein S9, putative	ribosomal protein S9	0.4282
	PFI0375w	23613597	Ribosomal protein L35 with long N-terminal extension, putative	ribosomal protein L35	0.3780
	PFE0545c	23613132	Histamine-releasing factor, putative	TCTP (potential GDI for eEF1 GTPase) Mss4-like fold, may also have cytoskeletal role	0.4065
	PF10_0038	23507842	Ribosomal protein S20e, putative	ribosomal protein S20e	0.4106
	MAL3P7.35, PFC1020c	16805310	40S ribosomal protein S3A, putative	ribosomal protein S3a	0.3487
	PF11_0386	23508576	30S ribosomal protein S14, putative	Ribosomal protein S14	0.4590
	PFB0888w	23593330	Hypothetical protein	ribosome associated membrane protein 4. RAMP4	0.4842
Lipid/fatty acid/ isoprenoid metabolism	PFB0695c	16805038	Acyl-CoA synthetase	Secreted. long-chain acyl-CoA synthetase (AMP-binding enzyme)	3.3677
	PF14_0751	23509972	Fatty acyl coenzyme A synthetase-1, putative	Secreted. long-chain acyl-CoA synthetase (AMP-binding enzyme)	3.6245
	PFL0035c	23508704	Octapeptide-repeat antigen, putative	Secreted. long-chain acyl-CoA synthetase (AMP-binding enzyme)	2.1448
	PF14_0155	23509376	Hypothetical protein	Sphingolipid biosynthesis; Signal + Tm + Aminotransferase class I and	3.1630

				II . Lcb2p-like serine C-palmitoyltransferase	
	PF14_0017	23509238	Lysophospholipase, putative	lysophospholipase homolog; alpha/beta-hydrolase fold 23509960	6.0919
	PF14_0738	23509960	Lysophospholipase, putative	lysophospholipase homolog; alpha/beta-hydrolase fold (N terminal Tm)	2.3505
	PF14_0298	23509520	Hypothetical protein	CTL2/NG22 family possible lipid transporter	0.4245
	PF14_0453	23509675	Hypothetical protein	SPAC1783.02c/Vps66p - like membrane associated Phosphate acyltransferases (plsC)	0.1503
	PF10_0016	23507820	Acyl CoA binding protein, putative	Acyl-CoA Binding Protein. pdb 1HBK	0.3188
	PFL0415w	23508780	Acyl carrier protein, mitochondrial precursor, putative	Acp1p family acyl carrier protein. PP-binding, Phosphopantetheine attachment domain	0.2840
	PFL0695c	23508836	Geranylgeranyl transferase type2 beta subunit, putative	geranylgeranyl transferase type2 beta. Tm + Prenyltransferase and squalene oxidase repeats	0.4379
	PFB0420w	16804983	2C-methyl-D-erythritol 2,4-cyclodiphosphate synthase	Tm + 2C-Methyl-D-erythritol 2,4-cyclodiphosphate synthase (Bacillus chorismate mutase-like fold) Nonmevalonate terpenoid biosynthesis pathway; fifth step. 2-phospho-4-(cytidine5'-diphospho)-2-C-methyl-D-erythritol = 2-C-methyl-D-erythritol2,4-cyclodiphosphate + CMP.	0.3193
	PF11_0370	23508561	Hypothetical protein	Tsc13p/synaptic glycoprotein sc2 (RHP methylase)	0.4522
	PFB0385w	23593289	Acyl carrier protein, putative	Secreted. acyl carrier protein	0.3381
	PF13_0285	23619464	Hypothetical protein, conserved	phosphoinositide phosphatase (synaptojanin-like phosphatase domain)	0.3397
Miscellaneous enzymatic activities	PFL1260w	23508946	Hydrolase / phosphatase, putative	Cof-like hydrolases of the HAD superfamily (bacterial)	5.7777
	MAL8P1.154	23612987	Hypothetical protein	amine oxidase, flavin-containing + C term C cluster (2 Ring finger?)	3.3963
	PF14_0384	23509606	Hypothetical protein	Allantoicase	3.5750
	MAL6P1.41	23612120	Hypothetical protein	A protein with C2 domain +Transglutaminase-type peptidase domain, found in all apicomplexans	2.9111
	PF14_0664	23509886	Biotin carboxylase subunit of acetyl CoA carboxylase, putative	acetyl-CoA carboxylase; Carbamoyl-phosphate synthase L chain, N-terminal domain + ATP binding domain +Biotin carboxylase C-terminal domain	2.4515

				+biotin_lipoyl domain +Carboxyl transferase domain	
	PF14_0415	23509637	Dephospho-CoA kinase, putative	CoaE-like Dephospho-CoA kinase (bacterial). P-loop ATPase	0.4724
	PF10505c	23613623	Hypothetical protein	selenide, water dikinase (AIR synthase related protein, C-terminal domain). N term plasmodium specific.	0.4484
	PFB0590w	16805017	Hypothetical protein	Monoxygenase (Ferrodoxin-like fold related to bacterial antibiotic synthesis monooxygenases 1N5V)	0.4218
	PF14_0248	23509470	Ubiquinol-cytochrome c reductase hinge protein, putative	Ubiquinol-cytochrome C reductase hinge protein	0.3888
	PFL0490c	23508795	Hypothetical protein	ATP11 - like. ATP synthase mitochondrial F1 complex assembly factor 1	0.4014
	MAL13P1.248	23619414		Hydrolase of MutT (Nudix) family. (bacterial)	
	PF13_0349	23619586	Nucleoside diphosphate kinase b; putative	NM23/NDPK-A nucleoside diphosphate kinase (Ferrodoxin-like fold)	0.3860
	PF14_0641	23509863	1-deoxy-D-xylulose 5-phosphate reductoisomerase	1-deoxy-D-xylulose 5-phosphate reductoisomerase (bacterial)	0.3778
	MAL7P1.114	23612585	T gondii P36-like protein	apicomplexan P36 family of proteins, appears to be a divergent HAD family phosphatase	0.3387
	PF11340w	23613790	Fumarate hydratase, putative	fumarate hydratase class I (bacterial)	0.3203
	PFD0350w	23510061	Hypothetical protein, conserved	has Tm + Oms1p-like ubiE ubiquinone/menaquinone biosynthesis methyltransferase	0.3302
Miscellaneous proteins with conserved domains	MAL8P1.14	23612733	Hypothetical protein	Oxa1 (mitochondrial membrane protein involved in assembly of inner membrane complexes)	0.3717
	PF14_0566	23509788	Hypothetical protein	Optic atrophy 3 protein (OPA3) (Mitochondrial function associated protein ?)	0.2847
	PFB0425c	23593293	Hypothetical protein	Ymr027wp/CG11474-like C terminal domain. brings C terminus of Pank4 pantothenate kinase 4	2.3522
	PFL2205w	23509133	Hypothetical protein	C rich middle domain of vacuolar sorting receptor + TM	4.7076
	PF11_0480	23508667	Hypothetical protein	Low complexity. c term C cluster/ZnF	2.3660
	PFD0875c	23510165	Hypothetical protein	Plasmodium specific. N terminal domain same as N term of SIT4-ASSOCIATING PROTEIN	2.1893

				SAP185 -like *	
	PF08_0065	23612855	Hypothetical protein, conserved	WD40 rpts	3.1236
	MAL13P1.139	23619205	Hypothetical protein, conserved	TPR repeats TTCB-like	0.2462
	MAL13P1.172	23619275	Hypothetical protein, conserved	Human AMMECR1 ortholog (highly conserved enzyme with GCIG motif) protein	0.3828
	MAL13P1.257	23619434	Hypothetical protein, conserved	Ycr090cp/CG4646-like highly conserved cysteine **	0.2750
	PF14_0383	23509605	Hypothetical protein	B-box zinc finger domain containing protein	0.4570
	MAL3P5.12, PFC0630w	16805233	Hypothetical protein	SWIM zinc finger	0.4220
	PFC0126c	16805130	Hypothetical protein	ZnF. (CDGSH-type zinc finger)	0.4900
	PFE0420c	23613108	Guanidine nucleotide exchange factor, putative	RCC1 domain containing protein	0.3942
	PFB0770c	23593320	Hypothetical protein	apicomplexan-specific transmembrane protein	0.3296
	PF10_0215	23508018	Hypothetical protein	CG17219/Yil110wp methyltransferase	0.4077
	PF10_0140	23507944	Hypothetical protein	SPRY domain (artificial fusion of membrane protein and Nuclear membrane SPRY domain)	0.4242
	MAL3P5.4, PFC0590c	23820927	Hypothetical protein	Signal and Tm. Plasmodium specific. Der1-like family+tm Check	0.4453
	MAL3P6.7, PFC0730w	16805251	Conserved protein, putative	Yop1p-like TB2/DP1, HVA22 family (deleted in polyposis)	0.3693
	PF13_0106	23619137	Hypothetical protein	KIAA1390-like protein. conserved in eukaryotes	2.8741
	MAL7P1.3	23612418	Hypothetical protein, conserved	integral membrane protein PFB0995w-like 23613539	2.4243
	PFB0095c	16804919	Erythrocyte membrane protein 3	low complexity GQQNTGLKNTPSE repeats	2.6210
	PFD0075w	23510007	Hypothetical protein, conserved in <i>P. falciparum</i>	Signal and Tm. N terminal alpha helical (EKLEKEIL rpts) Falciparum specific C terminus with H and C	2.3968
	MAL3P5.20, PFC0680w	23820932	Hypothetical protein	Apicomplexan specific. large low complexity with PFL0360c pfal like Znfinger	3.6691
	PF14_0263	23509485	Hypothetical protein	WD40s + Low complexity	2.6197
	PF14_0505	23509727	Hypothetical protein	Apicomplexa group.N term C cluster (found in N term of Dynactin)	2.5818
	MAL8P1.139	23612963	Hypothetical protein	Plasmodium specific. Wd40+Tms+Wd40	0.3483
	PF10085c	23613539	Hypothetical protein	integral membrane protein PFB0995w-like	0.2974
	PF14_0369	23509591	Hypothetical protein	Transmembrane protein (paralogs 23509591 and 23509433)	0.2253
	MAL13P1.329	23619577		Transmembrane protein	
	MAL3P7.36, PFC1025w	16805311	F49C12.11-like protein	Either RNA and not protein or exon of some other	0.3045

				protein. 54aa No hit	
	PF14_0169	23509390	Hypothetical protein	RNA not protein?	0.3826
Apicomple xa specific	PF10_0033	23507837	Hypothetical protein	Conserved CDRxxxDxHD	0.2790
	PF13_0246	23619390	Hypothetical protein		0.3029
	PFD0760c	23510141	Hypothetical protein		0.3328
	PFL0640w	23508825	Hypothetical protein		0.3598
	PFE1025c	23613227	Hypothetical protein		0.3605
	PFE1555c	23613330	Hypothetical protein		0.3473
	MAL13P1.14 3	23619210	Hypothetical protein		0.3518
	PFC0281w	23957734	Hypothetical protein		0.3716
	PF10_0048	23507852	Hypothetical protein		0.3770
	PFE0620c	23613147	Hypothetical protein		0.3877
	PFI0870w	23613696	Hypothetical protein		0.4074
	PF13_0337	23619558	Hypothetical protein		0.3831
	MAL7P1.74	23612526	Hypothetical protein	Secreted. conserved Cs	0.3989
	PFE1175w	23613257	Hypothetical protein		0.3756
	PF14_0186	23509407	Hypothetical protein		0.4078
	PF10_0029	23507833	Hypothetical protein		0.4056
	PFD0365c	23510064	Hypothetical protein		0.4207
	PF13_0249	23619393	Hypothetical protein		0.4312
	MAL1P1.48, PFA0285c	23613416	Hypothetical protein		0.4474
	PF14_0592	23509814	Hypothetical protein		0.4678
	PF07_0014	23612440	Hypothetical protein	CxD repeats	2.2927
	PFI0495w	23613621	Hypothetical protein	Low complexity	2.2368
	MAL13P1.12 3	23619171			
	MAL6P1.100	23612180	Hypothetical protein	C and N term C cluster.	2.3571
	PF10_0350	23508153	Hypothetical protein	Secreted.low complexity repeats	2.2277
	PF14_0531	23509753	Hypothetical protein		2.4436
	PF14_0512	23509734	Hypothetical protein	chk	2.4689
	MAL1P1.18, PFA0135w	23613386	Hypothetical protein	Secreted. Tryptophan rich	2.4741
	MAL6P1.200	23612306	Hypothetical protein		2.3881
	PF10_0296	23508099	Hypothetical protein		2.4606
	PF10_0292	23508095	Hypothetical protein	low complexity repeats	2.5240
	PFL1025c	23508899	Hypothetical protein	Low complexity	2.5846
	MAL13P1.11 2	23619152	Hypothetical protein		2.8576
	PF14_0165	23509386	Hypothetical protein		2.9722
	PF10_0284	23508087	Hypothetical protein		3.0492
	PFE0070w	23613038	Interspersed repeat antigen, putative	Low complexity	3.2486
	PF10_0265	23508068	Hypothetical protein	Conserved Cs,D and H metal binding	3.3591
	PF14_0544	23509766	Hypothetical protein		3.3824
	PF10_0161	23507965	Hypothetical protein	<i>Plasmodium falciparum</i> expansion	4.7357
	PFD0435c	23510078	Hypothetical protein	Signal and Tm. <i>Plasmodium</i> specific (C term YYDD patch)	4.9040
	PF14_0211	23509433	Hypothetical protein	Signal and Tm. Transmembrane protein (paralogs 23509591 and 23509433)	0.1936
	MAL3P7.34,	16805309	Hypothetical protein	Plasmodium Specific	0.2285

	PFC1015c			expansion	
	MAL3P5.18, PFC0670c	16805238	Hypothetical protein	Secreted*. <i>Plasmodium</i> specific	0.2693
	PFE1315w	23613285	Hypothetical protein	<i>Plasmodium</i> and <i>Theileria</i> specific	0.2789
	PF11_0146	23508337	Hypothetical protein	Apicomlexan specific.	0.2938
	PFB0810w	23593322	Hypothetical protein	<i>Plasmodium</i> and <i>Theileria</i> specific.	0.2943
	PF07_0081	23612568	Hypothetical protein	<i>Plasmodium</i> and <i>Theileria</i> specific	0.3061
	PF11_0309	23508500	Hypothetical protein	<i>Plasmodium</i> specific	0.3478
	PF11_0215	23508406	Hypothetical protein	<i>Plasmodium</i> specific. has cxxc	0.3388
	PFB0395w	16804978	Hypothetical protein	Signal. <i>Plasmodium</i> specific	0.3384
	PFI0575c	23613637	Hypothetical protein	<i>Plasmodium</i> specific.	0.3377
	PFB0886c	23593329	Hypothetical protein	<i>Plasmodium</i> specific.	0.3472
	MAL3P6.23, PFC0820w	16805269	Hypothetical protein	Apicomplexa specific	0.3467
	PFD0940w	23510178	Hypothetical protein	Signal and Tm. <i>Plasmodium</i> specific *	0.3890
	PF10_0059	23507863	Hypothetical protein	<i>Plasmodium</i> Specific.	0.3360
	MAL1P1.31, PFA0205w	23613400	Hypothetical protein	<i>Plasmodium</i> specific	0.3594
	PFC0261c	23957729	Hypothetical protein	<i>Plasmodium</i> specific. chk	0.3582
	PFE0910w	23613204		<i>Plasmodium</i> specific	
	PF14_0691	23509913	Hypothetical protein	Signal+ Tms. Apicomplexa specific	0.3924
	PFE0295w	23613083	Hypothetical protein	<i>Plasmodium</i> specific	0.3819
	PFL0720w	23508841	Hypothetical protein	Apicomplexan specific transmembrane protein	0.3901
	PF11_0064	23508260	Hypothetical protein	Signal and Tm. <i>Plasmodium</i> specific	0.4158
	MAL7P1.17	23612443	Hypothetical protein	<i>falciparum</i> specific	0.4309
	PF07_0118	23612647	Hypothetical protein	<i>Plasmodium</i> specific	0.3955
	PF14_0572	23509794	Hypothetical protein	<i>Plasmodium</i> specific. conserved C and Hs	0.4003
	PF07_0082	23612569	Hypothetical protein	<i>Plasmodium</i> specific. None	0.4038
	PF14_0253	23509475	Hypothetical protein	<i>Plasmodium</i> specific	0.4561
	MAL3P6.2,P FC0705c	16805246	Hypothetical protein	<i>Plasmodium</i> Specific	0.4446
	PFC0282w	23957735	Hypothetical protein	Signal and Tm. <i>Plasmodium</i> specific. chk	0.4426
	MAL13P1.14 I	23619208		<i>Plasmodium</i> and <i>Theileria</i> specific.	
	PF14_0394	23509616	Hypothetical protein	<i>Plasmodium</i> specific	0.4868
	MAL8P1.152	23612981	Hypothetical protein	Apicomplexan specific. ???	2.2519
	PFB0075c	16804915	Hypothetical protein	<i>falciparum</i> specific (3 to 4)	2.3527
	PFE0065w	23613037	Skeleton binding protein	<i>falciparum</i> specific. Low complexity	2.3181
	PFL1055c	23508905	Hypothetical protein	<i>Plasmodium</i> specific	2.6650
	PF07_0028	23612465	Hypothetical protein	<i>Plasmodium</i> specific.	2.6676
	PFE1180c	23613258	Hypothetical protein	<i>Plasmodium</i> specific	2.7667
	PF07_0107	23612628	Hypothetical protein	<i>falciparum</i> specific. Low complexity	3.0758
	PFB0106c	23593263	Hypothetical protein	<i>Plasmodium</i> specific	3.2894
	PF11_0038	23508234	Hypothetical protein	<i>Plasmodium</i> specific	3.3874
	MAL3P8.15, PFC0085c	16805122	Hypothetical protein	<i>Plasmodium</i> specific	5.1610
	PFD0225w	23510034	Hypothetical protein	<i>Plasmodium</i> specific	5.4695
Low	PF14_0153	23509374	Hypothetical protein	<i>Plasmodium</i> specific	0.2318

complexity					
	PFC1011c	23957783	Hypothetical protein		0.2488
	PFL0170w	23508731	Hypothetical protein	Signal + TMs	0.2572
	PF08_0060	23612843	Asparagine-rich antigen		2.0623
	PF14_0404	23509626	Hypothetical protein	<i>Plasmodium</i> specific some conserved Cs.	2.1419
	PF10_0024	23507828	Hypothetical protein	<i>Plasmodium</i> Specific	2.5498
	PFB0650w	16805029	Hypothetical protein		2.5639
	PFI1520w	23613826	Hypothetical protein		2.6034
	PF14_0029	23509250	Hypothetical protein	<i>Plasmodium</i> specific	2.7968
	PFL0070c	23508711	Hypothetical protein	Tm	2.9539
	MAL7P1.171	23612672		Tm	
	PFI1720w	23613866	Hypothetical protein		2.9353
	PFD0545w	23510099	Hypothetical protein		3.3289
	PF14_0706	23509928	Hypothetical protein	with GAQNT rpts	3.3462
	MAL13P1.125	23619174	Hypothetical protein		3.4659
	PF14_0644	23509866	Hypothetical protein		3.4668
	PF14_0758	23509979	Hypothetical protein		4.3368
	PF14_0631	23509853	Hypothetical protein		3.2463
	MAL13P1.313, PF13_0332	23619548	Hypothetical protein		3.8527
	PF11_0035	23508231	Hypothetical protein	Coiled coil	5.2519
No Hits	PF11_0459	23508646	Hypothetical protein	Signal and Tm.	0.2852
	MAL8P1.86	23612865	Hypothetical protein		0.3198
	PF14_0299	23509521	Hypothetical protein	C cluster	0.3589
	PFI0405w	23613603	Hypothetical protein	Signal and Tm.	0.3779
	PF10_0207	23508010	Hypothetical protein		0.4046
	PF10_0065	23507869	Hypothetical protein		0.4318
	PF14_0219	23509441	Hypothetical protein		2.7729
	PFL0195w	23508736	Hypothetical protein		2.7961
	PF08_0005	23612719	Hypothetical protein		2.7843
	MAL3P8.14, PFC0080c	16805121	Hypothetical protein		3.0816
	PFB0923c	23593334	Hypothetical protein		8.4170

Chapter 3

The Pathogenesis of Cerebral Malaria

Background. Cerebral malaria (CM) is defined as unarousable coma not attributable to other causes in patients with *Plasmodium falciparum* malaria (9). In contrast to fever, an invariable symptom of infection in non-immune individuals, the clinical outcome of CM occurs in only a minority of malaria cases (approximately 1% of *P. falciparum*-infected individuals). However, although neurological complications are a rare consequence of infection, due to its high mortality rate (15-20%), CM is the most common cause of malaria death. CM primarily affects young children in sub-Saharan Africa and adults in South East Asia (13). This geographical variation in susceptibility to CM is a consequence of differences in the transmission dynamics and therefore immunological status of individuals between the two regions. In Africa, where transmission is intense, the burden of CM lies in young children who mount an ineffective and often dysregulated immune response to the parasite. In South East Asia, where transmission is moderate, primary infection often occurs in adulthood and although the clinical course of CM typically differs by age, little or no immunity in adults also results in susceptibility to CM.

Currently, the prevention and management of CM is limited to the administration of anti-malarial drugs. The development of a vaccine that will prevent disease but not necessarily infection is considered by many scientists to be the best and most cost effective method currently available in reducing deaths caused by CM. Similarly, adjunct therapies that will reverse the rapid clinical deterioration associated with CM are needed. Decades of research have resulted in the development of an effective murine model and the identification of key parasite and host markers of CM. However, a further

understanding of the sequence of events leading to the development of CM and the downstream effector molecules that produce the symptoms of CM will be important in identifying potential anti-disease vaccine candidates and therapeutic drug targets.

The Pathogenesis of CM. Three hypotheses regarding the pathogenesis of CM have been proposed and intensely debated in the field of malaria. The mechanical hypothesis postulates that sequestration, the binding of *P. falciparum* parasitized erythrocytes to the endothelium, causes obstruction of blood flow, tissue hypoxia, and ultimately death (3). The cytokine hypothesis states that a malaria toxin is released on merozoite rupture which elicits an inflammatory response that leads to vascular damage in the brain, coma, and eventually death (5). The permeability hypothesis suggests that a toxin released by the parasite initiates the cascade of events leading to CM by increasing the permeability of the blood brain barrier (BBB) (17). Agreement is now emerging among scientists that CM cannot be explained by any one hypothesis alone but rather is a complex disease initiated by the parasite's ability to sequester and maintained by a multitude of host immunopathological and biochemical processes.

Sequestration. The sequestration of mature forms of parasitized erythrocytes within the brain microvasculature is considered the hallmark of cerebral malaria. Sequestration is the process by which parasites adhere to cells within the body and is a direct consequence of cytoadherence, molecular interactions between parasite molecules found on the surface of the erythrocyte and host molecules on the surface of endothelial cells. Sequestration has been reported in a wide array of host organs including brain, lung, and placental tissue.

Erythrocyte Membrane Protein 1 (EMP1) is believed to be the major parasite protein involved in the process of sequestration. Several features unique to EMP1 make this protein an effective virulence factor. EMP1 is encoded by a polymorphic family of 60 *var* genes (23), and only a single *var* gene is expressed at any given time by the parasite (21). Therefore, despite the relative immunogenicity of the *var* genes, repeated exposure to the parasite is required to develop protective immunity to all members of the *var* family. The principle function of EMP1, cytoadherence to host tissue, prevents filtration and therefore destruction and removal by the spleen. A number of host receptors participate in direct binding to EMP1 but differ by location. ICAM-1 appears to be the major host receptor implicated in sequestration of parasites within the brain (24).

Experimental CM. Similar to *falciparum* malaria, the murine *P. berghei* ANKA strain (Pb-A) of malaria is known for its ability to sequester within the microvasculature and has therefore become the parasite of choice for *in vivo* murine studies of cerebral malaria (9). Infection with Pb-A parasites results in death in 100% of mice. However, the cause of death varies greatly based on the mouse genetic background, and mouse strains are broadly categorized as susceptible or resistant to CM. In susceptible mouse strains (C57BL6 and CBA/J), approximately 80% mice develop cerebral malaria 6-10 days post-infection, and these mice die with relatively low parasitemia (approximately 10%). Experimental CM (ECM) in these mice resembles the features of *P. falciparum* clinical disease in humans including hemi or para-plegia, ataxia, deviation of the head, tendency to roll over upon stimulation, and convulsions (16). Similar to previous studies, we demonstrated the presence of hemorrhaging, lesions, sequestration of monocytes and to a

lesser extent parasitized red blood cells (pRBCs) by histological staining of brain sections from mice with ECM (FIG. 11).

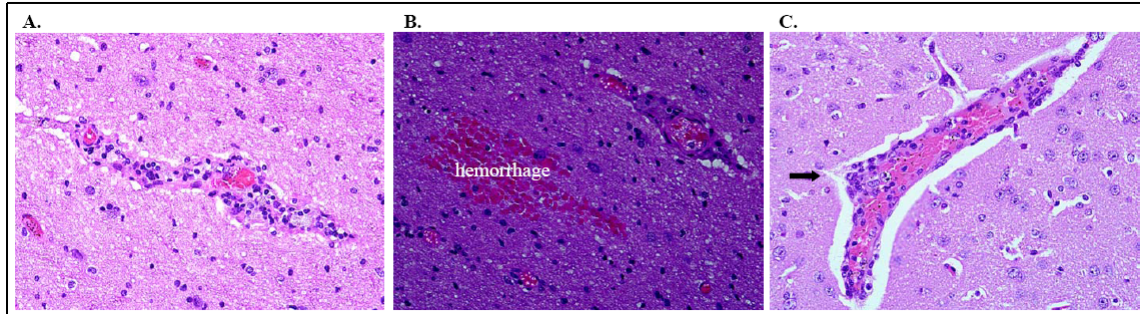


Figure 11. Histological features of ECM. H and E staining of brain tissue collected from susceptible (CBA/J) mice displaying symptoms of ECM demonstrates monocyte sequestration (A), hemorrhaging (B), and the formation of early lesions (C). Malaria pigment in the brain appears white under polarized light (B).

Resistant mice (BALB/c) do not develop any of the clinical or pathological features that resemble cerebral malaria, but instead succumb to anemia and hyperparasitemia approximately 15-18 days after infection with Pb-A. Susceptible mice that do not develop ECM (approximately 20%) follow a clinical course of disease similar to these resistant mice (9, 10, 16). Studies performed using the Pb-A murine model of ECM have illustrated an important role for T cells, Th1 cytokines, and elements of the hemostasis system in the pathogenesis of CM.

T cells. The requirement for T lymphocytes in ECM was initially established by a study demonstrating that athymic nude mice were resistant to ECM when challenged with PbA (11). Immunohistological analysis of human and mouse brain tissue has revealed that mechanical obstruction involves the accumulation of activated leukocytes in addition

to infected red blood cells (11, 19). Studies have suggested that both $CD4^+$ and $CD8^+$ T cells play a key role in the pathogenesis of cerebral malaria. Importantly, $CD4^+$ T cells appear to be critical in the induction of cerebral malaria, whereas $CD8^+$ T cells appear to play an effector role in the terminal stage of cerebral malaria, and recent studies suggest this effector role is mediated by disruption of the blood brain barrier by perforin.

CD4⁺ T cells. Due to the absence of MHC molecules on the surface of mature erythrocytes, an effective antibody response during the short window after schizont rupture and prior to reinvasion is important during blood stage infection of the parasite. While a Th1 mediated immune response is believed to be important in maintaining the parasite burden early in infection, an effective Th2 antibody response is associated with parasite clearance from the host. Several studies have suggested a role of $CD4^+$ T cells in the immunopathogenesis of CM. First, the $CD4^+$ T cell population is increased in the brains of mice with CM relative to those without CM (2). Second, both CD4 deficient mice and mice treated with monoclonal antibodies against CD4 are resistant to CM. However, the timing of CD4 depletion is critical; depletion prior to or early in infection results in resistance to CM (2, 12, 27), whereas depletion later in infection has no effect on susceptibility to CM. This suggests that $CD4^+$ T cells play a role in the induction phase of cerebral malaria.

CD8⁺ T cells. Antibody depletion studies and studies using knockout mice suggest that $CD8^+$ T cells may be principle mediators of CM pathogenesis. Both CD8 knockout (KO) mice (4) and mice homozygous for the null allele of the B2 microglobulin gene (27) are resistant to ECM. While $CD4^+$ T cells appear to play a role in the induction phase of cerebral malaria, depletion studies have demonstrated that $CD8^+$ T cells appear

to play an effector role in the terminal stage of cerebral malaria; antibody depletion of CD8⁺ T cells on day 6 post-infection prevented the development of CM and mice instead died of hyper-parasitemia and anemia in the third week after infection (2). A direct role for CD8⁺ T cells in CM has been implicated by adoptive transfer of splenic CD8⁺ T cells from wildtype mice with CM to RAG-2 deficient mice. CD8⁺ T cells were shown to migrate to the brain and induce CM shortly after administration of splenic CD8⁺ T cells (19). Phenotyping of the CD8⁺ T cell population has established that CD8 V β 8.1,2⁺ T cells are increased in the peripheral blood (4) and also form 50% of the $\alpha\beta$ CD8⁺ T cells in whole brain-sequestered leukocytes (BSL) of CM mice (2).

The increase in total brain CD8⁺ T cells during CM is relatively small and scientists hypothesize that CD8⁺ T cells may induce CM by disrupting the blood brain barrier through direct damage of the endothelium (27). This hypothesis is supported by recent studies showing that perforin knockout mice are also resistant to CM (19, 20).

Perforin. The two principle mechanisms of T cell mediated cytotoxicity against pathogens are the perforin and fas dependent molecular pathways of targeted cell death. Nitcheu *et al* demonstrated that CM pathogenesis is dependent on the expression of perforin by measuring susceptibility of PFP-KO, *lpr*, and *gld* infected mice to CM over the course of a *P. berghei* ANKA infection (19). Similar to WT, *lpr*, and *gld* mice, which contain mutations in the Fas and FasL genes respectively, developed CM between days 6 and 10 post-infection. In contrast, PFP-KO mice were completely resistant to CM and instead succumbed to anemia and hyper-parasitemia between days 17 and 28.

Similar to WT infected mice, the brains of PFP-KO mice contained sequestered pRBCs, signs of severe edema, and accumulation of a remarkably similar repertoire of

CD4⁺ and CD8⁺ T cells, most of which were differentiated memory cells. Although morphologic changes suggest activation of endothelial cells in both WT and PFP-KO infected mice, apoptosis of endothelial cells was significant in WT mice only (20). The type of antigen presented by brain endothelial cells is currently unknown. However, adoptive transfer studies suggest that activation of CD8⁺ T cells occurs in the spleen and development of CM requires both presence of parasite and trafficking of activated lymphocytes to the brain (19).

Blood Brain Barrier. It has been proposed that CD8⁺ T cell mediated apoptosis of brain endothelial cells may damage the blood brain barrier. Disruption of the BBB could have two important consequences. First, its breakdown may lead to cerebral edema and consequently an increase in intracranial pressure (22). Second, an intact BBB regulates the passage of molecules from the blood into the CNS and its permeability depends on both the size and charge of the molecule. Therefore, disruption of the BBB may lead to an increased influx of larger molecules such as inflammatory cytokines (1).

Soluble Mediators and Effector Molecules. The observations that CM often occurs in the absence of sequestration and that sequestration often occurs in patients without CM, led Clark *et al* to propose that local production of cytokines is responsible for the clinical symptoms of CM (5). The potential toxic effect of cytokines was initially demonstrated for TNF- α ; while moderate levels of TNF- α are associated with uncomplicated malaria fever, overproduction of TNF- α was shown to be associated with CM (15). Subsequent studies have demonstrated that other T helper 1 (Th1) proinflammatory cytokines such as IFN- γ and lymphotoxin are associated with the

immunopathogenesis of CM while Th2 anti-inflammatory cytokines such as IL-10 and TGF- β abrogate disease (14).

The synthesis of pro-inflammatory cytokines leads to increased production of nitric oxide (NO). Although NO has been shown to play a significant role in host resistance to infection, local production of NO in areas of the brain with a high density of sequestered parasites could damage neurons. Increased expression of inducible Nitric Oxide Synthase (iNOS) has been reported in endothelial cells and neurons during CM (18). In addition, CM is readily reversible and participation of a transient molecule such as NO in the pathogenesis of CM could account for this.

Hemostasis. Two elements of the hemostasis system, platelets and microparticles, have recently been shown to play an increasing role in the pathogenesis of CM. Platelets, small cell fragments that are crucial for blood clotting, may contribute to the pathogenesis of CM by augmenting mechanical obstruction and inflammation. Platelet accumulation has been well documented in brain vessels during CM and depletion of platelets has been shown to have a protective effect (7). Platelets have also been found to occur in rosettes (25), clumps of parasitized and unparasitized erythrocytes, and this may also contribute to mechanical obstruction. Lastly, platelets are potent modulators of the immune response, expressing chemokine receptors and releasing soluble mediators such as cytokines and chemokines from granules (26). Therefore, activation of platelets during primary hemostasis may augment the immunopathogenesis of CM.

Microparticles are submicron plasma membrane fragments derived primarily from platelets but also from erythrocytes, leukocytes, and endothelial cells. Human studies initially demonstrated a correlation between CM and elevated levels of circulating

endothelial microparticles in Malawian children (8). The most compelling evidence supporting a role of microparticles in the pathogenesis of CM is a study demonstrating that ABC1^{-/-} mice, which lack the ability to generate microparticles, are completely resistant to ECM (6).

Objectives

- I. To identify novel host biomarkers associated with cerebral malaria
- II. To examine the mechanism of T cell mediated pathogenesis of cerebral malaria by exploring the role of CD8⁺ T cells and perforin in susceptibility to ECM

REFERENCES

1. **Adams, S., H. Brown, and G. Turner.** 2002. Breaking down the blood-brain barrier: signaling a path to cerebral malaria? *Trends Parasitol* **18**:360-366.
2. **Belnoue, E., M. Kayibanda, A. M. Vigario, J. C. Deschemin, N. van Rooijen, M. Viguier, G. Snounou, and L. Renia.** 2002. On the pathogenic role of brain-sequestered alphabeta CD8+ T cells in experimental cerebral malaria. *J Immunol* **169**:6369-6375.
3. **Berendt, A. R., G. D. Tumer, and C. I. Newbold.** 1994. Cerebral malaria: the sequestration hypothesis. *Parasitol Today* **10**:412-414.
4. **Boubou, M. I., A. Collette, D. Voegtli, D. Mazier, P. A. Cazenave, and S. Pied.** 1999. T cell response in malaria pathogenesis: selective increase in T cells carrying the TCR V(beta)8 during experimental cerebral malaria. *Int Immunol* **11**:1553-1562.
5. **Clark, I. A., and K. A. Rockett.** 1994. The cytokine theory of human cerebral malaria. *Parasitol Today* **10**:410-412.
6. **Combes, V., N. Coltel, M. Alibert, M. van Eck, C. Raymond, I. Juhan-Vague, G. E. Grau, and G. Chimini.** 2005. ABCA1 gene deletion protects against cerebral malaria: potential pathogenic role of microparticles in neuropathology. *Am J Pathol* **166**:295-302.
7. **Combes, V., A. R. Rosenkranz, M. Redard, G. Pizzolato, H. Lepidi, D. Vestweber, T. N. Mayadas, and G. E. Grau.** 2004. Pathogenic role of P-selectin in experimental cerebral malaria: importance of the endothelial compartment. *Am J Pathol* **164**:781-786.
8. **Combes, V., T. E. Taylor, I. Juhan-Vague, J. L. Mege, J. Mwenechanya, M. Tembo, G. E. Grau, and M. E. Molyneux.** 2004. Circulating endothelial microparticles in Malawian children with severe falciparum malaria complicated with coma. *Jama* **291**:2542-2544.
9. **de Souza, J. B., and E. M. Riley.** 2002. Cerebral malaria: the contribution of studies in animal models to our understanding of immunopathogenesis. *Microbes Infect* **4**:291-300.
10. **Engwerda, C., E. Belnoue, A. C. Gruner, and L. Renia.** 2005. Experimental models of cerebral malaria. *Curr Top Microbiol Immunol* **297**:103-143.
11. **Finley, R. W., L. J. Mackey, and P. H. Lambert.** 1982. Virulent *P. berghei* malaria: prolonged survival and decreased cerebral pathology in cell-dependent nude mice. *J Immunol* **129**:2213-2218.
12. **Hermesen, C., T. van de Wiel, E. Mommers, R. Sauerwein, and W. Eling.** 1997. Depletion of CD4+ or CD8+ T-cells prevents *Plasmodium berghei* induced cerebral malaria in end-stage disease. *Parasitology* **114 (Pt 1)**:7-12.
13. **Hunt, N. H., J. Golenser, T. Chan-Ling, S. Parekh, C. Rae, S. Potter, I. M. Medana, J. Miu, and H. J. Ball.** 2006. Immunopathogenesis of cerebral malaria. *Int J Parasitol* **36**:569-582.
14. **Hunt, N. H., and G. E. Grau.** 2003. Cytokines: accelerators and brakes in the pathogenesis of cerebral malaria. *Trends Immunol* **24**:491-499.
15. **Kwiatkowski, D.** 1990. Tumour necrosis factor, fever and fatality in falciparum malaria. *Immunol Lett* **25**:213-216.

16. **Lou, J., R. Lucas, and G. E. Grau.** 2001. Pathogenesis of cerebral malaria: recent experimental data and possible applications for humans. *Clin Microbiol Rev* **14**:810-820, table of contents.
17. **Maegraith, B., and A. Fletcher.** 1972. The pathogenesis of mammalian malaria. *Adv Parasitol* **10**:49-75.
18. **Maneerat, Y., P. Viriyavejakul, B. Punpoowong, M. Jones, P. Wilairatana, E. Pongponratn, G. D. Turner, and R. Udomsangpetch.** 2000. Inducible nitric oxide synthase expression is increased in the brain in fatal cerebral malaria. *Histopathology* **37**:269-277.
19. **Nitcheu, J., O. Bonduelle, C. Combadiere, M. Tefit, D. Seilhean, D. Mazier, and B. Combadiere.** 2003. Perforin-dependent brain-infiltrating cytotoxic CD8⁺ T lymphocytes mediate experimental cerebral malaria pathogenesis. *J Immunol* **170**:2221-2228.
20. **Potter, S., T. Chan-Ling, H. J. Ball, H. Mansour, A. Mitchell, L. Maluish, and N. H. Hunt.** 2006. Perforin mediated apoptosis of cerebral microvascular endothelial cells during experimental cerebral malaria. *Int J Parasitol* **36**:485-496.
21. **Ralph, S. A., and A. Scherf.** 2005. The epigenetic control of antigenic variation in *Plasmodium falciparum*. *Curr Opin Microbiol* **8**:434-440.
22. **Shapiro, B. K., P. J. Accardo, and A. J. Capute.** 1979. Factors affecting walking in a profoundly retarded population. *Dev Med Child Neurol* **21**:369-373.
23. **Su, X. Z., V. M. Heatwole, S. P. Wertheimer, F. Guinet, J. A. Herrfeldt, D. S. Peterson, J. A. Ravetch, and T. E. Wellems.** 1995. The large diverse gene family var encodes proteins involved in cytoadherence and antigenic variation of *Plasmodium falciparum*-infected erythrocytes. *Cell* **82**:89-100.
24. **Turner, G. D., H. Morrison, M. Jones, T. M. Davis, S. Looareesuwan, I. D. Buley, K. C. Gatter, C. I. Newbold, S. Pukritayakamee, B. Nagachinta, and et al.** 1994. An immunohistochemical study of the pathology of fatal malaria. Evidence for widespread endothelial activation and a potential role for intercellular adhesion molecule-1 in cerebral sequestration. *Am J Pathol* **145**:1057-1069.
25. **van der Heyde, H. C., J. Nolan, V. Combes, I. Gramaglia, and G. E. Grau.** 2006. A unified hypothesis for the genesis of cerebral malaria: sequestration, inflammation and hemostasis leading to microcirculatory dysfunction. *Trends Parasitol* **22**:503-508.
26. **Weyrich, A. S., and G. A. Zimmerman.** 2004. Platelets: signaling cells in the immune continuum. *Trends Immunol* **25**:489-495.
27. **Yanez, D. M., D. D. Manning, A. J. Cooley, W. P. Weidanz, and H. C. van der Heyde.** 1996. Participation of lymphocyte subpopulations in the pathogenesis of experimental murine cerebral malaria. *J Immunol* **157**:1620-1624.

Chapter 4

CD8⁺ T cell-Mediated Pathogenesis of Cerebral Malaria

Abstract

Cerebral malaria is the most severe complication of malaria. We have investigated the role of CD8⁺ T cells and perforin in the pathogenesis of CM using the *Plasmodium berghei* ANKA (Pb-A) murine model of experimental cerebral malaria (ECM). By performing high density microarray analysis of wildtype, CD8⁺-KO, and perforin-KO C57BL/6 mice, we have identified an array of host genes associated with CD8⁺ T cell mediated pathogenesis of ECM. Specifically, a network of chemokines are significantly altered in the both the brain and the spleen of mice with ECM, and a proportion of genes in the brain are devoted to both the induction and suppression of apoptosis. Histological analysis of OX40, a protein expressed by activated T cells, suggests that this molecule is expressed by CD8⁺ T cells in the brain during ECM. Protein quantification of galectin-3, a protein involved in the suppression of apoptosis of its native cell and promotion of apoptosis of T cells, suggests a correlation between transcription of RNA and translation of proteins in our study. In conclusion, we have identified novel host molecular factors that are involved in CD8⁺ T cell and perforin mediated pathogenesis of ECM. Further studies will confirm the role of these molecules in ECM and help elucidate the mechanism of how CD8⁺ T cell mediate the pathogenesis of ECM.

Introduction

Cerebral malaria (39) caused by *Plasmodium falciparum* infections is the most severe form of malaria pathogenesis. It is mostly experienced in young children, and is a major contributing factor in many of the 1-2 million malaria associated deaths each year. The *P. berghei* ANKA (Pb-A) murine model of experimental cerebral malaria (ECM) reproduces the clinical symptoms of human CM, and studies using this murine model have identified an array of host molecular and cellular factors involved in the pathogenesis of CM. The clinical characteristics of ECM in mice include hemi or paraplegia, ataxia, deviation of the head, tendency to roll over upon stimulation, convulsions, and coma. Figure 12A shows a moribund C57BL/6 mouse on day 6 post-infection with Pb-A, while a non-moribund mouse (FIG. 12B) has no apparent symptoms at the same time post-parasite infection.

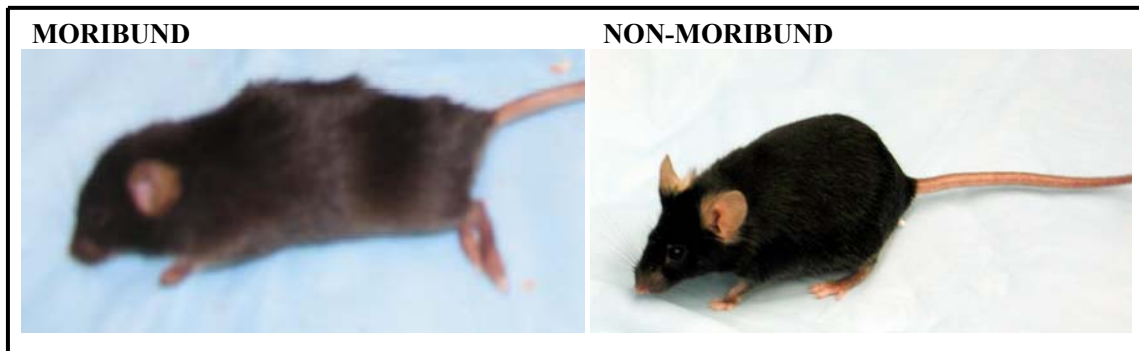


Figure 12. Symptoms of ECM. A moribund mouse (a) exhibits classical symptoms of CM including hemi or para-plegia, ataxia, deviation of the head, tendency to roll over upon stimulation, and seizures while a non-moribund mouse (b) appears healthy.

The importance of T cells in the pathogenesis of ECM was first recognized when it was reported that athymic nude mice do not develop symptoms of ECM during a Pb-A infection (24). Depletion of T cell subsets during a Pb-A infection later established that both CD4⁺ and CD8⁺ T cells are required for the development of ECM (61). Importantly, CD4⁺ T cells are critical for the induction of ECM, whereas CD8⁺ T cells are crucial during the effector phase of ECM. Additional studies demonstrating resistance to ECM of 1) mice homozygous for the null allele of the B2-microglobulin gene (B2M) (which lack functional CD8⁺ T cells) (61) and 2) CD8⁺-KO mice (11) confirmed an important role for CD8⁺ T cells in the pathogenesis of ECM.

Despite their significance in the pathogenesis of disease, CD8⁺ T cells comprise a very small subset of brain sequestered lymphocytes (BSLs) during ECM (8, 19). Remarkably, analysis of the BSL population of mice exhibiting symptoms of ECM revealed that 90% of sequestered T cells were CD4⁺CD8⁻ T cells. In contrast, only 4% (20,000 – 50,000 cells) of BSLs were CD8⁺ T cells. Furthermore, 50% of αβ CD8⁺ T cells (36% of total CD8⁺ BSLs) were phenotyped as CD8⁺ Vβ8.1,2⁺ T cells. In another study, more than 50% of brain sequestered CD8⁺ T cells isolated from mice with ECM were also characterized as differentiated memory cells (48).

The two principle mechanisms of T cell mediated cytotoxicity against pathogens are the perforin and fas dependent molecular pathways of targeted cell death. Nitecheu *et al* demonstrated that ECM pathogenesis is dependent on the expression of perforin by measuring susceptibility of PFP-KO, *lpr*, and *gld* infected mice to ECM over the course of a *P. berghei* ANKA infection (48). Similar to wildtype (WT), *lpr*, and *gld* mice, which contain mutations in the Fas and FasL genes respectively, developed ECM, whereas PFP-

KO mice were completely resistant to ECM. Similar to WT infected mice, the brains of PFP-KO mice contain sequestered pRBCs, signs of severe edema, and accumulation of a remarkably similar repertoire of CD4⁺ and CD8⁺ T cells, most of which were differentiated memory cells (51). In spite of these reports, a complete picture regarding how CD8⁺ T cells mediate the pathogenesis of ECM is far from complete.

In an effort to further define the mechanism of CD8⁺ T cell-mediated pathogenesis of ECM, we have compared the global gene expression profiles of Pb-A infected WT mice during the effector phase of ECM with Pb-A infected resistant CD8⁺-KO (deficient in the CD8 antigen, α chain) and PFP-KO mice on the C57BL/6 background. It is important to note that these knockout mice differ from their WT counterparts only in a single gene locus and therefore, any alterations observed in the gene expression profiling should reflect the specific mechanisms of ECM mediated by CD8 antigen or perforin molecules. We find that in Pb-A infected mice, loss of CD8 locus leads to alteration in 166 genes in the brain and 224 genes in the spleen, while 9 genes in the brain and 124 genes in the spleen exhibited altered expression in perforin knockout mice.

Analysis of the altered genes in WT mice in our dataset suggest that CD8⁺ T cells are strongly activated during ECM. In addition, in WT mice with ECM, a network of chemokines are significantly altered in the both the brain and the spleen and a proportion of genes in the brain are devoted to both the induction and suppression of apoptosis. Interestingly, two PFP-KO mice were able to self resolve their infection suggesting that absence of perforin, in addition to conferring resistance to ECM, may also produce an anti-parasitic effect that allows conversion of a highly virulent infection into a

nonvirulent one. Lastly, CCL21b, a chemokine strongly associated with experimental autoimmune encephalomyelitis (the murine model of multiple sclerosis) is significantly over-expressed in both uninfected and infected WT mice compared to respective PFP-KO mice. Further biological and functional analyses of the identified molecules will provide a complete picture of the role CD8⁺ T cells and perforin in the pathogenesis of ECM in the *berghei ANKA*-murine model.

Material and Methods

Mice and parasite infections. Six- to eight-week old female CD8⁺-KO (deficient in the CD8 antigen, α chain), PFP-KO, and WT mice on the C57BL/6 background were purchased from The Jackson Laboratory (Bar Harbor, ME). Parasite infection was initiated by intraperitoneal injection of 10^6 *Plasmodium berghei* ANKA parasites previously grown in donor mice with the same genetic background. Mice were monitored for clinical symptoms of ECM (hemi or para-plegia, deviation of the head, tendency to roll over upon stimulation, ataxia, and convulsions) between days 6 – 10 days post-infection. Parasitemias (parasitized RBCs/ total RBCs x 100) were enumerated daily by examination of Giemsa-stained thin blood films.

Sample Collection. Brain and spleen tissue was collected simultaneously from infected CD8⁺-KO, PFP-KO, and WT mice (six mice per group) between days 6 – 10 post-infection. Tissue was harvested from each of the three groups when WT mice exhibited symptoms of ECM, weighed, and stored at -80°C until use. Tissue was also harvested from uninfected CD8⁺-KO, PFP-KO, and WT mice (three mice per group) in order to determine inherent differences in basal gene expression between WT and knockout mice. Progression of infection was monitored to Day 14 in 5 additional CD8⁺-KO mice and 4 additional PFP-KO mice to ensure that these mice were resistant to ECM as reported in previously publications.

Statistical Analysis of Spleen Size. Spleen size of susceptible (C57BL/6 WT) and resistant (C57BL/6 CD8⁺-KO, C57BL/6 PFP-KO, and BALB/C WT) mice (6 mice per group) was analyzed using a t test for independent samples. Spleen size was

expressed as percentage of body weight (spleen weight/ body weight x 100) for statistical analysis to eliminate the potential confounder of a large spleen size due to variations in body weight of individual mice. Statistical analysis was performed on both untransformed and ln-transformed data using the natural logarithm (a logarithm that has the potential to convert data with a non-normal distribution to new data with a normal distribution).

Preparation of whole brain and spleen RNA. For preparation of high quality RNA, frozen tissue was homogenized in Tri-Reagent (Molecular Research Center, Cincinnati, OH), and RNA was isolated following two chloroform extractions, isopropanol precipitation, and resuspension in DEPC treated water. RNA quantity was determined by optical densitometry, and its quality was evaluated by agarose gel electrophoresis. Microarray expression profiles were determined from RNA samples isolated from six mice per group.

Microarray analysis. Tissue specific (brain and spleen) expression profiles of infected WT mice was compared with infected CD8⁺-KO mice and infected PFP-KO mice using pooled tissue (brain or spleen) from uninfected mice as a common reference to determine the array of host genes associated with T cell mediated pathogenesis of ECM. Differential gene expression was also compared in uninfected mice in order to determine the inherent differences in basal gene expression between WT and knockout mice prior to infection. cDNA was synthesized from 30 µg of RNA extracted from host brain and spleen tissue and then labeled as described in the *Materials and Methods* section of Chapter 2. Labeled cDNA was then hybridized to a murine oligonucleotide chip containing 16,600 oligonucleotide probes (Qiagen, Valencia, CA), and the slide was

scanned by a GenePix microarray scanner. Microarray data were analyzed with GenePix Pro 6.0 software (Axon Instruments, Inc. Union City, CA), filtered using the NIAID microarray database tools (<http://madb-niaid.cit.nih.gov>), and extracted spots were normalized to the precalculated 50th percentile (median). All hybridizations performed in this study are shown in Table 3.

Table 3. Groups of Mice used in Microarray Hybridizations

DAY ¹	CY5	CY3	BRAIN	SPLEEN
6	WT infected 060509	R	MO-179	MO-183
6	WT infected 060510	R	MO-180	MO-184
6	WT infected 060511	R	MO-161	MO-185
6	WT infected 060512	R	MO-157	MO-186
7	WT infected 060513	R	MO-171	MO-187
9	WT infected 060517	R	MO-172	MO-188
NA	WT uninfected	R	MO-173	MO-189
NA	WT uninfected	R	MO-174	MO-190
NA	WT uninfected	R	MO-175	MO-191
6	Perforin KO infected 060498	R	MO-178	MO-193
6	Perforin KO infected 060499	R	MO-182	MO-194
6	Perforin KO infected 060500	R	MO-156	MO-195
6	Perforin KO infected 060501	R	MO-162	MO-196
7	Perforin KO infected 060502	R	MO-169	MO-197
9	Perforin KO infected 060503	R	MO-170	MO-198
NA	perforin KO uninfected	R	MO-158	MO-199
NA	perforin KO uninfected	R	MO-159	MO-200
NA	perforin KO uninfected	R	MO-160	MO-201
6	CD8 KO infected 060487	R	MO-181	MO-202
6	CD8 KO infected 060488	R	MO-177	MO-203
6	CD8 KO infected 060489	R	MO-163	MO-204
6	CD8 KO infected 060490	R	MO-155	MO-205
7	CD8 KO infected 060491	R	MO-167	MO-206
9	CD8 KO infected 060492	R	MO-168	MO-207
NA	CD8 KO uninfected	R	MO-164	MO-208
NA	CD8 KO uninfected	R	MO-165	MO-209
NA	CD8 KO uninfected	R	MO-166	MO-210

¹Days post-challenge with 10⁶ P. berghei ANKA parasites
R: Common Reference (uninfected pooled tissue)

Data were analysed using the significance analysis of microarrays (SAM) program. Genes with a false discovery rate of $< 5\%$ and an average twofold increase (upregulation) or decrease (downregulation) were considered statistically significant. For each dataset, an FDR was chosen that would yield a set of genes that were statistically significant and also manageable in size for in depth functional analysis (FIG. 13).

WT vs. CD8 ⁺ KO mice BRAIN SAMPLES	WT vs. CD8 ⁺ KO mice SPLEEN SAMPLES	WT vs. Perforin KO mice BRAIN SAMPLES	WT vs. Perforin KO mice SPLEEN SAMPLES
Criterion: 1) FDR = 2.2 2) include genes with an average 2 fold increase or decrease in expression	Criterion: 1) FDR = 1.0 2) include genes with an average 2 fold increase or decrease in expression	Criterion: 1) FDR = 4.2 2) include genes with an average 2 fold increase or decrease in expression	Criterion: 1) FDR = 3.1 2) include genes with an average 2 fold increase or decrease in expression
Input Data: 12 Array 35,108 oligonucleotides	Input Data: 12 Arrays 35,169 oligonucleotides	Input Data: 12 Arrays 34,973 oligonucleotides	Input Data: 12 Arrays 35,254 oligonucleotides
FDR = 2.2 → 34,695 oligonucleotides excluded	FDR = 1.0 → 34,914 oligonucleotides excluded	FDR = 4.2 → 34,945 oligonucleotides excluded	FDR = 3.1 → 34,850 oligonucleotides excluded
230 oligonucleotides excluded for having an (unaltered) average fold change ratio between .5 and 2	17 oligonucleotides excluded for having an (unaltered) average fold change ratio between .5 and 2	19 oligonucleotides excluded for having an (unaltered) average fold change ratio between .5 and 2	273 oligonucleotides excluded for having an (unaltered) average fold change ratio between .5 and 2
Output Data: 12 Arrays, 188 oligonucleotides 166 genes (92% up-regulated, 8% down-regulated)	Output Data: 12 Arrays, 238 oligonucleotides 224 genes (16% up-regulated, 84% down-regulated)	Output Data: 12 Arrays, 9 oligonucleotides 9 genes (78% up-regulated, 22% down-regulated)	Output Data: 12 Arrays, 131 oligonucleotides 124 genes (22% up-regulated, 78% down-regulated)

Figure 13. Analysis of genes altered in expression in brain and spleen tissue. Data was analyzed using significance analysis of microarrays (SAM) program. Importantly, for each dataset, a false discovery rate (FDR) was chosen that would yield a set of genes that were both statistically significant and manageable for in depth functional analysis. After SAM analysis, a fold change criteria was instituted; genes having an average fold change ratio between .5 and 2 were excluded from the dataset.

Western blot analysis. Protein was prepared as a 10% brain homogenate, and tissue specific galectin-3 protein was detected using a mouse anti-galectin-3 monoclonal antibody specific for human recombinant galectin-3 protein (Biosource, Camarillo, CA) and a commercially obtained chemiluminescence-linked western blot kit (Western Light Tropic, Bedford, Mass.). Protein bands were visualized following incubation with ECL detection reagents, and the integrated optical densities (IOD) for each lane were measured using Meta Morph 6.1 software.

Immunohistological Studies. Tissue sections were prepared from the brains of moribund WT and CD8⁺-KO mice for immunohistological staining of OX40. Sections were fixed in acetone and then stained with a goat antibody specific for recombinant mouse OX40 (R&D Systems, Minneapolis, MN). A rabbit anti-goat antibody (Vector Laboratories, Burlingame, CA) was used for the next detection step by following the manufacture's instructions. Stained sections were examined by light microscopy.

Results and Discussion

CD8⁺-KO and PFP-KO mice are resistant to ECM. Before proceeding with further studies, we thought it was important to verify that CD8⁺-KO and PFP-KO C57BL/6 mice were resistant to ECM, as previously reported by other groups (11, 48). In our study, 60% of C57BL/6 WT mice (nine of fifteen mice) developed symptoms of ECM between days 6-10 post-infection. None of the mice that survived past Day 10, developed any symptoms of ECM but instead exhibited symptoms of severe anemia and high parasitemia between days 14-16 (FIG. 14).

We followed five WT BALB/c, five CD8⁺-KO C57BL/6, and four PFP-KO C57BL/6 up to 14-16 days post-infection. Unlike C57BL/6 wildtype mice, the other three groups were completely resistant to ECM, and their course of parasitemia was monitored until at least day 14 post-infection (FIG. 14). BALB/c mice, however, were particularly prone to develop high parasitemia and exhibit symptoms of severe anemia. Due to ethical consideration, two of these mice, that had developed high anemia, were sacrificed before completion of the study.

Surprisingly, two PFP-KO mice were able to self resolve their infection. In our hands and to our knowledge, self resolution of a *Pb*. ANKA infection has never been observed. It is possible that absence of perforin, in addition to conferring resistance to ECM, may also produce an anti-parasitic effect that allows conversion of a highly virulent infection into a nonvirulent one. However, these results will need to be reproduced in a larger group of PFP-KO mice.

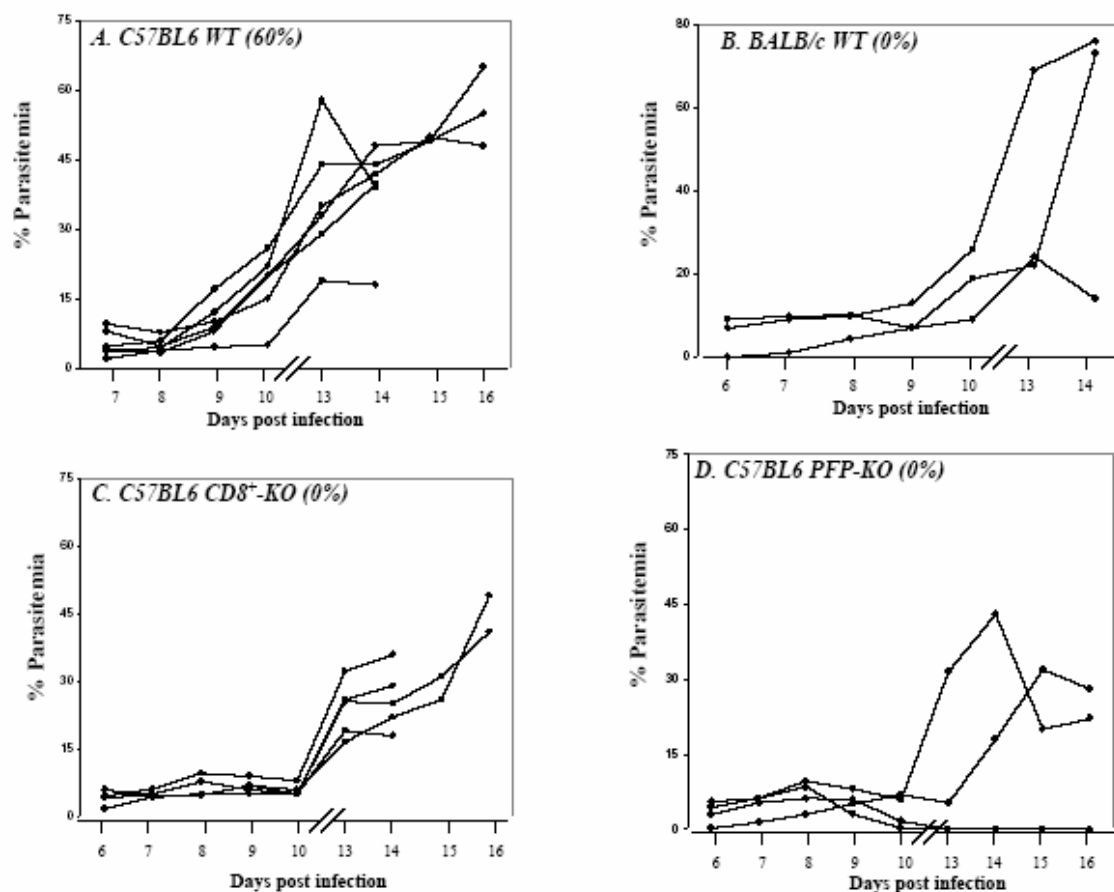


Figure 14. Susceptibility of C57BL/6 wildtype (A), BALB/c wildtype (B), C57BL/6 CD8⁺-KO (C), and PFP-KO (D) mice to ECM and course of parasitemia following infection with *P.berghei* ANKA parasites. Percentages of mice susceptible to ECM are shown in the top left hand corner.

Relationship between ECM and Spleen Size. The spleen has been shown to play an important role in immunity against blood form malaria parasites (60). Reports from field studies suggest that adults that have undergone splenectomy become more susceptible to parasite reinfection (6). In murine *P. chabaudi adami* malaria, presence of spleen is necessary for the expression of B-cell independent immunity in mice (29), and splenectomy results in the loss of re-infection immunity against *P. vinckei* malaria in

mice (20, 21). Although the spleen is known as an important immune organ, there is no information in the literature regarding the role of the spleen in the pathogenesis of CM. Therefore, we decided to investigate any possible relationship between splenic size and susceptibility to ECM.

Based on previous observations in our lab that mice displaying symptoms of ECM appear to have smaller spleens relative to mice without ECM, we hypothesized that there is an inverse correlation between manifestation of ECM and spleen size. Spleens were harvested simultaneously from susceptible (C57BL/6 WT) and resistant (C57BL/6 CD8⁺-KO, C57BL/6 PFP-KO, and BALB/C WT) mice (n=6 per group) between days 6-9 post-infection. To eliminate the potential confounder of a large spleen size due to variations in body weight of individual mice, spleen size was expressed as percentage of body weight (spleen weight/ body weight x 100) as shown in Figure 15. Average spleen sizes expressed as percentage of body weight were 1.23% (C57BL/6 WT), 1.31% (C57BL/6 CD8⁺-KO), 1.46% (C57BL/6 PFP-KO) and 1.87% (BALB/C WT). Although these results are consistent with our hypothesis (mice with small spleens are more likely to exhibit symptoms of ECM), there is significant variation in the data (particularly in the CD8⁺-KO group of mice) (FIG. 15).

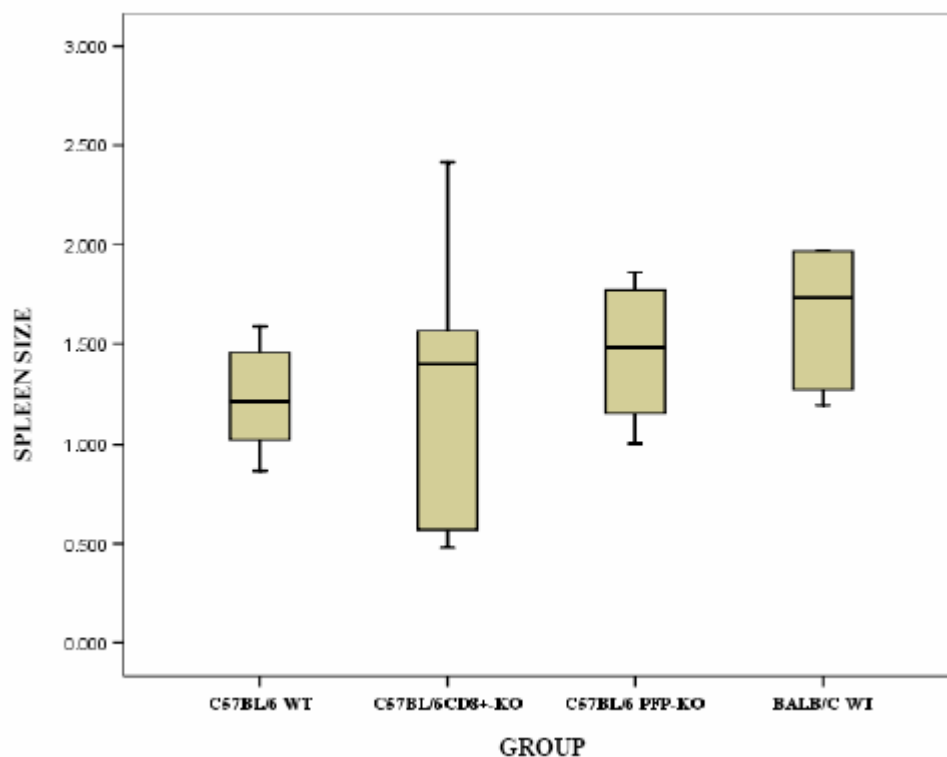


Figure 15. Boxplots for Data of Spleen Size

The statistical significance was next measured by comparing the means using a t test for independent samples (equal variance assumed). Spleen size of mice exhibiting symptoms of ECM (C57BL/6 WT) was compared to the three groups of mice that were resistant to ECM (CD8⁺-KO C57BL/6, PFP-KO C57BL/6, and BALB/C WT). Using 0.05 as the level of significance, we can conclude that there is no detectable difference in spleen size between susceptible C57BL/6 WT mice and resistant C57BL/6 CD8⁺-KO and C57BL/6 PFP-KO mice (Table 4). However, although not statistically significant, difference in spleen size between susceptible C57BL/6 WT mice and resistant BALB/C WT mice approached significance ($p=.088$ and $.061$ for untransformed and ln-transformed data, respectively). Importantly, the sample size of this study was very small.

Therefore, the possibility that there is inverse correlation between spleen size and manifestation of ECM should not be eliminated until further studies with a larger sample size have been conducted.

Interestingly, the level of significance greatly varies between the three groups of resistant mice (Table 4) and this may be due to differences in their genotype. The spleen is an immune organ and the site of activation and proliferation of CD8⁺ T cells during an infection. Therefore, the lack of functional CD8⁺ T cells in CD8⁺-KO C57BL/6 mice and even the perforin protein (a protein expressed by CD8⁺ T cells) in PFP-KO C57BL/6 mice could account for differences in spleen size between the three groups of resistant mice.

RESISTANT MICE	SIGNIFICANCE	
	SPLEEN SIZE	SPLEEN SIZE (LN_TRANSFORM)
CD8 ⁺ KO	.816	.812
PFP KO	.230	.243
BALB/C	.088	.061

Table 4. Statistical significance between susceptibility to ECM and spleen size. Spleen size (expressed as spleen weight/ body weight x 100) of susceptible mice was compared to 3 groups of resistant mice (n=6 per group) using the t test for independent samples (equal variance assumed). Level of significance was determined for both untransformed and ln-transformed data.

Measuring the alterations in the gene expression during ECM. We compared the expression profiles of host genes in the brain and spleen tissue of WT mice exhibiting

symptoms of ECM to CD8⁺KO and PFP-KO mice which displayed no clinical symptoms of ECM. Altered expression was defined as significant only if a gene had met the following two criteria: 1) had a false discovery rate of < 5 % and 2) exhibited an average two-fold increase (upregulation) or decrease (downregulation) in expression. For each dataset, an FDR was chosen that would yield a set of genes that were statistically significant and also manageable in size for in depth functional analysis (Table 5).

Our first observation was that presence of the *CD8* (WT genotype) resulted in a disproportionate number of upregulated genes in the brain and downregulated genes in the spleen; 92% of genes in the brain were upregulated in WT mice compared to CD8⁺-KO mice, whereas 84% of genes in the spleen were downregulated (Table 5). The effect of perforin yielded a similar trend: 78% of genes in the brain were upregulated in WT mice compared to PFP-KO mice, whereas 78% of genes in the spleen were downregulated. The precise reason for a generalized downregulation in expression of genes in the spleen is not clear. Among possible mechanisms of this phenomenon include suppression in genes involved in immune function, erythropoiesis and other splenic functions during a virulent infection. Similarly, a global upregulation in the gene expression in the brain suggests an active and vigorous response on the host side to protect from the undergoing deleterious response associated with the pathogenesis of cerebral malaria.

It has been reported that B2M^{-/-} mice can produce a robust Th1 response in the spleen during viral infection to compensate for absence of the CTL arm of T cell immunity (56). It is possible that this may be the case for CD8⁺-KO mice too. Because presence of the *CD8* gene results in susceptibility to ECM, we hypothesized that the

disproportionate number of over-expressed genes in the brain may be, at least in part, a consequence of 1) activity of CD8⁺ T cells 2) induction and manifestation of ECM and 3) a host response to insult to the brain. Therefore, we were surprised that presence of the *pfp* gene, also a determinant of susceptibility to ECM, resulted in altered expression of only 9 genes in the brain of infected mice (FDR .0419). Nonetheless, the fact that only a very small number of molecules had altered gene expression due to presence of perforin greatly renders specificity to the approach used to identify the molecules and their implicated pathways involved in the process of infection induced pathogenesis.

Protein	Tissue	Upregulated	Downregulated	Total	FDR ¹
CD8	Brain	153	13	166	2.2
	Spleen	36	188	224	1.0
Perforin	Brain	7	2	9	4.2
	Spleen	27	97	124	3.1

¹ False Discovery Rate

Table 5. Effect of the *CD8* and *pfp* genes on tissue-specific gene expression in the *P. berghei* ANKA murine model of ECM.

Measuring alterations in gene expression in uninfected knockout mice. In

order to determine whether these transcriptional changes were a consequence of infection and not due to inherent differences in basal gene expression between WT and knockout mice, we measured differential gene expression in uninfected WT mice verses uninfected CD8⁺ KO and PFP-KO mice (Table 6). Using a FDR of < 5% and a fold change ratio of > 2 or < -2 as criteria for significance, we found that presence of the *CD8* gene resulted

differential expression of only one gene (*CD8b1*) in the spleen. However, we found that presence of the *CD8* gene resulted in no transcriptional changes in the brain. This is not surprising because in the absence of infection, the brain is regarded as an immunoprivileged site. However, greater differences in basal gene expression may have been observed if a larger samples size had been used.

Surprisingly, presence of perforin resulted in differential expression of thirteen genes in the brain and four genes in the spleen. Among these genes, a similar transcriptional change (13.8) in *CCL21b* was also observed in infected WT mice (with ECM) compared to infected resistant PFP-KO mice. However, differential expression of a gene prior to infection should not necessarily eliminate a potential role for the gene in the pathogenesis of ECM.

Gene	Tissue	Genes Altered	GI Number	Fold Δ
<i>CD8</i>	Brain	None	NA	NA
<i>CD8</i>	Spleen	CD8 antigen, beta chain 1	6753358	15.7
<i>Perforin</i>	Brain	chemokine (C-C motif) ligand 21b	14547891	13.7
		similar to 4933409K07Rik protein (predicted)	94371693	8.4
		Ligand dependent nuclear receptor corepressor-like	—	2.7
		acyl-Coenzyme A oxidase 1, palmitoyl	66793429	2.7
		centaurin, delta 1, transcript variant 2	94376294	2.4
		gene model 288 (predicted)	38076082	-4.0
		vacuolar protein sorting 37D	29243920	-4.1
		procollagen C-endopeptidase enhancer protein	125490382	-2.7
		gene model 749	85702211	-3.5
		Insulin-like growth factor 2	—	-3.2
		uncoupling protein 2	31543920	-2.1
		solute carrier family 12, member 7	6755534	-2.1
		translocator protein	31981875	-2.1
<i>Perforin</i>	Spleen	similar to Ig kappa chain V-V region L6 precursor (predicted)	82901259	-4.8
		similar to immunoglobulin kappa chain (predicted)	—	-4.4
		Immunoglobulin light chain productive VJ rearrangement, J606 myeloma	—	-3.2
		CMRF-35-like molecule 3	40353230	-6.8

Table 6. Effect of *CD8* and *perforin* genes on brain and spleen gene expression in uninfected mice.

CD8⁺ T cells and the pathogenesis of ECM. Comparison of WT to CD8⁺-KO mice has enabled us to examine in depth the role of CD8⁺ T cells in the pathogenesis of ECM. Analysis of genes in our dataset suggest that CD8⁺ T cells are strongly activated during ECM. In addition, a network of chemokines are significantly altered in the both the brain and the spleen, and a proportion of genes in the brain are devoted to both the induction and suppression of apoptosis. We also find that, CCL21b, a chemokine strongly associated with experimental autoimmune encephalomyelitis (the murine model of multiple sclerosis), is significantly downregulated in both uninfected and infected PFP-KO mice suggesting a role of perforin in the regulation of the CCL21b chemokine.

Activation of CD8⁺ T cells. Several genes that are markers of activated CD8⁺ T cells are over-expressed in WT mice with ECM compared to resistant CD8⁺-KO mice. These include effector molecules of CTL-mediated apoptosis such as cathepsin C, granzyme A, and granzyme B. Upregulation of CTL-mediated apoptosis is fully consistent with the recent reports that demonstrated CD8⁺ T cell dependent killing of endothelial cells leading to a disruption of the blood brain barrier (51). These results also point towards at least one plausible mechanism of how CD8⁺ T cells mediate the pathogenesis of cerebral malaria. Other genes in our dataset that are associated with activation of T cells are molecules such as regulated upon activation, normal T cell expressed and secreted (RANTES) and OX40 which have dual roles in both arms of T cell immunity.

OX40, a member of the tumor necrosis factor receptor superfamily, is found be expressed only on activated T cells (32). Although OX40 is typically expressed by CD4⁺ T cells, strong activation can induce expression on CD8⁺ T cells (53). OX40L is

expressed on a variety of antigen presenting cells including vascular endothelial. Ligation of the two molecules elicits costimulation, and under the restricted condition that both T cells and APCs are found to be activated (32). Studies have shown that OX40 plays a significant role in the generation of memory T cells (31, 50, 59). Importantly, Nitcheu et al reported that more than 50% of brain infiltrating CD8⁺ T cells during Pb-A induced ECM were memory T cells (CD44⁺CD62L⁻) (48), suggesting the importance of OX40 during ECM.

To find out if there is a correlation between the presence of OX40 and the expression of cerebral malaria, we determined the presence of OX40 in brain sections from WT and CD8⁺-KO mice. We stained brain sections with a goat anti-mouse OX40 antibody. While OX40 antibody reacted very specifically with tissue samples harvested from WT (moribund) mice, reactivity to CD8⁺-KO was completely negative (FIG.16). Although the cell type that expressed OX40 was not determined, it is highly possible that CD8⁺ T cells were the source of OX40 detected in samples from moribund mice. However, future studies double staining T cells from mice with ECM with antibodies against both OX40 and a phenotypic marker of CD8⁺ T cells by histology or flow cytometry will be needed to firmly establish CD8⁺ T cell specific expression of OX40 during ECM.

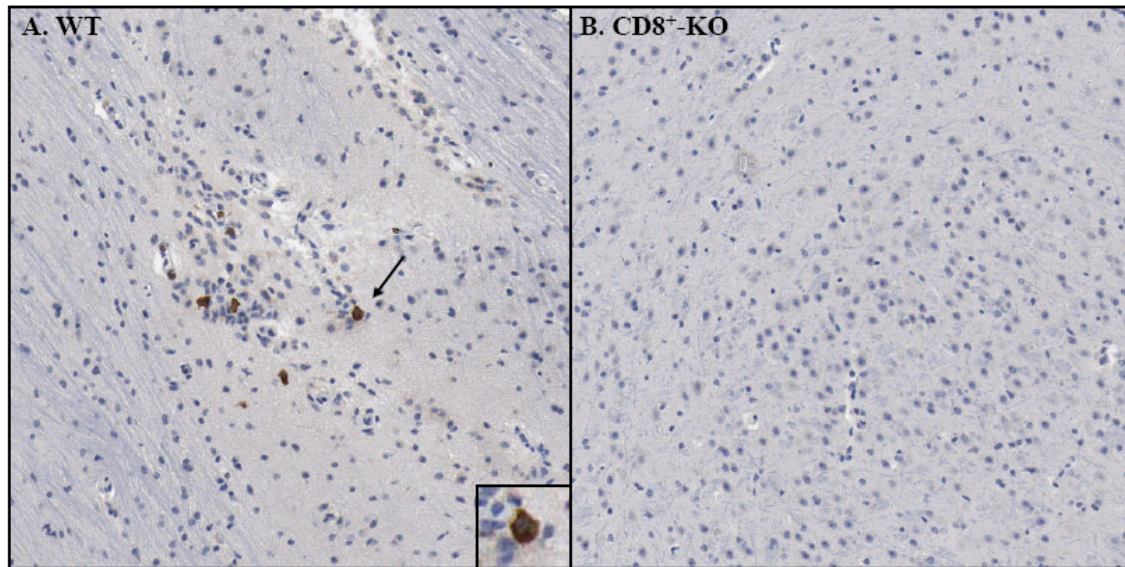


Figure 16. Immunohistological staining of brain sections from infected wildtype (moribund) mice with ECM (a) and infected CD8⁺-KO mice without ECM (b) at 40X magnification. Immunostaining with a goat antibody specific for mouse OX40 resulted in strong but highly specific staining of a small subset of cells within the brain of wildtype mice. In contrast, brain sections from CD8⁺-KO mice were negative for OX40. Anti-OX40 staining of a single cell at 100X magnification can be visualized in the bottom right hand corner of 16A.

Apoptosis. Several genes in our dataset are involved in either the promotion or suppression of apoptosis (Table 7). Cathepsin C, granzyme A, granzyme B, and high mobility box 2 (HMG-2) play particularly important roles in T cell mediated cytotoxicity. Genes such as CCAAT/enhancer binding protein (C/EBP β), Serum/glucocorticoid regulated kinase (SGK1), Growth arrest and DNA-damage-inducible 45 beta (GADD45 β), B-cell leukemia/lymphoma 2 related protein A1a (BCL-2a1a), and B-cell leukemia/lymphoma 2 related protein A1b (BCL-2a1b) suppress apoptosis. p21 and

galectin-3 can induce or inhibit apoptosis depending on the subcellular location of the proteins they encode.

GENE NAME	GI No.	FOLD Δ^1	APOPTOSIS
Granzyme A	6754102	8.3	+
Galectin-3	33859580	5.5	+/-
High mobility group box 2	6680229	4.3	+
B-cell leukemia/lymphoma 2 related protein A1b	6671626	4.2	-
Granzyme B	7305123	4.1	+
Cyclin-dependent kinase inhibitor 1A (P21)	6671726	4.0	+/-
B-cell leukemia/lymphoma 2 related protein A1a	11024684	3.8	-
Cathepsin C	31560607	3.2	+
CCAAT/enhancer binding protein	6753404	3.2	-
Serum/glucocorticoid regulated kinase	6755490	2.9	-
Lamin A	9506843	2.4	+
Growth arrest and DNA-damage-inducible 45 beta	6678980	2.2	-

Table 7. Mediators of apoptosis with altered expression in the brain during ECM.

¹ Fold Δ of moribund wildtype mice compared to resistant CD8⁺-KO mice

CTL mediated cytotoxicity. The principle mechanism by which CTLs act is by release of lytic granules upon recognition of foreign antigen in a target cell. Granules are composed of 1) perforin, which upon polymerization forms transmembrane pores in the target cell and 2) granzymes, a group of serine proteases which induce apoptosis of the target cell. Not surprisingly, several genes involved in T cell mediated cytotoxicity are strongly upregulated in WT mice with ECM compared to resistant CD8⁺-KO mice.

Cathepsin C, an endopeptidase that converts granzymes from inactive pro-enzymes into active enzymes (37) is upregulated by 3.2 fold. Furthermore, granzyme A and B are overexpressed by 8.3 and 4.1 fold, respectively.

Granzyme A is the most abundant protease in granules of CTLs (27, 28). Expression of granzyme A is upregulated approximately three to five days after naïve T cells are induced to differentiate into CTLs (38). Granzyme A induces a unique caspase independent cell death pathway by targeting the endoplasmic reticulum associated SET complex. Three members of the SET complex (nucleosome assembly protein SET, the DNA bending protein HMG-2, the base excision repair endonuclease Ape1) are direct substrates of granzyme A and cleavage destroys all of their known functions (10, 22, 23).

One member of the SET complex, HMG-2 is over-expressed by 4.3 fold in wildtype mice with ECM compared to resistant CD8⁺-KO mice. HMG-2 is a nuclear protein that can bind single-stranded DNA, unwind double-stranded DNA, and increase transcription (58). HMG-2 contains two DNA binding HMG-box domains and has a long acidic C-terminal domain. Although HMG-2 can bind DNA without sequence specificity, it binds preferentially to bent or altered DNA and is capable of bending linear DNA (55). Granzyme A cleavage of HMG-2 promotes cell death by impairing its ability to repair DNA. Over-expression of HMG-2 in the moribund WT mice but not in CD8⁺-KO mice that don't experience ECM strongly suggests the involvement of a Granzyme A-mediated, caspase-independent cell death pathway during the course of ECM.

Granzyme B is capable of inducing caspase-dependent and independent cell death. Granzyme B has a strong preference for proteolytic cleavage of acidic aspartate residues (49), and caspase-3 and 8 are known substrates of granzyme B (5, 42).

Granzyme B induces caspase-independent cell death by cleavage of the molecule BH3-interacting domain death agonist (BID) into a truncated form. This disrupts the outer mitochondrial membrane resulting in the release of cytochrome c, HtrA2/OMI, and endonuclease G. Cytochrome c activates pro-caspase 9, HtrA2/OMI is a serine protease that inhibits IAP (an inhibitor of apoptosis), and endonuclease G induces DNA damage (37).

Although the functions of granzyme A and B overlap, granzyme A is particularly important in promoting apoptosis of cells that overexpress bcl-2 (9), a mitochondrial protein that regulates apoptosis by blocking the release of cytochrome c. Two genes in the bcl-2 family (bcl-2a1a and bcl-2a1b) are robustly over-expressed in wildtype mice with ECM compared to resistant CD8⁺-KO mice. Therefore, Granzyme A may have a pertinent role in the apoptosis of bcl-2a1a and bcl-2a1b producing cells during the pathogenesis of ECM.

Suppressors of Apoptosis. In addition to bcl-2a1a and bcl-2a1b, several other altered genes encode proteins involved in protection from apoptosis (Table 7). For example, expression of GADD45 β is upregulated by 2.2 fold during ECM. GADD45 β is a TNF- α inducible gene that mediates NF- κ B suppression of the pro-apoptotic JNK signaling pathway by inhibiting the JNK kinase, mitogen-activated protein kinase kinase 7 (MKK7) (47). Another molecule, C/EBP β is over-expressed by 3.2 in WT mice compared to CD8⁺-KO mice and is one of six CCAAT/enhancer binding protein (C/EBP) transcription factors that regulate cell cycle arrest through direct interactions with palindromic DNA sites. C/EBP β is ubiquitously expressed and is identified as the effector of cyclin D1 activity in human cancer (34).

Galectin-3. Compared to CD8⁺-KO mice, expression of galectin-3 was enhanced by 5.5 fold in WT mice. Interestingly, galectin-3 possesses both pro and anti-apoptotic activities depending on its cellular localization; intracellular galectin-3 appears to suppress apoptosis of its native cell, whereas extracellular galectin-3 promotes apoptosis of T cells (18). The precise mechanism of intracellular galectin-3 mediated protection from apoptosis has not been clearly elucidated. However, the molecule does possess the anti-death motif (1) shown to be critical for the anti-apoptotic activity of bcl-2 (30). Similar to Bcl-2, galectin-3 may regulate apoptosis by inhibiting the release of cytochrome c from mitochondria (40, 45). Furthermore, Kim et al demonstrated that activation of cyclin D1 by galectin-3 may accelerate the cell cycle during the apoptosis sensitive point in early G1 phase (35).

Extracellular galectin-3 has been shown to induce apoptosis of human T cells. Galectin-3 has three binding partners on the surface of CTLs. Binding to the T cell CD29/CD7 complex results in apoptosis of T cells through release of mitochondria cytochrome c and activation of caspase-3 (26). Galectin-3 can also bind to the T cell death receptor CD98 (25). Lastly, galectin-3 can bind to the T cell receptor (TCR) complex. However, this does not induce apoptosis but instead down-regulates T cell activity (16). Tumor cells produce and secrete high levels of galectin-3, and this may prevent CTL mediated killing of tumors (46).

We examined differential expression of galectin-3 at the level of translation in order to determine whether a correlation exists between synthesis of mRNA and synthesis of protein. While our microarray results indicate that transcription of galectin-3 in the moribund WT mice is 5.5 fold greater than expression in resistant CD8⁺-KO mice,

quantification of galectin-3 protein by western blot revealed a similar fold increase (4.3) (FIG. 17).

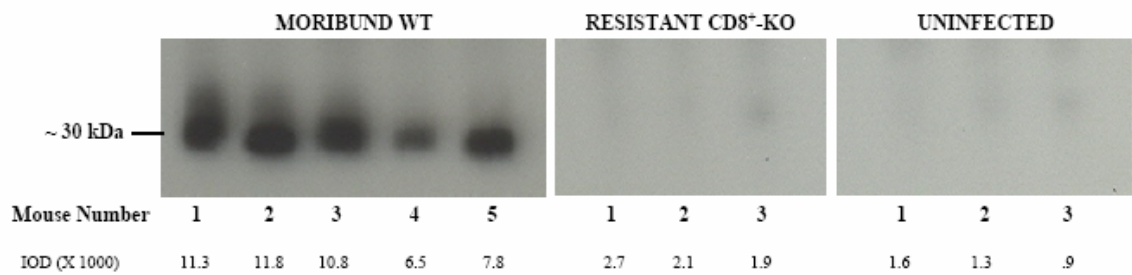


FIG. 17. CD8⁺ T cell mediated expression of galectin-3. Expression of murine galectin-3 protein was measured by western blot analysis using a mouse anti-human galectin-3 antibody. Quantitative analysis based on intensity of bands gave average IOD units of 9645 (moribund WT), 2226 (resistant CD8⁺-KO), and 1266 (uninfected), demonstrating a 4.3 fold upregulation of galectin-3 in moribund mice compared to CD8⁺-KO mice. Protein bands were visualized following incubation with ECL detection reagents and the integrated optical densities (IOD) for each lane were measured using Meta Morph 6.1 software.

The observation in our dataset showing an altered expression in both apoptosis and anti-apoptosis genes suggests that multiple cellular mechanisms are simultaneously occurring during the pathogenesis of cerebral malaria. These processes probably reflect the vigorous host effort to prevent en masse damage to brain tissue from the inflammatory responses characteristics of CM. This is potentially accomplished by activating the expression of anti-apoptotic molecules that serve as neuroprotectants.

Chemokines. We find that CCL3, CCL5, CCL9, and CCL25 are overexpressed in brain tissue of WT mice with ECM compared to resistant CD8⁺ KO mice. CCL3, also known as macrophage inflammatory protein 1 α (MIP-1 α) is produced by activated macrophages to recruit other inflammatory cells including macrophages themselves (41, 43). CCL25, also known as thymus expressed chemokine (TECK), plays a role in T cell development and anti-apoptosis of T cells (62). Overexpression of CCL3 (produced by activated macrophages) coincides with the possibility that activated macrophages in ECM contribute towards pathogenesis by producing inflammatory cytokines such as TNF- α and oxygen radicals, factors associated with the pathogenesis of CM.

CCL5, also known as regulated upon activation, normal T cell expressed and secreted (RANTES), is overexpressed by 4.1 fold in WT mice with ECM compared to resistant CD8⁺-KO mice. RANTES is produced predominantly by CD8⁺ T cells, epithelial cells, fibroblasts, and platelets and plays an important role in the chemotaxis and activation of T cells (3). RANTES, in addition to perforin and granzyme A, is degranulated by activated CD8⁺ T cells (57).

Previously, two studies have addressed the role of CCR5, a RANTES chemokine receptor, in murine ECM. Nitcheu et al reported increased mRNA expression of CCR5 in activated CD8⁺ T cells isolated from both moribund WT and resistant PFP-KO mice (48). “A modest, but consistent, delayed effect of CCR5-KO on the onset of ECM” was observed when susceptibility of CCR5-KO mice to ECM was examined during the same study. In a previous study, Belnoue et al reported that only 20% of CCR5 KO mice exhibited symptoms of ECM compared to 70-85% of wildtype mice (7). Together, these studies show that the absence of CCR5 is associated with a delayed or reduced expression

of the pathogenesis of ECM. In our microarray data set, we find a 1.34 fold upregulation of CCR5 in the brain of WT mice with ECM compared to resistant CD8⁺-KO mice, suggesting a rather weak association between CCR5 and pathogenesis of CM. It is highly possible that only slightly elevated levels of CCR5 is sufficient to exert its pathogenic effect.

Data presented on the role of RANTES in the pathogenesis of human CM is conflicting. In one study, expression of both RANTES and its receptor CCR5 have been shown to be significantly upregulated in the brains of those who died of CM (52). In contrast, another study performed by John et al showed that decreased levels of RANTES were observed in children with CM compared to those without CM, and low levels of RANTES were also associated with death due to CM (33).

Analysis of our dataset shows that three members of the macrophage chemoattractant protein (MCP) subgroup of CC chemokines (MCP-1, -3, -5) are down-regulated in the spleen of WT mice with ECM compared to resistant CD8⁺-KO mice. MCPs are a group of structurally and genetically related proteins named for their potent ability to attract macrophages. Although MCP-1, -3, and -5 all bind to CCR2 receptor, their biological activities are non-redundant. MCP-1 attracts monocytes and memory T cells, stimulates Th2 polarization, and also has been shown to induce the pro-apoptotic transcription factor MCPIP (MCP induced protein) in cardiovascular disease (13, 14, 63). MCP-3 is capable of recognizing multiple chemokine receptors and therefore is one of the most pluripotent chemokines, activating a very broad range of target cells (monocytes, lymphocytes, natural killer cells, granulocytes, and dendritic cells) (44). Further experiments will be needed to find an association between reduced expression of

the MCP subgroup of chemokines in the spleen and ECM. A summary of the chemokines altered in our study, their associated receptors, as well as pertinent functions has been illustrated in Figure 18.

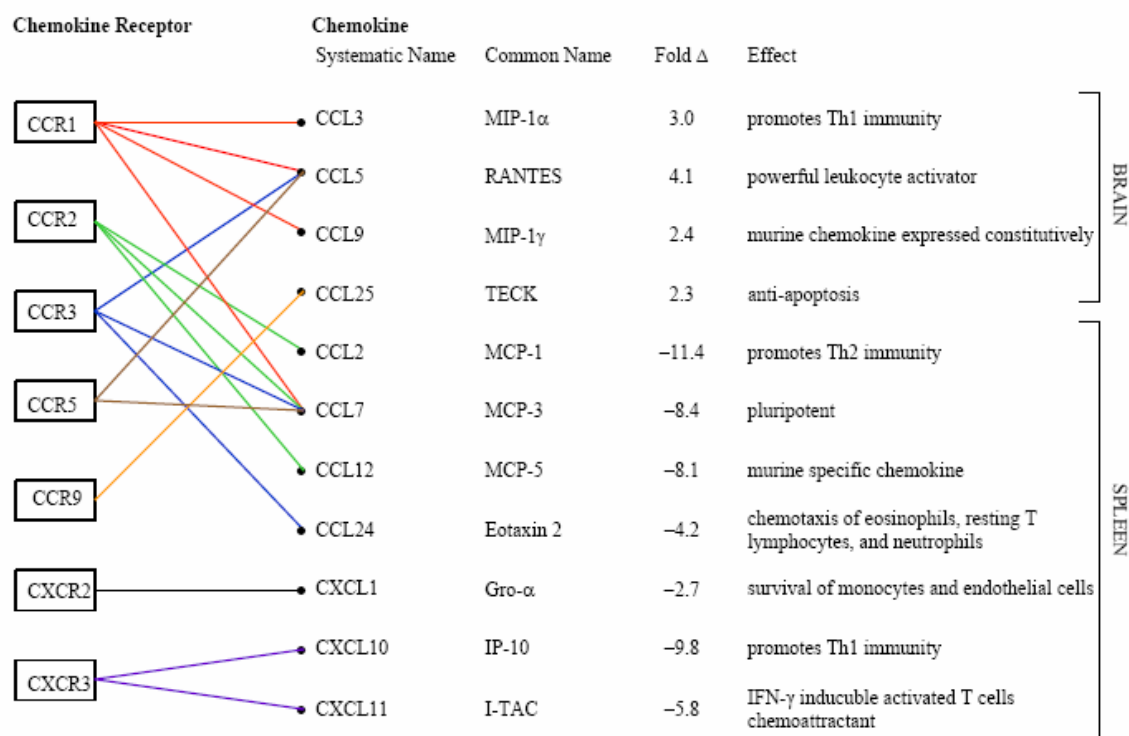


Figure 18. A summary of chemokines that exhibited altered expression levels in the brain and spleen tissues of wildtype (moribund) mice compared to CD8⁺-KO (resistant) mice. Colored lines link chemokines with their associated receptor(s).

Perforin and Pathogenesis of ECM. Only nine molecules were altered by presence of the *ppp* gene during a Pb-A infection when using both 1) FDR of .0419 and 2) two-fold change in expression as criteria for significant differential gene expression (Table 8). Of particular interest was the overexpression (2.5 fold) of two serpins, *serpina3n* and *3c*, in WT moribund mice compared to PFP-KO resistant mice. Serpins are serine protease inhibitors that may be particularly important in abrogating extracellular

damage induced by serine proteases such as Granzyme B. It is feasible that increased levels of serpin3n and 3c may lead to significant inhibition in the activity of serine proteases and may be a compensatory host response to prevent further damage to the CNS. Further studies will be needed to clarify the precise role of serpins during the pathogenesis of ECM.

GENE NAME	GI NUMBER	FOLD Δ
Chemokine (C-C motif) ligand 21b	14547891	13.8
Achaete-scute complex homolog-like 2	66792798	2.7
Serpina3n	6678093	2.5
Serpina3c	6680586	2.5
WD repeat and FYVE domain containing 1	21312280	2.5
Kruppel-like factor 10	7305571	2.1
RIKEN cDNA	40254303	2.1
Lymphocyte antigen 6 complex, locus A	6754580	-2.3
Lymphocyte antigen 6 complex, locus C	—	-2.4

Table 8. Genes significantly altered in expression by presence of the *ppp* gene during a *P. berghei* ANKA infection.

Effect of Perforin on the Expression of CCL21b. We were particularly interested in the association between CCL21b expression and presence of perforin in our study. CCL21b was significantly upregulated in both uninfected (13.7) and infected (13.8 fold) wildtype mice compared to respective uninfected and infected PFP-KO mice. CCL21 possesses at least three functions that may be pertinent to the pathogenesis of ECM. First, CCL21 is a potent arrest chemokine (36). Second, CCL21 promotes inflammatory T cell migration across and ligation to the BBB during EAE, the murine model of MS (2). Lastly, CCL21 is believed to play a prominent role in the activation of microglia by damaged neurons (15).

CCL21 is a potent arrest chemokine, participating in the immobilization of circulating lymphocytes from a rolling to a firmly adherent state. CCL21 has been shown to arrest T lymphocytes in vitro and in vivo. CCL21 has been shown to induce B2 integrin-dependent arrest of naïve T cells on ICAM-1 (12, 54) in vitro. T lymphocyte arrest has also been demonstrated in vivo by ligation of the CCR7 chemokine receptor with CCL21 on high endothelial cells (12).

The hallmark of EAE is the circulation of encephalitogenic T cells within the immunoprivileged CNS. A study performed by Alt et al. demonstrated the presence of CCL21 in CNS venules during EAE, as well as paralleled expression of its receptor CCR7 on inflammatory T cells surrounding these venules (2). These T cells migrated towards CCL21 in a concentration dependent manner. Furthermore, in addition to inducing chemotaxis, binding assays demonstrated that CCL21 has a functional role in providing adhesion strength to encephalitogenic T cells to inflamed venules in the brain.

CCL21 may also participate in the activation of microglia, the first cells in the CNS to become activated upon neuronal injury. Damaged neurons have been shown to upregulate the expression of CCL21 mRNA (4), and it is hypothesized that CCL21 protein is sorted into vesicles and released from neurons where it can activate microglia via its chemokine receptor CXCR3 (15, 17). Although uninfected as well as infected WT mice exhibit an approximately 13-fold higher expression of CCL21b compared to respective PFP-KO mice, due to the important role of CCL21b in immunoregulation (including T lymphocyte arrest on endothelial cells, a factor that could be critical in the pathogenesis of CM), a direct role for CCL21b in the pathogenesis of ECM cannot be eliminated.

REFERENCES

1. **Akahani, S., P. Nangia-Makker, H. Inohara, H. R. Kim, and A. Raz.** 1997. Galectin-3: a novel antiapoptotic molecule with a functional BH1 (NWGR) domain of Bcl-2 family. *Cancer Res* **57**:5272-5276.
2. **Alt, C., M. Laschinger, and B. Engelhardt.** 2002. Functional expression of the lymphoid chemokines CCL19 (ELC) and CCL 21 (SLC) at the blood-brain barrier suggests their involvement in G-protein-dependent lymphocyte recruitment into the central nervous system during experimental autoimmune encephalomyelitis. *Eur J Immunol* **32**:2133-2144.
3. **Appay, V., and S. L. Rowland-Jones.** 2001. RANTES: a versatile and controversial chemokine. *Trends Immunol* **22**:83-87.
4. **Aronow, S., and J. M. Bruner.** 1975. Editorial views: Electrosurgery. *Anesthesiology* **42**:525-526.
5. **Atkinson, E. A., M. Barry, A. J. Darmon, I. Shostak, P. C. Turner, R. W. Moyer, and R. C. Bleackley.** 1998. Cytotoxic T lymphocyte-assisted suicide. Caspase 3 activation is primarily the result of the direct action of granzyme B. *J Biol Chem* **273**:21261-21266.
6. **Bach, O., M. Baier, A. Pullwitt, N. Fosiko, G. Chagaluka, M. Kalima, W. Pfister, E. Straube, and M. Molyneux.** 2005. Falciparum malaria after splenectomy: a prospective controlled study of 33 previously splenectomized Malawian adults. *Trans R Soc Trop Med Hyg* **99**:861-867.
7. **Belnoue, E., M. Kayibanda, J. C. Deschemin, M. Viguier, M. Mack, W. A. Kuziel, and L. Renia.** 2003. CCR5 deficiency decreases susceptibility to experimental cerebral malaria. *Blood* **101**:4253-4259.
8. **Belnoue, E., M. Kayibanda, A. M. Vigario, J. C. Deschemin, N. van Rooijen, M. Viguier, G. Snounou, and L. Renia.** 2002. On the pathogenic role of brain-sequestered alphabeta CD8⁺ T cells in experimental cerebral malaria. *J Immunol* **169**:6369-6375.
9. **Beresford, P. J., Z. Xia, A. H. Greenberg, and J. Lieberman.** 1999. Granzyme A loading induces rapid cytolysis and a novel form of DNA damage independently of caspase activation. *Immunity* **10**:585-594.
10. **Beresford, P. J., D. Zhang, D. Y. Oh, Z. Fan, E. L. Greer, M. L. Russo, M. Jaju, and J. Lieberman.** 2001. Granzyme A activates an endoplasmic reticulum-associated caspase-independent nuclease to induce single-stranded DNA nicks. *J Biol Chem* **276**:43285-43293.
11. **Boubou, M. I., A. Collette, D. Voegtli, D. Mazier, P. A. Cazenave, and S. Pied.** 1999. T cell response in malaria pathogenesis: selective increase in T cells carrying the TCR V(beta)8 during experimental cerebral malaria. *Int Immunol* **11**:1553-1562.
12. **Campbell, J. J., J. Hedrick, A. Zlotnik, M. A. Siani, D. A. Thompson, and E. C. Butcher.** 1998. Chemokines and the arrest of lymphocytes rolling under flow conditions. *Science* **279**:381-384.
13. **Conti, I., and B. J. Rollins.** 2004. CCL2 (monocyte chemoattractant protein-1) and cancer. *Semin Cancer Biol* **14**:149-154.

14. **Daly, C., and B. J. Rollins.** 2003. Monocyte chemoattractant protein-1 (CCL2) in inflammatory disease and adaptive immunity: therapeutic opportunities and controversies. *Microcirculation* **10**:247-257.
15. **de Jong, E. K., I. M. Dijkstra, M. Hensens, N. Brouwer, M. van Amerongen, R. S. Liem, H. W. Boddeke, and K. Biber.** 2005. Vesicle-mediated transport and release of CCL21 in endangered neurons: a possible explanation for microglia activation remote from a primary lesion. *J Neurosci* **25**:7548-7557.
16. **Demetriou, M., M. Granovsky, S. Quaggin, and J. W. Dennis.** 2001. Negative regulation of T-cell activation and autoimmunity by Mgat5 N-glycosylation. *Nature* **409**:733-739.
17. **Dijkstra, I. M., S. Hulshof, P. van der Valk, H. W. Boddeke, and K. Biber.** 2004. Cutting edge: activity of human adult microglia in response to CC chemokine ligand 21. *J Immunol* **172**:2744-2747.
18. **Dumic, J., S. Dabelic, and M. Flögel.** 2006. Galectin-3: an open-ended story. *Biochim Biophys Acta* **1760**:616-635.
19. **Engwerda, C., E. Belnoue, A. C. Gruner, and L. Renia.** 2005. Experimental models of cerebral malaria. *Curr Top Microbiol Immunol* **297**:103-143.
20. **Fabiani, G., J. Orfila, and G. Bonhoure.** 1957. [Effect of splenectomy on malaria in white rats previously infected by *Plasmodium vinckei*.]. *C R Seances Soc Biol Fil* **151**:2135-2137.
21. **Fabiani, G., J. Orfila, and G. Bonhoure.** 1958. [Influence of splenectomy on the natural resistance of white rats to *Plasmodium vinckei*.]. *C R Seances Soc Biol Fil* **152**:337-339.
22. **Fan, Z., P. J. Beresford, D. Zhang, and J. Lieberman.** 2002. HMG2 interacts with the nucleosome assembly protein SET and is a target of the cytotoxic T-lymphocyte protease granzyme A. *Mol Cell Biol* **22**:2810-2820.
23. **Fan, Z., P. J. Beresford, D. Zhang, Z. Xu, C. D. Novina, A. Yoshida, Y. Pommier, and J. Lieberman.** 2003. Cleaving the oxidative repair protein Ape1 enhances cell death mediated by granzyme A. *Nat Immunol* **4**:145-153.
24. **Finley, R. W., L. J. Mackey, and P. H. Lambert.** 1982. Virulent *P. berghei* malaria: prolonged survival and decreased cerebral pathology in cell-dependent nude mice. *J Immunol* **129**:2213-2218.
25. **Fukumori, T., Y. Takenaka, N. Oka, T. Yoshii, V. Hogan, H. Inohara, H. O. Kanayama, H. R. Kim, and A. Raz.** 2004. Endogenous galectin-3 determines the routing of CD95 apoptotic signaling pathways. *Cancer Res* **64**:3376-3379.
26. **Fukumori, T., Y. Takenaka, T. Yoshii, H. R. Kim, V. Hogan, H. Inohara, S. Kagawa, and A. Raz.** 2003. CD29 and CD7 mediate galectin-3-induced type II T-cell apoptosis. *Cancer Res* **63**:8302-8311.
27. **Garcia-Sanz, J. A., H. R. MacDonald, D. E. Jenne, J. Tschopp, and M. Nabholz.** 1990. Cell specificity of granzyme gene expression. *J Immunol* **145**:3111-3118.
28. **Garcia-Sanz, J. A., F. Velotti, H. R. MacDonald, D. Masson, J. Tschopp, and M. Nabholz.** 1988. Appearance of granule-associated molecules during activation of cytolytic T-lymphocyte precursors by defined stimuli. *Immunology* **64**:129-134.
29. **Grun, J. L., C. A. Long, and W. P. Weidanz.** 1985. Effects of splenectomy on antibody-independent immunity to *Plasmodium chabaudi adami* malaria. *Infect Immun* **48**:853-858.

30. **Hanada, M., C. Aime-Sempe, T. Sato, and J. C. Reed.** 1995. Structure-function analysis of Bcl-2 protein. Identification of conserved domains important for homodimerization with Bcl-2 and heterodimerization with Bax. *J Biol Chem* **270**:11962-11969.
31. **Hendriks, J., Y. Xiao, J. W. Rossen, K. F. van der Sluijs, K. Sugamura, N. Ishii, and J. Borst.** 2005. During viral infection of the respiratory tract, CD27, 4-1BB, and OX40 collectively determine formation of CD8⁺ memory T cells and their capacity for secondary expansion. *J Immunol* **175**:1665-1676.
32. **Hori, T.** 2006. Roles of OX40 in the pathogenesis and the control of diseases. *Int J Hematol* **83**:17-22.
33. **John, C. C., R. Opika-Opoka, J. Byarugaba, R. Idro, and M. J. Boivin.** 2006. Low levels of RANTES are associated with mortality in children with cerebral malaria. *J Infect Dis* **194**:837-845.
34. **Johnson, P. F.** 2005. Molecular stop signs: regulation of cell-cycle arrest by C/EBP transcription factors. *J Cell Sci* **118**:2545-2555.
35. **Kim, H. R., H. M. Lin, H. Biliran, and A. Raz.** 1999. Cell cycle arrest and inhibition of anoikis by galectin-3 in human breast epithelial cells. *Cancer Res* **59**:4148-4154.
36. **Ley, K.** 2003. Arrest chemokines. *Microcirculation* **10**:289-295.
37. **Lieberman, J.** 2003. The ABCs of granule-mediated cytotoxicity: new weapons in the arsenal. *Nat Rev Immunol* **3**:361-370.
38. **Lieberman, J., and Z. Fan.** 2003. Nuclear war: the granzyme A-bomb. *Curr Opin Immunol* **15**:553-559.
39. **MacMicking, J. D.** 2004. IFN-inducible GTPases and immunity to intracellular pathogens. *Trends Immunol* **25**:601-609.
40. **Matarrese, P., N. Tinari, M. L. Semeraro, C. Natoli, S. Iacobelli, and W. Malorni.** 2000. Galectin-3 overexpression protects from cell damage and death by influencing mitochondrial homeostasis. *FEBS Lett* **473**:311-315.
41. **Maurer, M., and E. von Stebut.** 2004. Macrophage inflammatory protein-1. *Int J Biochem Cell Biol* **36**:1882-1886.
42. **Medema, J. P., R. E. Toes, C. Scaffidi, T. S. Zheng, R. A. Flavell, C. J. Melief, M. E. Peter, R. Offringa, and P. H. Krammer.** 1997. Cleavage of FLICE (caspase-8) by granzyme B during cytotoxic T lymphocyte-induced apoptosis. *Eur J Immunol* **27**:3492-3498.
43. **Menten, P., A. Wuyts, and J. Van Damme.** 2002. Macrophage inflammatory protein-1. *Cytokine Growth Factor Rev* **13**:455-481.
44. **Menten, P., A. Wuyts, and J. Van Damme.** 2001. Monocyte chemotactic protein-3. *Eur Cytokine Netw* **12**:554-560.
45. **Moon, B. K., Y. J. Lee, P. Battle, J. M. Jessup, A. Raz, and H. R. Kim.** 2001. Galectin-3 protects human breast carcinoma cells against nitric oxide-induced apoptosis: implication of galectin-3 function during metastasis. *Am J Pathol* **159**:1055-1060.
46. **Nakahara, S., N. Oka, and A. Raz.** 2005. On the role of galectin-3 in cancer apoptosis. *Apoptosis* **10**:267-275.
47. **Nakano, H.** 2004. Signaling crosstalk between NF-kappaB and JNK. *Trends Immunol* **25**:402-405.

48. **Nitcheu, J., O. Bonduelle, C. Combadiere, M. Tefit, D. Seilhean, D. Mazier, and B. Combadiere.** 2003. Perforin-dependent brain-infiltrating cytotoxic CD8⁺ T lymphocytes mediate experimental cerebral malaria pathogenesis. *J Immunol* **170**:2221-2228.
49. **Odake, S., C. M. Kam, L. Narasimhan, M. Poe, J. T. Blake, O. Krahenbuhl, J. Tschopp, and J. C. Powers.** 1991. Human and murine cytotoxic T lymphocyte serine proteases: subsite mapping with peptide thioester substrates and inhibition of enzyme activity and cytolysis by isocoumarins. *Biochemistry* **30**:2217-2227.
50. **Pan, P. Y., Y. Zang, K. Weber, M. L. Meseck, and S. H. Chen.** 2002. OX40 ligation enhances primary and memory cytotoxic T lymphocyte responses in an immunotherapy for hepatic colon metastases. *Mol Ther* **6**:528-536.
51. **Potter, S., T. Chan-Ling, H. J. Ball, H. Mansour, A. Mitchell, L. Maluish, and N. H. Hunt.** 2006. Perforin mediated apoptosis of cerebral microvascular endothelial cells during experimental cerebral malaria. *Int J Parasitol* **36**:485-496.
52. **Sarfo, B. Y., S. Singh, J. W. Lillard, A. Quarshie, R. K. Gyasi, H. Armah, A. A. Adjei, P. Jolly, and J. K. Stiles.** 2004. The cerebral-malaria-associated expression of RANTES, CCR3 and CCR5 in post-mortem tissue samples. *Ann Trop Med Parasitol* **98**:297-303.
53. **Takasawa, N., N. Ishii, N. Higashimura, K. Murata, Y. Tanaka, M. Nakamura, T. Sasaki, and K. Sugamura.** 2001. Expression of gp34 (OX40 ligand) and OX40 on human T cell clones. *Jpn J Cancer Res* **92**:377-382.
54. **Tangemann, K., M. D. Gunn, P. Giblin, and S. D. Rosen.** 1998. A high endothelial cell-derived chemokine induces rapid, efficient, and subset-selective arrest of rolling T lymphocytes on a reconstituted endothelial substrate. *J Immunol* **161**:6330-6337.
55. **Thomas, J. O.** 2001. HMG1 and 2: architectural DNA-binding proteins. *Biochem Soc Trans* **29**:395-401.
56. **Vikingsson, A., K. Pederson, and D. Muller.** 1996. Altered kinetics of CD4⁺ T cell proliferation and interferon-gamma production in the absence of CD8⁺ T lymphocytes in virus-infected beta2-microglobulin-deficient mice. *Cell Immunol* **173**:261-268.
57. **Wagner, L., O. O. Yang, E. A. Garcia-Zepeda, Y. Ge, S. A. Kalams, B. D. Walker, M. S. Pasternack, and A. D. Luster.** 1998. Beta-chemokines are released from HIV-1-specific cytolytic T-cell granules complexed to proteoglycans. *Nature* **391**:908-911.
58. **Wanschura, S., E. F. Schoenmakers, C. Huysmans, S. Bartnitzke, W. J. Van de Ven, and J. Bullrdiek.** 1996. Mapping of the human HMG2 gene to 4q31. *Genomics* **31**:264-265.
59. **Weinberg, A. D., D. E. Evans, C. Thalhoffer, T. Shi, and R. A. Prell.** 2004. The generation of T cell memory: a review describing the molecular and cellular events following OX40 (CD134) engagement. *J Leukoc Biol* **75**:962-972.
60. **Wyler, D. J.** 1983. The spleen in malaria. *Ciba Found Symp* **94**:98-116.
61. **Yanez, D. M., D. D. Manning, A. J. Cooley, W. P. Weidanz, and H. C. van der Heyde.** 1996. Participation of lymphocyte subpopulations in the pathogenesis of experimental murine cerebral malaria. *J Immunol* **157**:1620-1624.
62. **Youn, B. S., K. Y. Yu, J. Oh, J. Lee, T. H. Lee, and H. E. Broxmeyer.** 2002. Role of the CC chemokine receptor 9/TECK interaction in apoptosis. *Apoptosis* **7**:271-276.
63. **Zhou, L., A. Azfer, J. Niu, S. Graham, M. Choudhury, F. M. Adamski, C. Younce, P. F. Binkley, and P. E. Kolattukudy.** 2006. Monocyte chemoattractant protein-1

induces a novel transcription factor that causes cardiac myocyte apoptosis and ventricular dysfunction. *Circ Res* **98**:1177-1185.

Table S2. Differential gene expression in relation to WT C57BL6 mice with ECM and CD8⁺ KO C57BL6 with no ECM in the Brain

Description	Fold Δ
cytotoxic T lymphocyte-associated protein 2 alpha (Ctla2a), mRNA.	8.9948
cytotoxic T lymphocyte-associated protein 2 alpha (Ctla2a), mRNA.	8.9865
granzyme A (Gzma), mRNA.	8.3315
GRANZYME B(G,H) PRECURSOR (EC 3.4.21.79) (CYTOTOXIC CELL PROTEASE 1) (CCP1) (CTLA-1) (FRAGMENTIN 2). [Source:SWISSPROT;Acc:P04187]	6.8155
lectin, galactose binding, soluble 3 (Lgals3), mRNA.	6.7903
heme oxygenase (decycling) 1 (Hmox1), mRNA.	6.3266
Fc fragment of IgG, low affinity IIIa, receptor (Fcgr3a), mRNA.	6.2845
SMALL INDUCIBLE CYTOKINE A5 PRECURSOR (CCL5) (T-CELL SPECIFIC RANTES PROTEIN) (SIS-DELTA) (MURANTES). [Source:SWISSPROT;Acc:P30882]	5.6416
zinc finger protein 36 (Zfp36), mRNA.	5.4219
CTLA-2-beta protein precursor (Fragment). [Source:Uniprot/SWISSPROT;Acc:P12400]	5.4125
glycoprotein 49 A (Gp49a), mRNA.	5.3459
uncoupling protein 2 (mitochondrial, proton carrier) (Ucp2), mRNA.	5.0887
membrane-spanning 4-domains, subfamily A, member 4B (Ms4a4b), mRNA.	4.7746
formyl peptide receptor, related sequence 2 (Fpr-rs2), mRNA.	4.5642
membrane-spanning 4-domains, subfamily A, member 6C (Ms4a6c), mRNA.	4.4701
serine (or cysteine) peptidase inhibitor, clade A, member 3N (Serpina3n), mRNA.	4.4484
PLACENTAL CALCIUM-BINDING PROTEIN (18A2) (PEL98) (MTS1 PROTEIN) (METASTATIC CELL PROTEIN). [Source:SWISSPROT;Acc:P07091]	4.4071
arrestin domain containing 2 (Arrdc2), mRNA.	4.3469
high mobility group box 2 (Hmgb2), mRNA.	4.2910
epithelial membrane protein 1 (Emp1), mRNA.	4.2516
B-cell leukemia/lymphoma 2 related protein A1b (Bcl2a1b), mRNA.	4.2057
centromere protein A (Cenpa), mRNA.	4.1628
granzyme B (Gzmb), mRNA.	4.1367

lectin, galactose binding, soluble 3 (Lgals3), mRNA.	4.1308
ENSMUST00000058434	4.1239
chemokine (C-C motif) ligand 5 (Ccl5), mRNA.	4.1196
mitogen-activated protein kinase kinase kinase 6 (Map3k6), mRNA.	4.0947
Unknown	4.0905
Aryl sulfotransferase (EC 2.8.2.1) (Phenol sulfotransferase) (PST-1) (Sulfokinase) (Phenol/aryl sulfotransferase) (ST1A4). [Source:Uniprot/SWISSPROT;Acc:P52840]	4.0796
RIKEN cDNA 3930401B19 gene	4.0785
adrenomedullin (Adm), mRNA.	4.0579
RIKEN cDNA A130040M12 gene (A130040M12Rik) on chromosome 4.	4.0108
cyclin-dependent kinase inhibitor 1A (P21) (Cdkn1a), mRNA.	3.9789
membrane-spanning 4-domains, subfamily A, member 4B (Ms4a4b), mRNA.	3.9629
Metallothionein-I (MT-I). [Source:Uniprot/SWISSPROT;Acc:P02802]	3.9449
metallothionein 2 (Mt2), mRNA.	3.8845
B-cell leukemia/lymphoma 2 related protein A1a (Bcl2a1a), mRNA.	3.8356
Interferon inducible GTPase 1	3.7640
serine (or cysteine) peptidase inhibitor, clade A, member 3C (Serpina3c), mRNA.	3.6337
GLI pathogenesis-related 2 (Glipr2), mRNA.	3.6142
Unknown	3.5686
RIKEN cDNA 4930591A17 gene (4930591A17Rik), mRNA.	3.5301
B-cell linker (Blnk), mRNA.	3.4768
RIKEN cDNA 1700030N03 gene	3.3931
RIKEN cDNA A130040M12 gene (A130040M12Rik) on chromosome 4.	3.3370
PREDICTED: hect domain and RLD 5 (Herc5), mRNA.	3.2961
RAS-related C3 botulinum substrate 2 (Rac2), mRNA.	3.2944
FK506 binding protein 5 (Fkbp5), mRNA.	3.2910
nuclear factor of kappa light chain gene enhancer in B-cells inhibitor, alpha (Nfkbia), mRNA.	3.2865
glial fibrillary acidic protein (Gfap), mRNA.	3.2605
metallothionein 1 (Mt1), mRNA.	3.2466

cathepsin C (Ctsc), mRNA.	3.2289
CCAAT/enhancer binding protein (C/EBP), beta (Cebpb), mRNA.	3.2079
v-maf musculoaponeurotic fibrosarcoma oncogene family, protein F (avian) (Maff), mRNA.	3.1959
interleukin 2 receptor, gamma chain (Il2rg), mRNA.	3.1748
proteasome (prosome, macropain) subunit, beta type 9 (large multifunctional peptidase 2) (Psmb9), mRNA.	3.1250
plasma membrane associated protein, S3-12 (S3-12), mRNA.	3.1185
mitogen activated protein kinase kinase kinase kinase 1 (Map4k1), mRNA.	3.1166
CD8 antigen, beta chain 1 (Cd8b1), mRNA.	3.1095
ENSMUST00000049805	3.0983
cold inducible RNA binding protein (Cirbp), mRNA.	3.0921
RNA binding motif protein 3 (Rbm3), mRNA.	3.0499
patatin-like phospholipase domain containing 2 (Pnpla2), mRNA.	3.0251
phospholipase A1 member A (Pla1a), mRNA.	3.0048
transgelin (Tagln), mRNA.	2.9974
chemokine (C-C motif) ligand 3 (Ccl3), mRNA.	2.9891
AXIN1 up-regulated 1 (Axud1), mRNA.	2.9860
nanos homolog 2 (Drosophila) (Nanos2), mRNA.	2.9732
signal transducer and activator of transcription 1 (Stat1), mRNA.	2.9717
cytochrome b-245, beta polypeptide (Cybb), mRNA.	2.9535
complement component 4A (Rodgers blood group) (C4a), mRNA.	2.9400
Phospholipase A2, group III	2.9279
transgelin (Tagln), mRNA.	2.9157
RIKEN cDNA 4833432E10 gene	2.9124
serum/glucocorticoid regulated kinase (Sgk), mRNA.	2.8995
protein tyrosine phosphatase, receptor type, C polypeptide-associated protein (Ptprcap), mRNA.	2.8934
complement component 1, r subcomponent (C1r), mRNA.	2.8879
colony stimulating factor 2 receptor, beta 1, low-affinity (granulocyte-macrophage) (Csf2rb1), mRNA.	2.8770
S100 calcium binding protein A6 (calcyclin) (S100a6), mRNA.	2.8627

Inhibitory PAS domain protein. [Source:Uniprot/SPTREMBL;Acc:Q8VHR1]	2.8501
Fc receptor, IgG, low affinity III (Fcgr3), mRNA.	2.8370
linker for activation of T cells (Lat), mRNA.	2.8328
transgelin (Tagln), mRNA.	2.8318
Unknown	2.7952
Fc receptor, IgG, low affinity IIb (Fcgr2b), transcript variant 2, mRNA.	2.7462
Unknown	2.7450
IKAROS family zinc finger 1 (Ikzf1), transcript variant 2, mRNA.	2.7223
FK506 binding protein 5	2.7142
C-type lectin domain family 4, member a2	2.7095
phospholipase A2, group III (Pla2g3), mRNA.	2.6938
PREDICTED: RIKEN cDNA A530050D06 gene, transcript variant 10 (A530050D06Rik), mRNA.	2.6912
PREDICTED: RIKEN cDNA A130082M07 gene (A130082M07Rik), mRNA.	2.6823
transforming growth factor, beta induced (Tgfb1), mRNA.	2.6718
achaete-scute complex homolog-like 2 (Drosophila) (Ascl2), mRNA.	2.6510
Cysteine-rich protein 1 (intestinal)	2.6407
calcium/calmodulin-dependent protein kinase kinase 1, alpha (Camkk1), mRNA.	2.6385
RIKEN cDNA 4930535B03 gene	2.6385
cysteine-rich protein 1 (intestinal) (Crip1), mRNA.	2.5528
UDP glucuronosyltransferase 1 family, polypeptide A7C (Ugt1a7c), mRNA.	2.5236
leukocyte immunoglobulin-like receptor, subfamily B, member 4 (Lilrb4), mRNA.	2.5079
cDNA sequence BC032204 (BC032204), mRNA.	2.4898
RIKEN cDNA 1700093K21 gene (1700093K21Rik), mRNA.	2.4827
cadherin 5 (Cdh5), mRNA.	2.4447
protein tyrosine phosphatase, receptor type, C (Ptprc), mRNA.	2.4346
myeloid differentiation primary response gene 116 (Myd116), mRNA.	2.4310
Solute carrier family 1 (glial high affinity glutamate transporter), member 3	2.4255
lamin A (Lmna), transcript variant 2, mRNA.	2.4236

Unknown	2.3977
pyruvate dehydrogenase kinase, isoenzyme 4 (Pdk4), mRNA.	2.3935
ornithine decarboxylase, structural 1 (Odc1), mRNA.	2.3923
chemokine (C-C motif) ligand 9 (Ccl9), mRNA.	2.3874
runt related transcription factor 1 (Runx1), mRNA.	2.3809
glia maturation factor, gamma (Gmfg), transcript variant 2, mRNA.	2.3499
tumor necrosis factor receptor superfamily, member 4 (Tnfrsf4), mRNA.	2.3430
ADP-ribosylation factor 4-like (Arf14), mRNA.	2.3375
lymphocyte specific 1 (Lsp1), mRNA.	2.3299
proteasome (prosome, macropain) subunit, beta type 10 (Psm10), mRNA.	2.3198
RIKEN cDNA 2010002N04 gene (2010002N04Rik), mRNA.	2.3159
Unknown	2.3077
Histone 2, H2bb	2.3067
PREDICTED: similar to macrophage expressed gene 1 (LOC671359), mRNA.	2.2807
Small nucleolar RNA, C/D box 22	2.2801
lymphocyte cytosolic protein 1 (Lcp1), mRNA.	2.2739
Solute carrier family 1 (glial high affinity glutamate transporter), member 3	2.2650
Chemokine (C-C motif) ligand 25	2.2592
RIKEN cDNA 1110007F12 gene (1110007F12Rik), mRNA.	2.2557
UDP-Gal:betaGlcNAc beta 1,4- galactosyltransferase, polypeptide 1 (B4galt1), mRNA.	2.2464
hematopoietic cell specific Lyn substrate 1 (Hcls1), mRNA.	2.2382
histone cluster 1, H3e (Hist1h3e), mRNA.	2.2191
gasdermin domain containing 1 (Gsdmdc1), mRNA.	2.2190
histone cluster 1, H3d (Hist1h3d), mRNA.	2.2098
UDP glucuronosyltransferase 1 family, polypeptide A6B (Ugt1a6b), mRNA.	2.2089
histone cluster 1, H3b (Hist1h3b), mRNA.	2.2056
Unknown	2.2018
cDNA sequence BC040758 (BC040758), mRNA.	2.1976

	2.1955
plasminogen activator, urokinase receptor (Plaur), mRNA.	
colony stimulating factor 2 receptor, beta 2, low-affinity (granulocyte-macrophage) (Csf2rb2), mRNA.	2.1946
	2.1922
Nudix (nucleoside diphosphate linked moiety X)-type motif 6	
	2.1867
cofilin 1, non-muscle (Cfl1), mRNA.	
PREDICTED: similar to Leucine-rich repeat-containing protein 32 precursor (GARP protein) (Garpin) (Glycoprotein A repetitions predominant) (LOC434215), mRNA.	2.1712
	2.1712
PREDICTED: hypothetical protein LOC665756 (LOC665756), mRNA.	
	2.1671
PREDICTED: LOC434061 (LOC434061)	
PREDICTED: AN1, ubiquitin-like, homolog (Xenopus laevis), transcript variant 2 (Anub1), mRNA.	2.1539
	2.1488
growth arrest and DNA-damage-inducible 45 beta (Gadd45b), mRNA.	
PREDICTED: similar to UDP-glucuronosyltransferase 1-1 precursor (UDPGT) (UGT1*1) (UGT1-01) (UGT1.1) (UGT1A1) (UGTBR1) (LOC673061), mRNA.	2.1459
	2.1436
major facilitator superfamily domain containing 2 (Mfsd2), mRNA.	
	2.1338
GATA binding protein 2 (Gata2), mRNA.	
	2.1015
cytochrome P450, family 4, subfamily x, polypeptide 1 (Cyp4x1), mRNA.	
	2.0870
serum deprivation response (Sdpr), mRNA.	
	2.0767
microrchidia 4 (Morc4), mRNA.	
	2.0740
thioredoxin interacting protein (Txnip), transcript variant 2, mRNA.	
	2.0695
thyroid hormone receptor interactor 10 (Trip10), mRNA.	
	2.0651
IKAROS family zinc finger 1 (Ikzf1), transcript variant 2, mRNA.	
	2.0616
myelocytomatosis oncogene (Myc), mRNA.	
SULFOTRANSFERASE FAMILY, CYTOSOLIC, 2B, MEMBER 1; HYDROXYSTEROID SULFOTRANSFERASE; EXPRESSED SEQUENCE BB173635. [Source:RefSeq;Acc:NM_017465]	2.0570
	2.0513
calponin 2 (Cnn2), mRNA.	
	2.0442
zyxin (Zyx), mRNA.	
	2.0414
actin, beta, cytoplasmic (Actb), mRNA.	
	2.0391
membrane-spanning 4-domains, subfamily A, member 11 (Ms4a11), mRNA.	
	2.0383
proteoglycan 1, secretory granule (Prg1), mRNA.	
	2.0349
transferrin receptor 2 (Trfr2), mRNA.	
	2.0305
regulator of G-protein signaling 1 (Rgs1), mRNA.	

ornithine decarboxylase, structural 1 (Odc1), mRNA.	2.0274
interferon gamma (Ifng), mRNA.	2.0181
chitinase 3-like 4 (Chi3l4), mRNA.	2.0168
dual-specificity tyrosine-(Y)-phosphorylation regulated kinase 3 (Dyrk3), mRNA.	2.0123
Fas (TNF receptor superfamily member) (Fas), mRNA.	2.0048
predicted gene, EG622320 (EG622320), mRNA.	0.4641
CYTOSKELETAL PROTEIN. [Source:SPTREMBL;Acc:O08614]	0.4616
potassium channel, subfamily K, member 13 (Kcnk13), mRNA.	0.4457
CDNA clone IMAGE:6411272	0.4451
integral membrane protein 2A (Itm2a), mRNA.	0.4294
cysteine and histidine-rich domain (CHORD)-containing, zinc-binding protein 1 (Chordc1), mRNA.	0.4293
TRANSCRIPTION ELONGATION REGULATOR 1 (CA150); TRANSCRIPTION FACTOR CA150B; COACTIVATOR OF 150 KD; TATA BOX BINDING PROTEIN (TBP)-ASSOCIATED FACTOR, RNA POLYMERASE II, S, 150KD. [Source:RefSeq;Acc:NM_019512]	0.4267
McKusick-Kaufman syndrome protein (Mkks), mRNA.	0.3743
Splicing factor proline/glutamine rich (polypyrimidine tract binding protein associated)	0.3690
UDP galactosyltransferase 8A (Ugt8a), mRNA.	0.3629
TRANSCRIPTION ELONGATION REGULATOR 1 (CA150); TRANSCRIPTION FACTOR CA150B; COACTIVATOR OF 150 KD; TATA BOX BINDING PROTEIN (TBP)-ASSOCIATED FACTOR, RNA POLYMERASE II, S, 150KD. [Source:RefSeq;Acc:NM_019512]	0.3604
G protein-coupled receptor 17 (Gpr17), mRNA.	0.2942
RNA binding motif protein 3 (Rbm3), mRNA.	0.2848
fatty acid binding protein 7, brain (Fabp7), mRNA.	0.2701
G protein-coupled receptor 34 (Gpr34), mRNA.	0.2685

Table S3. Differential gene expression in relation to WT C57BL6 mice with ECM and CD8⁺ KO C57BL6 with no ECM in the spleen.

Description	GI #	Fold Change
CD8 antigen, beta chain 1 (Cd8b1), mRNA.	6753358	13.4451
3-hydroxy-3-methylglutaryl-Coenzyme A synthase 2 (Hmgcs2), mRNA.	31560689	6.4773
pyruvate dehydrogenase kinase, isoenzyme 4 (Pdk4), mRNA.	7305375	6.3688
acyl-CoA thioesterase 1 (Acot1), mRNA.	6753550	6.2296
metallothionein 1 (Mt1), mRNA.	7305285	5.8018
Unknown	NA	5.4255
pyruvate dehydrogenase kinase, isoenzyme 4 (Pdk4), mRNA.	7305375	5.2336
dual specificity phosphatase 1 (Dusp1), mRNA.	7305423	4.4848
Aryl sulfotransferase (EC 2.8.2.1) (Phenol sulfotransferase) (PST-1) (Sulfokinase) (Phenol/aryl sulfotransferase) (ST1A4). [Source:Uniprot/SWISSPROT;Acc:P52840]	NA	4.3839
Ras association (RalGDS/AF-6) and pleckstrin homology domains 1	NA	4.0273
eosinophil-associated, ribonuclease A family, member 1 (Ear1), mRNA.	6681249	3.5958
RIKEN cDNA C630010D07 gene	NA	3.5807
glutamate-ammonia ligase (glutamine synthetase) (Glul), mRNA.	31982332	3.5784
VASCULAR CELL ADHESION PROTEIN 1 PRECURSOR (V-CAM 1). [Source:SWISSPROT;Acc:P29533]	NA	3.5483
Glucocorticoid-induced leucine zipper protein. [Source:Uniprot/SWISSPROT;Acc:Q9Z2S7]	NA	3.5091
PREDICTED: upstream transcription factor 2 (Usf2), mRNA.	94379911	3.4103
ELAV (embryonic lethal, abnormal vision, Drosophila)-like 1 (Hu antigen R)	NA	3.3857
eosinophil-associated, ribonuclease A family, member 3 (Ear3), mRNA.	8393283	3.3435
zinc finger protein 36, C3H type-like 2 (Zfp36l2), mRNA.	49249965	3.3059
RIKEN cDNA A630066F11 gene	NA	3.0934
TSC22 domain family 3 (Tsc22d3), mRNA.	31982796 11073540	3.0061
selenoprotein P, plasma, 1 (Sepp1), transcript variant 2, mRNA.	8	2.9250
vascular cell adhesion molecule 1 (Vcam1), mRNA.	31981430	2.8646
DIRAS family, GTP-binding RAS-like 2 (Diras2), mRNA.	71725385	2.7918
centaurin, gamma 2 (Centg2), transcript variant 2, mRNA.	80978937	2.7499
Unknown	NA	2.5512
defensin related cryptdin 22 (Defcr22), mRNA.	50263038	2.5371
neuromedin B (Nmb), mRNA.	13386018	2.5330

RIKEN cDNA 2810403D21 gene	NA	2.4536
PREDICTED: RIKEN cDNA 1700109H08 gene, transcript variant 1 (1700109H08Rik), mRNA.	51710784	2.4235
RIKEN cDNA 9330133O14 gene (9330133O14Rik), mRNA.	28892761	2.3348
ZINC FINGER PROTEIN 207. [Source:RefSeq;Acc:NM_011751]	NA	2.2568
Nudix (nucleoside diphosphate linked moiety X)-type motif 5	NA	2.1683
PREDICTED: similar to 40S ribosomal protein S25 (LOC629595), mRNA.	82943174	2.1634
acetyl-Coenzyme A acyltransferase 2 (mitochondrial 3-oxoacyl-Coenzyme A thiolase) (Acaa2), mRNA.	29126205	2.1569
RIKEN cDNA 2610044O15 gene	NA	2.0790
nei like 3 (E. coli) (Neil3), mRNA.	22122759	2.0592
olfactory receptor 816 (Olf816), mRNA.	33239334	1.9493
kinesin family member 4 (Kif4), mRNA.	6680568	1.9468
serum/glucocorticoid regulated kinase (Sgk), mRNA.	6755490	1.9143
solute carrier family 25 (mitochondrial carrier, adenine nucleotide translocator), member 5 (Slc25a5), mRNA.	22094075	1.8576
growth factor, erv1 (S. cerevisiae)-like (augmenter of liver regeneration) (Gfer), mRNA.	46909575	0.6092
polyribonucleotide nucleotidyltransferase 1 (Pnpt1), mRNA.	25188204	0.5915
C-type lectin domain family 4, member d (Clec4d), mRNA.	61098075	0.5655
START domain containing 3 (Stard3), mRNA.	10946984	0.5473
CDNA sequence BC005537	NA	0.5437
Rho GTPase activating protein 17 (Arhgap17), mRNA.	21362323	0.5300
bone morphogenetic protein 7 (Bmp7), mRNA.	31982487	0.5207
PREDICTED: Cdc42 binding protein kinase alpha, transcript variant 5 (Cdc42bpa), mRNA.	82883279	0.5133
ring finger protein 31 (Rnf31), mRNA.	40254409 11415867	0.5129
Luc7 homolog (S. cerevisiae)-like (Luc7l), transcript variant 2, mRNA.	7	0.5065
ubiquitin D (Ubd), mRNA.	12963519	0.5011
RIKEN cDNA 1190005F20 gene (1190005F20Rik), mRNA.	74959790	0.4892
transmembrane protein 67 (Tmem67), mRNA.	29244458	0.4888
amyotrophic lateral sclerosis 2 (juvenile) homolog (human) (Als2), mRNA.	17505210	0.4888
solute carrier family 2 (facilitated glucose transporter), member 6 (Slc2a6), mRNA.	27369954	0.4845
ENSMUST00000057160	NA	0.4811
SIMILAR TO CORONIN, ACTIN BINDING PROTEIN, 2A (FRAGMENT). [Source:SPTREMBL;Acc:Q8R0L6]	NA	0.4786
transmembrane 4 superfamily member 1 (Tm4sf1), mRNA.	6678762	0.4784
histidine decarboxylase (Hdc), mRNA.	28173556	0.4773
kelch-like 26 (Drosophila) (Klhl26), transcript variant 1, mRNA.	25286713	0.4705
ficolin B (Fcnb), mRNA.	77404440	0.4695
Testis protein TEX17. [Source:Uniprot/SPTREMBL;Acc:Q99MW2]	NA	0.4643

serine (or cysteine) peptidase inhibitor, clade A, member 3F (Serpina3f), mRNA.	85701824	0.4633
hexokinase 3 (Hk3), mRNA.	84370288	0.4607
nuclear factor, erythroid derived 2, like 2 (Nfe2l2), mRNA.	6754832	0.4605
ring finger protein 135 (Rnf135), mRNA.	21312628	0.4587
methyltransferase-like 3 (Mettl3), mRNA.	77627973	0.4569
Mortality factor 4 like 1	NA	0.4562
v-ral simian leukemia viral oncogene homolog A (ras related) (Rala), mRNA.	34328471	0.4507
interferon induced transmembrane protein 3 (Ifitm3), mRNA.	21539593	0.4491
potassium voltage-gated channel, subfamily Q, member 3 (Kcnq3), mRNA.	23097333	0.4432
v-maf musculoaponeurotic fibrosarcoma oncogene family, protein K (avian) (Mafk), mRNA.	6754612	0.4412
transmembrane protein 106A (Tmem106a), mRNA.	21450215	0.4406
leucine rich repeat containing 16 (Lrrc16), mRNA.	57864122	0.4402
interleukin 27 (Il27), mRNA.	21704110	0.4384
phosphoinositide-3-kinase adaptor protein 1 (Pik3ap1), mRNA.	13878195	0.4373
5'-nucleotidase, cytosolic III (Nt5c3), mRNA.	27229034	0.4358
RIKEN cDNA 4632417K18 gene (4632417K18Rik), mRNA.	13386132	0.4343
similar to CDNA sequence BC023105 (LOC225594), mRNA.	77861889	0.4287
histocompatibility 2, T region locus 24 (H2-T24), mRNA.	6680153	0.4274
PREDICTED: tetratricopeptide repeat domain 18 (Ttc18), mRNA.	94396678	0.4236
ATPase, class V, type 10A (Atp10a), mRNA.	23510329	0.4218
brain-specific angiogenesis inhibitor 1 (Bai1), mRNA.	92110033	0.4146
vascular endothelial growth factor A (Vegfa), transcript variant 2, mRNA.	40254603	0.4127
lymphocyte antigen 6 complex, locus H (Ly6h), mRNA.	6754586	0.4116
v-maf musculoaponeurotic fibrosarcoma oncogene family, protein F (avian) (Maff), mRNA.	6754608	0.4038
RNA binding motif protein 3 (Rbm3), mRNA.	37497112	0.4007
hematopoietic SH2 domain containing (Hsh2d), mRNA.	37537546	0.3983
Nuclear transcription factor-Y alpha	NA	0.3897
RIKEN cDNA 1600014C10 gene (1600014C10Rik), mRNA.	21312338	0.3892
olfactory receptor 49 (Olfr49), mRNA.	6754932	0.3878
RIKEN cDNA A630077B13 gene (A630077B13Rik), mRNA.	31982193	0.3835
immediate early response 3 (Ier3), mRNA.	19526808	0.3820
Unknown	NA	0.3791
RIKEN cDNA 2600010E01 gene (2600010E01Rik), mRNA.	31560751	0.3776
PREDICTED: RIKEN cDNA 4933412E12 gene (4933412E12Rik), mRNA.	94389693	0.3771
PREDICTED: hect domain and RLD 5 (Herc5), mRNA.	82901528	0.3731
solute carrier family 25 (mitochondrial carrier, glutamate), member 22 (Slc25a22), mRNA.	21311845	0.3730

poly (ADP-ribose) polymerase family, member 11 (Parp11), mRNA.	31088906	0.3725
eukaryotic translation initiation factor 2-alpha kinase 2 (Eif2ak2), mRNA.	6755160	0.3722
chemokine (C-X-C motif) ligand 1 (Cxcl1), mRNA.	6680109	0.3703
DNA segment, Chr 11, Lothar Hennighausen 2, expressed (D11Lgp2e), mRNA.	70608133	0.3655
interferon induced with helicase C domain 1 (Ifih1), mRNA.	23956208	0.3646
vascular endothelial growth factor A (Vegfa), transcript variant 2, mRNA.	40254603	0.3632
PREDICTED: similar to immunity-related GTPase family, cinema 1 (LOC631323), mRNA.	94390113	0.3628
MIT, microtubule interacting and transport, domain containing 1 (Mitd1), mRNA.	11062571 0	0.3621
PREDICTED: immunoresponsive gene 1 (Irg1), mRNA.	94397329	0.3560
adenosine deaminase, RNA-specific (Adar), transcript variant 1, mRNA.	31981009	0.3534
PREDICTED: platelet-activating factor receptor (Ptafr), mRNA.	38079353	0.3520
component of Sp100-rs (Csprs), mRNA.	31542429	0.3516
TRANSCRIPTION ELONGATION REGULATOR 1 (CA150); TRANSCRIPTION FACTOR CA150B; COACTIVATOR OF 150 KD; TATA BOX BINDING PROTEIN (TBP)-ASSOCIATED FACTOR, RNA POLYMERASE II, S, 150KD. [Source:RefSeq;Acc:NM_019512]	NA	0.3463
Fas death domain-associated protein (Daxx), mRNA.	11218118 5	0.3459
tryptophanyl-tRNA synthetase (Wars), mRNA.	34328206	0.3444
PREDICTED: cDNA sequence BC013672, transcript variant 1 (BC013672), mRNA.	82917484	0.3435
RIKEN cDNA 5830443L24 gene	NA	0.3426
LYMPHOCYTE ANTIGEN LY-6C PRECURSOR. [Source:SWISSPROT;Acc:P09568]	NA	0.3406
Nuclear antigen Sp100	NA	0.3392
cDNA sequence BC057170 (BC057170), mRNA.	27370144	0.3385
coiled-coil domain containing 52 (Ccdc52), mRNA.	31559964	0.3304
bone marrow stromal cell antigen 2 (Bst2), mRNA.	37674242	0.3295
2-cell-stage, variable group, member 3 (Tctsv3), mRNA.	23943805	0.3293
PREDICTED: similar to cyclin fold protein 1 (LOC625291), mRNA.	94411176	0.3293
SLAM family member 8 (Slamf8), mRNA.	11062580 4	0.3291
Z-DNA binding protein 1 (Zbp1), mRNA.	11496253	0.3262
ubiquitin-conjugating enzyme E2L 6 (Ube2l6), mRNA.	9910602	0.3217
nuclear factor of kappa light polypeptide gene enhancer in B-cells inhibitor, epsilon (Nfkbie), mRNA.	31543321	0.3200
colony stimulating factor 3 receptor (granulocyte) (Csf3r), mRNA.	6681051	0.3173
PREDICTED: RIKEN cDNA 1700113H08 gene (1700113H08Rik), mRNA.	94388522	0.3173
Unknown	NA	0.3170
DnaJ (Hsp40) homolog, subfamily B, member 10 (Dnajb10), transcript variant 1, mRNA.	9937996	0.3168
Z-DNA BINDING PROTEIN 1 (TUMOR STROMA AND ACTIVATED MACROPHAGE PROTEIN DLM-1). [Source:SWISSPROT;Acc:Q9QY24]	NA	0.3154

RIKEN cDNA 2700019D07 gene (2700019D07Rik), mRNA.	30794380	0.3132
interferon, alpha-inducible protein 27 (Ifi27), mRNA.	44771124	0.3126
tumor necrosis factor (ligand) superfamily, member 10 (Tnfsf10), mRNA.	6678431	0.3097
cyclin D1 (Ccnd1), mRNA.	6680868	0.3092
UDP-Gal:betaGlcNAc beta 1,4-galactosyltransferase, polypeptide 5 (B4galt5), mRNA.	11608930 6	0.3083
Jun oncogene (Jun), mRNA.	6754402	0.3083
interleukin 4 induced 1 (Il4i1), mRNA.	6753872	0.3074
free fatty acid receptor 2 (Ffar2), mRNA.	22122727	0.3072
PREDICTED: similar to Gamma-interferon-inducible protein Ifi-16 (Interferon-inducible myeloid differentiation transcriptional activator) (IFI 16) (LOC672540), mRNA.	94365824	0.3023
T cell receptor gamma chain	NA	0.3010
histocompatibility 2, M region locus 10.2 (H2-M10.2), mRNA.	29244570	0.2992
cDNA sequence BC023105 (BC023105), mRNA.	93352547	0.2991
interleukin 12 receptor, beta 1 (Il12rb1), mRNA.	6680399	0.2990
Unknown	NA	0.2985
nuclear factor of kappa light polypeptide gene enhancer in B-cells 2, p49/p100 (Nfkb2), mRNA.	9506921	0.2973
poly (ADP-ribose) polymerase family, member 14 (Parp14), mRNA.	87299607	0.2964
poly (ADP-ribose) polymerase family, member 12 (Parp12), mRNA.	27370366	0.2950
killer cell lectin-like receptor family E member 1 (Klre1), mRNA.	30520371	0.2931
tumor necrosis factor (Tnf), mRNA.	7305585	0.2925
interferon gamma inducible protein 47 (Ifi47), mRNA.	6680359	0.2923
ENSMUST00000046104	NA	0.2913
RIKEN cDNA 2700055K07 gene (2700055K07Rik), mRNA.	13385968	0.2895
interferon gamma induced GTPase (Igtf), mRNA.	31980875	0.2887
DNA segment, Chr 11, Lothar Hennighausen 2, expressed (D11Lgp2e), mRNA.	70608133	0.2878
PREDICTED: cDNA sequence BC006779, transcript variant 3 (BC006779), mRNA.	94369093	0.2854
receptor transporter protein 4 (Rtp4), mRNA.	31981001	0.2841
basic leucine zipper transcription factor, ATF-like 2 (Batf2), mRNA.	28077033	0.2824
DNA segment, Chr 13, ERATO Doi 608, expressed (D13Ertd608e), mRNA.	85701640	0.2806
2'-5' oligoadenylate synthetase 1B (Oas1b), mRNA.	21728364	0.2795
T-cell specific GTPase (Tgtp), mRNA.	31543861	0.2792
RIKEN cDNA A530030E21 gene	NA	0.2770
toll-like receptor 9 (Tlr9), mRNA.	13626030	0.2765
PREDICTED: sterile alpha motif domain containing 9-like, transcript variant 3 (Samd9l), mRNA.	82802395	0.2751
PREDICTED: expressed sequence AW011738 (AW011738), mRNA.	94374136	0.2743

programmed cell death 1 ligand 2 (Pdcd1lg2), mRNA.	10946740	0.2738
PREDICTED: similar to poly (ADP-ribose) polymerase family, member 10 (LOC671535), mRNA.	94399567	0.2711
PREDICTED: expressed sequence AI481105, transcript variant 4 (AI481105), mRNA.	82887296	0.2694
interferon inducible GTPase 1 (Iigp1), mRNA.	49274637	0.2672
PREDICTED: cDNA sequence BC020489, transcript variant 3 (BC020489), mRNA.	82958239	0.2660
C-type lectin domain family 5, member a (Clec5a), transcript variant 2, mRNA.	10946692	0.2660
Stannin	NA	0.2657
protocadherin 18 (Pcdh18), mRNA.	31982589	0.2648
tripartite motif protein 30 (Trim30), mRNA.	6677815	0.2637
tripartite motif protein 34 (Trim34), mRNA.	13507607	0.2634
signal transducer and activator of transcription 2 (Stat2), mRNA.	9910572	0.2609
signal transducer and activator of transcription 1 (Stat1), mRNA.	11432648 2	0.2609
PREDICTED: RIKEN cDNA 4930599N23 gene (4930599N23Rik), misc RNA.	NA	0.2604
solute carrier organic anion transporter family, member 3a1 (Slco3a1), transcript variant 1, mRNA.	84579880	0.2602
RIKEN cDNA A630038E17 gene	NA	0.2578
PREDICTED: similar to Interferon-activatable protein 204 (Ifi-204) (Interferon-inducible protein p204) (LOC672526), mRNA.	94365817	0.2553
myxovirus (influenza virus) resistance 1 (Mx1), mRNA.	6996930	0.2552
interleukin 1 beta (Il1b), mRNA.	6680415	0.2487
PREDICTED: gene model 1966, (NCBI), transcript variant 2 (Gm1966), mRNA.	82907383	0.2475
interferon-induced protein with tetratricopeptide repeats 3 (Ifit3), mRNA.	6754288	0.2456
poly (ADP-ribose) polymerase family, member 14 (Parp14), mRNA.	87299607	0.2443
PREDICTED: similar to T cell receptor gamma MNG8 (LOC434531)	NA	0.2408
interferon activated gene 205 (Ifi205), mRNA.	31982556	0.2407
natural cytotoxicity triggering receptor 1 (Ncr1), mRNA.	31981638	0.2383
chemokine (C-C motif) ligand 24 (Ccl24), mRNA.	9625035	0.2378
radical S-adenosyl methionine domain containing 2 (Rsad2), mRNA.	31543946	0.2324
GTPase, very large interferon inducible 1 (Gvin1), transcript variant B, mRNA.	11527096 8	0.2307
interferon inducible GTPase 2 (Iigp2), mRNA.	31980894	0.2306
plasminogen activator, urokinase (Plau), mRNA.	6679377	0.2300
2'-5' oligoadenylate synthetase 1A (Oas1a), mRNA.	21630283	0.2298
T-cell receptor gamma, constant region	NA	0.2252
RNA binding motif protein 3 (Rbm3), mRNA.	37497112	0.2250
Unknown	NA	0.2248
myxovirus (influenza virus) resistance 1 (Mx1), mRNA.	6996930	0.2226
myxovirus (influenza virus) resistance 2 (Mx2), mRNA.	7549779	0.2164

DNA segment, Chr 14, ERATO Doi 668, expressed (D14Ert668e), mRNA.	39841029	0.2125
Unknown	NA	0.2108
ADP-ribosyltransferase 2b (Art2b), mRNA.	11081585	
	1	0.2105
2-cell-stage, variable group, member 1 (Tctst1), mRNA.	9055256	0.2090
receptor transporter protein 4 (Rtp4), mRNA.	31981001	0.2077
ubiquitin-conjugating enzyme E2L 6 (Ube2l6), mRNA.	9910602	0.2074
RIKEN cDNA B020031M17 gene (B020031M17Rik), mRNA.	85702077	0.2023
poly (ADP-ribose) polymerase family, member 3 (Parp3), mRNA.	25014095	0.2000
PREDICTED: similar to PHD finger protein 11 (LOC236451), mRNA.	94420092	0.1988
tripartite motif protein 30 (Trim30), mRNA.	6677815	0.1978
PREDICTED: sterile alpha motif domain containing 9-like, transcript variant 3 (Samd9l), mRNA.	82802395	0.1978
2'-5' oligoadenylate synthetase-like 1 (Oas1l), mRNA.	21630289	0.1969
thymidylate kinase family LPS-inducible member (Tyki), mRNA.	15805018	0.1963
2'-5' oligoadenylate synthetase 1A (Oas1a), mRNA.	21630283	0.1948
schlafen 1 (Slfn1), mRNA.	6755568	0.1946
	11632598	
PREDICTED: interferon activated gene 203, transcript variant 9 (Ifi203), mRNA.	1	0.1940
DNA segment, Chr 11, ERATO Doi 759, expressed (D11Ert759e), mRNA.	90855774	0.1926
2'-5' oligoadenylate synthetase-like 2 (Oas12), mRNA.	16924024	0.1908
Proteasome (prosome, macropain) 28 subunit, beta	NA	0.1894
PREDICTED: similar to Interferon-activatable protein 204 (Ifi-204) (Interferon-inducible protein p204) (LOC240921), mRNA.	82883182	0.1889
	11432648	
signal transducer and activator of transcription 1 (Stat1), mRNA.	2	0.1857
PREDICTED: hypothetical protein LOC675673 (LOC675673), mRNA.	94391273	0.1836
expressed sequence AI451617 (AI451617), mRNA.	40255281	0.1766
chemokine (C-X-C motif) ligand 11 (Cxcl11), mRNA.	9507071	0.1739
interferon regulatory factor 7 (Irf7), mRNA.	8567364	0.1730
interferon-induced protein 44 (Ifi44), mRNA.	19527086	0.1724
membrane-spanning 4-domains, subfamily A, member 4C (Ms4a4c), mRNA.	13386406	0.1710
schlafen 4 (Slfn4), mRNA.	84490391	0.1694
similar to 2-cell-stage, variable group, member 3 (LOC625360), mRNA.	85702324	0.1657
RIKEN cDNA E430029J22 gene (E430029J22Rik), mRNA.	85701874	0.1638
Unknown	NA	0.1632
PREDICTED: similar to interferon-induced protein with tetratricopeptide repeats 1 (LOC669129), mRNA.	94406702	0.1595
PREDICTED: hypothetical protein LOC675673 (LOC675673), mRNA.	94391273	0.1586
2'-5' oligoadenylate synthetase 3 (Oas3), mRNA.	21644585	0.1546
interleukin 1 receptor antagonist (Il1rn), transcript variant 2, mRNA.	89257344	0.1544
PREDICTED: hect domain and RLD 5, transcript variant 1 (Herc5), mRNA.	94378601	0.1506

matrix metalloproteinase 13 (Mmp13), mRNA.	6678896	0.1462
cDNA sequence AF067061 (AF067061), mRNA.	39979622	0.1405
ISG15 ubiquitin-like modifier (Isg15), mRNA.	7657240	0.1309
PREDICTED: hect domain and RLD 5, transcript variant 1 (Herc5), mRNA.	94378601	0.1293
chemokine (C-C motif) ligand 12 (Ccl12), mRNA.	6755420	0.1231
Z-DNA binding protein 1 (Zbp1), mRNA.	11496253	0.1224
interferon-induced protein with tetratricopeptide repeats 2 (Ifit2), mRNA.	6680363	0.1199
chemokine (C-C motif) ligand 7 (Ccl7), mRNA.	7305463	0.1186
expressed sequence AI447904 (AI447904), mRNA.	27923921	0.1146
suppressor of cytokine signaling 1 (Socs1), mRNA.	6753424	0.1128
RIKEN cDNA 4122401K19 gene	NA	0.1054
ubiquitin specific peptidase 18 (Usp18), mRNA.	6755927	0.1049
chemokine (C-X-C motif) ligand 10 (Cxcl10), mRNA.	10946576	0.1022
2'-5' oligoadenylate synthetase 2 (Oas2), mRNA.	21644597	0.0911
PREDICTED: hypothetical LOC625046 (LOC625046), mRNA.	82998312	0.0910
SMALL INDUCIBLE CYTOKINE A12 PRECURSOR (CCL12) (MONOCYTE CHEMOTACTIC PROTEIN 5) (MCP-5) (MCP-1 RELATED CHEMOKINE). [Source:SWISSPROT;Acc:Q62401]	NA	0.0881
chemokine (C-C motif) ligand 2 (Ccl2), mRNA.	6755430	0.0848
interferon-induced protein with tetratricopeptide repeats 1 (Ifit1), mRNA.	11062610 4	0.0841

Table S4. Differential gene expression in relation to WT C57BL6 mice with ECM and PFP-KO C57BL6 with no ECM in the Brain.

Description	GI Number	Fold Δ
chemokine (C-C motif) ligand 21b (Ccl21b), mRNA.	14547891	13.7859
PREDICTED: similar to 4933409K07Rik protein (LOC545605), mRNA.	94371693	6.8993
PREDICTED: hypothetical protein LOC674214 (LOC674214), mRNA.	94371793	2.6813
achaete-scute complex homolog-like 2 (Drosophila) (Ascl2), mRNA.	66792798	2.6712
serine (or cysteine) peptidase inhibitor, clade A, member 3N (Serpina3n), mRNA.	6678093	2.4658
Kruppel-like factor 10 (Klf10), mRNA.	7305571	2.0701
WD repeat and FYVE domain containing 1 (Wdfy1), mRNA.	21312280	2.5198
serine (or cysteine) peptidase inhibitor, clade A, member 3C (Serpina3c), mRNA.	6680586	2.4755
RIKEN cDNA 8030451F13 gene (8030451F13Rik), mRNA.	40254303	2.0875
lymphocyte antigen 6 complex, locus A (Ly6a), mRNA.	6754580	0.4428
Lymphocyte antigen 6 complex, locus C	NA	0.4136

Table S5. Differential gene expression in relation to WT C57BL6 mice with ECM and PFP-KO C57BL6 with no ECM in the Spleen.

Description	GI Number	Fold Δ
PREDICTED: similar to 4933409K07Rik protein (LOC545605), mRNA.	94371693	4.1157
myosin binding protein C, fast-type (Mybpc2), mRNA.	22122731	4.0623
CD300e antigen (Cd300e), mRNA.	25286711	3.8070
PREDICTED: upstream transcription factor 2 (Usf2), mRNA.	94379911	2.9710
solute carrier family 26, member 11 (Slc26a11), mRNA.	85540463	2.7394
myosin IC (Myo1c), mRNA.	6678986	2.3928
PREDICTED: tensin 1 (Tns1), mRNA.	94363690	2.3168
PREDICTED: RIKEN cDNA 1700109H08 gene, transcript variant 1 (1700109H08Rik)	51710784	2.2888
RIKEN cDNA 1810057P16 gene	NA	2.2782
RIKEN cDNA A730082K24 gene	NA	2.2693
nanos homolog 3 (Drosophila) (Nanos3), mRNA.	34610217	2.2464
PREDICTED: RIKEN cDNA 1700080G18 gene (1700080G18Rik), mRNA.	94377197	2.2305
Ribosomal protein S6 kinase, polypeptide 5	NA	2.2299
RIKEN cDNA 2900022I03 gene	NA	2.1599
DIRAS family, GTP-binding RAS-like 2 (Diras2), mRNA.	71725385	2.1584
Zinc finger protein 787	NA	2.1575
RIKEN cDNA 1110012D08 gene (1110012D08Rik), mRNA.	30017375	2.1561
makorin, ring finger protein, 1 (Mkrn1), mRNA.	9055274	2.1354
RIKEN cDNA E430014L09 gene	NA	2.1129
RIKEN cDNA A830058I18 gene	NA	2.0715
RIKEN cDNA 0610010E21 gene (0610010E21Rik), mRNA.	110815822	2.0588
RIKEN cDNA 8030451F13 gene (8030451F13Rik), mRNA.	40254303	2.0482
troponin T3, skeletal, fast (Tnnt3), mRNA.	6755845	2.0476
DIRAS family, GTP-binding RAS-like 2 (Diras2), mRNA.	71725385	2.0428
PREDICTED: RIKEN cDNA B230112C05 gene (B230112C05Rik), mRNA.	82952216	

		2.0411
RIKEN cDNA 1700019N12 gene (1700019N12Rik), mRNA.	95772156	2.0305
Kruppel-like factor 15 (Klf15), mRNA.	12963561	2.0239
ectonucleoside triphosphate diphosphohydrolase 4 (Entpd4), mRNA.	18093090	2.0114
F-box protein 28 (Fbxo28), mRNA.	28201989	0.4977
RIKEN cDNA 5830411E10 gene (5830411E10Rik), mRNA.	30844321	0.4926
PREDICTED: RIKEN cDNA 2310047C04 gene, transcript variant 7 (2310047C04Rik)	94400572	0.4916
MIT, microtubule interacting and transport, domain containing 1 (Mitd1), mRNA.	110625710	0.4914
nuclear factor, erythroid derived 2, like 2 (Nfe2l2), mRNA.	6754832	0.4847
RIKEN cDNA C130045F17 gene	NA	0.4818
ectodermal-neural cortex 1 (Enc1), mRNA.	40254359	0.4790
glucosaminyl (N-acetyl) transferase 2, I-branching enzyme (Gcnt2), transcript variant 1	39995100	0.4789
Transcribed locus	NA	0.4780
Unknown	NA	0.4774
inhibin beta-B (Inhbb), mRNA.	74315992	0.4772
Choline/ethanolaminephosphotransferase 1	NA	0.4761
interferon induced with helicase C domain 1 (Ifih1), mRNA.	23956208	0.4741
RAD23a homolog (S. cerevisiae)	NA	0.4722
bone marrow stromal cell antigen 2 (Bst2), mRNA.	37674242	0.4698
PREDICTED: RIKEN cDNA 4631424J17 gene, transcript variant 4 (4631424J17Rik)	82934393	0.4678
RIKEN cDNA A630077B13 gene (A630077B13Rik), mRNA.	31982193	0.4663
early growth response 2 (Egr2), mRNA.	23956052	0.4657
poly (ADP-ribose) polymerase family, member 14 (Parp14), mRNA.	87299607	0.4624
interferon gamma inducible protein 47 (Ifi47), mRNA.	6680359	0.4565
PREDICTED: RIKEN cDNA 5830431A10 gene (5830431A10Rik), misc RNA.	NA	0.4563
MIS12 homolog (yeast) (Mis12), mRNA.	21313120	0.4555
dynein light chain LC8-type 1 (Dync1l1), mRNA.	31981035	0.4542
PML-RAR alpha-regulated adaptor molecule 1 (Pram1), mRNA.	50726896	0.4515
Tubulin, alpha 3	NA	0.4485
C-type lectin domain family 5, member a (Clec5a), transcript variant 2, mRNA.	10946692	0.4471
PREDICTED: RIKEN cDNA 2310047C04 gene, transcript variant 7 (2310047C04Rik), mRNA.	94400572	0.4468

Z-DNA binding protein 1	NA	0.4385
secreted phosphoprotein 1 (Spp1), mRNA.	6678113	0.4373
coiled-coil domain containing 52 (Ccde52), mRNA.	31559964	0.4338
myxovirus (influenza virus) resistance 2 (Mx2), mRNA.	7549779	0.4323
vascular endothelial growth factor A (Vegfa), transcript variant 2, mRNA.	40254603	0.4255
signal transducer and activator of transcription 1 (Stat1), mRNA.	114326482	0.4240
DNA segment, Chr 4, Wayne State University 53, expressed (D4Wsu53e), mRNA.	31560078	0.4194
PREDICTED: sterile alpha motif domain containing 9-like, transcript variant 3 (Samd9l)	82802395	0.4190
PREDICTED: similar to cyclin fold protein 1 (LOC625291), mRNA.	94411176	0.4186
Killer cell lectin-like receptor subfamily C, member 1	NA	0.4178
component of Sp100-rs (Csprs), mRNA.	31542429	0.4174
RIKEN cDNA 5830443L24 gene (5830443L24Rik), mRNA.	83776551	0.4151
REV3-like, catalytic subunit of DNA polymerase zeta RAD54 like (S. cerevisiae)	NA	0.4137
PREDICTED: cDNA sequence BC013672, transcript variant 1 (BC013672), mRNA.	82917484	0.4034
Unknown	NA	0.4029
Unknown	NA	0.4018
Potassium voltage-gated channel, subfamily Q, member 1	NA	0.4010
2'-5' oligoadenylate synthetase 1B (Oas1b), mRNA.	21728364	0.4007
PREDICTED: RIKEN cDNA 2310047C04 gene, transcript variant 7 (2310047C04Rik), mRNA.	94400572	0.3996
C-type lectin domain family 2, member d (Clec2d), mRNA.	16716407	0.3973
PREDICTED: expressed sequence AW011738 (AW011738), mRNA.	94374136	0.3970
MAX-like protein X (Mlx), mRNA.	31560537	0.3947
chemokine (C-C motif) receptor 2 (Ccr2), mRNA.	6753466	0.3912
DNA segment, Chr 13, ERATO Doi 608, expressed (D13Ert608e), mRNA.	85701640	0.3840
RNA binding motif protein 3 (Rbm3), mRNA.	37497112	0.3760
2-cell-stage, variable group, member 1 (Tcstv1), mRNA.	9055256	0.3749
Unknown	NA	0.3718
interferon inducible GTPase 2 (Iigp2), mRNA.	31980894	0.3697
tumor necrosis factor (ligand) superfamily, member 10 (Tnfsf10), mRNA.	6678431	0.3653
adenosine deaminase, RNA-specific (Adar), transcript variant 1, mRNA.	31981009	0.3628

cDNA sequence AF067061 (AF067061), mRNA.	39979622	0.3608
PREDICTED: hypothetical protein LOC675673 (LOC675673), mRNA.	94391273	0.3426
PREDICTED: hect domain and RLD 5 (Herc5), mRNA.	82901528	0.3415
PREDICTED: immunoresponsive gene 1 (Irg1), mRNA.	94397329	0.3376
Lymphocyte antigen 6 complex, locus F	NA	0.3373
RIKEN cDNA A530030E21 gene	NA	0.3367
interferon gamma induced GTPase (Igtp), mRNA.	31980875	0.3339
		0.3232
schlafen 4 (Slfn4), mRNA.	84490391	
receptor transporter protein 4 (Rtp4), mRNA.	31981001	0.3202
ADP-ribosyltransferase 2b (Art2b), mRNA.	11081585 1	0.3175
		0.3113
basic leucine zipper transcription factor, ATF-like 2 (Batf2), mRNA.	28077033	
mast cell protease 4 (Mcpt4), mRNA.	114205406	0.3065
2'-5' oligoadenylate synthetase-like 2 (Oasl2), mRNA.	16924024	0.3019
thymidylate kinase family LPS-inducible member (Tyki), mRNA.	117606366	0.2989
mast cell protease 1 (Mcpt1), mRNA.	6678836	0.2964
LYMPHOCYTE ANTIGEN LY-6C PRECURSOR. [Source:SWISSPROT;Acc:P09568]		0.2928
poly (ADP-ribose) polymerase family, member 14 (Parp14), mRNA.	87299607	0.2923
PREDICTED: similar to Gamma-interferon-inducible protein Ifi-16 (Interferon-inducible myeloid differentiation transcriptional activator) (IFI 16) (LOC672540), mRNA.	94365824	0.2906
cDNA sequence BC023105 (BC023105), mRNA.	93352547	0.2886
suppressor of cytokine signaling 1 (Socs1), mRNA.	6753424	0.2836
Z-DNA binding protein 1 (Zbp1), mRNA.	11496253	0.2766
expressed sequence AI451617 (AI451617), mRNA.	40255281	0.2702
formyl peptide receptor 1 (Fpr1), mRNA.	7305065	0.2681
tumor necrosis factor (ligand) superfamily, member 10 (Tnfsf10), mRNA.	6678431	0.2651
similar to 2-cell-stage, variable group, member 3 (LOC625360), mRNA.	85702324	0.2647
RIKEN cDNA B020031M17 gene (B020031M17Rik), mRNA.	85702077	0.2616
interferon-induced protein 44 (Ifi44), mRNA.	19527086	0.2531
PREDICTED: hypothetical protein LOC675673 (LOC675673), mRNA.	94391273	0.2521
2'-5' oligoadenylate synthetase 2 (Oas2), mRNA.	21644597	

0.2514

interleukin 1 receptor antagonist (Il1rn), transcript variant 2, mRNA.	89257344	0.2495
ISG15 ubiquitin-like modifier (Isg15), mRNA.	7657240	0.2480
interferon regulatory factor 7 (Irf7), mRNA.	8567364	0.2313
PREDICTED: CD8 antigen, alpha chain, transcript variant 1 (Cd8a), mRNA.	63544289	0.2308
DNA segment, Chr 14, ERATO Doi 668, expressed (D14Erttd668e), mRNA.	39841029	0.2237
chemokine (C-C motif) ligand 4 (Ccl4), mRNA.	7305459	0.2237
PREDICTED: hect domain and RLD 5, transcript variant 1 (Herc5), mRNA.	94378601	0.2168
RNA binding motif protein 3 (Rbm3), mRNA.	37497112	0.2147
2'-5' oligoadenylate synthetase 3 (Oas3), mRNA.	21644585	0.2112
expressed sequence AI447904 (AI447904), mRNA.	27923921	0.2072
serum amyloid A 3 (Saa3), mRNA.	6755396	0.1883
PREDICTED: similar to interferon-induced protein with tetratricopeptide repeats 1 (LOC669129), mRNA.	94406702	0.1860
ubiquitin specific peptidase 18 (Usp18), mRNA.	6755927	0.1609
interferon-induced protein with tetratricopeptide repeats 1 (Ifit1), mRNA.	110626104	0.1475
chemokine (C-C motif) ligand 3 (Ccl3), mRNA.	6755432	0.1451
PREDICTED: hypothetical LOC625046 (LOC625046), mRNA.	82998312	0.1286

Chapter 5

Host Molecular Markers of Cerebral Malaria

Abstract

Cerebral malaria (CM) is a rare but often lethal outcome of infection with the *Plasmodium falciparum* species of human malaria and is responsible for a large portion of the 1-2 million deaths due to malaria every year. Using the *P. berghei* ANKA murine model of experimental cerebral malaria (ECM) and high density oligonucleotide microarray analysis, we have identified 210 host molecules in the brain that are strongly associated with the manifestation of ECM. While a small subset of these molecules have previously been identified as proteins associated with CM, the majority of our dataset consists of novel biomarkers of CM. Through in depth functional analysis, we were able to classify these proteins into eleven categories based on function and subcellular localization. In addition to several molecules of the immune system, a wide variety of host genes encoding transcription factors, receptors, transporters and proteins involved in signal transduction and cell adhesion are transcriptionally altered during ECM. One notable result of this study is the finding that low levels of hemoglobin may be associated with ECM. In clinical cerebral malaria, low oxygen levels are considered the primary cause of coma and eventual death. Furthermore, upregulation of a large proportion of genes during ECM appears to be a direct response to injury to the brain.

Introduction

Human malaria is caused by infection with four species of the Genus *Plasmodium*. Among these, *Plasmodium falciparum* is the most lethal and responsible for more than 90% of deaths mostly in children under the age of five. One characteristic feature of *falciparum* malaria is the clinical manifestation termed as cerebral malaria (41), a rare but serious complication that often results in death. Among the 1–2 million deaths due to malaria per year, mostly in children living in sub-Saharan Africa, the majority are a consequence of CM or severe anemia. The molecular factors and mechanisms underlying the pathogenesis of CM are poorly understood, and there is an urgent need to improve the current methods available for the diagnosis, treatment, and management of CM.

A vaccine that will prevent disease but not necessarily infection is considered by many malaria experts to be the most promising method for the prevention of CM. Administration of adjunct therapies that can reverse the rapid clinical deterioration associated with CM in combination with anti-malarials will also reduce the number of deaths due to malaria. A further understanding of the sequence of events leading to the development of CM and the downstream effector molecules that produce the symptoms of CM will be important in identifying potential anti-disease vaccine candidates and therapeutic drug targets.

Susceptibility to CM is believed to result from a combination of parasite and host factors. The ability of the parasite to sequester within the deep vascular beds of brain tissue is believed to be the dominant parasite factor required for CM (44). The goal of

this study was to identify novel host molecular markers and associated biological pathways that are responsible for the pathological manifestations of CM. In previous studies, an association between a number of host genes and susceptibility to CM has been established (68). The majority of these genes, including TNF- α and IFN- γ , encode proteins of the immune system. However, the brain is a complex system composed of a variety of cells, networks, and pathways. Therefore, in order to obtain a more accurate and complete picture of the pathogenesis of CM, we have determined the repertoire of genes altered in whole brain tissue during a clinical episode of CM using the *P. berghei* ANKA (Pb-A) murine model of experimental cerebral malaria (ECM).

Similar to *P. falciparum* malaria, the murine Pb-A strain of malaria is known for its ability to sequester within the microvasculature and has therefore become the parasite of choice for in vivo murine studies of cerebral malaria (19). Infection with Pb-A parasites results in death in 100% of mice. However, the cause of death varies greatly based on the mouse genetic background, and mouse strains are broadly categorized as susceptible or resistant to CM (19). In susceptible mouse strains (C57BL6 and CBA/J), approximately 80% mice develop cerebral malaria 6-10 days post-infection, and these mice die with relatively low parasitemia (approximately 10%). ECM in these mice resembles the features of *P. falciparum* clinical disease in humans: hemi- or paraplegia, tendency to roll over on stimulation, deviation of the head, ataxia, and convulsions. In contrast, resistant mice (BALB/c) do not develop any of the clinical or pathological features that resemble cerebral malaria (19) but instead succumb to anemia and hyperparasitemia approximately 15-18 days after infection with Pb-A. Susceptible mice that do

not develop ECM (approximately 20%) follow a clinical course of disease similar to the resistant mice and eventually die of hyperparasitemia and severe malaria.

Using high density microarray chips, we compared whole brain tissue expression profiles of C57BL6 mice with ECM (moribund) to: 1) C57BL/6 mice without ECM (non-moribund) and 2) BALB/c mice without ECM (resistant). Based on differential expression in brain tissue samples taken from mice that were terminally ill with the symptoms of ECM, a total of 210 host genes were strongly associated with the manifestation of ECM. Further studies will be needed to assess their role in the pathogenesis or protection from ECM. These include studies measuring the effect of candidate genes on susceptibility to ECM using knockout mice or following antibody depletion of protein over the course of an infection in wildtype mice, as well as immunohistological analysis of brain sections to determine the cellular localization of these newly identified markers of CM.

Based on gene expression profiling, our studies have identified several novel molecules that could be involved either in susceptibility to or protection from the pathogenesis of CM. Identification of such molecules (biomarkers) in the brain that are also altered in the blood may lead to the development of a method for early detection of CM and offer novel targets to develop anti-disease vaccines and drugs. However, further biological studies will be needed to elucidate the precise role of individual molecules and intricate biological pathways involved in the pathogenesis of CM.

Material and Methods

Mice and parasite infections. Six- to eight- week old female C57BL/6 and BALB/c mice were purchased from The Jackson Laboratory (Bar Harbor, ME). Parasite infection was induced by intraperitoneal injection of 10^6 *P. berghei* ANKA parasites and mice were monitored for clinical symptoms of ECM (hemi or para-plegia, deviation of the head, tendency to roll over upon stimulation, ataxia, and convulsions) beginning on Day 5 post-infection. Parasitemias (parasitized RBCs/ total RBCs x 100) were enumerated by examining a Giemsa-stained thin blood films prepared every day beginning on Day 3 post-infection and at the time of sample collection.

Manifestations of experimental cerebral malaria and tissue collection. Based on their clinical symptoms displayed post-parasite challenge, mice were classified into three groups: 1) moribund, 2) non-moribund, and 3) resistant mice. Brain tissue samples were collected simultaneously from the three groups (five mice per group) and stored at -80°C until use. Moribund mice were defined as susceptible mice (infected C57BL/6) exhibiting symptoms of ECM. Non-moribund mice were defined as susceptible mice (infected C57BL/6) displaying no apparent clinical symptoms of ECM. Infected BALB/C mice, which never exhibit symptoms of ECM, were classified as resistant (Table 9).

GROUP	STRAIN	SUSCEPTIBLE	ECM*
Moribund	C57BL6	Yes	Yes
Non-moribund	C57BL6	Yes	No
Resistant	BALB/C	No	No

Table 9. Criteria (strain, susceptibility to disease, and clinical symptoms exhibited) used for the classification of mice into moribund, non-moribund, and resistant groups.*ECM: Experimental cerebral malaria.

Preparation of whole brain RNA. For preparation of high quality RNA, frozen tissue was homogenized in Tri-Reagent (Molecular Research Center, Cincinnati, OH), and RNA was isolated following two chloroform extractions, isopropanol precipitation, and resuspension in DEPC treated water. RNA quantity was determined by optical densitometry, and its quality was evaluated by agarose gel electrophoresis.

Microarray analysis. The global gene expression profiles of moribund mice was compared with both non-moribund and resistant mice to determine the array of host genes induced and repressed during the induction and expression of cerebral malaria. Microarray expression profiles were determined from RNA samples isolated from five mice per group. Hybridizations were performed as shown in Table 10.

Table 10. Groups of Mice used in Microarray Hybridizations

DAY*	CY5	CY3	BRAIN
5	Moribund 13	Non-moribund 14	MO-221
6	Moribund 1	Non-moribund 4	MO-213
6	Moribund 2	Non-moribund 5	MO-215
6	Moribund 3	Non-moribund 6	MO-217
6	Moribund 10	Non-moribund 11	MO-219
5	Moribund (C57BL6) 13	Resistant (BALB/c) 15	MO-222
6	Moribund (C57BL6) 1	Resistant (BALB/c) 7	MO-214
6	Moribund (C57BL6) 2	Resistant (BALB/c) 8	MO-216
6	Moribund (C57BL6) 3	Resistant (BALB/c) 9	MO-218
6	Moribund (C57BL6) 10	Resistant (BALB/c) 12	MO-220

* Days post challenge with 10^6 *P. berghei* ANKA parasites

cDNA was synthesized from 30 µg of RNA extracted from host brain tissue and then labeled with cy3 or cy5 as described in the Material and Methods section of Chapter 2. Labeled cDNA was then hybridized to a murine oligonucleotide chip containing 16,600 oligonucleotide probes (Qiagen, Valencia, CA) and the slide was scanned by a GenePix microarray scanner. Microarray data were analyzed with GenePix Pro 6.0 software (Axon Instruments, Inc. Union City, CA), filtered using the NIAID microarray database tools (<http://madb-niaid.cit.nih.gov>), and extracted spots were normalized to the precalculated 50th percentile (median).

Altered expression of an individual gene was defined as significant only if two criteria were met: 1) moribund mice exhibited an average two-fold or greater increase

(upregulation) or decrease (downregulation) in gene expression compared to both non-moribund and resistant mice (p value <0.05 by two-tailed Student t-test) and 2) moribund mice exhibited an two-fold or greater increase (upregulation) or decrease (downregulation) in 3 of the 5 arrays per group.

Western blot analysis. Protein was prepared as a 10% brain homogenate, and tissue specific p21 protein was detected using a mouse anti-p21 monoclonal antibody specific for human recombinant p21^{WAF1} protein (Biosource, Camarillo, CA) and a commercially obtained chemiluminescence-linked western blot kit (Western Light Tropix, Bedford, Mass.). Protein bands were visualized following incubation with ECL detection reagents, and the integrated optical densities (IOD) for each lane were measured using Meta Morph 6.1 software.

Results and Discussion

Measuring the alterations in the gene expression during ECM. We compared the global expression profiles of host genes in the brains of mice with (moribund) and without (non-moribund and resistant) ECM to identify novel biomarkers of disease by performing microarray hybridizations with RNA samples isolated in five mice per group. Altered expression of an individual gene was defined as significant only if two criteria were met: 1) moribund mice exhibited an average two-fold or greater increase (upregulation) or decrease (downregulation) in gene expression compared to both non-moribund and resistant mice (p value <0.05 by two-tailed Student t-test) and 2) moribund mice exhibited a twofold or greater increase (upregulation) or decrease (downregulation) in 3 of the 5 arrays per group.

When comparing moribund to non-moribund C57Bl/6 mice, the input data were 5 arrays and 34,928 genes. 34,144 genes were excluded by criteria 1 and 172 additional genes were excluded by criteria 2. When comparing moribund C57Bl/6 to resistant BALB/c mice, the input data were 5 arrays and 34,826 genes. 33,543 genes were excluded by criteria 1 and 169 additional genes were excluded by criteria 2. A total of 612 genes were considered significantly altered when comparing moribund to non-moribund mice and 1,114 genes were considered significantly altered when comparing moribund to resistant mice. Of these 1,726 genes, 210 genes (66% upregulated, 34% downregulated) were significantly altered in both groups. The microarray analysis has been summarized in FIG 19. These genes were next categorized by function, and a subset of our dataset is displayed in Table 12.

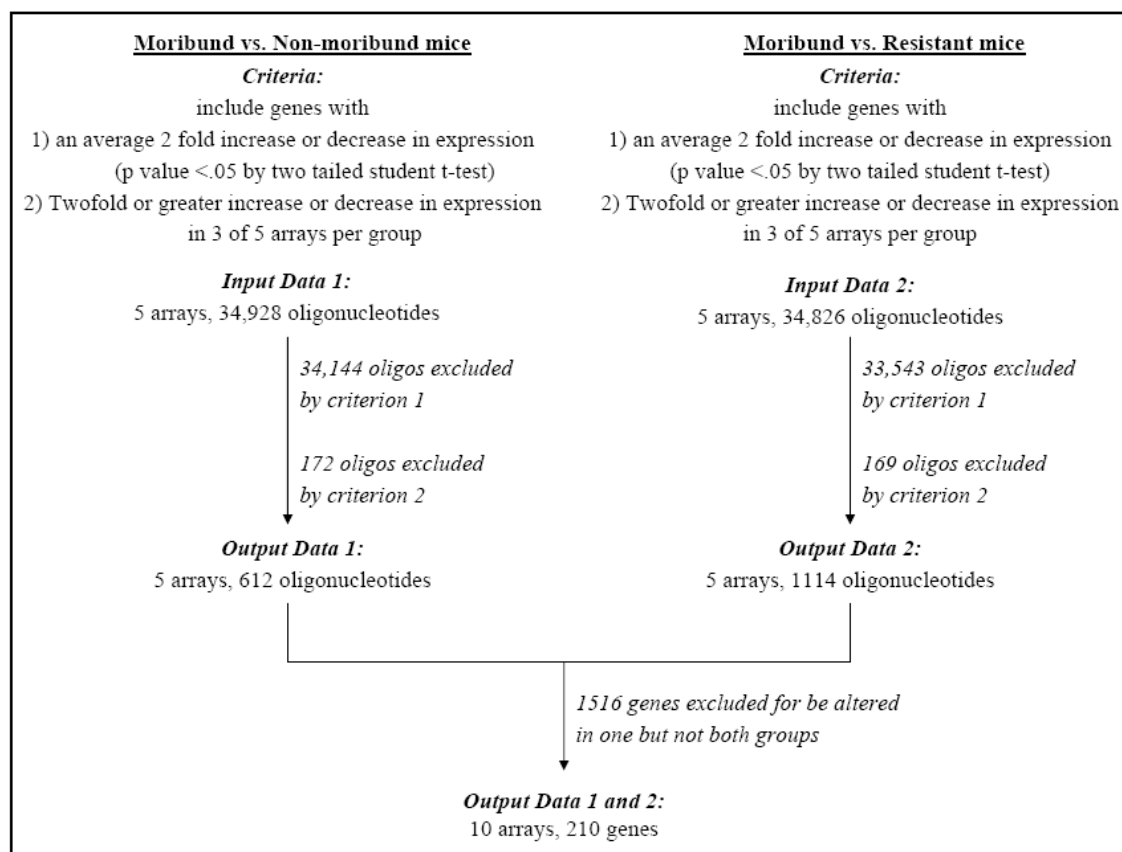


Figure 19. Diagram of Microarray Analysis.

Table 11. Biological functions of a subset of ECM related genes in our dataset.

Function	Gene Name	GI Number	Average Fold Δ^1	
			Resistant	Non-MB
Immune Modulators	Cytotoxic T lymphocyte-associated protein 2 α	6681077	5.3	15.7
	CTLA-2-beta protein precursor	—	3.2	5.1
	CD14	6753332	2.7	6.0
	Lipocalin 2	34328049	2.6	3.2
	TSAD	70909334	2.0	2.3
	OX40	6755909	2.0	2.2
	Toll-like receptor 11	45429992	-2.5	-2.4
Hemoglobin Syn.	Heme Oxygenase (decycling) 1	6754212	2.4	7.8
	Hemoglobin α , adult chain 1	6680175	-4.3	-5.8
	Hemoglobin β , adult major chain	31982300	-18.7	-16.2
	Hemoglobin β , adult minor chain	17647499	-19.2	-19.7
Stress Response	DNA Repair			
	DNA-damage-inducible transcript 4	21312868	2.6	2.6
	Growth arrest and DNA-damage-inducible 45 gamma	6753938	2.2	2.6
	S1 RNA binding domain 1 (Predicted)	94404154	-2.2	-2.2
	Splicing factor proline/glutamine rich (polypyrimidine tract binding protein associated)	—	-3.8	-3.8
	Proteases			
	Preproacrosin	7304853	3.3	3.3
	HtrA serine peptidase 1	9625027	2.4	2.2
	Kallikrein 1-related peptidase b11	28875780	2.2	2.0
	Transmembrane protease, serine 5	13507652	-2.2	-2.2
	Apoptosis			
	Angiopoietin-like 4	10181164	2.4	3.8
	TSC22 domain family 3	11651734 2	2.3	3.1
	Nuclear factor of kappa light chain gene enhancer in B-cells inhibitor	6754840	2.5	2.6
	AXIN1 up-regulated 1	23463295	2.6	2.6
	Lamin A	9506843	2.2	2.5
	Unc-5 homolog C	—	-2.6	-2.3
	TRAIL	6678431	-3.2	-2.9
	Protein phosphatase 1F	28849881	-2.0	-2.1

Other	Metallothionein 2	33468863	5.9	8.4
	Metallothionein 1	7305285	3.7	4.9
	Uncoupling protein 2 (mitochondrial, proton carrier)	31543920	2.3	4.3
Transcription Factors	Protein phosphatase 1, regulatory (inhibitor) subunit 12C (predicted)	82902891	4.8	2.4
	FBJ osteosarcoma oncogene B	6679827	4.4	3.6
	Kruppel-like factor 4	6754456	3	2.1
	Transcriptional regulator, sin3b	28212270	2.4	2.7
	v-maf musculoaponeurotic fibrosarcoma oncogene family, protein K	6754612	2.3	2.6
	Kruppel-like factor 9	31542239	2.2	2.2
	Jun proto-oncogene related gene d1	6754404	2.2	2
	Tripartite motif-containing 66	79750343	2.1	2.6
	Homeo box A5	6754232	-3.8	-2.5
	Zinc finger protein 715	66793402	-3.5	-3.6
	Zinc finger protein 54	6756063	-2.1	-2.4
	SRY-box containing gene 5	6755608	-2.4	-3.1
Signal Transduction				
	Kinase Activity			
	Mitogen-activated protein kinase kinase kinase 6	66392595	4.6	3.1
	Serum/glucocorticoid regulated kinase	6755490	2.8	2.8
	Casein kinase 2, α prime polypeptide	—	2.7	2.2
	Calcium/calmodulin-dependent protein kinase kinase 1	9256525	2.5	2.3
	Protein kinase, AMP-activated, β 2 non-catalytic subunit	72384347	2.4	2.2
	Tousled-Like Kinase 2	—	2.3	2.2
	Phosphorylase kinase α 1	—	-2.5	-2.5
	GTPases			
	ADP-ribosylation factor 4-like	13384792	3.4	2.6
	Guanylate nucleotide binding protein 2	6753950	2.4	2.4
	Regulator of G-protein signaling 1	7657512	2.2	3.0
	GTP binding protein	6753972	2.2	2.5
	TBC1 domain family	—	-2.8	-2.1
	RAB28	—	-2.0	-2.0
Cell Cycle				
	p21	6671726	4.4	5.5
	SAM and SH3 domain containing 1	112821670	4.7	4.7
	Cullin 2	19482162	2.7	2.3
	Spindle assembly 6 homolog	58037301	-2.2	-2.6

Lipid Metabolism	Aryl sulfotransferase	—	4.2	4.5
	Arachidonate 12-lipoxygenase, 12R type	6753040	3.2	2.4
	Patatin-like phospholipase domain containing 2	21313274	2.4	3.5
	Thyroid hormone responsive SPOT14 homolog	6678345	2.4	2.3
	Arachidonate lipoxygenase 3	6753042	2.3	2.2
	Phospholipase A1 member A	31982575	2.1	2.8
	Phospholipase A2	—	2.1	2.4
	Fatty acid binding protein 7, brain	10946572	-3.2	-2.6
Transporters	Solute carrier family 10, member 6	21313062	8.0	7.5
	Solute carrier family 2, member 3	31543726	2.5	2.2
	Solute carrier family 6, member 8	19527208	2.4	2.8
	ATP-binding cassette, sub-family A, member 8a	23346593	-2.5	-2.2
	Potassium inwardly-rectifying channel, subfamily J, member 9	11160744 3	-2.1	-2.1
Receptors	Vomeronasal 1 receptor, F3	21717723	4.3	4.6
	Neuropeptide Y receptor Y6	6754884	3.8	2.2
	Bradykinin receptor, beta 1	6671632	3.2	2.6
	Olfactory receptor 705	22128881	2.9	2.4
	G protein-coupled receptor, family C, group 5, member A	31126968	2.0	2.2
	Purinergic receptor P2Y, G-protein coupled 12	31980659	-3.0	-2.6
Cell Adhesion	Cysteine rich protein 61	6753594	3.8	4.7
	Epithelial membrane protein 1	6753748	2.2	3.5
	Syndecan 4	6755442	2.2	2.6
	Epithelial membrane protein 2	11115405 9	-2.3	-2.1
Cytoskeleton	Connective tissue growth factor	6753878	4.4	2.8
	Similar to claudin 20 (Predicted)	82981734	3.6	2.9
	Cofilin 1, non-muscle	6680924	3.3	2.3
	Transgelin	6755714	2.8	3.3
	Internexin neuronal intermediate filament protein	—	2.8	2.3
	Coronin, actin binding protein 1C	31542413	2.5	2.2
	Actin, beta, cytoplasmic	6671509	2.4	2.8
	Bassoon	—	2.2	2.7
	Claudin 11	6679186	2.2	2.1

¹ Average fold Δ represents genes induced or repressed in moribund mice compared to resistant or non-moribund mice

Immune Modulators of Pathogenesis. Several molecules with differentially altered expression in our dataset are modulators of the innate and adaptive immune responses. The first molecule of importance is CD14, which is significantly up-regulated (2.7, 6 fold) in brain tissue of mice displaying symptoms of cerebral malaria. The molecule exists in two forms. Membrane CD14 (mCD14) is expressed on the surface of myeloid cells, whereas soluble CD14 (sCD14) exists free in plasma and differs from mCD14 structurally by the absence of a phosphoinositol glycolipid tail (45). CD14 was the first lipopolysaccharide (LPS) receptor to be characterized. It is now known that binding of LPS to CD14 in conjunction with TLR4 initiates inflammatory gene expression through NF κ B and MAPK signal transduction (10). Furthermore, a correlation between high concentrations of sCD14 and septic shock has been demonstrated (40).

CD14 also plays an important role in the recognition and clearance of apoptotic cells (17). However, interaction of CD14 with self molecules produces a very different response. CD14 recognition of apoptotic cells increases phagocytosis but does not induce the release of inflammatory cytokines from macrophages (17).

Studies are beginning to emerge on the role of CD14 during infection of protozoan parasites. A hallmark of innate immunity is the ability of the host to recognize non-self antigens through direct interactions of toll-like receptors (TLRs) and pathogen associated molecular patterns (PAMPs). Data suggest that a complex of TLR2-TLR6 and CD14 is involved in the recognition of *Trypanosoma cruzi* glycosylphosphatidylinositol (GPI) anchors (23, 52). However, while the recognition of *P. falciparum* derived GPI anchors by a TLR2-TLR1 heterodimer has been shown to induce the synthesis of TNF, a

requirement for CD14 in this recognition has not been established (23). How the CD14 molecule participates in the pathogenesis ECM remains to be determined.

OX40, a member of the tumor necrosis factor receptor superfamily, is also upregulated in the brain during ECM. OX40 is expressed only on activated T cells. Although OX40 is more commonly expressed on the CD4⁺ subset of T cells, expression has also been observed on CD8⁺ T cells that are strongly activated (63). Its functional partner, OX40L, is expressed on antigen presenting cells such as myeloid and plasmacytoid dendritic cells, B cells, mast cells, natural killer cells, and vascular endothelial cells. Ligation of OX40 triggers costimulatory signals in T cells when both T cells and APCs are activated. Of particular interest is the interaction of OX40L on vascular endothelial cells and OX40 on activated T cells. This interaction induces the production of RANTES (32), a chemokine that may be associated with CM (54), by vascular endothelial cells, suggesting a possible mechanism regarding the role of OX40 in ECM. It is also possible that upregulation of OX40 could be due to active proliferation in the T cell subset-populations that are known to contribute towards the pathogenesis of cerebral malaria (9). The role of OX40 in ECM is under investigation in our laboratory.

Other immune modulators in our dataset include two cysteine proteinases expressed by T cells (CTLA-2 α and CTLA-2 β protein precursor), T cell specific adapter protein (TSAd), Toll like receptor 11 (TLR11), and lipocalin 2. TSAd is a signal transduction molecule expressed by NK cells and T cells and is associated with the regulation of autoimmunity (42). TLR11 (a receptor present in mice but not humans), is involved in pathogenesis of uropathogenic *E. coli* and protection from Toxoplasmosis

(72). Lipocalin 2 is a cytoplasmic protein induced by TLRs on immune cells that has been shown to limit bacterial growth by sequestering iron (21).

Changes in Hemoglobin Content. Expression of genes that encode the alpha and beta chains of hemoglobin are considerably down-regulated during ECM. Down regulation of the hemoglobin chains could be a consequence of changes in expression at the level of transcription, a decrease in erythrocyte production, or obstruction of blood flow. Because erythropoiesis occurs in the bone marrow and spleen, a decrease in the expression of hemoglobin mRNA within the brain is most likely a reflection of obstruction of blood flow and/or dyserythropoiesis, a reduction in the output of erythrocytes, which has been reported in clinical cases of severe malaria (1, 50). Irregardless of the cause, a reduction in hemoglobin levels within the brain will profoundly compromise the ability of brain cells to obtain and utilize oxygen. This finding is highly significant because hypoxia or low-oxygen content in the brain is a symptom commonly seen in cerebral malaria patients (53) and possibly the cause of non-arousable coma, a characteristic of CM disease before death. In addition, similar to previous findings published by Schluesener et al (55), we find that heme oxygenase 1, an enzyme essential for the catabolism of heme, is upregulated during ECM.

Stress Response. A large number of transcriptional changes due to ECM appear to be a direct response to stress including genes involved in DNA repair, the induction or repression of apoptosis, and oxidative stress. A number of genes that had altered expression during ECM such as uncoupling protein 2 (UCP2) and the metallothioneins, have been characterized in previous publications as neuroprotective (43, 48).

UCP2, a mitochondrial proton carrier, is up-regulated by greater than 2 fold in mice with ECM. Uncoupling proteins are a family of anion carrier transporters present in the inner mitochondrial membrane. Unlike other members of the mitochondrial carrier superfamily, UCP2 is expressed in neurons and microglial cells of the brain (33, 51), and has been demonstrated to play a major role in neuroprotection by reducing the mitochondrial membrane potential (67) and controlling the production of reactive oxygen species (ROS) (7). While studies clearly demonstrate that UCP2 negatively regulates the production of ROS in the mitochondria, Mattiasson et al has proposed that UCP2 may also influence the cellular-distribution of ROS by serving as a channel for the transport of ROS from the mitochondria to the cytoplasm, and that this dissipation could induce the expression of neuroprotective proteins in the cytoplasm such as manganese superoxide dismutase and Bcl-2 (43).

In agreement with a recent report published in 2006 by Wiese et al (71), mice displaying symptoms of ECM in our study had increased expression of the genes encoding metallothionein I and II (MT-I and II). MT-I and II belong to a family of highly conserved, low molecular weight, cysteine rich metalloproteins and are capable of participating in a wide array of neuroprotective activities ranging from immunoregulation, cell survival and brain repair. In the brain, astrocytes are the main source of MT-I and II (71). However, MT-I and II are distributed both intra- and extracellularly (13) and primarily protect neurons (12, 13, 37, 49). Increased expression is seen in various pathologies of the brain including traumatic injury, multiple sclerosis (MS), Alzheimer's disease (AD), Parkinson's disease (PD), and amyotrophic lateral sclerosis (ALS) (48).

MT-I and II may play an active role in reducing damage to the CNS induced by the parasite during ECM by two potential mechanisms. First, MT-I and II reduce the activation and recruitment of macrophages and T cells, and they also inhibit the production and secretion of inflammatory cytokines including TNF- α and lymphotoxin (58). Second, MT I and II are powerful scavengers of free radicals (66) and therefore may moderate oxidative stress and prevent apoptosis during ECM.

Transcription Factors. Twelve members of our dataset are regulators of transcription varying in expression from -2.4 to 4.8 fold change. Of particular interest is MafK, a gene upregulated during ECM that is a subunit of the NF-E2 (Nuclear Factor-Erythroid 2) transcription factor. NF-E2 is a heterodimer composed of a small ubiquitous member of the Maf protein family and the much larger p45 subunit (5, 6). NF-E2 is expressed in erythroid cells, megakaryocytes (progenitors of platelets), and mast cells (4). Two functions have been assigned to NF-E2. First, it is believed to be involved in the transcriptional activation of the globin genes (24). Second, it is essential for normal platelet production (57). Interestingly, targeted disruption of the p45 subunit in mice resulted in severe thrombocytopenia but little defect in erythropoiesis suggesting a functional redundancy in the latter (57). Targeted disruption of p18/MafK resulted in no phenotypic abnormalities suggesting that other members of the Maf protein family such as MafG can replace MafK in NF-E2 (38).

Studies have demonstrated that NF-E2 is activated by reactive oxygen species (35), which are produced in excess during ECM. It may seem counterintuitive that the genes that encode the α and β chains of hemoglobin are significantly down-regulated during ECM while the transcriptional activator of these genes is upregulated. However, it

is plausible that synthesis of MafK may be a compensatory response to the observed downregulation of hemoglobin chains during ECM.

Signal Transduction. Seven molecules in our dataset possess kinase activity. Of particular interest is Casein Kinase 2 (CK2), a ubiquitous and conserved nuclear and cytoplasmic serine/threonine protein kinase involved in cell growth and proliferation and the suppression of apoptosis. CK2 consists of two catalytic (α and α') and two regulatory (β) subunits forming one of three possible heterotetrameric configurations: $\alpha_2\beta_2$, $\alpha\alpha'\beta_2$, or $\alpha'_2\beta_2$ (2). The α' subunit of CK2, which is expressed solely in brain and testis (20), is upregulated by two-fold in mice with CM. Dysregulation of CK2 has been reported in all cancers examined to date (27, 65) and is capable of phosphorylating more than 100 different substrates. While its role in cell growth and proliferation is established, recent studies demonstrating an inverse correlation between expression of CK2 and apoptosis suggests an important role as a cell survival factor; CK2 upregulation inhibits, while its downregulation promotes, apoptosis mediated by death receptor ligands such as TNF- α , TRAIL, and FasL (69).

At least five molecules in our dataset are GTPases each differing widely by their function and intrinsic GTPase activity. Guanylate nucleotide binding protein 2 (GBP2) is upregulated in mice with ECM, exhibits robust GTPase activity, and is a member of the p65 GBP family of interferon inducible GTPases. Expression of GBP2 is induced in macrophages by IFN- γ and LPS and in endothelial and fibroblast cells by TNF- α and IL-1 β (41, 46). Promotion of fibroblast proliferation is the most definitive function assigned to GBP2 to date (25). GTP binding protein (GEM) is also upregulated in mice with ECM, but displays very low levels of GTPase activity (14), and is one of four RGK (Rad, Gem,

Kir) proteins, small Ras related GTP binding proteins consisting of a Ras-like core with extensions at both the N and C termini. GEM is a suppressor of voltage dependent calcium channels (VDCCs) (8) and plays a role in cytoskeletal remodeling, such as increased neurite formation in neuroblastoma cells (39), by inhibiting Rho kinase β (70).

Cell Cycle. Expression of the gene that encodes the kinase inhibitor p21 is significantly upregulated during ECM. p21, a member of the Cip/Kip family of cell cycle inhibitors, was the first cyclin dependent kinase (CDK) inhibitor to be identified (18, 28) and has been shown to possess both pro- and anti-proliferative activities depending on its subcellular localization. Nuclear localization is associated with the ability of p21 to induce cell cycle arrest in response to DNA damage by blocking CDK activity and DNA replication (22). Cytosolic p21 has been shown to be an important survival factor involved in the regulation of apoptosis. For example, cytoplasmic p21 prevents apoptosis during neuronal differentiation (64) by inhibiting the catalytic activity of stress activated protein kinase (SAPK) (56), and mitochondrial p21 prevents Fas-mediated apoptosis by inhibiting caspase 3 activation through direct interactions with its precursor procaspase-3 (61, 62).

Expression of p21 increases when cells are damaged, and it is believed that p21 is a key element of the cellular response to oxidative stress (47). Inguaggiato *et al* demonstrated that overexpression of heme oxygenase 1, an enzyme that catalyses the degradation of heme and is significantly upregulated in mice with ECM, upregulates p21 and confers resistance to apoptosis in renal epithelial cells (34).

We examined the expression of p21 at the level of translation in order to further establish the role of p21 during ECM and determine whether a correlation exists between

synthesis of mRNA and synthesis of protein. Our microarray results indicate that expression of p21 in moribund mice is 5.5 fold greater than expression in non-moribund mice at the level of transcription. Quantification of p21 protein by western blot demonstrated a 14.5 fold increase in expression at the level of translation (FIG. 20). Therefore, although differential expression of p21 protein was significantly higher than p21 mRNA, our results demonstrate that synthesis of both p21 mRNA and protein is strongly induced during ECM.

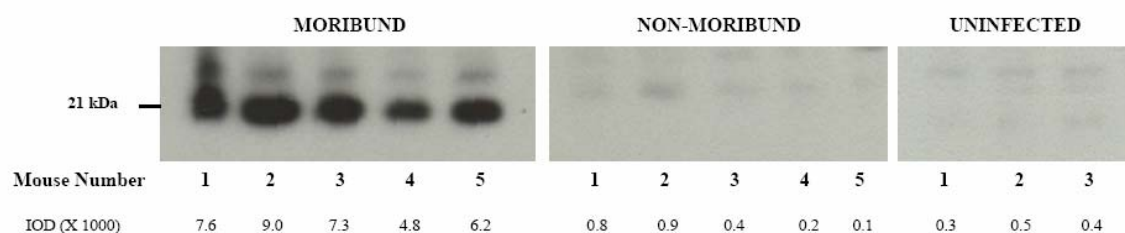


Figure 20. p21 protein expression during experimental cerebral malaria (ECM).

Expression of murine p21 protein in individual C57Bl/6 mice was measured by western blot analysis using a mouse anti-human p21 antibody. Quantitative analysis based on intensity of bands gave average IOD units of 6968 (moribund), 482 (non-moribund), and 386 (uninfected), demonstrating a 14.5 fold upregulation of p21 in moribund mice compared to non-moribund mice. Protein bands were visualized following incubation with ECL detection reagents, and the integrated optical densities (IOD) for each lane were measured using Meta Morph 6.1 software.

Receptors. Six receptors had altered expression during ECM. P2Y₁₂, one of two adenosine diphosphate (ADP) receptors expressed on platelets, was significantly down-regulated (–2.6 to –3 fold) during ECM. We were particularly interested in this molecule

due to its role in platelet activation. In vessel injury, platelets are activated and play an important role in the arrest of bleeding (29). Platelet activation requires three subsequent events: 1) rapid change of shape 2) release of granule contents and 3) platelet-to-platelet aggregation (29). In this process, nucleotides act in a positive feedback mechanism to amplify activation of platelets. The effect of adenine nucleotides on platelets are mediated through P2 receptors. Two of these receptors, P2Y₁ and P2Y₁₂ are activated by ADP and are essential for platelet aggregation (29, 59). P2Y₁ is required for initiation of ADP-induced platelet aggregation (30, 31), and P2Y₁₂ is necessary for continued amplification of the process (60). In P2Y₁₂ deficient mice, platelets aggregate poorly in response to ADP (36). P2Y₁₂ receptor activation also amplifies granule secretion, P-selectin expression, and the formation of microparticles (59). Grau and colleagues have conducted a number of studies suggesting an important role for platelets and microparticles in the pathogenesis of ECM. In these studies, expression of P-selectin on endothelial cells (but not platelets) (15) and microparticle formation (16) are both associated with the development of ECM. Studies have also documented an association between CM and thrombocytopenia (3). Therefore, downregulation of P2Y₁₂ during ECM may be a consequence of low levels of platelets in diseased mice.

Cytoskeleton. Nine members of our dataset are involved in cytoskeleton organization and remodeling, and all are upregulated during ECM. At least two molecules, actin β and claudin-11 are components of intercellular tight junctions. Claudin-11, also known as oligodendrocyte-specific protein (OSP) encodes a 218 amino acid protein that contributes towards the 7% of total protein in purified myelin (11). Studies performed in OSP null mice suggest that this gene plays a pivotal role in the

formation of intramyelinic tight junctions in the CNS; myelin sheaths from OSP knockout mice are shown to lack the tight junction strands. These mice also exhibit hindlimb weakness and slowed conduction velocities in the CNS (26). The upregulation in the cytoskeleton organization proteins suggest that the induction of cerebral malaria leads to drastic disruption in the cellular structures and possibly their function. For example, elevated OSP levels in moribund mice may lead to CNS dysfunction and hence contribute towards the neurological syndromes of CM.

REFERENCES

1. **Abdalla, S. H.** 1990. Hematopoiesis in human malaria. *Blood Cells* **16**:401-416; discussion 417-409.
2. **Ahmad, K. A., G. Wang, J. Slaton, G. Unger, and K. Ahmed.** 2005. Targeting CK2 for cancer therapy. *Anticancer Drugs* **16**:1037-1043.
3. **Akingbola, T. S., W. A. Shokunbi, and P. E. Olumese.** 2006. Coagulation profile in Nigerian children with cerebral malaria. *Niger Postgrad Med J* **13**:195-199.
4. **Andrews, N. C.** 1998. The NF-E2 transcription factor. *Int J Biochem Cell Biol* **30**:429-432.
5. **Andrews, N. C., H. Erdjument-Bromage, M. B. Davidson, P. Tempst, and S. H. Orkin.** 1993. Erythroid transcription factor NF-E2 is a haematopoietic-specific basic-leucine zipper protein. *Nature* **362**:722-728.
6. **Andrews, N. C., K. J. Kotkow, P. A. Ney, H. Erdjument-Bromage, P. Tempst, and S. H. Orkin.** 1993. The ubiquitous subunit of erythroid transcription factor NF-E2 is a small basic-leucine zipper protein related to the v-maf oncogene. *Proc Natl Acad Sci U S A* **90**:11488-11492.
7. **Arsenijevic, D., H. Onuma, C. Pecqueur, S. Raimbault, B. S. Manning, B. Miroux, E. Couplan, M. C. Alves-Guerra, M. Gubern, R. Surwit, F. Bouillaud, D. Richard, S. Collins, and D. Ricquier.** 2000. Disruption of the uncoupling protein-2 gene in mice reveals a role in immunity and reactive oxygen species production. *Nat Genet* **26**:435-439.
8. **Beguin, P., K. Nagashima, T. Gono, T. Shibasaki, K. Takahashi, Y. Kashima, N. Ozaki, K. Geering, T. Iwanaga, and S. Seino.** 2001. Regulation of Ca²⁺ channel expression at the cell surface by the small G-protein kir/Gem. *Nature* **411**:701-706.
9. **Belnoue, E., M. Kayibanda, A. M. Vigario, J. C. Deschemin, N. van Rooijen, M. Viguier, G. Snounou, and L. Renia.** 2002. On the pathogenic role of brain-sequestered alphabeta CD8⁺ T cells in experimental cerebral malaria. *J Immunol* **169**:6369-6375.
10. **Bochkov, V. N., A. Kadl, J. Huber, F. Gruber, B. R. Binder, and N. Leitinger.** 2002. Protective role of phospholipid oxidation products in endotoxin-induced tissue damage. *Nature* **419**:77-81.
11. **Bronstein, J. M., P. E. Micevych, and K. Chen.** 1997. Oligodendrocyte-specific protein (OSP) is a major component of CNS myelin. *J Neurosci Res* **50**:713-720.
12. **Chung, R. S., P. A. Adlard, J. Dittmann, J. C. Vickers, M. I. Chuah, and A. K. West.** 2004. Neuron-glia communication: metallothionein expression is specifically up-regulated by astrocytes in response to neuronal injury. *J Neurochem* **88**:454-461.
13. **Chung, R. S., and A. K. West.** 2004. A role for extracellular metallothioneins in CNS injury and repair. *Neuroscience* **123**:595-599.
14. **Cohen, L., R. Mohr, Y. Y. Chen, M. Huang, R. Kato, D. Dorin, F. Tamanai, A. Goga, D. Afar, N. Rosenberg, and et al.** 1994. Transcriptional activation of a

- ras-like gene (kir) by oncogenic tyrosine kinases. *Proc Natl Acad Sci U S A* **91**:12448-12452.
15. **Combes, V., A. R. Rosenkranz, M. Redard, G. Pizzolato, H. Lepidi, D. Vestweber, T. N. Mayadas, and G. E. Grau.** 2004. Pathogenic role of P-selectin in experimental cerebral malaria: importance of the endothelial compartment. *Am J Pathol* **164**:781-786.
 16. **Combes, V., T. E. Taylor, I. Juhan-Vague, J. L. Mege, J. Mwenechanya, M. Tembo, G. E. Grau, and M. E. Molyneux.** 2004. Circulating endothelial microparticles in Malawian children with severe falciparum malaria complicated with coma. *Jama* **291**:2542-2544.
 17. **Devitt, A., O. D. Moffatt, C. Raykundalia, J. D. Capra, D. L. Simmons, and C. D. Gregory.** 1998. Human CD14 mediates recognition and phagocytosis of apoptotic cells. *Nature* **392**:505-509.
 18. **el-Deiry, W. S., T. Tokino, V. E. Velculescu, D. B. Levy, R. Parsons, J. M. Trent, D. Lin, W. E. Mercer, K. W. Kinzler, and B. Vogelstein.** 1993. WAF1, a potential mediator of p53 tumor suppression. *Cell* **75**:817-825.
 19. **Engwerda, C., E. Belnoue, A. C. Gruner, and L. Renia.** 2005. Experimental models of cerebral malaria. *Curr Top Microbiol Immunol* **297**:103-143.
 20. **Faust, M., and M. Montenarh.** 2000. Subcellular localization of protein kinase CK2. A key to its function? *Cell Tissue Res* **301**:329-340.
 21. **Flo, T. H., K. D. Smith, S. Sato, D. J. Rodriguez, M. A. Holmes, R. K. Strong, S. Akira, and A. Aderem.** 2004. Lipocalin 2 mediates an innate immune response to bacterial infection by sequestering iron. *Nature* **432**:917-921.
 22. **Gartel, A. L., M. S. Serfas, and A. L. Tyner.** 1996. p21--negative regulator of the cell cycle. *Proc Soc Exp Biol Med* **213**:138-149.
 23. **Gazzinelli, R. T., and E. Y. Denkers.** 2006. Protozoan encounters with Toll-like receptor signalling pathways: implications for host parasitism. *Nat Rev Immunol* **6**:895-906.
 24. **Gong, Q. H., J. C. McDowell, and A. Dean.** 1996. Essential role of NF-E2 in remodeling of chromatin structure and transcriptional activation of the epsilon-globin gene in vivo by 5' hypersensitive site 2 of the beta-globin locus control region. *Mol Cell Biol* **16**:6055-6064.
 25. **Gorbacheva, V. Y., D. Lindner, G. C. Sen, and D. J. Vestal.** 2002. The interferon (IFN)-induced GTPase, mGBP-2. Role in IFN-gamma-induced murine fibroblast proliferation. *J Biol Chem* **277**:6080-6087.
 26. **Gow, A., C. M. Southwood, J. S. Li, M. Pariali, G. P. Riordan, S. E. Brodie, J. Danias, J. M. Bronstein, B. Kachar, and R. A. Lazzarini.** 1999. CNS myelin and sertoli cell tight junction strands are absent in Osp/claudin-11 null mice. *Cell* **99**:649-659.
 27. **Guerra, B., and O. G. Issinger.** 1999. Protein kinase CK2 and its role in cellular proliferation, development and pathology. *Electrophoresis* **20**:391-408.
 28. **Harper, J. W., G. R. Adami, N. Wei, K. Keyomarsi, and S. J. Elledge.** 1993. The p21 Cdk-interacting protein Cip1 is a potent inhibitor of G1 cyclin-dependent kinases. *Cell* **75**:805-816.
 29. **Hechler, B., M. Cattaneo, and C. Gachet.** 2005. The P2 receptors in platelet function. *Semin Thromb Hemost* **31**:150-161.

30. **Hechler, B., A. Eckly, P. Ohlmann, J. P. Cazenave, and C. Gachet.** 1998. The P2Y1 receptor, necessary but not sufficient to support full ADP-induced platelet aggregation, is not the target of the drug clopidogrel. *Br J Haematol* **103**:858-866.
31. **Hechler, B., C. Leon, C. Vial, P. Vigne, C. Frelin, J. P. Cazenave, and C. Gachet.** 1998. The P2Y1 receptor is necessary for adenosine 5'-diphosphate-induced platelet aggregation. *Blood* **92**:152-159.
32. **Hori, T.** 2006. Roles of OX40 in the pathogenesis and the control of diseases. *Int J Hematol* **83**:17-22.
33. **Horvath, T. L., C. H. Warden, M. Hajos, A. Lombardi, F. Goglia, and S. Diano.** 1999. Brain uncoupling protein 2: uncoupled neuronal mitochondria predict thermal synapses in homeostatic centers. *J Neurosci* **19**:10417-10427.
34. **Inguaggiato, P., L. Gonzalez-Michaca, A. J. Croatt, J. J. Haggard, J. Alam, and K. A. Nath.** 2001. Cellular overexpression of heme oxygenase-1 up-regulates p21 and confers resistance to apoptosis. *Kidney Int* **60**:2181-2191.
35. **Jaiswal, A. K.** 2004. Nrf2 signaling in coordinated activation of antioxidant gene expression. *Free Radic Biol Med* **36**:1199-1207.
36. **Kauffenstein, G., W. Bergmeier, A. Eckly, P. Ohlmann, C. Leon, J. P. Cazenave, B. Nieswandt, and C. Gachet.** 2001. The P2Y(12) receptor induces platelet aggregation through weak activation of the alpha(IIb)beta(3) integrin--a phosphoinositide 3-kinase-dependent mechanism. *FEBS Lett* **505**:281-290.
37. **Kohler, L. B., V. Berezin, E. Bock, and M. Penkowa.** 2003. The role of metallothionein II in neuronal differentiation and survival. *Brain Res* **992**:128-136.
38. **Kotkow, K. J., and S. H. Orkin.** 1996. Complexity of the erythroid transcription factor NF-E2 as revealed by gene targeting of the mouse p18 NF-E2 locus. *Proc Natl Acad Sci U S A* **93**:3514-3518.
39. **Leone, A., N. Mitsiades, Y. Ward, B. Spinelli, V. Poulaki, M. Tsokos, and K. Kelly.** 2001. The Gem GTP-binding protein promotes morphological differentiation in neuroblastoma. *Oncogene* **20**:3217-3225.
40. **LeVan, T. D., J. W. Bloom, T. J. Bailey, C. L. Karp, M. Halonen, F. D. Martinez, and D. Vercelli.** 2001. A common single nucleotide polymorphism in the CD14 promoter decreases the affinity of Sp protein binding and enhances transcriptional activity. *J Immunol* **167**:5838-5844.
41. **MacMicking, J. D.** 2004. IFN-inducible GTPases and immunity to intracellular pathogens. *Trends Immunol* **25**:601-609.
42. **Marti, F., P. E. Lapinski, and P. D. King.** 2005. The emerging role of the T cell-specific adaptor (TSAd) protein as an autoimmune disease-regulator in mouse and man. *Immunol Lett* **97**:165-170.
43. **Mattiasson, G., M. Shamloo, G. Gido, K. Mathi, G. Tomasevic, S. Yi, C. H. Warden, R. F. Castilho, T. Melcher, M. Gonzalez-Zulueta, K. Nikolich, and T. Wieloch.** 2003. Uncoupling protein-2 prevents neuronal death and diminishes brain dysfunction after stroke and brain trauma. *Nat Med* **9**:1062-1068.
44. **Miller, L. H., D. I. Baruch, K. Marsh, and O. K. Doumbo.** 2002. The pathogenic basis of malaria. *Nature* **415**:673-679.
45. **Nguyen, M. D., J. P. Julien, and S. Rivest.** 2002. Innate immunity: the missing link in neuroprotection and neurodegeneration? *Nat Rev Neurosci* **3**:216-227.

46. **Nguyen, T. T., Y. Hu, D. P. Widney, R. A. Mar, and J. B. Smith.** 2002. Murine GBP-5, a new member of the murine guanylate-binding protein family, is coordinately regulated with other GBPs in vivo and in vitro. *J Interferon Cytokine Res* **22**:899-909.
47. **O'Reilly, M. A.** 2005. Redox activation of p21Cip1/WAF1/Sdi1: a multifunctional regulator of cell survival and death. *Antioxid Redox Signal* **7**:108-118.
48. **Penkowa, M.** 2006. Metallothioneins are multipurpose neuroprotectants during brain pathology. *Febs J* **273**:1857-1870.
49. **Penkowa, M., and J. Hidalgo.** 2001. Metallothionein treatment reduces proinflammatory cytokines IL-6 and TNF-alpha and apoptotic cell death during experimental autoimmune encephalomyelitis (EAE). *Exp Neurol* **170**:1-14.
50. **Phillips, R. E., S. Looareesuwan, D. A. Warrell, S. H. Lee, J. Karbwang, M. J. Warrell, N. J. White, C. Swasdichai, and D. J. Weatherall.** 1986. The importance of anaemia in cerebral and uncomplicated falciparum malaria: role of complications, dyserythropoiesis and iron sequestration. *Q J Med* **58**:305-323.
51. **Richard, D., R. Rivest, Q. Huang, F. Bouillaud, D. Sanchis, O. Champigny, and D. Ricquier.** 1998. Distribution of the uncoupling protein 2 mRNA in the mouse brain. *J Comp Neurol* **397**:549-560.
52. **Ropert, C., and R. T. Gazzinelli.** 2004. Regulatory role of Toll-like receptor 2 during infection with *Trypanosoma cruzi*. *J Endotoxin Res* **10**:425-430.
53. **Sanni, L. A.** 2001. The role of cerebral oedema in the pathogenesis of cerebral malaria. *Redox Rep* **6**:137-142.
54. **Sarfo, B. Y., S. Singh, J. W. Lillard, A. Quarshie, R. K. Gyasi, H. Armah, A. A. Adjei, P. Jolly, and J. K. Stiles.** 2004. The cerebral-malaria-associated expression of RANTES, CCR3 and CCR5 in post-mortem tissue samples. *Ann Trop Med Parasitol* **98**:297-303.
55. **Schluesener, H. J., P. G. Kremsner, and R. Meyermann.** 2001. Heme oxygenase-1 in lesions of human cerebral malaria. *Acta Neuropathol (Berl)* **101**:65-68.
56. **Shim, J., H. Lee, J. Park, H. Kim, and E. J. Choi.** 1996. A non-enzymatic p21 protein inhibitor of stress-activated protein kinases. *Nature* **381**:804-806.
57. **Shivdasani, R. A., M. F. Rosenblatt, D. Zucker-Franklin, C. W. Jackson, P. Hunt, C. J. Saris, and S. H. Orkin.** 1995. Transcription factor NF-E2 is required for platelet formation independent of the actions of thrombopoietin/MGDF in megakaryocyte development. *Cell* **81**:695-704.
58. **Stankovic, R. K., R. S. Chung, and M. Penkowa.** 2007. Metallothioneins I and II: neuroprotective significance during CNS pathology. *Int J Biochem Cell Biol* **39**:484-489.
59. **Storey, R. F.** 2006. Biology and pharmacology of the platelet P2Y₁₂ receptor. *Curr Pharm Des* **12**:1255-1259.
60. **Storey, R. F., H. M. Sanderson, A. E. White, J. A. May, K. E. Cameron, and S. Heptinstall.** 2000. The central role of the P(2T) receptor in amplification of human platelet activation, aggregation, secretion and procoagulant activity. *Br J Haematol* **110**:925-934.

61. **Suzuki, A., Y. Tsutomi, K. Akahane, T. Araki, and M. Miura.** 1998. Resistance to Fas-mediated apoptosis: activation of caspase 3 is regulated by cell cycle regulator p21WAF1 and IAP gene family ILP. *Oncogene* **17**:931-939.
62. **Suzuki, A., Y. Tsutomi, N. Yamamoto, T. Shibutani, and K. Akahane.** 1999. Mitochondrial regulation of cell death: mitochondria are essential for procaspase 3-p21 complex formation to resist Fas-mediated cell death. *Mol Cell Biol* **19**:3842-3847.
63. **Takasawa, N., N. Ishii, N. Higashimura, K. Murata, Y. Tanaka, M. Nakamura, T. Sasaki, and K. Sugamura.** 2001. Expression of gp34 (OX40 ligand) and OX40 on human T cell clones. *Jpn J Cancer Res* **92**:377-382.
64. **Tanaka, H., T. Yamashita, M. Asada, S. Mizutani, H. Yoshikawa, and M. Tohyama.** 2002. Cytoplasmic p21(Cip1/WAF1) regulates neurite remodeling by inhibiting Rho-kinase activity. *J Cell Biol* **158**:321-329.
65. **Tawfic, S., S. Yu, H. Wang, R. Faust, A. Davis, and K. Ahmed.** 2001. Protein kinase CK2 signal in neoplasia. *Histol Histopathol* **16**:573-582.
66. **Taylor, D. M., S. Minotti, J. N. Agar, and H. D. Durham.** 2004. Overexpression of metallothionein protects cultured motor neurons against oxidative stress, but not mutant Cu/Zn-superoxide dismutase toxicity. *Neurotoxicology* **25**:779-792.
67. **Teshima, Y., M. Akao, S. P. Jones, and E. Marban.** 2003. Uncoupling protein-2 overexpression inhibits mitochondrial death pathway in cardiomyocytes. *Circ Res* **93**:192-200.
68. **van der Heyde, H. C., J. Nolan, V. Combes, I. Gramaglia, and G. E. Grau.** 2006. A unified hypothesis for the genesis of cerebral malaria: sequestration, inflammation and hemostasis leading to microcirculatory dysfunction. *Trends Parasitol* **22**:503-508.
69. **Wang, G., K. A. Ahmad, and K. Ahmed.** 2005. Modulation of death receptor-mediated apoptosis by CK2. *Mol Cell Biochem* **274**:201-205.
70. **Ward, Y., S. F. Yap, V. Ravichandran, F. Matsumura, M. Ito, B. Spinelli, and K. Kelly.** 2002. The GTP binding proteins Gem and Rad are negative regulators of the Rho-Rho kinase pathway. *J Cell Biol* **157**:291-302.
71. **Wiese, L., J. A. Kurtzhals, and M. Penkowa.** 2006. Neuronal apoptosis, metallothionein expression and proinflammatory responses during cerebral malaria in mice. *Exp Neurol* **200**:216-226.
72. **Yarovinsky, F., and A. Sher.** 2006. Toll-like receptor recognition of *Toxoplasma gondii*. *Int J Parasitol* **36**:255-259.

Table S6. A complete list of ECM related genes in our study.

Description	GI Number	Average Fold Δ	
		Resistant	Non-MB
Unknown	NA	9.6699	18.129
RIKEN cDNA 1700058C13 gene (1700058C13Rik), mRNA.	58037321	9.0300	12.5004
solute carrier family 10 (sodium/bile acid cotransporter family), member 6 (Slc10a6), mRNA.	21313062	8.0098	7.4886
chitinase 3-like 3 (Chi3l3), mRNA.	6753416	6.4979	9.4846
metallothionein 2 (Mt2), mRNA.	33468863	5.9281	8.3874
arrestin domain containing 2 (Arrdc2), mRNA.	58037219	5.4463	3.4694
cytotoxic T lymphocyte-associated protein 2 alpha (Ctla2a), mRNA.	6681077	5.3175	15.411
cytotoxic T lymphocyte-associated protein 2 alpha (Ctla2a), mRNA.	6681077	5.1938	15.9449
PREDICTED: protein phosphatase 1, regulatory (inhibitor) subunit 12C, transcript variant 4 (Ppp1r12c), mRNA.	82902891	4.7691	2.4070
SAM and SH3 domain containing 1 (Sash1), mRNA.	112821670	4.6885	4.6488
mitogen-activated protein kinase kinase kinase 6 (Map3k6), mRNA.	66392595	4.5517	3.0951
cyclin-dependent kinase inhibitor 1A (P21) (Cdkn1a), mRNA.	6671726	4.4316	5.5363
FBJ osteosarcoma oncogene B (Fosb), mRNA.	6679827	4.3753	3.5498
connective tissue growth factor (Ctgf), mRNA.	6753878	4.3552	2.7946
vomeroneasal 1 receptor, F3 (V1rf3), mRNA.	21717723	4.2504	4.5490
RIKEN cDNA 4930591A17 gene (4930591A17Rik), mRNA.	13386084	4.2243	5.9102
Aryl sulfotransferase (EC 2.8.2.1) (Phenol sulfotransferase) (PST-1) (Sulfokinase) (Phenol/aryl sulfotransferase) (ST1A4). [Source:Uniprot/SWISSPROT;Acc:P52840]	NA	4.1744	4.4623
PREDICTED: RIKEN cDNA 1700057K13 gene (1700057K13Rik), mRNA.	23593059	4.0243	3.9217
Glucosamine	NA	3.8706	4.2752
neuropeptide Y receptor Y6 (Npy6r), mRNA.	6754884	3.8214	2.1872
RNA binding motif protein 3 (Rbm3), mRNA.	37497112	3.8130	4.7272
histone cluster 1, H1c (Hist1h1c), mRNA.	9845257	3.7585	2.8581
<i>cysteine rich protein 61 (Cyr61), mRNA.</i>	6753594	3.7571	4.6535
metallothionein 1 (Mt1), mRNA.	7305285	3.7323	4.9079
PREDICTED: similar to claudin 20 (LOC621628), mRNA.	82981734	3.6294	2.8889
neuronal pentraxin 2 (Nptx2), mRNA.	7949098	3.5912	2.4922
Unknown	NA	3.5736	4.6733
Unknown	NA	3.5501	4.1910
Proteasome (prosome, macropain) activator subunit 4	NA	3.5427	2.7676

cold inducible RNA binding protein (Cirbp), mRNA.	6680946	3.5313	3.1915
PREDICTED: similar to Ig heavy chain V region 441 precursor (LOC668418), mRNA.	94393200	3.4854	2.8990
RIKEN cDNA 4833432E10 gene	NA	3.4469	2.8937
RIKEN cDNA 4930434J08 gene	NA	3.4379	2.6555
B-cell translocation gene 3 (Btg3), mRNA.	6753208	3.4157	2.5010
Unknown	NA	3.3844	2.0120
ADP-ribosylation factor 4-like (Arf14), mRNA.	13384792	3.3607	2.6233
RIKEN cDNA A130040M12 gene (A130040M12Rik) on chromosome 4.	NA	3.3069	4.4642
preproacrosin (Acr), mRNA.	7304853	3.2723	3.3383
cofilin 1, non-muscle (Cfl1), mRNA.	6680924	3.2712	2.2512
PREDICTED: RAB11 family interacting protein 1 (class I), transcript variant 1 (Rab11fip1), mRNA.	82916552	3.2625	3.8285
RIKEN cDNA 1700030N03 gene	NA	3.2468	3.9198
CTLA-2-beta protein precursor (Fragment). [Source:Uniprot/SWISSPROT;Acc:P12400]	NA	3.2446	5.1150
bradykinin receptor, beta 1 (Bdkrb1), mRNA.	6671632	3.2305	2.5495
Metallothionein-I (MT-I). [Source:Uniprot/SWISSPROT;Acc:P02802]	NA	3.2173	4.2207
arachidonate 12-lipoxygenase, 12R type (Alox12b), mRNA.	6753040	3.2086	2.4240
Kruppel-like factor 4 (gut) (Klf4), mRNA.	6754456	3.0303	2.0779
Transgelin	NA	3.0099	3.4160
PREDICTED: cytochrome P450, family 4, subfamily f, polypeptide 18 (Cyp4f18), mRNA.	94384155	2.9678	2.5542
PREDICTED: transmembrane protein 52, transcript variant 1 (Tmem52), mRNA.	20850871	2.9661	2.4072
PREDICTED: transmembrane protein 52, transcript variant 1 (Tmem52), mRNA.	20850871	2.9661	2.4072
Unknown	NA	2.9190	3.4325
olfactory receptor 705 (Olfir705), mRNA.	22128881	2.9173	2.4341
Unknown	NA	2.8982	2.8981
Unknown	NA	2.8842	2.1816
RIKEN cDNA A130040M12 gene (A130040M12Rik) on chromosome 4.	NA	2.8815	3.8253
alanine-glyoxylate aminotransferase 2-like 1 (Agxt2l1), mRNA.	21313030	2.8654	2.0530
Unknown	NA	2.8565	2.5170
fibulin 5 (Fbln5), mRNA.	6753824	2.8342	2.3307
Unknown	NA	2.7967	2.4994
serum/glucocorticoid regulated kinase (Sgk), mRNA.	6755490	2.7945	2.7549
transgelin (Tagln), mRNA.	6755714	2.7833	3.3238
Internexin neuronal intermediate filament protein, alpha	NA	2.7601	2.2932
Casein kinase 2, alpha prime polypeptide	NA	2.7319	2.2010
vacuolar protein sorting 37D (yeast) (Vps37d), mRNA.	29243920	2.7178	2.1616

Dysbindin (dystrobrein binding protein 1) domain containing 2	NA	2.7117	2.3844
cullin 2 (Cul2), mRNA.	19482162	2.6867	2.2630
CD14 antigen (Cd14), mRNA.	6753332	2.6826	5.9668
protein kinase, AMP-activated, beta 2 non-catalytic subunit (Prkab2), mRNA.	72384347	2.6375	2.3431
transgelin (Tagln), mRNA.	6755714	2.6322	3.2566
AXIN1 up-regulated 1 (Axud1), mRNA.	23463295	2.6269	2.5756
FK506 binding protein 5 (Fkbp5), mRNA.	6753884	2.6118	2.5090
calcium regulated heat stable protein 1 (Carhsp1), mRNA.	13385290	2.6052	2.1279
DNA-damage-inducible transcript 4 (Ddit4), mRNA.	21312868	2.5821	2.5463
actin, beta, cytoplasmic (Actb), mRNA.	6671509	2.5726	3.0354
Unknown	NA	2.5627	2.4447
actin, beta, cytoplasmic (Actb), mRNA.	6671509	2.5523	3.0296
lipocalin 2 (Lcn2), mRNA.	34328049	2.5508	3.2024
<i>gene model 749, (NCBI) (Gm749), mRNA.</i>	85702211	2.5476	2.0498
coronin, actin binding protein 1C (Coro1c), mRNA.	31542413	2.5180	2.1758
major facilitator superfamily domain containing 2 (Mfsd2), mRNA.	58037449	2.5102	2.4778
major facilitator superfamily domain containing 2 (Mfsd2), mRNA.	58037449	2.5102	2.4778
RIKEN cDNA 4930535B03 gene	NA	2.4907	2.4639
nestin (Nes), mRNA.	50363232	2.4776	2.0290
<i>nuclear factor of kappa light chain gene enhancer in B-cells inhibitor, alpha (Nfkbia), mRNA.</i>	6754840	2.4699	2.6112
calcium/calmodulin-dependent protein kinase kinase 1, alpha (Camkk1), mRNA.	9256525	2.4654	2.3096
solute carrier family 2 (facilitated glucose transporter), member 3 (Slc2a3), mRNA.	31543726	2.4621	2.1722
Ca ²⁺ -dependent activator protein for secretion 2 (Cadps2), mRNA.	30520367	2.4619	2.8015
RIKEN cDNA 2410018G20 gene (2410018G20Rik), mRNA.	21312988	2.4602	2.6048
heme oxygenase (decycling) 1 (Hmox1), mRNA.	6754212	2.4339	7.7732
<i>HtrA serine peptidase 1 (Htra1), mRNA.</i>	9625027	2.4334	2.1909
actin, beta, cytoplasmic (Actb), mRNA.	6671509	2.4242	2.7908
angiotensin-like 4 (Angptl4), mRNA.	10181164	2.4204	3.8083
solute carrier family 6 (neurotransmitter transporter, creatine), member 8 (Slc6a8), mRNA.	19527208	2.4177	2.7898
patatin-like phospholipase domain containing 2 (Pnpla2), mRNA.	21313274	2.4062	3.4487
microorchidia 4 (More4), mRNA.	30794186	2.4047	2.7340
F-box and leucine-rich repeat protein 5	NA	2.4043	2.3625
transcriptional regulator, SIN3B (yeast) (Sin3b), mRNA.	28212270	2.4009	2.6900
5' nucleotidase, ecto (Nt5e), mRNA.	6754900	2.3984	2.1106
t-complex protein 10a (Tcpl0a), mRNA.	6678261	2.3883	2.0052
guanylate nucleotide binding protein 2 (Gbp2), mRNA.	6753950	2.3750	2.4250

PREDICTED: HtrA serine peptidase 4 (Htra4), mRNA.	28483736	2.3701	2.3846
a disintegrin-like and metallopetidase (reprolysin type) with thrombospondin type 1 motif, 16 (Adamts16), mRNA.	88196786	2.3663	2.1697
ornithine decarboxylase, structural 1 (Odc1), mRNA.	7305337	2.3630	2.4964
RIKEN cDNA A930018C05 gene	NA	2.3566	2.4549
RIKEN cDNA C030019I05 gene (C030019I05Rik), mRNA.	28892985	2.3549	2.4557
Unknown	NA	2.3496	2.0904
thyroid hormone responsive SPOT14 homolog (Rattus) (Thrsp), mRNA.	6678345	2.3457	2.3291
uncoupling protein 2 (mitochondrial, proton carrier) (Ucp2), mRNA.	31543920	2.3446	4.3372
Small nucleolar RNA, C/D box 22	NA	2.3319	3.0450
actin, beta, cytoplasmic (Actb), mRNA.	6671509	2.3284	2.6758
PREDICTED: Kruppel-like factor 9 (Klf9), mRNA.	94406143	2.3225	2.0603
PREDICTED: similar to axonemal dynein heavy chain 7 (LOC227058)	NA	2.3148	2.2089
<i>TSC22 domain family 3 (Tsc22d3), transcript variant 2, mRNA.</i>	116517342	2.3135	2.1384
<i>TSC22 domain family 3 (Tsc22d3), transcript variant 2, mRNA.</i>	116517342	2.3135	2.1384
RIKEN cDNA 2410006H16 gene	NA	2.3043	2.6002
RIKEN cDNA 2010004A03 gene (2010004A03Rik), mRNA.	33239433	2.2995	2.5681
RIKEN cDNA 1700093K21 gene (1700093K21Rik), mRNA.	40254498	2.2980	2.3735
H3 histone, family 3B (H3f3b), mRNA.	6680161	2.2949	2.8015
Unknown	NA	2.2912	2.8301
arachidonate lipoxygenase 3 (Aloxe3), mRNA.	6753042	2.2841	2.2080
plasma membrane associated protein, S3-12 (S3-12), mRNA.	10181204	2.2802	2.1130
plasma membrane associated protein, S3-12 (S3-12), mRNA.	10181204	2.2802	2.1130
v-maf musculoaponeurotic fibrosarcoma oncogene family, protein K (avian) (Mafk), mRNA.	6754612	2.2779	2.6080
kelch-like 15 (Drosophila) (Klh15), transcript variant 3, mRNA.	84794643	2.2727	2.3019
TOUSLED-LIKE KINASE 2; TOUSLED-LIKE KINASE (ARABIDOPSIS); PROTEIN KINASE U-ALPHA; TOUSLED-LIKE KINASE 2 (ARABIDOPSIS). [Source:RefSeq;Acc:NM_011903]	NA	2.2670	2.2391
hypothetical protein A630085K21 (A630085K21)	NA	2.2633	4.4696
<i>lamin A (Lmna), transcript variant 2, mRNA.</i>	9506843	2.2396	2.5334
<i>syndecan 4 (Sdc4), mRNA.</i>	6755442	2.2323	2.5949
GTP binding protein (gene overexpressed in skeletal muscle) (Gem), mRNA.	6753972	2.2254	2.4846
GTP binding protein (gene overexpressed in skeletal muscle) (Gem), mRNA.	6753972	2.2254	2.4846
protein phosphatase 1, regulatory (inhibitor) subunit 1B (Ppp1r1b), mRNA.	21536256	2.2155	2.1791
claudin 11 (Cldn11), mRNA.	6679186	2.2071	2.0770
growth arrest and DNA-damage-inducible 45 gamma (Gadd45g), mRNA.	6753938	2.2070	2.6054
Kruppel-like factor 9 (Klf9), mRNA.	31542239	2.2065	2.0262
actin, beta, cytoplasmic (Actb), mRNA.	6671509	2.2045	2.6780

relaxin 1 (Rln1), mRNA.	51093876	2.2037	2.1867
regulator of G-protein signaling 1 (Rgs1), mRNA.	7657512	2.2025	3.0249
Jun proto-oncogene related gene d1 (Jund1), mRNA.	6754404	2.2008	2.0175
RIKEN cDNA 2010002N04 gene (2010002N04Rik), mRNA.	19527364	2.1979	2.2238
RIKEN cDNA E030010A14 gene (E030010A14Rik), mRNA.	34147189	2.1867	2.2081
kallikrein 1-related peptidase b11 (Klk1b11), mRNA.	28875780	2.1715	2.0085
Bassoon	NA	2.1666	2.7117
protein kinase, AMP-activated, beta 2 non-catalytic subunit (Prkab2), mRNA.	72384347	2.1644	2.0847
dysbindin (dystrobrevin binding protein 1) domain containing 2 (Dbnbd2), transcript variant 1, mRNA.	115299764	2.1621	2.0322
epithelial membrane protein 1 (Emp1), mRNA.	6753748	2.1560	3.5286
tripartite motif-containing 66 (Trim66), mRNA.	79750343	2.1335	2.6488
phospholipase A1 member A (Pla1a), mRNA.	31982575	2.1278	2.8298
Phospholipase A2, group III	NA	2.1267	2.3951
RNA binding motif protein 22 (Rbm22), mRNA.	110625591	2.1188	2.0285
hyaluronan and proteoglycan link protein 2 (Hapln2), mRNA.	15042971	2.0958	2.1157
SH2 domain protein 2A (Sh2d2a), transcript variant 2, mRNA.	70909334	2.0458	2.3376
G protein-coupled receptor, family C, group 5, member A (Gprc5a), mRNA.	31126968	2.0241	2.2332
RIKEN cDNA 2600006K01 gene	NA	2.0213	2.1849
tumor necrosis factor receptor superfamily, member 4 (Tnfrsf4), mRNA.	6755909	2.0137	2.1650
RAB28, member RAS oncogene family	NA	0.4921	0.4922
protein phosphatase 1F (PP2C domain containing) (Ppm1f), mRNA.	28849881	0.4898	0.4746
RIKEN cDNA 4930413O22 gene	NA	0.4868	0.4443
RNA binding protein gene with multiple splicing	NA	0.4865	0.4908
RIKEN cDNA 9930013L23 gene (9930013L23Rik), mRNA.	38638700	0.4822	0.3883
zinc finger protein 54 (Zfp54), mRNA.	6756063	0.4724	0.4176
Unknown	NA	0.4723	0.4224
Unknown	NA	0.4697	0.4758
RIKEN cDNA 9430037G07 gene	NA	0.4687	0.4824
potassium inwardly-rectifying channel, subfamily J, member 9 (Kcnj9), mRNA.	111607443	0.4681	0.4800
<i>H-2 class I histocompatibility antigen, Q8 alpha chain precursor.</i> [Source:Uniprot/SWISSPROT;Acc:P14430]	NA	0.4675	3.4204
DNA segment, Chr 19, Brigham & Women's Genetics 1357 expressed (D19Bwg1357e), mRNA.	29126213	0.4663	0.4057
PREDICTED: S1 RNA binding domain 1 (Srbd1), mRNA.	94404154	0.4642	0.4518
<i>CD48 antigen</i>	NA	0.4609	2.1128
Unknown	NA	0.4598	0.4886
galactose-3-O-sulfotransferase 1 (Gal3st1), mRNA.	31980855	0.4587	0.4086

transmembrane 6 superfamily member 2 (Tm6sf2), mRNA.	31559811	0.4556	0.4660
transmembrane 6 superfamily member 2 (Tm6sf2), mRNA.	31559811	0.4556	0.4660
spindle assembly 6 homolog (C. elegans) (Sass6), mRNA.	58037301	0.4541	0.3798
<i>histocompatibility 2, Q region locus 6 (H2-Q6), mRNA.</i>	46559400	0.4502	3.0048
transmembrane protease, serine 5 (spinesin) (Tmprss5), mRNA.	13507652	0.4493	0.4457
Hypothetical gene supported by AK083927	NA	0.4452	0.4194
Unknown	NA	0.4416	3.2588
predicted gene, EG622320 (EG622320), mRNA.	85702330	0.4407	0.3859
epithelial membrane protein 2 (Emp2), mRNA.	111154059	0.4393	0.4738
PREDICTED: similar to Tubulin alpha-3 chain (Alpha-tubulin 3) (LOC384401), mRNA.	NA	0.4353	0.4108
peroxisome biogenesis factor 5 (Pex5), transcript variant 1, mRNA.	113930737	0.4332	0.4498
Oocyte specific homeobox 5	NA	0.4326	0.4745
zinc finger and BTB domain containing 26 (Zbtb26), mRNA.	71037369	0.4289	0.4552
Dlx6 opposite strand transcript 1	NA	0.4234	0.3738
SRY-box containing gene 5 (Sox5), mRNA.	6755608	0.4210	0.3264
RIKEN cDNA C030029H02 gene TRANSCRIPTION ELONGATION REGULATOR 1 (CA150); TRANSCRIPTION FACTOR CA150B; COACTIVATOR OF 150 KD; TATA BOX BINDING PROTEIN (TBP)- ASSOCIATED FACTOR, RNA POLYMERASE II, S, 150KD. [Source:RefSeq;Acc:NM_019512]	NA	0.4127	0.3328
RIKEN cDNA C130045F17 gene	NA	0.4102	0.4228
DnaJ (Hsp40) homolog, subfamily C, member 19	NA	0.4081	0.4742
tubulin, delta 1 (Tubd1), mRNA. TRANSCRIPTION ELONGATION REGULATOR 1 (CA150); TRANSCRIPTION FACTOR CA150B; COACTIVATOR OF 150 KD; TATA BOX BINDING PROTEIN (TBP)- ASSOCIATED FACTOR, RNA POLYMERASE II, S, 150KD. [Source:RefSeq;Acc:NM_019512]	9790053	0.4034	0.4125
Unknown	NA	0.4022	0.4426
ATP-binding cassette, sub-family A (ABC1), member 8a (Abca8a), mRNA.	23346593	0.4006	0.4630
toll-like receptor 11 (Tlr11), mRNA.	45429992	0.4000	0.4185
Phosphorylase kinase alpha 1	NA	0.3980	0.4027
Fuzzy homolog (Drosophila) TRANSCRIPTION ELONGATION REGULATOR 1 (CA150); TRANSCRIPTION FACTOR CA150B; COACTIVATOR OF 150 KD; TATA BOX BINDING PROTEIN (TBP)- ASSOCIATED FACTOR, RNA POLYMERASE II, S, 150KD. [Source:RefSeq;Acc:NM_019512]	NA	0.3964	0.4859
methytransferase-like 3 (Mettl3), mRNA.	77627973	0.3940	0.4263
Cleavage and polyadenylation factor subunit homolog (S. cerevisiae)	NA	0.3940	0.3789
Unknown	NA	0.3896	0.4932
steroid receptor-interacting SNF2 domain protein. [Source:RefSeq;Acc:NM_030730]	NA	0.3886	0.4739
predicted gene, EG317677 (EG317677), mRNA.	27805393	0.3875	2.0280

PREDICTED: RIKEN cDNA D430007A19 gene, transcript variant 3 (D430007A19Rik), mRNA.	82997007	0.3863	0.4316
Unknown	NA	0.3793	0.3886
Unc-5 homolog C (C. elegans)	NA	0.3792	0.4412
Unc-5 homolog C (C. elegans)	NA	0.3792	0.4412
RIKEN cDNA 9530059O14 gene	NA	0.3792	0.4298
Recombining binding protein suppressor of hairless (Drosophila)	NA	0.3735	0.3867
RIKEN cDNA 6332401O19 gene (6332401O19Rik), mRNA.	28892879	0.3730	0.3826
cysteine and histidine-rich domain (CHORD)-containing, zinc-binding protein 1 (Chordc1), mRNA.	13385324	0.3715	0.3853
tumor necrosis factor (ligand) superfamily, member 10 (Tnfsf10), mRNA.	6678431	0.3626	0.3950
nuclear autoantigenic sperm protein (histone-binding) (Nasp), mRNA.	13384598	0.3606	0.3563
RIKEN cDNA 2210009G21 gene (2210009G21Rik), transcript variant 1, mRNA.	21312668	0.3560	0.3428
<i>colony stimulating factor 2 receptor, beta 1, low-affinity (granulocyte-macrophage) (Csf2rb1), mRNA.</i>	75677418	0.3548	2.7849
TBC1 domain family, member 4	NA	0.3519	0.4857
Myeloid/lymphoid or mixed lineage-leukemia translocation to 3 homolog (Drosophila)	NA	0.3514	0.4187
<i>neutrophil cytosolic factor 4 (Ncf4), mRNA.</i>	6679022	0.3468	2.9632
RIKEN cDNA 9330118A15 gene	NA	0.3386	0.3234
Unknown	NA	0.3375	0.3569
purinergic receptor P2Y, G-protein coupled 12 (P2ry12), mRNA.	31980659	0.3299	0.3892
Hypothetical protein 6430584L05	NA	0.3269	0.4753
RIKEN cDNA 4930558O21 gene (4930558O21Rik), mRNA.	13386152	0.3239	0.3967
TRANSCRIPTION ELONGATION REGULATOR 1 (CA150); TRANSCRIPTION FACTOR CA150B; COACTIVATOR OF 150 KD; TATA BOX BINDING PROTEIN (TBP)-ASSOCIATED FACTOR, RNA POLYMERASE II, S, 150KD. [Source:RefSeq;Acc:NM_019512]	NA	0.3143	0.4043
fatty acid binding protein 7, brain (Fabp7), mRNA.	10946572	0.3142	0.3911
0 day neonate thymus cDNA, RIKEN full-length enriched library, clone:A430098J12 product:unclassifiable, full insert sequence	NA	0.3135	0.3981
McKusick-Kaufman syndrome protein (Mkks), mRNA.	10946954	0.3059	0.3146
zinc finger protein 715 (Zfp715), mRNA.	66793402	0.2824	0.2777
UDP galactosyltransferase 8A (Ugt8a), mRNA.	31543926	0.2801	0.3478
RNA binding motif protein 3 (Rbm3), mRNA.	37497112	0.2761	0.3576
Hypothetical protein 9330117O12	NA	0.2741	0.3615
tumor necrosis factor (ligand) superfamily, member 10 (Tnfsf10), mRNA.	6678431	0.2696	0.3134
homeo box A5 (Hoxa5), mRNA.	6754232	0.2630	0.4080
Splicing factor proline/glutamine rich (polypyrimidine tract binding protein associated)	NA	0.2601	0.2626
hemoglobin alpha, adult chain 1 (Hba-a1), mRNA.	6680175	0.2347	0.1934
SRY-box containing gene 21 PREDICTED: RIKEN cDNA 4933433K01 gene, transcript variant 1 (4933433K01Rik), mRNA.	NA	0.2311	0.3028
	82934570	0.0859	0.3897

HEMOGLOBIN EPSILON-Y2 CHAIN. [Source:SWISSPROT;Acc:P02104]	NA	0.0659	0.0688
hemoglobin, beta adult major chain (Hbb-b1), mRNA.	31982300	0.0535	0.0617
hemoglobin, beta adult minor chain (Hbb-b2), mRNA.	17647499	0.0520	0.0509

Discussion of Results

Malaria is one of the earliest diseases known to mankind; the first recorded description of symptoms of the disease is found in ancient Chinese medical writings in 2700 BC in the Nei Ching, The Canon of Medicine. Today, malaria is a major cause of illness and death throughout the world, accounting for 300 to 500 million cases and more than 1 million deaths annually (4). In fact, malaria is on the rise; today there are more case of malaria than 30 years ago. The primary factors that are attributed to the increase in the global problem of malaria are exponential rise in human population, environmental degradation, human migration and probably most importantly the rapid emergence and spread of parasite strains that have developed resistance against the major anti-malaria drugs. (26).

Malaria is caused by a protozoan parasite from the genus *Plasmodium* that is transmitted through the bite of the female *Anopheles* mosquito. There are more than 100 species of *Plasmodium* that infect reptiles, birds and mammals of which only four species, *P. falciparum*, *P. vivax*, *P. ovale*, and *P. malariae* are known to cause infections in human. Infections with human *Plasmodium* species cause a wide array of clinical illness varying from asymptomatic, symptomatic, and severe disease (20). The outcome of clinical disease is determined by several factors including parasite species and host genetics.

Among the four *Plasmodium* species, *P. falciparum* is the most virulent and alone is responsible for more than 90% of malaria related deaths; approximately 90% of these deaths occur in children under the age of five living in sub-Saharan Africa (4). Why *P. falciparum* has evolved to cause the most virulent form of malaria is not clear; however,

the majority of *falciparum*-associated deaths in young children are caused by the pathological syndromes of cerebral malaria and severe anemia. One unique feature of the biology of *P. falciparum* parasites is that only early ring form parasites are detected in blood films; mature blood forms of the parasite sequester in different organs, including in the brain that causes an obstruction in blood flow. Parasite sequestration is considered by many to be the primary cause of the pathogenesis of cerebral malaria, a clinical feature seen only during *P. falciparum* infections; some murine malarias also display the pathophysiological symptoms that closely resemble the human cerebral malaria disease.

Rupturing infected erythrocytes and releasing merozoites are known to cause malaria fever and chills, the clinical symptoms most closely associated with malaria. Another common feature of malaria is the presence of severe anemia mostly experienced during primary infections. The degree of anemia experienced during malaria is not always directly proportional to the parasite density and has been shown to be caused by destruction of both infected and uninfected erythrocytes and dyserythropoiesis (21).

I. Molecular Factors and Biochemical Pathways Induced in Response to Malaria Fever

Febrile illness experienced during primary infections with *Plasmodium* parasites is the most common and benign clinical symptom of malaria. Even long before the discovery that malaria was caused by intra-erythrocytic protozoan parasites, the cyclical nature of malaria fever was the most identifiable feature of this disease. Clinical descriptions of malaria primarily based on malaria fever were described in several ancient writings including by the Chinese, Indians and Greeks.

Malaria fever is induced by parasite products released by rupturing schizonts that account for the clinical observations that each wave of malaria fever coincides with the length of the intra-erythrocytic stage developmental cycle. Several parasite factors have been identified as candidate “malaria toxins” that induce malaria fever and are responsible for other aspects of malaria pathogenesis such as upregulation of the host endothelial receptors (28), severe anemia (19), and several physiological disturbances such as acute acidosis and hypoglycemia (6). The most studied malaria toxin for *P. falciparum* is glycosylphosphatidylinositol (GPI), a glycolipid that is a constituent of several surface membrane proteins (27). GPI molecules act on monocytes to produce excess amounts of TNF – α , a cytokine associated with febrile illness (15).

Another major candidate toxin molecule is malaria pigment – hemozoin (Hz) that was first implicated in 1912 as the parasite factor responsible for the malaria paroxysm (5). Although immunologically inert, recent studies suggest that *P. falciparum* Hz can serve as a novel non-DNA ligand for Toll-like receptor (TLR) 9 and can activate the

innate immune response to produce cytokines, chemokines, and up-regulation of costimulatory molecules (7).

Observations arising from neurosyphilis studies performed in the 1930s and 1940s (2) and from a few recent studies have led many researchers to believe that malaria febrile illness is an evolutionary adaptation that benefits both the parasite and its host (17, 32). According to this hypothesis, elevated host temperature induces a cascade of molecular events that maintain the total parasite burden at a threshold level by limiting its replication rate, allowing host defense mechanisms to activate and mature. Although inhibition of exponential parasite growth caused by febrile temperature may appear to aid only the host, it may also provide the parasite sufficient time to further transmit infection, making it a potential parasite survival strategy. Given the important role of febrile temperature on the survival and virulence of malaria parasites, surprisingly information regarding the molecular factors and its associated biological pathways induced in malaria parasites in response to febrile illness remains very limited.

In this Ph.D. dissertation, I studied the effect of febrile temperatures on the in vitro survival of intra-erythrocytic parasites and performed experiments to determine the mechanism of febrile illness induced death in *P. falciparum* parasites. We also studied the molecular factors altered in response to febrile temperature by measuring differential expression levels of individual parasite genes using high-density oligonucleotide microarray technology and by performing biological assays in asexual-stage *P. falciparum* parasite cultures incubated at 37°C and 41°C (an elevated temperature that is equivalent to malaria induced febrile illness in the host). We also performed in-depth sensitive computational analyses to identify the changes in the major parasite biologic

networks and pathways that occurred in response to growth at febrile temperatures. In addition, we performed a few biological assays to verify the results obtained by microarray chip based gene expression analysis and its implied alterations in biological pathways.

A Summary Discussion of Results. Our studies show that elevated temperature had a deleterious effect on parasite survival in both synchronous and asynchronous cultures. In synchronous ring stage cultures, in relation to survival at 37°C, following 2, 8, 16, and 24 h of cultivation at 41°C, parasite survival was reduced by 25%, 60%, 95%, and 88% respectively. Thirty-two hours of cultivation at 41°C caused elimination of 100% of cultured *P. falciparum* parasites. In asynchronous cultures, following 2 and 8 hours of cultivation at 41°C, parasite survival was reduced by 23% and 66%, respectively, and 16 h of cultivation at febrile temperature resulted in the death of 100% of cultured parasites. These results are in agreement with an earlier report showing an inhibitory effect of temperatures characteristic of the malaria paroxysm on in vitro parasite growth (15, 17) and suggest that the malaria paroxysm plays a significant role in limiting the exponential growth of parasites in a non-immune host.

To explore the mechanism of the febrile temperature induced killing of blood form parasites, we examined Giemsa-stained *P. falciparum* blood films for the presence of pyknotic “crisis forms” that give the appearance of parasites undergoing death. By light microscopy, we find that treatment of parasite at 41°C revealed the distinct presence of “crisis form” trophozoites and schizonts, while rings appear to be immune to heat-induced destruction. Presence of “crisis forms” has been ascribed as a marker of apoptotic cell death in malaria parasites (9). Previously, “crisis forms” of trophozoites

and schizonts has been described in *P. falciparum* cultures undergoing death induced by treatment with anti-malaria drugs and other experimentally induced forms of stress (9, 22). We were also able to demonstrate a strong TUNEL-activity in 41°C cultured parasites. The TUNEL assay is widely used as a marker for apoptotic cell death. Existence of TUNEL-reactivity in blood forms of malaria parasites has been a subject of controversy. In a recent review article, Deponete and Becker have reported TUNEL-activity in *P. falciparum* blood stage schizonts treated with anti-malaria drugs and H₂O₂ (9), although no experimental data to sustain their claim was presented. Other studies have failed to detect a TUNEL-positive assay in *P. falciparum* parasites treated *in vitro* with known anti-malarial drugs (22, 23). Thus, our results are the first documented demonstration of a TUNEL-positive assay in blood form malaria parasites. Together, based on our results, presence of “crisis forms” and TUNEL-positive parasites suggests that febrile temperature induced parasite killing is mediated by the mechanism of apoptotic cell death.

The molecular factors and biologic pathways triggered in response to febrile illness during a malaria infection are not known. We identified the molecular factors altered in response to febrile temperature by measuring differential expression levels of individual genes using high-density oligonucleotide microarray technology and by performing biological assays in asexual-stage *P. falciparum* parasite cultures incubated at 37°C and 41°C (an elevated temperature that is equivalent to malaria induced febrile illness in the host). Elevated temperature had a profound influence on expression of individual genes; 336 of approximately 5,300 genes (6.3% of the genome) had altered expression profiles. Of these, 163 genes (49%) were upregulated by 2 fold or greater, and

173 genes (51%) were downregulated by 2 fold or greater. In-depth sensitive sequence-profile analysis revealed that febrile temperature-induced responses caused significant alterations in the major parasite biologic networks and pathways, and that these changes are well coordinated and intricately linked. Using our sensitive computational analysis, we were also able to assign biochemical or biologic functional predictions for at least 100 distinct genes previously annotated as “hypothetical” and thus improved the overall database for the *P. falciparum* genome.

One of the most notable transcriptional changes was that about 47% of the genes that show altered transcription are predicted to be either transmembrane or secreted proteins, suggesting that a major component of the transcriptional response to temperature is directed at altering the cell-surface and/or interactions with the host. About 22% (75 proteins) of the transcriptionally altered genes are predicted to contain the recently described Pexel motif or host target signal (consensus R/KxLxE/Q) (13, 16). The Pexel motif has been demonstrated to serve as a key signal for protein export into the erythrocytes, and such exported proteins are known to reside either in the host cytoplasm or the host membrane and are identified as parasite virulence molecules. In our studies, 72% of the proteins (54 of 75) with reliably predicted Pexel motifs encoded by the temperature-affected genes are upregulated, suggesting that there is a major extrusion of proteins into the host cytoplasm or membrane upon temperature elevation.

We also find that a generalized upregulation in the expression of genes that are identified as virulence factors and potential erythrocyte remodeling proteins strongly suggest that febrile illness directly affects malaria pathogenesis. In this regard, we find a consistent upregulation in the expression of 5 *var* genes or erythrocyte membrane

protein-1 (EMP-1) (average fold change 2.8, range 2.6–3.0). EMP-1 is the most studied virulence protein of *P. falciparum* and is anchored on the surface of infected erythrocytes where it serves as a parasite ligand that binds to receptors on host endothelial cells (20).

In an earlier study, Udomsangpetch et al. detected EMP-1 expression on the surface of ring and mature trophozoite IRBCs incubated at 40°C but not at 37°C (32), suggesting that febrile temperatures can induce the expression level and trafficking of EMP-1 to the surface of erythrocytes. However, by fluorescence analysis, we detected equal amounts of EMP-1 in *P. falciparum* parasites treated at 37°C and 41°C, suggesting that febrile temperature had no effect of surface expression of EMP-1.

These in vitro studies suggest that in an infected host, febrile illness could have both protective and deleterious effects. While febrile temperature could directly kill in vivo parasites by causing physiologic stress, it can also simultaneously prevent parasite immunologic clearance by en masse trafficking of parasite virulence proteins on the erythrocyte surface and thus allowing enhanced sequestration within the deep venules of the host tissues that could contribute toward the pathogenesis of cerebral malaria.

The genome of *P. falciparum* possesses an intact pathway for the synthesis of GPI anchors for membrane proteins, and this is consistent with the presence of several GPI-anchored proteins on the parasite membranes (31). In this study, five key enzymes in the GPI anchor biosynthesis pathway, including GPI transamidase and glycosyltransferase are consistently downregulated. This suggests that in response to elevated temperature, GPI-anchored proteins are likely to be depleted from the parasite membrane. Given the identified role of *Plasmodium* GPIs as malaria toxins, febrile temperature induced down-

regulation in GPI expression may have significance in modulating the parasite's pathogenic response.

We noted significant changes in the expression of the category of genes that are involved in the heat-shock response and protein stability. Two chaperones, the HSP70 and HSP90 orthologs, which have been implicated in the heat-shock response across the phylogenetic spectrum of life, show an increased expression. *P. falciparum*, in contrast to other *Plasmodium* species and other Apicomplexa, shows a dramatic lineage-specific expansion of a particular family of DnaJ-domain proteins (1). Nine members of this DnaJ expansion show an elevated expression in our study. Febrile temperature induced upregulation in the expression of the heat shock protein family is well known (12) and is considered an adaptation to protect the cell from environmental stress.

Another significant finding of our study was that ten different genes for proteins of the ubiquitin metabolism system were observed to be consistently downregulated. These include proteasomal enzymes, different E1 and E3 enzymes, as well as some ubiquitin C-terminal hydrolases. As a validation of our microarray results, we noted that polyubiquitin, the only ubiquitin pathway gene found to be upregulated in our dataset (1.53 fold change), was also upregulated in response to elevated temperature in an earlier published report (14). We further confirmed our microarray results by measuring the total ubiquitination of proteins isolated from parasites incubated at 37°C and 41°C, using a rabbit polyclonal bovine anti-ubiquitin antibody. Comparison of expression levels obtained by ECL-based semi-quantitative western blot analysis of *P. falciparum* parasite extracts collected after incubation at 37°C or 41°C 2 h demonstrated that temperature elevation caused a 14.8-fold downregulation in the ubiquitination process. An overall

depression of the ubiquitin pathway suggests that modulation of protein degradation could be a parasite survival mechanism to increase the half-life of certain proteins under stressful conditions. In addition to degradation of misfolded proteins, the ubiquitin pathway has a second important function of regulation of the cell cycle by selective degradation of cyclins (10). Therefore, heat induced down-regulation of the parasite ubiquitin pathway may also be an effector mechanism employed by the parasite to maintain the parasite burden below a threshold that is lethal to the host.

We also find that eight genes for chromatin components are upregulated; in comparison, only two genes are downregulated. The upregulated genes include the histones (H2B and H4) and the NAD-dependent histone deacetylase of the Sir2p family (PfSir2). Several genes of the DNA replication and repair systems, including the RP-A and RF-C are downregulated, whereas a Rad25-like helicase/ATPase and a DNA repair nuclease, Dem1p of the RecB family are upregulated. The exact implication of these changes in the expression pattern of the nuclear proteins is unclear, but it might indicate a tendency for condensation of chromatin and a possible slow-down in replication.

Another striking observation was that about 26% (90 genes) of the genes showing a change in transcription in response to febrile conditions map to the sub-telomeric gene arrays that, in addition to members of the *rif*, *var* and DNAJ families, also encode several other proteins. This observation indicates a strong bias in the preferential regulation of genes associated with chromosome ends and points to probable special chromatin-related changes in the sub-telomeric regions. In particular, we noticed that at least 70% of sub-telomeric genes found in our dataset were over-expressed, suggesting there might be an

increased accessibility of particular regions of sub-telomeric chromatin to allow increased transcription of certain genes.

In conclusion, by using a combination of gene expression data, sequence analysis, and biologic experiments, we have determined the potential global biological response in *P. falciparum* parasites that occurs in response to a febrile temperature. We find that a large number of proteins that are predicted or known to be exported into the host cell or expressed on the host cell surface are over-expressed to varying degrees under temperature stress. As a general intracellular response, the upregulation of several genes related to mRNA metabolism and splicing appears to suggest a major post-transcriptional regulatory response. We also find a general tendency to slow down the synthesis of proteins involved in protein stability, trafficking, and protein synthesis itself, and also a down regulation in the synthesis of new proteins and degradation of existing proteins by the ubiquitin pathway. Several *Plasmodium*- or Apicomplexan-specific gene families and other enzymes with no close homologs in humans are over-expressed in response to febrile temperature suggesting that these molecules might serve as potential targets for therapeutic intervention or as vaccine candidates.

Future research avenues arising from this study. We believe that in this study, we offer for the first time a comprehensive view of the alterations in gene expression and predicted biochemical pathways in a malaria parasite that occur in response to exposure to a febrile temperature condition. Data generated from these experiments have provided a glimpse of several biological findings that were previously not known. Our data have for the first time clearly shown the presence of an apoptosis-like cell death mechanism in blood form malaria parasites. The fact that we were able to measure febrile temperature

induced parasite destruction (a natural physiological process that also occurs in the human host) opens up prospects for further research that will enable identification of the parasite molecules and pathway involved in apoptosis-mediated cell death and thus offer novel targets for drugs and vaccine intervention.

The next major finding is that febrile temperature triggers the transcription of proteins involved in the remodeling of the host erythrocyte, especially proteins containing the Pexel motif or host target signal that are considered virulence proteins. Temperature induced expression of GFP-tagged expression plasmids encoding these molecules will enable studies to be made that examine the trafficking of malarial antigens to the erythrocyte surface and determination of their role in cytoadherence to host endothelial cells. These studies will greatly increase the repertoire of malaria virulence proteins that are attractive vaccine targets.

Our observation that five key enzymes in the GPI anchor biosynthesis pathway, including GPI transamidase and glycosyltransferase are consistently downregulated suggests that febrile illness alters the synthesis of malaria toxins. This observation warrants further investigations to determine the role of the individual genes of the GPI-pathway in parasite survival by targeted gene deletion studies. A further analysis of the altered genes in our dataset might lead to the identification of additional malaria toxins that induce malaria pathogenesis.

Finally, our finding (by microarray and western blot) showing that a febrile response could lead to a generalized shutdown in the *P. falciparum* ubiquitin pathway might spur studies in protein degradation in malaria parasites. We also think that deletion

of genes in the ubiquitin pathway could lead to the generation of growth attenuated malaria parasites for use as candidate vaccines.

Overall, we believe that our studies have opened many avenues that will allow 1) detailed knowledge regarding the apoptotic parasite death mechanism, 2) identification of novel virulence and cytoadherence molecules of malaria pathogenesis, 3) cell biology studies to study the transport of malarial proteins across the cytoplasm to the erythrocyte surface and 5) understanding the ubiquitin pathway and protein degradation in malaria parasites. Eventually, identification of novel molecules that are responsible for parasite survival and virulence offer new targets for the development of drugs and vaccines against malaria.

II. Host Molecular Factors that Contribute Towards the Susceptibility or Resistance to Cerebral Malaria

The most severe pathological consequence of malaria is the clinical syndromes collectively termed as cerebral malaria (CM). Among human malarias, only infection with *P. falciparum* is known to cause CM, although some murine *Plasmodium* species cause a pathological syndrome that closely resemble human CM. In contrast to fever, an invariable symptom of infection in non-immune individuals, the clinical outcome of CM occurs in only a minority of malaria cases. However, although neurological complications are a rare consequence of infection, due to its high mortality rate, CM is the most common cause of malaria death.

Although the pathogenesis of CM is a primary factor in malaria-associated deaths, only limited information is available regarding the host molecular factors that contribute towards the pathogenesis of CM. In Africa, most children develop immunity against the pathogenesis of CM by the age of 10. However, in a community where every child receives an equal amount of parasite exposure, the fact that a small subset of children will suffer from the pathogenesis of CM strongly suggests that host genetics play an important role.

As stated earlier, even after decades of research, the host molecular factors and its associated biochemical pathways that contribute towards the pathogenesis of cerebral malaria are poorly defined. An obvious reason behind the limited progress is because of the fact that in young children, many of the desired studies of immunology and pathogenesis can not be performed due to practical and ethical reasons. For this reason, we decided to rely on *P. berghei* ANKA (Pb-A), an experiment murine malaria model of cerebral malaria to study the pathogenesis of CM (8).

We used the *P. berghei* ANKA (Pb-A) murine model of experimental cerebral malaria (ECM) to examine the role of host gene expression in susceptibility or resistance to disease. Infection with Pb-A parasites is lethal in 100% of mice. However, the cause of death varies greatly based on the mouse genetic background, and mouse strains are broadly categorized as susceptible or resistant to CM. Using high density microarray chips, we compared whole brain tissue expression profiles of C57BL/6 mice with ECM (moribund) to: 1) C57BL/6 mice without ECM (non-moribund) and 2) BALB/c mice without ECM (resistant). Based on differential expression in brain tissue samples taken

from mice that were terminally ill with the symptoms of ECM, a total of 210 host genes were strongly associated with the manifestation of ECM.

ECM can be divided into two distinct phases of disease: 1) induction phase and 2) effector phase. The induction phase can be defined as the events preceding the onset of symptoms, and in the Pb-A model of ECM occur between days 0-5 post-infection. The effector phase can be defined as the events mediating the disease process and occurs during and after the onset of symptoms (days 6-10 post-infection).

We have identified 210 host genes that we believe are associated with the effector phase of ECM by determining the set of genes transcriptionally altered in terminally ill mice. These genes can be divided into two functional groups: 1) genes mediating the disease process and 2) genes responding to disease process. Genes in the latter group include genes involved in DNA and tissue repair and in the prevention of oxidative stress and apoptosis. Identification of novel biomarkers of ECM will pave new avenues for future research in the prevention, diagnosis, and treatment of CM.

Prevention. The development of a vaccine that will prevent disease but not necessarily infection is considered by many scientists to be the best and most cost effective method currently available in reducing deaths caused by CM. An understanding of the events involved in the induction of CM is crucial for identifying potential anti-disease vaccine targets. However, a major dilemma in studying factors associated with the induction of ECM in the Pb-A model is the inability to predict which susceptible mice will go on to develop symptoms of ECM. This inability to predict is due to the fact that only a proportion of susceptible mice actually develop ECM (60% in our study) and progression of disease occurs very rapidly (within hours). In terms of host gene

expression, we predict that there is significant overlap between the induction and effector phases of disease; some genes that are significantly overexpressed during the effector phase may be moderately overexpressed during the induction phase. Identification of reliable biomarkers of the induction phase will be required before valid studies of the early events of ECM can be performed.

Diagnosis. Identification of biomarkers in the brain that are also altered in the blood may lead to the development of a method for early detection of CM. Further experiments will be needed to detect the presence of these biomarkers in the blood of mice during different stages of progression during infection with Pb-A and should be performed with caution. For example, the most promising biomarkers of ECM that may also be detectable in the blood are the genes that encode the hemoglobin chains; these genes are significantly down-regulated during ECM and are also expressed in the reticulocytes of the bloodstream. However, because anemia (including malaria anemia) is common in malaria endemic countries, they may not be good candidates for the diagnosis of CM.

For these biomarkers to become of prognostic value in determining whether *P. falciparum* infection in a child would progress into CM, carefully designed field studies will be needed. However, availability of a test that could be predictive of CM during a *P. falciparum* infection will be of great value in early treatment and may potentially save the lives of children.

Treatment. Adjunct therapies that will reverse the rapid clinical deterioration associated with CM are needed. We have identified 210 host genes that we believe are associated with the effector phase of ECM, the phase most pertinent to the treatment of

CM. As stated previously, these genes can be divided into two functional groups: 1) genes mediating the disease process and 2) genes responding to disease process.

Candidate genes from both groups may be promising therapeutic drug targets.

We are particularly interested in addressing the role of CD14 in the pathogenesis of ECM. In our study, CD14 was significantly up-regulated (2.7, 6 fold) in brain tissue of mice displaying symptoms of cerebral malaria. CD14 was the first lipopolysaccharide (LPS) receptor to be characterized. It is now known that binding of LPS to CD14 in conjunction with TLR4 initiates inflammatory gene expression through NF κ B and MAPK signal transduction (3). A correlation between high concentrations of sCD14 and septic shock has been demonstrated (16). Although the recognition of *P. falciparum* derived GPI anchors by a TLR2-TLR1 heterodimer has been shown to induce the synthesis of TNF, a requirement for CD14 in this recognition has not been established (11). Experiments testing the susceptibility of CD14-KO mice to ECM are under way in our lab.

A large number of transcriptional changes due to ECM appear to be a direct response to stress including genes involved in DNA repair, the induction or repression of apoptosis, and oxidative stress. A number of genes that had altered expression during ECM have been characterized in previous publications as neuroprotective (18, 24). In particular, metallothionein I and II were both upregulated during ECM. The metallothioneins are highly conserved, low molecular weight, cysteine rich metalloproteins and are capable of participating in a wide array of neuroprotective activities ranging from immunoregulation, cell survival and brain repair. Increased expression is seen in various pathologies of the brain including traumatic injury, multiple

sclerosis (MS), Alzheimer's disease (AD), Parkinson's disease (PD), and amyotrophic lateral sclerosis (ALS) {16640552}.

MT-I and II may play an active role in reducing damage to the CNS induced by the parasite during CM by at least two mechanisms. First, MT-I and II reduce the activation and recruitment of macrophages and T cells and also inhibit the production and secretion of inflammatory cytokines including TNF- α and lymphotoxin (29). Second, MT I and II are powerful scavengers of free radicals (30) and therefore may moderate oxidative stress and prevent apoptosis during CM. Importantly, exogenous treatment of MT-I and II is also neuroprotective, is well tolerated, and has been shown to inhibit experimental autoimmune encephalomyelitis (EAE) (25), the murine model of MS. Future studies testing the ability of exogenous metallothioneins, as well as other neuroprotectants to reverse the symptoms of ECM should be performed.

REFERENCES

1. **Aravind, L., L. M. Iyer, T. E. Wellems, and L. H. Miller.** 2003. *Plasmodium* biology: genomic gleanings. *Cell* **115**:771-785.
2. **Becker, F. T.** 1949. Induced Malaria as a therapeutic agent, vol. II. W.B. Saunders Company, Philadelphia and London.
3. **Bochkov, V. N., A. Kadl, J. Huber, F. Gruber, B. R. Binder, and N. Leitinger.** 2002. Protective role of phospholipid oxidation products in endotoxin-induced tissue damage. *Nature* **419**:77-81.
4. **Breman, J. G., A. Egan, and G. T. Keusch.** 2001. The intolerable burden of malaria: a new look at the numbers. *Am J Trop Med Hyg* **64**:iv-vii.
5. **Brown, W. D.** 1912. Malarial pigment (hematin) as a factor in the production of the malarial paroxysm. *J Exp Med* **15**:579-597.
6. **Clark, I. A., F. M. al Yaman, and L. S. Jacobson.** 1997. The biological basis of malarial disease. *Int J Parasitol* **27**:1237-1249.
7. **Coban, C., K. J. Ishii, T. Kawai, H. Hemmi, S. Sato, S. Uematsu, M. Yamamoto, O. Takeuchi, S. Itagaki, N. Kumar, T. Horii, and S. Akira.** 2005. Toll-like receptor 9 mediates innate immune activation by the malaria pigment hemozoin. *J Exp Med* **201**:19-25.

8. **de Souza, J. B., and E. M. Riley.** 2002. Cerebral malaria: the contribution of studies in animal models to our understanding of immunopathogenesis. *Microbes Infect* **4**:291-300.
9. **Deponte, M., and K. Becker.** 2004. *Plasmodium falciparum*-do killers commit suicide? *Trends Parasitol* **20**:165-169.
10. **Doherty, F. J., S. Dawson, and R. J. Mayer.** 2002. The ubiquitin-proteasome pathway of intracellular proteolysis. *Essays Biochem* **38**:51-63.
11. **Gazzinelli, R. T., and E. Y. Denkers.** 2006. Protozoan encounters with Toll-like receptor signalling pathways: implications for host parasitism. *Nat Rev Immunol* **6**:895-906.
12. **Hasday, J. D., and I. S. Singh.** 2000. Fever and the heat shock response: distinct, partially overlapping processes. *Cell Stress Chaperones* **5**:471-480.
13. **Hiller, N. L., S. Bhattacharjee, C. van Ooij, K. Liolios, T. Harrison, C. Lopez-Estrano, and K. Haldar.** 2004. A host-targeting signal in virulence proteins reveals a secretome in malarial infection. *Science* **306**:1934-1937.
14. **Horrocks, P., and C. I. Newbold.** 2000. Intraerythrocytic polyubiquitin expression in *Plasmodium falciparum* is subjected to developmental and heat-shock control. *Mol Biochem Parasitol* **105**:115-125.
15. **Kwiatkowski, D.** 1990. Tumour necrosis factor, fever and fatality in falciparum malaria. *Immunol Lett* **25**:213-216.
16. **LeVan, T. D., J. W. Bloom, T. J. Bailey, C. L. Karp, M. Halonen, F. D. Martinez, and D. Vercelli.** 2001. A common single nucleotide polymorphism in the CD14 promoter decreases the affinity of Sp protein binding and enhances transcriptional activity. *J Immunol* **167**:5838-5844.
17. **Long, H. Y., B. Lell, K. Dietz, and P. G. Kremsner.** 2001. *Plasmodium falciparum*: in vitro growth inhibition by febrile temperatures. *Parasitol Res* **87**:553-555.
18. **Mattiasson, G., M. Shamloo, G. Gido, K. Mathi, G. Tomasevic, S. Yi, C. H. Warden, R. F. Castilho, T. Melcher, M. Gonzalez-Zulueta, K. Nikolich, and T. Wieloch.** 2003. Uncoupling protein-2 prevents neuronal death and diminishes brain dysfunction after stroke and brain trauma. *Nat Med* **9**:1062-1068.
19. **Menendez, C., A. F. Fleming, and P. L. Alonso.** 2000. Malaria-related anaemia. *Parasitol Today* **16**:469-476.
20. **Miller, L. H., D. I. Baruch, K. Marsh, and O. K. Doumbo.** 2002. The pathogenic basis of malaria. *Nature* **415**:673-679.
21. **Newton, C. R., P. A. Warn, P. A. Winstanley, N. Peshu, R. W. Snow, G. Pasvol, and K. Marsh.** 1997. Severe anaemia in children living in a malaria endemic area of Kenya. *Trop Med Int Health* **2**:165-178.
22. **Nyakeriga, A. M., H. Perlmann, M. Hagstedt, K. Berzins, M. Troye-Blomberg, B. Zhivotovsky, P. Perlmann, and A. Grandien.** 2006. Drug-induced death of the asexual blood stages of *Plasmodium falciparum* occurs without typical signs of apoptosis. *Microbes Infect* **8**:1560-1568.
23. **Pankova-Kholmyansky, I., A. Dagan, D. Gold, Z. Zaslavsky, E. Skutelsky, S. Gatt, and E. Flescher.** 2003. Ceramide mediates growth inhibition of the *Plasmodium falciparum* parasite. *Cell Mol Life Sci* **60**:577-587.

24. **Penkowa, M.** 2006. Metallothioneins are multipurpose neuroprotectants during brain pathology. *Febs J* **273**:1857-1870.
25. **Penkowa, M., and J. Hidalgo.** 2003. Treatment with metallothionein prevents demyelination and axonal damage and increases oligodendrocyte precursors and tissue repair during experimental autoimmune encephalomyelitis. *J Neurosci Res* **72**:574-586.
26. **Sachs, J. D.** 2002. A new global effort to control malaria. *Science* **298**:122-124.
27. **Schofield, L., M. C. Hewitt, K. Evans, M. A. Siomos, and P. H. Seeberger.** 2002. Synthetic GPI as a candidate anti-toxic vaccine in a model of malaria. *Nature* **418**:785-789.
28. **Schofield, L., S. Novakovic, P. Gerold, R. T. Schwarz, M. J. McConville, and S. D. Tachado.** 1996. Glycosylphosphatidylinositol toxin of *Plasmodium* up-regulates intercellular adhesion molecule-1, vascular cell adhesion molecule-1, and E-selectin expression in vascular endothelial cells and increases leukocyte and parasite cytoadherence via tyrosine kinase-dependent signal transduction. *J Immunol* **156**:1886-1896.
29. **Stankovic, R. K., R. S. Chung, and M. Penkowa.** 2007. Metallothioneins I and II: neuroprotective significance during CNS pathology. *Int J Biochem Cell Biol* **39**:484-489.
30. **Taylor, D. M., S. Minotti, J. N. Agar, and H. D. Durham.** 2004. Overexpression of metallothionein protects cultured motor neurons against oxidative stress, but not mutant Cu/Zn-superoxide dismutase toxicity. *Neurotoxicology* **25**:779-792.
31. **Templeton, T. J., L. M. Iyer, V. Anantharaman, S. Enomoto, J. E. Abrahante, G. M. Subramanian, S. L. Hoffman, M. S. Abrahamsen, and L. Aravind.** 2004. Comparative analysis of Apicomplexa and genomic diversity in eukaryotes. *Genome Res* **14**:1686-1695.
32. **Udomsangpetch, R., B. Pipitaporn, K. Silamut, R. Pinches, S. Kyes, S. Looareesuwan, C. Newbold, and N. J. White.** 2002. Febrile temperatures induce cytoadherence of ring-stage *Plasmodium falciparum*-infected erythrocytes. *Proc Natl Acad Sci U S A* **99**:11825-11829.

